FORMATION AND CHARACTERIZATION OF HYBRID MEMBRANES UTILIZING HIGH-PERFORMANCE POLYIMIDES AND CARBON MOLECULAR SIEVES

A Dissertation
Presented to
The Academic Faculty

By

John Douglas Perry

In Partial Fulfillment
Of the Requirements for the Degree
Doctor of Philosophy in the
School of Chemical & Biomolecular Engineering

Georgia Institute of Technology
August, 2007

FORMATION AND CHARACTERIZATION OF HYBRID MEMBRANES UTILIZING HIGH-PERFORMANCE POLYIMIDES AND CARBON MOLECULAR SIEVES

Approved by:

Dr. William J. Koros, Advisor
School of Chemical & Biomolecular Engineering
Georgia Institute of Technology

Dr. Satish Kumar
School of Polymer, Textile & Fiber Engineering
Georgia Institute of Technology

Dr. Victor Breedveld
School of Chemical & Biomolecular Engineering
Georgia Institute of Technology

Dr. Sankar Nair
School of Chemical & Biomolecular Engineering
Georgia Institute of Technology

Dr. Christopher W. Jones
School of Chemical & Biomolecular Engineering
Georgia Institute of Technology

Date Approved: April 16, 2007

ACKNOWLEDGEMENTS

I would like to acknowledge Dr. William J. Koros for being a truly amazing advisor. His understanding, cooperation, and outstanding ability to guide the research of his students make him the kind of advisor any graduate student would love to have. I consider myself very blessed for the time I was able to work with him.

I would also like to acknowledge the many members of the Koros research group that shared their time with me. I would especially like to thank Ted Moore, Bill Madden, and Jason Williams for all of their help and friendship as I was getting started with my research. Raymond Chafin, Preeti Chandra, Adam Kratochvil, and Ryan Adams also deserve special thanks for the very helpful conversations and numerous “favors” they provided that helped get me through.

Furthermore, I would like to acknowledge a lifetime of unfailing support that I have received from my family. My sisters have been amazing supporters throughout all of my education, and I honestly can not imagine having better parents.

Finally, I want to acknowledge Lindsay, my wife, my love, my best friend. I thank the Lord constantly for bringing her into my life.

TABLE OF CONTENTS

LIST OF TABLES

LIST OF FIGURES

SUMMARY

The industrial market for gas separation membranes is expected to grow considerably in the next several decades. Much of this expansion is dependent on the continued development of more efficient membranes. Current membrane technology is based on polymeric materials that are subject to a limiting tradeoff between productivity (permeability) and efficiency (selectivity). While other materials with better gas separation performance exist, such as zeolites and carbon molecular sieves, these materials are limited by physical characteristics that inhibit industrial scale membrane preparation. Hybrid membrane technology has shown the ability to combine the advantageous properties of these materials opening the door for the next generation of gas separation membranes. This research focuses on the application of hybrid membrane technology to a system comprised of carbon molecular sieves dispersed in an upper bound polymer matrix, 6FDA-6FpDA.

Development of hybrid membranes requires significant engineering to produce effective mass transfer across the interface between the two phases. Previous work has highlighted multiple issues associated with the production of hybrid membranes with "good" interfacial characteristics. In this work, the further challenge of forming membranes with 6FDA-6FpDA was added. The techniques that allowed the successful formation of hybrid membranes using other polymers required further modification for success with this system.

This work shows the sensitivity of the component materials to processing conditions and the importance of consistency in gas separation membrane production. In particular,

milling the sieves to reduce the size and using chemical linkage agents to bond to the polymer have considerable potential to alter the separation performance of the respective materials. Systematic analysis of multiple factors in this work provides important information regarding the source of unexpected properties in the hybrid membranes.

Hybrid membrane testing in this work shows a need for active elimination of particle agglomerates within the membrane dope prior to casting to produce effective membranes. Continual sonication during the preparation of the casting dope was able to eliminate the majority of the agglomerates present in earlier trials. Further reduction of stresses generated during the casting process was also necessary to produce membranes with enhanced selectivity. Annealing the hybrid films above the polymer T_g appears to repair the interfacial morphology and produce effective membranes. The use of these tools to enhance the gas separation performance of 6FDA-6FpDA represents the first known report of successful enhancement of the selectivity of an upper bound polymer using the hybrid membrane approach.

CHAPTER 1

INTRODUCTION

1.1. Gas Separation Membranes and Applications

Membrane based processes are useful in many industrial applications for both liquid and gas based separations [1]. Using a combination of the size, shape, and physicochemical properties of the components in a stream, membranes enable the preferential passage of certain species over others. Some separations, such as microfiltration and ultrafiltration, rely almost entirely on size differences to perform the separation [2]. Meanwhile more specialized processes, such as reverse osmosis and dialysis membranes, exploit physical *and* chemical interactions of components to perform the separation [3-6].

While the most popular historical uses of membranes have involved separations of solids and liquids (i.e. filtration), the use of membranes in pervaporation and gas separations continues to grow [7, 8]. Pervaporation involves a liquid phase upstream with a vapor phase permeate. In gas separations, the membrane enables separation of a gas mixture with two or more components based on the different permeation rates of each species in the feed. A broad range of industrially important membrane based gas separations have been investigated involving several gas pairs: O_2/N_2, CO_2/CH_4, H_2/CH_4, H_2/CO, H_2O/CH_4, and C_3H_6/C_3H_8 [8-11].

Advancements in membrane technology have allowed membranes to compete successfully with more traditional methods used for gas separations such as absorption, adsorption, pressure swing adsorption (PSA), and distillation (including cryogenic) [8,

12]. When properly implemented, membrane processes can provide lower capital investment, ease of installation, lower operational and maintenance costs, lower space and weight requirements, more environmentally friendly components, and more flexibility and adaptability relative to traditional methods [8]. Because of the limitations of the solution-diffusion mechanism of gas transport that dominates the performance of polymer based membranes (see chapter 2), the production of membranes with increased separation properties will likely require the development of new materials [13, 14]. ***The goal of this project is to establish a framework for the development of gas separation membranes based on hybrid (polymer-carbon) materials that exceed the performance capabilities currently available with polymeric membrane systems.***

1.2. History

Since the early 1950s membranes have been considered for a variety of gas separations including the removal of oxygen from air, helium from natural gas, and hydrogen from petroleum refinery gas [15]. Further developments have expanded the applications to other separations such as removal of carbon dioxide from natural gas and even the separation of olefins and paraffins [13, 16]. Membranes offer a separation alternative to the thermally driven and solvent based separations, such as distillation and adsorption, which traditionally dominate the field [8, 17].

Even though prior work had shown promise for industrial application of membranes, it was late in the 1970s before DuPont pioneered the use of small-diameter hollow fiber gas separation membranes [18]. Unfortunately, the low productivity in the first generation of hollow fibers was not economical for widespread gas separations. Monsanto Company overcame this problem by developing a mulitcomponent,

polysulfone hollow fiber membrane for hydrogen recovery [19]. By limiting the dense, selective region of the fiber to a very thin outer layer, the fiber productivity was greatly increased. This new technology was successfully applied to the separation of hydrogen from ammonia purge gases. Soon after, Separex Corp. developed the Separex® spiral wound cellulose acetate membranes for hydrogen separations and natural gas purification and dehydration [20]. The increased chemical resistance gave the cellulose acetate membranes better performance in the presence of hydrocarbon impurities. By the mid 1980s, membranes were being implemented more frequently and in further applications [21, 22]. In Japan, Ube introduced a polyimide membrane with the best heat- and solvent-resistance properties of its time [17]. Further development with new materials and processing has led to the continued advancement of membrane separations in the past twenty years.

1.3. Polymeric Gas Separation Membranes

The majority of membranes currently used for gas separations are produced from synthetic polymers with polysulfone, cellulose acetate, and the polyimide Matrimid® being the most common [23]. One of the major attractions to these materials besides their separation properties is the ability to spin them as asymmetric hollow fibers [10]. Figure 1.1 shows the surface area to volume ratio for the most common applied configurations for membrane separators [24]. The extremely high surface area obtained with the hollow fibers makes this form the most attractive for gas separations due to the enormous surface area needed to make membrane separations economically viable [25].

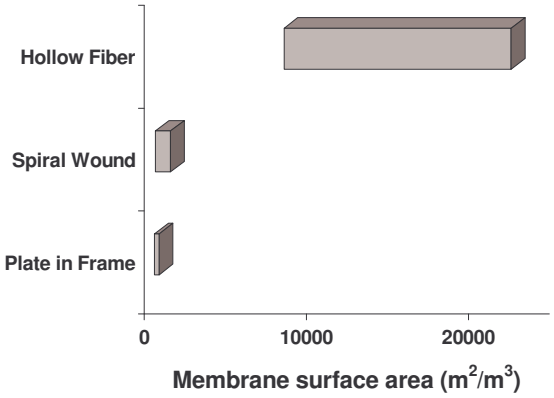

Figure 1.1 Surface area to volume ratios vary greatly for different membrane configurations [24].

Many polymer families have been examined for their gas transport characteristics including polymethacrylates, polycarbonates, polysulfones, polyesters, polyimides, and polypyrrolones [26]. Polyimides and polypyrrolones tend to have the highest transport performance properties of these polymer families, but even the best solution processible polymer membranes are limited by an upper bound of the permeability and selectivity attainable [14, 27]. In membrane systems there is a tradeoff between the permeability of the material (productivity) and the selectivity of the separation (efficiency). When plotted on a logarithmic scale, this tradeoff creates an upper bound that was established in 1991 by L.M. Robeson for several common gas separations [14]. Figure 1.2 shows this upper bound for the oxygen/nitrogen and carbon dioxide/methane separations. As the figure illustrates, new materials will be necessary to produce membranes with properties that exceed those available with solution processable polymers.

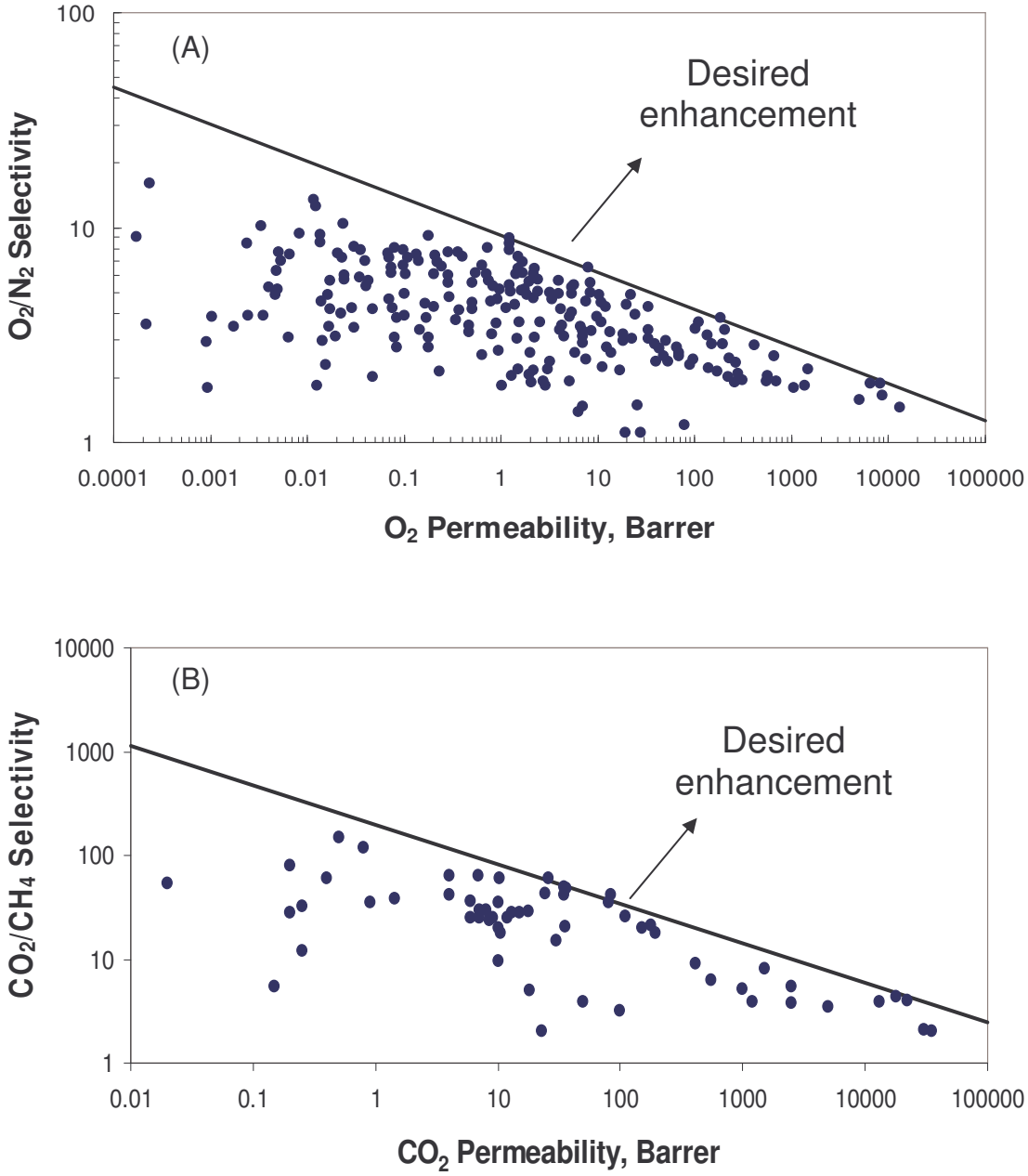

Figure 1.2 Permeation data for the O_2/N_2 (A) and CO_2/CH_4 (B) separations for various polymers illustrates the upper bound limit observed by Robeson [14].

1.4. Inorganic Gas Separation Membranes

There are materials, including zeolites and carbon molecular sieves (CMSs), that have separation properties exceeding the performance limit for solution processable polymers

[28-33]. Figure 1.3 provides some examples of the transport properties that may be obtained with these materials. These molecular sieves have rigid structures with pore sizes that approach the size of gas molecules. As a result of their molecular scale, rigid pores these materials are capable of much higher size- and shape-based selectivities than even the best performing polymers. These high selectivities, combined with relatively high permeabilities for the fast gas, allow many of these materials to operate above the upper bound limit for polymer membranes. Carbon molecular sieves are produced by the controlled high temperature pyrolysis of a polymer precursor [34], and this process will be discussed further in Chapter 2. By carefully controlling many of the parameters of the pyrolysis including atmosphere, sample geometry, precursor, temperature, "thermal soak" time, and post treatment conditions, it is possible to tune the transport properties of the sieves [33, 34]. This flexibility, combined with the ease of carbon formation and excellent transport properties, has generated a desire to use CMSs in membrane separation processes.

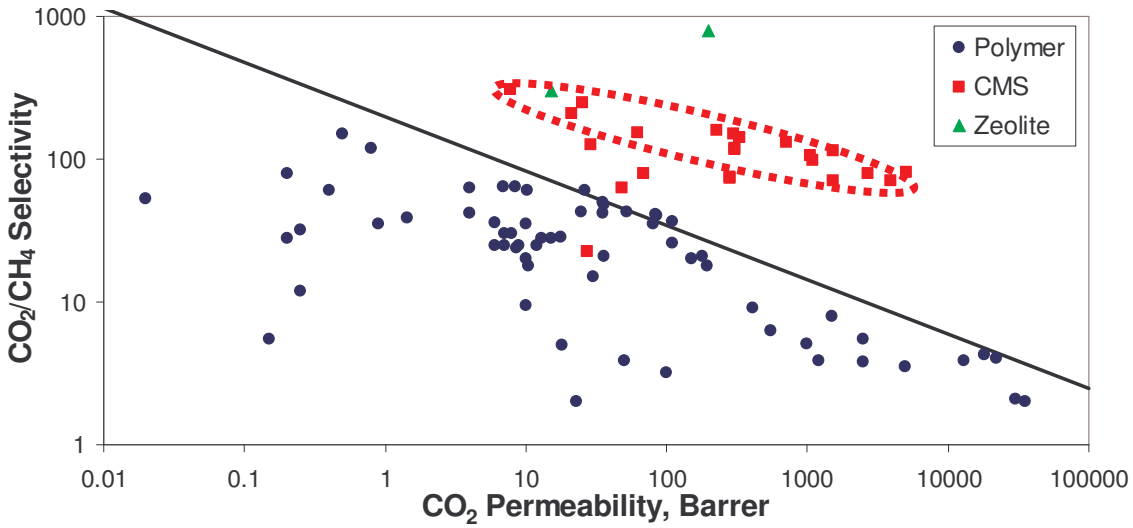

Figure 1.3 Permeation data for molecular sieves plotted against the upper bound plot for CO_2/CH_4 shows the much higher separation ability available with inorganic materials. The dotted line indicates a range of properties readily obtainable with CMS membranes [35].

While the rigid structure of the zeolites and CMSs is one of the primary reasons for their high selectivities in gas separations, this rigidity causes zeolite and CMS membranes to be very brittle. As a result, membrane processing with these materials is *very* expensive. In fact, estimates suggest that an industrial zeolite membrane unit could cost 100 to 1000 times more to construct than a polymer based membrane unit [36]. As well as making the production of a membrane unit cost prohibitive, the brittle nature of zeolite and CMS membranes also makes them less physically robust in the potentially harsh environment of a natural gas processing facility where catastrophic damage to the membrane could result from an incident that would have little effect on a polymer membrane. In order to overcome the obstacles present in the application of these membranes, the use of hybrid materials has been proposed as a possible solution [36-38].

1.5. Hybrid Gas Separation Membranes

To overcome the limitations of these current membrane technologies, development of a hybrid material that combines the excellent transport properties of the CMS membranes with the physically robust nature of the polymer membranes is desired. Otherwise known as “mixed matrix” membranes, these hybrid membranes composed of a continuous polymer network containing dispersed CMS particles (see Figure 1.4) combine the materials to provide enhanced separation performance from the CMS inserts while maintaining the necessary physical resilience of the polymer [39-41]. Such a membrane may be processed with only minor adjustments of the techniques used with neat polymer membranes, while providing improved transport properties from the dispersed sieve phase [39, 42]. Successful implementation of this technology should enable the production of robust membrane materials with separation performance

exceeding the upper bound noted by Robeson [14] but at a fraction of the cost of pure CMS membranes [39, 40].

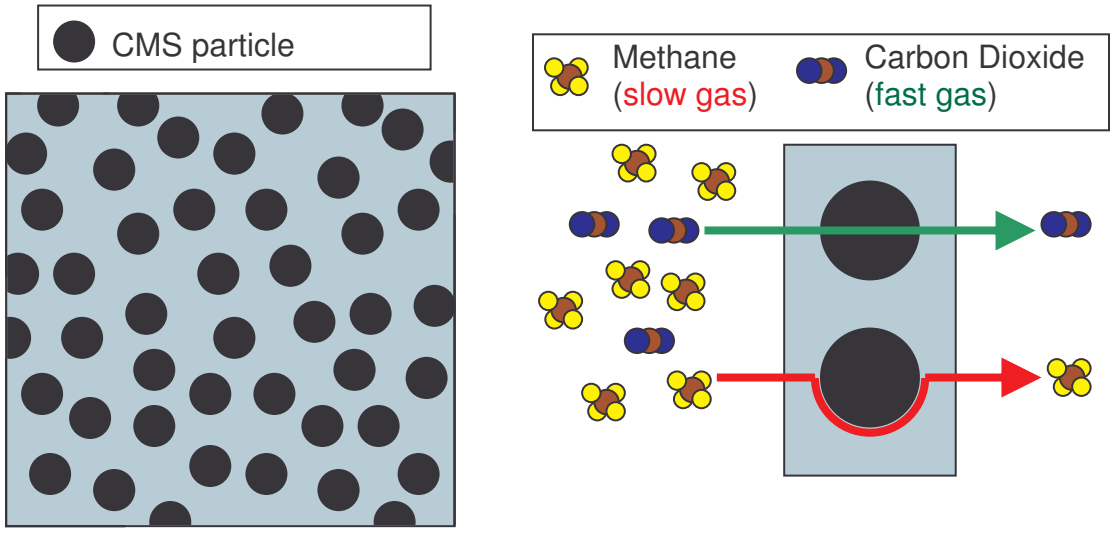

Figure 1.4 CMS particles homogeneously dispersed in a polymer matrix are used to enhance the gas separation performance of the membrane. Because of the excellent transport properties of the molecular sieves, the fast gas has increased permeability while the slow gas has decreased permeability.

The mixed matrix concept has been successfully demonstrated using both zeolite [42, 43] and CMS [39, 40] inserts; however, "successful" implementation of this technique using "upper bound" polymers has not been achieved previously [36]. Hybrid membranes often do not possess the predicted separation performance. Two primary reasons have been suggested for this failure: rigidification of the polymer matrix around the inserts and poor contact between the polymer and the sieve [23, 36, 38]. As the solvent evaporates from the films during casting, the polymer contracts, but the sieves cannot. This difference in the mobility of the two phases can cause localized stresses in the membrane resulting in these two problems [23, 44]. Compressive stress can cause rigidification of the polymer matrix around the sieve leading to lower diffusivity in that region. On the other hand, tensile stress can lead to delamination of the polymer and

sieve resulting in gaps at the interface. Several techniques such as surface modification, high formation temperature, the use of plasticizing agents, and chemical reaction techniques have been used to overcome some of these issues for zeolite particles and promote interfacial contact [23, 36, 38]. While these techniques offer potential solutions to the current problems with the interfacial region for zeolites, they have not been attempted with carbons due to poorly defined surface chemistry. The lack of success with previous attempts to produce mixed matrix membranes with “upper bound” polymers and CMS inserts suggests that further sieve preparation is required.

1.6. Applications of Gas Separation Membranes

The utilization of membranes in industrial gas separations has undergone substantial growth in several areas since 1980 when the first large scale application was developed by Permea for hydrogen separations [13, 17]. As Figure 1.5 indicates, the current membrane market is dominated by three major separations: nitrogen from air, natural gas purification, and hydrogen separations [13, 24]. The recovery of nitrogen from air currently accounts for nearly half of the current market for gas separation membranes. Because air is 80% nitrogen, the majority of air separation membranes operate to recover nitrogen. Approximately two thirds of the component expense for a membrane based air separation plant resides in the compressors needed for the operation [13]. Further improvements in the performance of air separation membranes still has significant potential for application in this area by reducing compressor size and increasing operation efficiency. There is also room for growth in the area of oxygen recovery from air if significantly advanced membranes can be developed to allow the economics to compete with current cryogenic processes. Figure 1.5 shows the membrane market in 2000 and a future “predicted” market for 2020 proposed by Baker,

but these changes rely on the development of alternative membrane materials besides solution processable polymers [13].

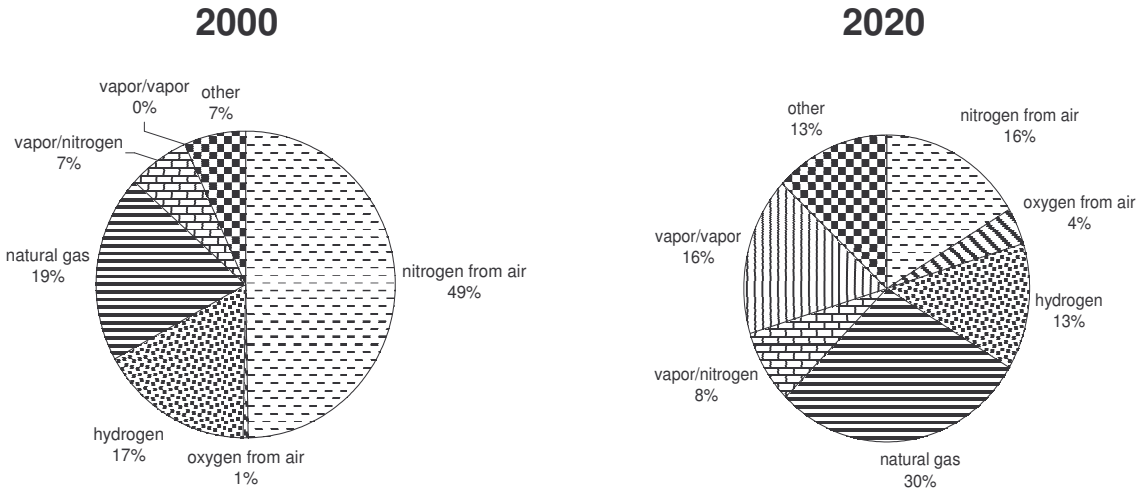

Figure 1.5 The membrane market is expected to see significant changes as new materials continue to improve the economics of membrane separations [13].

Another major application of gas separation membranes is in the purification of natural gas before it goes to the pipeline. Strict regulations control the concentrations of the contaminants in the natural gas streams (Meyer 1990; Lee 1994; Lee 1995), and over 40% of the proven raw reserves in the United States contain subquality natural gas [45]. Table 1.1 shows a comparison of typical feed concentrations and the sales specifications required before the gas can be introduced to the pipeline. Of these impurities, carbon dioxide occurs in the highest concentrations with approximately 17% of domestic raw natural gas reserves containing too much carbon dioxide [13]. Amine absorption is the technology most widely used to remove excess carbon dioxide from raw natural gas, however, these absorption facilities are very costly, the operation is complex, and maintenance is expensive and labor intensive [11, 46-49]. These issues become particularly important in smaller reserves and more remote locations where

building an absorption plant is cost prohibitive or impractical. In addition to the demands of current reservoirs, it is also anticipated that many of the gas reserves discovered in the future will be smaller, with lower quality gas and in more remote locations, such as offshore [36]. These expected trends suggest great potential for growth in the application of gas separation membranes for the purification of natural gas. The development of high performance gas separation membrane materials that can withstand more aggressive feed streams containing higher levels of condensable hydrocarbon impurities would also allow the application of membranes for natural gas purification to be widely expanded [13].

Table 1.1 Molar concentration of several components of natural gas wells and their respective sales specifications (Lee 1994; Lee 1995; Tabe-Mohammadi 1999).

Compound	***Typical Feed Concentration***	*Sales Specifications*
CH_4	70-80%	90%
CO_2	5-20%	<2%
C_2H_6	3-4%	3-4%
C3 to C5	3%	3%
N_2	1-4%	<4%
H_2S	<100 ppm	<4 ppm
H_2O	Saturated	<100 ppm
C6 and higher	0.5-1%	0.5-1%

Because of its very small size, hydrogen has one of the highest diffusivities of the permanent gases [50], and as a result, hydrogen recovery was the first industrial scale application of gas separation membranes [37]. Applications such as recovery of hydrogen from ammonia purge gas and adjustment of the hydrogen/carbon monoxide ratio in syngas plants are ideal applications of gas separation membranes because the gas is clean and free of condensable hydrocarbon vapors [13]. On the other hand, some of the best sources of new hydrogen are refinery fuel gas streams, pressure swing adsorption tail gas, and hydrocracker/hydrotreater off gas; however, these streams contain mixtures of light hydrocarbons (C_1-C_5) [50]. The development of more robust

materials that can resist plasticization in aggressive feed streams and operate at higher temperatures should allow significant expansion of membrane separations in these applications [37].

Other areas of application for gas separation membranes include the recovery of vapors from permanent gases and the separation of vapors. Of particular interest are the separations of light hydrocarbon vapor streams such as ethane/ethylene, propane/propylene, and n-butane/isobutene [13, 34]. Because these systems have such close boiling points, large towers and high reflux ratios are required to obtain high purities with distillation. While several reports have been published showing the application of membranes to these separations, further development will be necessary to produce membranes that can operate at the higher temperatures and pressures that will be required for industrial application in these separations [51-54]. This field may prove to be a situation where the high cost of inorganic membranes can be justified by their ability to withstand the harsh operating conditions [13, 34].

Clearly there is plenty of room for expansion of gas separation membrane applications with the continued development of more efficient and more robust membrane materials. Increased performance combined with the ability to withstand harsher operating conditions would allow membranes to economically compete in an ever broadening range of applications. Hybrid membrane development provides a pathway to further advance the material properties of gas separation membranes without the need for drastic changes in the production infrastructure.

1.7. Research Objectives

The previous section has established the importance of membranes for gas separations and the need for new materials with enhanced separation performance to broaden the scope of future membrane applications. This project seeks to establish the framework that will enable the development of membrane materials that exceed the performance ability of solution processable polymers. The overarching goal of the work is to apply the hybrid membrane concept using a carbon molecular sieve insert and an "upper bound" polymer thus producing a material with properties that exceed the performance limits of any neat polymer membranes. In order to work towards these goals, the following objectives were developed:

1. *Develop a methodology to stabilize CMS submicron particle suspensions to enable creation of a stable casting suspension for hybrid materials using an "upper bound" polymer and a tailored CMS insert.*
2. *Develop a surface treatment that does not adversely affect the transport properties of the CMS materials prior to incorporation in a hybrid membrane.*
3. *Develop a modification that does not adversely impact the transport properties of the polymer matrix used to produce the hybrid membranes.*
4. *Develop a surface treatment to enable tailoring interfacial interactions (adhesion/rigidification) to produce transport properties consistent with model predictions for hybrid membranes.*

1.7.1. Objective 1: Develop a methodology to stabilize CMS particle suspensions.

One of the primary obstacles in the production of successful hybrid membranes is the presence of particle agglomerates in the dope. These agglomerates can prevent the matrix polymer from fully covering the particles resulting in voids in the membrane that

cause defective transport properties. It is desirable to form suspensions for film formation using a polymer solution and sieve that have favorable interactions that prevent agglomeration from occurring. The modification used in this work improved the stability of the suspensions, but further processing was necessary to prevent the presence of agglomerates in the hybrid membranes as discussed in Chapter 6.

1.7.2. Objective 2: Develop a surface treatment that does not adversely affect CMS transport properties.

The surface treatment used in this work was designed to provide a covalent bond between the polymer and the sieve. In order for this technique to successfully provide enhancement of the transport properties of the final membrane, it is important that the modification does not impair the transport properties of the sieve prior to incorporation in the hybrid film. High pressure sorption analysis, shown in Chapter 4, demonstrated the ability of the sieves to maintain excellent gas transport properties after surface modification.

1.7.3. Objective 3: Develop a modification that does not adversely affect polymer transport properties.

Similar to the case for the sieves, the modification technique used must not impair the transport properties of the polymer used in the hybrid matrix. This work shows that the alteration of the backbone caused by the linkage unit can strongly impact the transport properties of the polymer; however, controlling the amount of modifier in the system is successful at eliminating these adverse effects as shown in Chapter 5.

1.7.4. Objective 4: Develop a surface treatment that controls the interface sufficiently to provide enhanced transport properties.

The membrane formation process plays a major role in the transport properties of the resulting hybrid material[23, 38]. The use of a chemical agent to enhance the interaction of the polymer and the sieve particles was employed along with some modifications to the formation process to produce membranes with enhanced transport properties. These process modifications and the steps involved in their development are described in Chapter 6.

1.8. Dissertation Overview

Chapter 2 provides background information and the theoretical basis relevant to this work, and the chapter closes with a review of previous research involving hybrid membranes. Chapter 3 gives the details of the materials and the procedures that were used in this work. The impact of processing conditions and modification on the CMS particles used in the hybrid membranes is discussed in Chapter 4. The changes that occur in the polymer matrix during hybrid film formation are examined in Chapter 5. Development of enhanced transport properties in a hybrid film containing an upper bound polymer as the matrix is discussed in Chapter 6. Finally, conclusions and recommendations for future work are presented in Chapter 7.

1.9. References

1. Rautenbach, R. and Albrecht, R. (1989). Membrane Processes. Chichester, John Wiley & Sons.
2. Cheryan, M. (1998). Ultrafiltration and Microfiltration Handbook. Lancaster, PA, Technomic Publishing.
3. Peters, T.A. (1991). "Desalination and Industrial-Waste Water-Treatment with the Rochem Disk Tube Module Dt." Desalination 83(1-3): 159-172.
4. Peters, T.A. (1998). "Purification Of Landfill Leachate With Reverse Osmosis And Nanofiltration." Desalination 119(1-3): 289-293.

5. Petersen, R.J. (1993). "Composite Reverse Osmosis And Nanofiltration Membranes." Journal of Membrane Science 83: 81-150.
6. Saki, K. (1994). "Determination Of Pore Size And Pore Size Distribution 2. Dialysis Membranes." Journal of Membrane Science 96: 91-130.
7. Lipnizki, F.F., Robert W., et al. (1999). "Pervaporation-Based Hybrid Process: A Review Of Process Design, Applications And Economics." Journal of Membrane Science 153: 183-210.
8. Spillman, R.W., Sherwin, M.B. (1990). "Gas Separation Membranes: The First Decade." Chemtech 20(6): 378-384.
9. Bessarabov, D.G. (1999). "Membrane Gas-Separation Technology In The Petrochemical Industry." Membrane Technology 107: 9-13.
10. Koros, W.J. and Fleming, G.K. (1993). "Membrane-Based Gas Separation." Journal of Membrane Science 83(1): 1-80.
11. Spillman, R.W. (1989). "Economics of Gas Separation Membranes." Chemical Engineering Progress 85(1): 41-62.
12. Spillman, R.W. and Cooley, T.E. (1989). "Membrane Gas Treating." Proceedings of the 68th Annual convention of the Gas Processors Association: 186-196.
13. Baker, R. W. (2002). "Future Directions Of Membrane Gas Separation Technology." Industrial & Engineering Chemistry Research 41(6): 1393-1411.
14. Robeson, L.M. (1991). "Correlation of Separation Factor Versus Permeability for Polymeric Membranes." Journal of Membrane Science 62(2): 165-185.
15. Weller, S. and Steiner, W.A. (1950). "Engineering Aspects of Separation of Gases - Fractional Permeation through Membranes." Chemical Engineering Progress 46(11): 585-590.
16. Burns, R.L. and Koros, W.J. (2003). "Defining The Challenges For C3H6/C3H8 Separation Using Polymeric Membranes." Journal of Membrane Science 211(2): 299-309.
17. Zolandz, R.R. and Fleming, G.K. (1992). Gas Permeation Applications. Membrane Handbook. W. S. W. Ho and K. K. Sirkar. New York, Chapman and Hall: 78-94.
18. Gardner, R.J., Crane, R.A., et al. (1977). "Hollow Fiber Permeater for Separating Gases." Chemical Engineering Progress 73(10): 76-78.
19. Henis, J.M.S. and Tripodi, M.K. (1980). Multicomponent Membranes for Gas Separations. U. S. P. Office. United States, Monsanto Company, St. Louis, Mo. 4,230,463: 34.
20. Schell, W.J. and Houston, C.D. (1982). "Spiral-Wound Permeators for Purification and Recovery." Chemical Engineering Progress 78(10): 33-37.
21. Bollinger, W.A., Long, S.P., et al. (1984). "Optimizing Hydrocracker Hydrogen." Chemical Engineering Progress 80(5): 51-57.
22. Bollinger, W.A., Maclean, D.L., et al. (1982). "Separation Systems for Oil Refining and Production." Chemical Engineering Progress 78(10): 27-32.
23. Moore, T.T. (2004). Effects of Materials, Processing, and Operating Conditions on the Morphology and Gas Transport Properties of Mixed Matrix Membranes. Chemical Engineering. Austin, TX, The University of Texas at Austin. Doctor of Philosophy: 312.
24. Kesting, R.E., Fritzsche, A.K. (1993). Polymeric Gas Separation Membranes. New York, John Wiley and Sons, Inc.
25. Wallace, D.W. (2004). Crosslinked Hollow Fiber Membranes for Natural Gas Purification and Their Manufacture from Novel Polymers. Chemical Engineering. Austin, The University of Texas at Austin. Doctor of Philosophy: 221.
26. Koros, W.J., Coleman, M.R., et al. (1992). "Controlled Permeability Polymer Membranes." Annual Review of Materials Science 22: 47-89.

27. Walker, D.R.B. (1993). Synthesis and Characterization of Polypyrrolones for Gas Separation Membranes. Chemical Engineering. Austin, TX, The University of Texas at Austin. Doctor of Philosophy: 168.
28. Caro, J., Noack, M., et al. (2000). "Zeolite Membranes - State Of Their Development And Perspective." Microporous and Mesoporous Materials 38(1): 3-24.
29. Ismail, A.F. and David, L.I.B. (2001). "A Review On The Latest Development Of Carbon Membranes For Gas Separation." Journal of Membrane Science 193: 1-18.
30. Jones, C.W. and Koros, W.J. (1994). "Carbon Molecular-Sieve Gas Separation Membranes.I. Preparation and Characterization Based on Polyimide Precursors." Carbon 32(8): 1419-1425.
31. Jones, C.W. and Koros, W.J. (1995). "Carbon Composite Membranes: A Solution To Adverse Humidity Effects." Industrial and Engineering Chemistry Research 34: 164.
32. Koresh, J.E., Soffer, A. (1983). "Molecular Sieve Carbon Permselective Membrane. Part 1. Presentation Of A New Device For Gas Mixture Separation." Separation Science and Technology 18: 723-734.
33. Steel, K.M. (2000). Carbon Membranes For Challenging Gas Separations. Chemical Engineering. Austin, TX, The University of Texas at Austin. Doctor of Philosophy.
34. Williams, P.J. (2006). Analysis of Factors Influencing the Performance of CMS membranes for Gas Separation. School of Chemical and Biomolecular Engineering. Atlanta, Georgia Institute of Technology. Doctor of Philosophy: 238.
35. Williams, P.J. (2004). Personal Communication.
36. Vu, D.Q. (2001). Formation and Characterization of Asymmetric Carbon Molecular Sieve and Mixed Matrix Membranes for Natural Gas Purification. Chemical Engineering. Austin, TX, The University of Texas at Austin. Doctor of Philosophy.
37. Koros, W.J. and Mahajan, R. (2000). "Pushing The Limits On Possibilities For Large Scale Gas Separation: Which Strategies?" Journal of Membrane Science 175(2): 181-196.
38. Mahajan, R. (2000). Formation, Characterization, and Modeling of Mixed Matrix Membrane Materials. Chemical Engienering. Austin, TX, The University of Texas at Austin. Doctor of Philosophy.
39. Vu, D.Q., Koros, W.J., et al. (2003). "Mixed Matrix Membranes Using Carbon Molecular Sieves - I. Preparation And Experimental Results." Journal of Membrane Science 211(2): 311-334.
40. Vu, D.Q., Koros, W.J., et al. (2003). "Mixed Matrix Membranes Using Carbon Molecular Sieves - II. Modeling Permeation Behavior." Journal of Membrane Science 211(2): 335-348.
41. Zimmerman, C.M., Singh, A., et al. (1997). "Tailoring Mixed Matrix Composite Membranes For Gas Separations." Journal of Membrane Science 137(1-2): 145-154.
42. Mahajan, R. and Koros, W.J. (2002). "Mixed Matrix Membrane Materials With Glassy Polymers. Part 1." Polymer Engineering and Science 42(7): 1420-1431.
43. Mahajan, R. and Koros, W.J. 2002). "Mixed Matrix Membrane Materials With Glassy Polymers. Part 2." Polymer Engineering and Science 42(7): 1432-1441.
44. Moore, T.T. Mahajan, R., et al. (2004). "Hybrid Membrane Materials Comprising Organic Polymers with Rigid Dispersed Phases." AIChE Journal 50(2): 311-321.
45. Meyer, H.S. (2000). "Volume and Distribution of Subquality Natural Gas in the United States." GasTIPS 6(1): 10-13.

46. Bhide, B.D. Stern, S.A. (1993). "Membrane Processes For The Removal Of Acid Gases From Natural Gas. I. Process Configurations And Optimization Of Operating Conditions." Journal of Membrane Science 81: 209-237.
47. Fournie, F.J.C. and Agostini, J.P. (1987). "Permeation Membranes Can Efficiently Replace Conventional Gas Treatment Processes." Journal of Petroleum Technology 39(6): 707-712.
48. Mazur, W.H. and Chan, M.C. (1982). "Membranes for Natural-Gas Sweetening and CO2 Enrichment." Chemical Engineering Progress 78(10): 38-43.
49. Schell, W.J., Houston, C.D., et al. (1983). "Membranes Can Efficiently Separate CO2 from Mixtures." Oil & Gas Journal 81(33): 52-56.
50. Perry, J.D., Nagai, K., et al. (2006). "Polymer Membranes For Hydrogen Separations." Mrs Bulletin 31(10): 745-749.
51. Krol, J.J., Boerrigter, M., et al. (2001). "Polyimide Hollow Fiber Gas Separation Membranes: Preparation And The Suppression Of Plasticization In Propane/Propylene Environments." Journal of Membrane Science 184(2): 275-286.
52. Shimazu, A., Miyazaki, T., et al. (2000). "Relationships Between The Chemical Structures And The Solubility, Diffusivity, And Permselectivity Of Propylene And Propane In 6FDA-Based Polyimides." Journal of Polymer Science Part B-Polymer Physics 38(19): 2525-2536.
53. Staudt-Bickel, C. and Koros, W. J. (2000). "Olefin/Paraffin Gas Separations With 6FDA-Based Polyimide Membranes." Journal of Membrane Science 170(2): 205-214.
54. Tanaka, K., Taguchi, A., et al. (1996). "Permeation And Separation Properties Of Polyimide Membranes To Olefins And Paraffins." Journal of Membrane Science 121(2): 197-207.

CHAPTER 2

BACKGROUND AND THEORY

The first part of this chapter discusses the fundamental concepts associated with the transport of gas molecules through a membrane. This information is then used to compare and contrast the most common materials used to produce gas separation membranes. Section 2.3 covers strategies for modeling the behavior of these systems, and the chapter closes with a review of previous work in the area of hybrid gas separation membranes.

2.1. Gas Transport

The utility of gas separation membranes relies entirely on the ability of a material to control the rate at which different gas molecules are allowed to pass through the material. As such, membranes are essentially a selective barrier for gas molecules or a molecular level filter. The fundamental principles that regulate the transport of gas molecules through the membrane materials are discussed in this section.

2.1.1. *Permeation*

Two primary orders of merit are used to establish the viability of a material as a gas separation membrane: permeability and permselectivity. Permeability is a material property that directly relates to how fast a gas can pass through a membrane. Experimentally, the permeability is derived from the flux of gas through the membrane normalized by the thickness and pressure drop as shown in Equation 2.1.

$$P_A = N_A \frac{\ell}{\Delta p_A} \tag{2.1}$$

where P_A is the permeability of component A through the membrane, N_A is the flux of component A, ℓ is the thickness of the membrane, and Δp_A is the partial pressure drop for component A across the membrane. The most common unit of permeability is the Barrer which was established for its relevance in industrial membrane applications:

$$1\text{Barrer} = 10^{-10} \frac{cm^3(STP) \cdot cm}{s \cdot cm^2 \cdot cmHg}. \tag{2.2}$$

In certain membrane morphologies such as asymmetric hollow fibers, it is difficult to accurately characterize the thickness of the separating layer, therefore, these membranes are often described by their permeance rather than permeability. Permeance is the flux through the membrane normalized by the pressure drop only, as indicated by Equation 2.3:

$$permeance_A = \frac{P_A}{\ell} = \frac{N_A}{\Delta p_A} \tag{2.3}$$

The most common unit used for permeance is the gas permeation unit (GPU):

$$1\text{GPU} = 10^{-6} \frac{cm^3(STP)}{s \cdot cm^2 \cdot cmHg}. \tag{2.4}$$

For a multicomponent gas mixture permeating through a membrane, the separation factor for component A relative to component B, α_{AB}, is defined by Equation 2.5:

$$\alpha_{AB} = \frac{(Y_A / Y_B)}{(X_A / X_B)} = \frac{Y_A X_B}{X_A Y_B} \tag{2.5}$$

where Y_i and X_i are the gas-phase concentrations of component *i* at the downstream and upstream faces of the membrane, respectively. When the downstream pressure is negligible relative to the upstream pressure, the separation factor can be written as the ratio of permeabilities, and is called the ideal selectivity, α^*_{AB}, or the permselectivity.

$$\alpha^*_{AB} = \frac{P_A}{P_B} \tag{2.6}$$

The slower of the two permeabilities is most commonly placed in the denominator leading to selectivity values greater than or equal to one. The permselectivity provides a great tool for comparing membrane materials since, like the permeability, the permselectivity is a material property independent of membrane geometry. An added advantage of the use of these properties is that most new materials are initially tested in systems with negligible downstream pressure.

Because the motion of gas molecules can be characterized as a "random walk" influenced by chemical potential gradients, Fick's Law governs the permeation of gas in a membrane [1]. This relationship allows Equation 2.1 to be rewritten as shown in Equation 2.7:

$$P_A = -D_A(C)\left[\frac{\partial C_A}{\partial x}\right]\frac{\ell}{p_{A2} - p_{A1}} \tag{2.7}$$

where $D_A(C)$ is the concentration dependent diffusion coefficient, C_A is the concentration of component A, and p_{A2} and p_{A1} are the upstream and downstream partial pressures of component A, respectively. When the permeability is measured with a negligible downstream pressure, the expression for permeability can be simplified to the form shown in Equation 2.8.

$$P_A = \overline{D}_A \cdot \overline{S}_A \tag{2.8}$$

$\overline{D}_A$ is the average diffusion coefficient and $\overline{S}_A$ is the sorption coefficient, and these values are described mathematically by Equations 2.9 and 2.10.

$$\overline{D}_A = \frac{\int_0^{C_{A2}} D_A dC_A}{C_{A2}} \tag{2.9}$$

$$\overline{S}_A = \frac{C_A}{p_A} \tag{2.10}$$

The average diffusion coefficient relates to the diffusivity, or kinetic mobility, of a molecule in the membrane. Diffusivity tells how quickly the molecule can move in the direction of decreasing concentration within the membrane. The sorption coefficient relates to the sorption capacity, or thermodynamic partitioning, of the gas into the membrane. The sorption coefficient tells how much of the gas can dissolve into the membrane material at a given pressure. These two components combine to become the solution-diffusion transport mechanism that dominates the permeation of gases through a membrane [2-5]. In this process, the gas molecule sorbs into the membrane on the

upstream side, diffuses through, and then desorbs out of the membrane on the downstream side, see Figure 2.1. In this system, the driving force for gas transport is a chemical potential gradient that is controlled by the difference in partial pressure of a gas on the upstream and downstream sides of the membrane [1, 6].

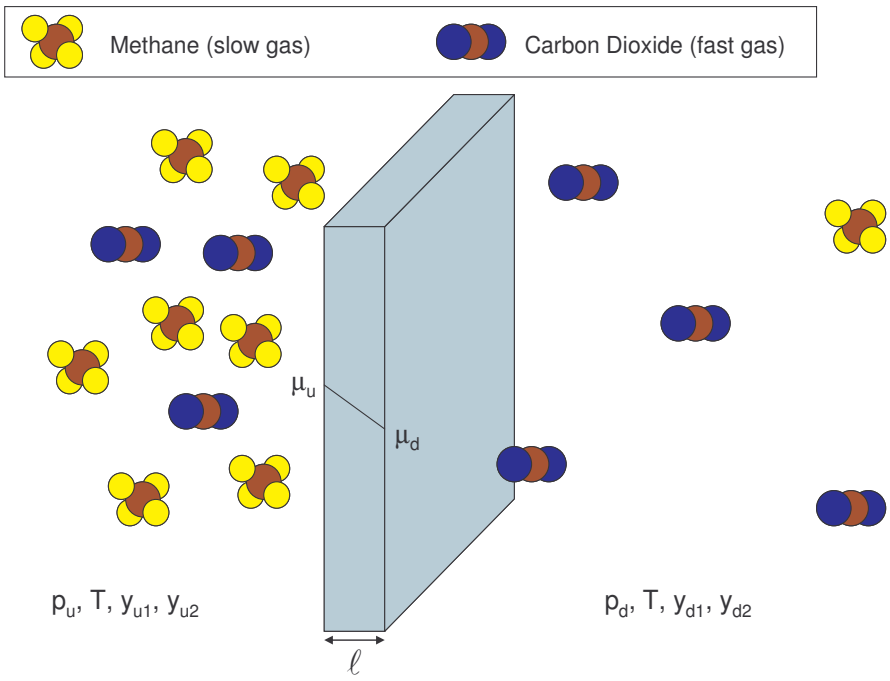

Figure 2.1 Carbon dioxide and methane are separated by a polymeric membrane operating by the solution-diffusion transport mechanism.

By combining Equations 2.6 and 2.8, the permselectivity can be factored into diffusion and sorption components as shown in Equation 2.11.

$$\frac{P_A}{P_B} = \left(\frac{D_A}{D_B}\right)\left(\frac{S_A}{S_B}\right) \tag{2.11}$$

This relationship introduces two new terms. The ratio of the effective diffusion coefficients, D_A/D_B, is referred to as the diffusivity selectivity, and the ratio of the sorption

coefficients, S_A/S_B, is referred to as the sorption selectivity. Improving the selectivity of a membrane requires an increase in at least one of these two components [7].

2.1.2. *Sorption*

As previously described, the first step in gas permeation that follows the solution-diffusion mechanism is that a gas molecule must be sorbed into the membrane. Although sorption follows considerably different mechanisms in different materials, the sorption coefficient has the same meaning for any given material. In particular, the sorption coefficient is defined as the amount of gas sorbed at a given external partial pressure as shown previously in Equation 2.10.

2.1.2.1. *Sorption in Glassy Polymers*

The most common model used to describe sorption in polymeric systems is the dual-mode model. In this model, sorption of penetrants is represented by two modes: "dissolved" and "holes" [8]. In the dissolved regions, sorption follows Henry's Law as molecules displace polymer chains to occupy space that would otherwise be filled by polymer. Sorption that follows Henry's Law is characterized by Equation 2.12,

$$C_A = k_{D,A} p_A \tag{2.12}$$

where $k_{D,A}$ is the Henry's Law coefficient. This equation characterizes sorption in rubbery polymers where the chain mobility allows the system to maintain equilibrium specific volume. When a polymer is taken below its glass transition temperature, the chain mobility becomes hindered [9], and the polymer can no longer reconfigure its chain orientation to reach an equilibrium volume. This phenomenon is illustrated in Figure 2.2.

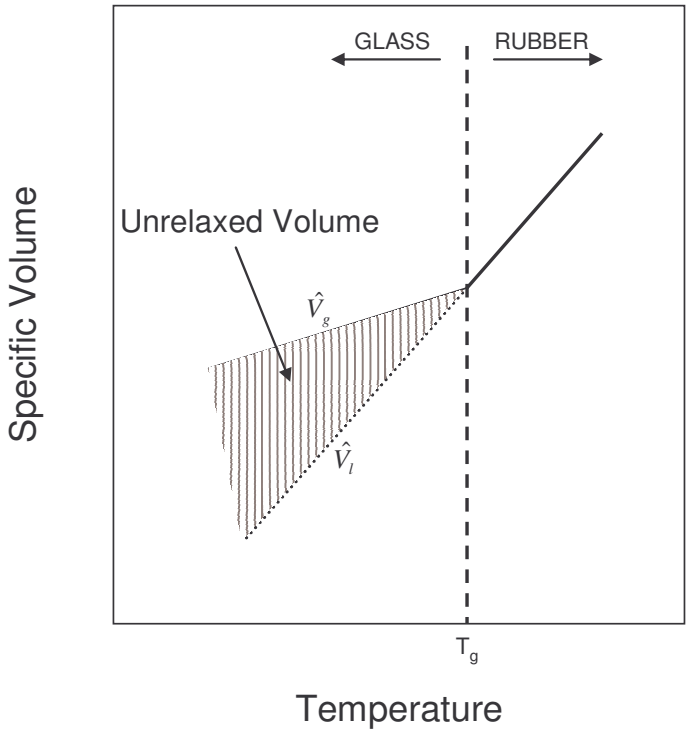

Figure 2.2 Restricted chain mobility in glassy polymers leads to unrelaxed volume [10].

As this figure shows, the specific volume of a polymer below its glass transition temperature, $\hat{V}_g$, is higher than the equilibrium volume predicted by the extrapolation of the volume in the rubbery region, $\hat{V}_l$. This difference in volume is caused by void space known as unrelaxed volume, and it provides increased sorption capacity for gas molecules [11, 12]. The sorption of gas into these regions follows the Langmuir model shown in Equation 2.13,

$$C_A = \frac{C'_{H,A} b_A p_A}{1 + b_A p_A}, \tag{2.13}$$

where $C'_{H,A}$ is the Langmuir hole filling capacity, and b_A is the Langmuir affinity constant. The summation of these two sorption modes for glassy polymers leads to the dual-mode model [13-16] shown in Equation 2.14.

$$C_A = k_{D,A} p_A + \frac{C'_{H,A} b_A p_A}{1 + b_A p_A} \tag{2.14}$$

Sorption in polymeric materials can also be the source of changes in material properties. Of particular interest to membrane systems are the phenomena of plasticization and antiplasticization. Plasticization occurs when the amount of sorption for exceeds a critical level in the membrane. When the sorption reaches this point, swelling of the polymer leads to increased sorption capacity and higher chain mobility [17]. As a result, the membrane permeability may be significantly increased. Plasticization, while inflating permeability, is almost always accompanied by a decrease in selectivity. The polymer used in this project is susceptible to plasticization by carbon dioxide at high pressures (see Chapter 5), but it may also occur in the presence of condensable impurities at lower concentrations. In contrast to plasticization, antiplasticization is marked by a decrease in permeability, and often an increase in selectivity [18]. The accepted cause of antiplasticization is the increased rigidity of the polymer matrix caused by a high affinity penetrant that acts to limit the mobility of the polymer segments [19-21]. Potential sources of antiplastication are traces of residual solvent in a membrane or highly condensable contaminants in the feed stream.

2.1.2.2. *Sorption in Molecular Sieves*

Unlike sorption in polymeric systems, the sorption in molecular sieves can only occur in specific locations. Molecular sieves lack the mobility needed to allow gas molecules to

occupy space that is not predefined by the structure of the material. As a result, the sorption in molecular sieves can be modeled by the dual mode sorption description with only a Langmuir term, and with the Henry's Law coefficient equal to zero for these systems since they do not possess a "dissolved" mode [22]. However, it is often necessary to account for heterogeneity among the sorption sites within a molecular sieving material by applying multiple modes of the Langmuir model with different hole filling capacities and affinity constants for the various Langmuir modes within the material. This is the case with carbon molecular sieves since the amorphous nature of the material and the relatively broad pore size distribution leads to significantly different adsorption energies for the pores [23, 24].

Molecular sieves do not show the same sensitivity to plasticization and antiplasticization that is seen in polymers because even high sorbent concentrations are generally not able to alter their rigid structures. Still, the pores of molecular sieves are subject to fouling and plugging that is not a major concern in polymers. Of particular interest is the ability of hydrophilic sieves to become plugged in the presence of even low concentrations of water. There are also issues dealing with chemisorption, such as surface oxidation, that are not faced by polymeric materials.

2.1.3. *Diffusion*

For permeation to continue after the gas molecule has sorbed into the membrane, the molecules must then move through the material to desorb from the downstream side. The movement of the molecule through the material is called diffusion. Diffusion can occur via several mechanisms depending upon the penetrant, the material, and the operating conditions. Two major classes of membranes are porous and nonporous [7]. The diffusion mechanisms for these materials are discussed in the following sections.

2.1.3.1. *Diffusion in Porous Membranes*

The mechanism of diffusion in porous membranes varies based on several factors including pressure, pore size, and the condensability of the penetrant. There are four primary mechanisms that occur in these porous materials: Knudsen diffusion, surface diffusion, capillary condensation, and molecular sieving.

Knudsen diffusion occurs when the conditions and pore size are such that the pore size is smaller than the mean free path of the molecule [25]; that is to say the diffusing species collides more frequently with the pore wall than with other diffusing molecules. The Knudsen diffusion coefficient can be calculated from kinetic theory for a cylindrical pore, of radius r, as shown in Equation 2.15,

$$D_A = 97.0r\left(\frac{T}{M_A}\right)^{1/2} \tag{2.15}$$

where D_A is the diffusion coefficient (m^2/s), T is the temperature (K), r is the pore radius (m), and M_A is the molecular weight of component A (g/mol). This equation allows the selectivity to be estimated for systems operating in the Knudsen diffusion region as shown in Equation 2.16.

$$\alpha_{A/B} = \sqrt{\frac{M_B}{M_A}} \tag{2.16}$$

Because the selectivity relies only on the molecular weight of the penetrants, Knudsen selectivities tend to be fairly low.

Surface diffusion takes place in systems when the molecules adsorb on the surface of the pores and subsequently move from one site to another of lower concentration. Surface diffusion is most common in systems with relatively large pore sizes and high condensabilities of the penetrants [1, 26].

Capillary condensation occurs when the pore size and the interactions of the penetrant with the pore walls cause condensation in the pore that influences the rate of diffusion across the membrane [27].

With molecular sieveing, the pore size approaches the size of the diffusing molecules leading to activated diffusion through the material [28]. Table 2.1 shows the kinetic and Lennard-Jones diameters for several gas molecules. The dimension of the "ultramicropore" approaches that of the diffusing molecules, and the larger micropore represents the sorption sites in the material. For a molecule to diffuse from one sorption site to another, it must overcome the repulsive interaction energy associated with the walls of the ultramicropores.

Table 2.1. Properties of several common gas molecules.

Compound	*Molecule*	*k X 10^{10} (m)* [a]	*σ X 10^{10} (m)* [b]
Helium	He	2.6	2.551
Ammonia	NH_3	2.6	2.900
Water	H_2O	2.65	2.641
Hydrogen	H_2	2.89	2.827
Carbon Dioxide	CO_2	3.3	3.941
Carbon Monoxide	CO	3.73	3.690
Oxygen	O_2	3.46	3.467
Nitrogen	N_2	3.64	3.798
Methane	CH_4	3.8	3.758
Propane	C_3H_8	4.3	5.118
BTX[c]	see note[c]	≥5.85	≥5.349

[a] kinetic diameter calculated from the minimum equilibrium cross-sectional diameter [29]
[b] Lennard-Jones collision diameter [1]
[c] BTX: Benzene (C_6H_6), Toluene (C_7H_8), and Xylene (C_8H_{10})

As the dimension of the ultramicropores approaches that of the diffusing molecule, very small changes in pore size can have a large impact on this activation energy of diffusion. This activated diffusion is often represented by an Arrhenius relationship:

$$D_A = D_{AO} \exp\left(\frac{-E_D}{RT}\right), \tag{2.17}$$

where D_{AO} is the pre-exponential term, E_D is the activation energy of diffusion, R is the ideal gas constant, and T is the absolute temperature. As the temperature increases, the diffusion rate increases; however, this increase most often favors the larger molecules leading to a decrease in observed selectivity. Diffusion through a molecular sieving pore is depicted in Figure 2.3.

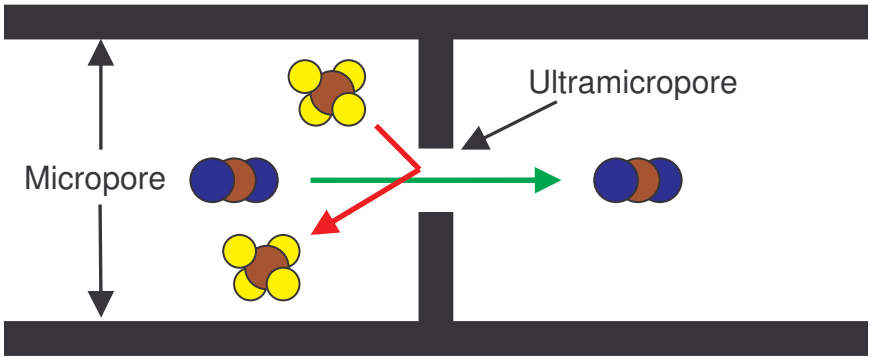

Figure 2.3 Transport through a molecular sieving pore is accomplished by activated jumps with associated energies strongly dependent on the size of the diffusing molecule. The atomic scale dimensions of the ultramicropore allow it to prohibit certain gas molecules based on size.

Another characteristic of molecular sieving materials is the significance of entropic selectivity [2, 3]. Because of the rigid structure of the pores, certain molecules may be required to orient in a particular direction before they can pass through the pore while other, smaller molecules may pass through regardless of orientation. As a result,

entropic selectivity is introduced because a greater number of configurations are allowed for the smaller molecule [3].

2.1.3.2. *Diffusion in Nonporous Membranes*

Gas separation membranes formed from polymeric materials are almost exclusively nonporous. The diffusion of gas molecules through a polymer membrane is facilitated by transient gaps created by the localized thermal fluctuations of chain segments [9, 30]. The small scale openings generated by these motions allow gas molecules to progress through the polymer in small jumps. The frequency and length of these jumps are dependent on several factors including the size of the penetrant, the flexibility and packing density of the polymer chains, and the cohesive energy of the polymer [31]. Contrary to molecular sieving, one of the results of this diffusion mechanism is limited selectivity. While larger molecules still tend to have lower diffusivities, polymers are not capable of the near-absolute size exclusion capable with molecular sieves. Temperature increases cause an increase in the fluctuations in the polymer chains leading to an increased diffusion coefficient that follows an Arrhenius expression [9]. In a manner similar to molecular sieves, the larger molecule typically benefits more from these increases leading to a decrease in selectivity with the increased permeability.

2.2. Materials for Gas Separation Membranes

Using the tools and fundamentals established in the previous section, it is now possible to effectively compare the various materials that are commonly used to produce gas separation membranes. Most industrial gas separation membranes are formed from glassy polymers, but membranes have also been produced using rubbery polymers and inorganic molecular sieves such as zeolites and carbon molecular sieves. This section

will look at the advantages and disadvantages of these different materials for gas separation membranes.

2.2.1. *Polymers*

Polymers were the first materials developed into large scale gas separation membranes [32, 33]. Most of the gas separation membranes currently in use are produced from amorphous, glassy polymers. Glassy polymers are generally preferred because the ability of a polymer to control the transport of gases is strongly related to the mobility of the polymer chains. As a result, glassy polymers, with limited chain segment mobility, tend to have much greater control over the permeating molecules than rubbery polymers. The selectivities obtained through glassy polymers tend to be greater; however, rubbery polymers tend to have higher permeabilities as shown in Figure 2.4.

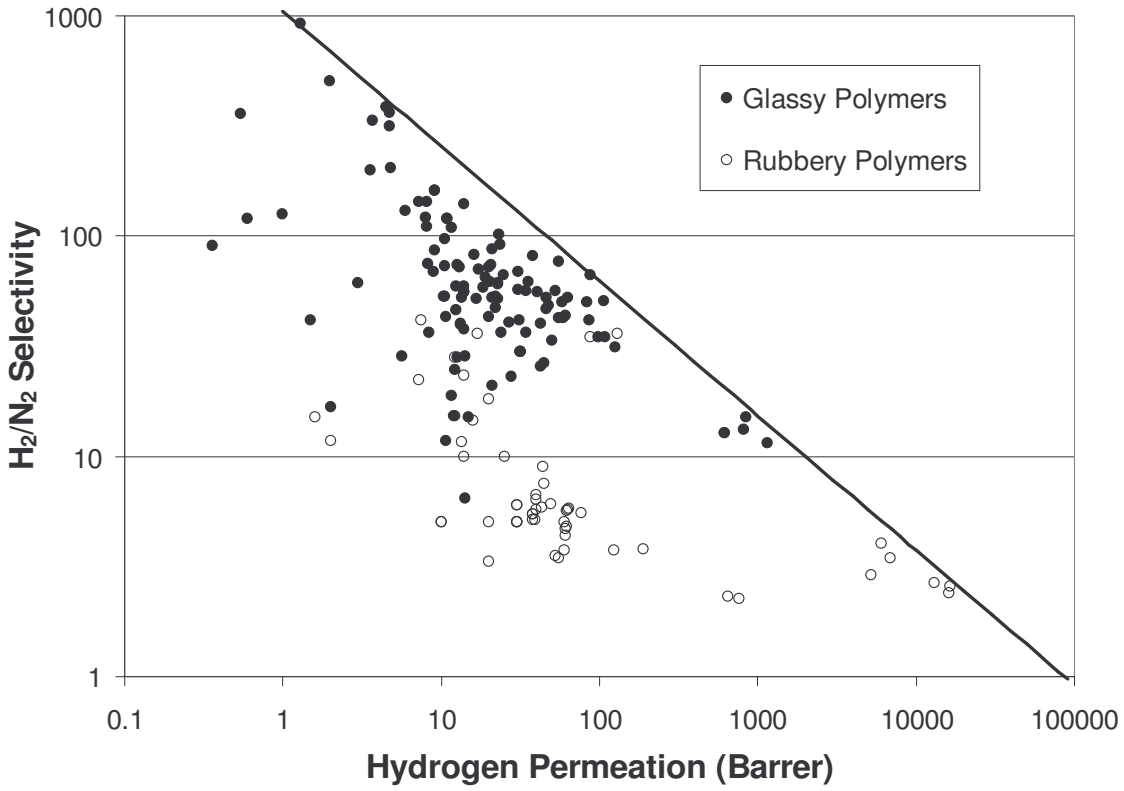

Figure 2.4 Glassy polymers tend to have higher selectivities and lower permeabilities than rubbery polymers.

Figure 2.4 is similar to Figure 1.2, but it shows the relationship between glassy and rubbery polymers that have been tested for the separation of hydrogen and nitrogen. While it is important to base selection criteria on a specific gas pair, the overall trends illustrated by Figure 2.4 would hold for most gas separations. One major exception to this rule is in the separation of a highly condensable species from a permanent gas, such as the removal of propane from hydrogen [7]. In cases such as this, rubbery polymers can sometimes be used, because of their lower diffusivity selectivities, to provide preferential selection of the more condensable component over the much less condensable hydrogen [34-40].

The use of semi-crystalline polymers for gas separation membranes is usually avoided for multiple reasons. Crystalline regions in the polymer tend to have little or no permeability to gas molecules inhibiting the transport through the polymer leading to lower permeability [41, 42]. Controlling the size, distribution, and orientation of crystalline regions in a membrane can also be difficult and have a considerable impact on the performance of the membrane. An additional factor that must be considered in dealing with semi-crystalline polymers is the impact of the permeating species on the crystallinity. If the interactions between the penetrant and the polymer are strong enough, the actual separation may have an unpredictable impact on the material performance leading to unreliable membranes.

One of the important reasons for the development of polymeric gas separation membranes is the processability of the polymeric materials. Because polymers can be processed in solution phase, the final membrane structure can be controlled to a great degree by careful design of the processing parameters without the need for exotic processing, excessively costly materials, or high amounts of energy [24, 43]. An

additional advantage of the solution processing process is the ability to spin asymmetric hollow fibers. This particular membrane conformation is especially effective because of its extremely high surface area to volume ratio as well as the very thin selective layer of the fibers that greatly reduces the resistance to gas transport while maintaining the selective properties of the material. The production of asymmetric hollow fibers is a process that continues to see significant development as it is improved and adapted to more specialized systems, and much more detailed information can be found elsewhere [44, 45].

In addition to processability, polymers are very attractive membrane materials because of their robust physical properties. The flexibility and increased strain to failure properties of polymers make them very capable of withstanding the mechanical forces that may be encountered in an industrial separation application. For instance, anomalies in the pressurized feed to the membrane system can sometimes result in a pressure wave that provides substantial mechanical shock to the membrane systems. The flexibility of polymer membranes also allows the formation of densely packed membrane modules where the fibers are tightly packed to increase surface area per unit volume [24]. The mechanical stability of the polymeric materials makes the production and application of membrane systems with these materials relatively straightforward from a mechanical engineering standpoint.

2.2.2. *Molecular Sieves*

Molecular sieves are another attractive set of materials for gas separation applications. They consist of a wide range of materials that posses rigid pore structures with angstrom-level dimensions that allow the discrimination of gas molecules based on their molecular dimensions. Two major categories of these materials are zeolites and carbon

molecular sieves. Zeolites are synthesized aluminosilicate materials, and carbon molecular sieves are generally produced from the high temperature pyrolysis of polymers or other precursor materials.

2.2.2.1. *Zeolites*

Zeolites have found significant area for application in the fields of high surface area supported catalysis and ion exchange [29]. Further, the ability of these materials to be synthesized in large quantities with regular, controlled pore sizes capable of controlling gas transport has made them the object of substantial research in the field of membrane separations. Figure 2.5 shows the unit cell structure of zeolite 4A, a common synthetic zeolite [23, 24]. The cell structure consists of a larger cavity inside the cell that provides most of the adsorptive capacity of the zeolite, while the smaller pore opening acts as a molecular sieve. These structural characteristics are further illustrated by the pore size distribution shown in Figure 2.6, where the sharp peaks at 3.8 Å and 11 Å represent the pore opening and cavity, respectively [24]. The highly crystalline and very controlled nature of the zeolite structure further enhances their attraction in gas separations. With a pore diameter of 3.8 Å, zeolite 4A is capable of providing selectivity approaching 40 even for the separation of similarly sized oxygen (3.46 Å) and nitrogen (3.64 Å). Other separations such as the removal of carbon dioxide from natural gas reserves may require the further development of new, more efficient zeolites before their application becomes economical.

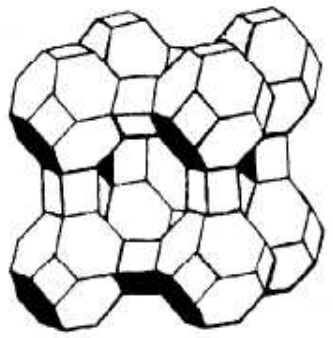

Figure 2.5 The regular crystal structure of zeolite 4A produces well structured pores capable of discriminating gas molecules based on size [23, 24].

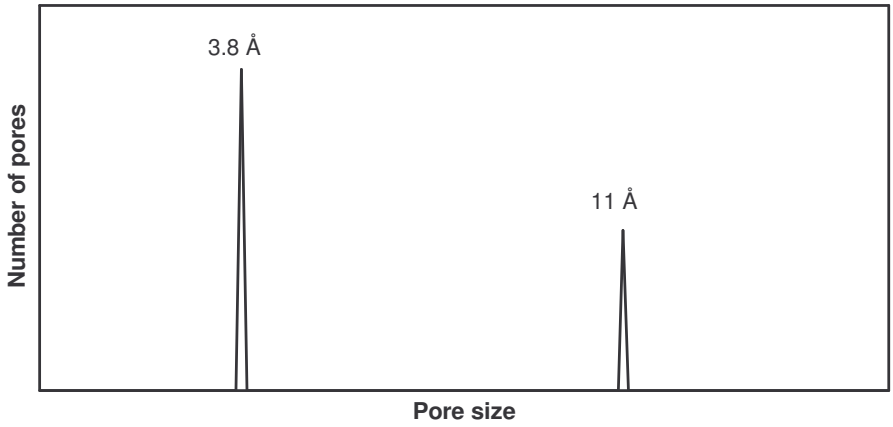

Figure 2.6 The pore size distribution of zeolite 4A is dominated by two sharp peaks representing the 3.8 Å pore openings and 11 Å cavities repeated in the unit cell of the crystal structure [24].

While there is still significant development being carried out with the production of new zeolite architectures, which could continue to enlarge the area of application for these materials, some limitations exist. The formation of homogeneous, defect-free zeolite membranes, even at the laboratory scale, has proven very challenging, and this is a necessary step before the full potential of these materials in gas separation membrane applications can be realized [24]. Another major obstacle to the large scale implementation of zeolite gas separation membranes is the brittle nature of the material. The successful use of these materials as gas separation membranes in an industrial

setting would require extreme measures to protect the mechanical integrity of the membranes because of the lack of resilience provided by the inherent properties of the zeolites.

2.2.2.2. *Carbon Molecular Sieves*

Unlike the crystalline nature of the zeolite structure, carbon molecular sieves are amorphous with no long range ordering of the pore structure [46]. The turbostratic carbon structure is formed from the irregular packing of sp^2 hybridized carbon "sheets" [46, 47], as shown in Figure 2.7. The high porosity of these materials provides relatively high permeabilities while the presence of the molecular sieving regions maintains the high selectivity. Unlike zeolites, the pore size of a carbon molecular sieve is described by a distribution rather than a characteristic length [47, 48] as shown in Figure 2.8.

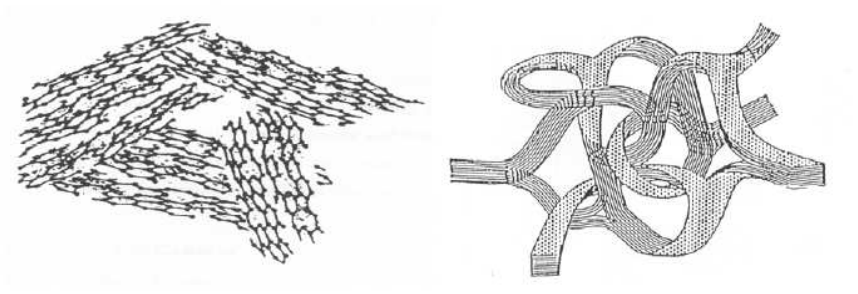

Figure 2.7 The amorphous, turbostratic structure of carbon molecular sieves is formed by the irregular packing of sp^2 hybridized carbon. Pictures taken from [46, 47].

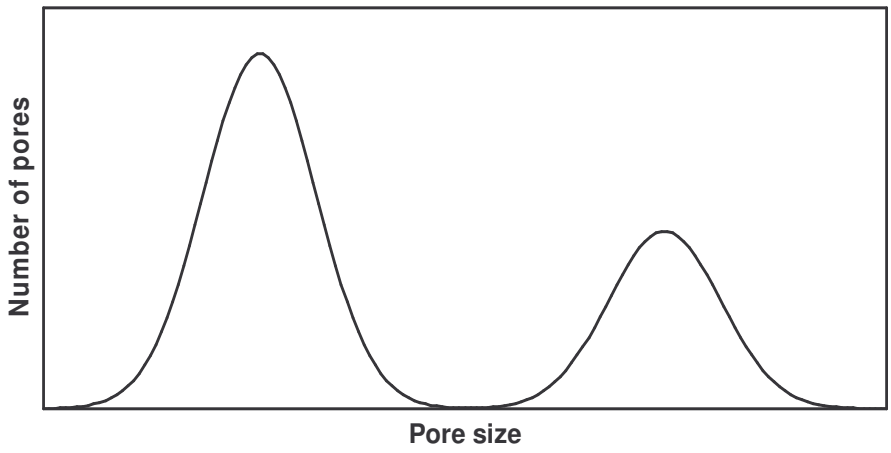

Figure 2.8 The amorphous nature of carbon molecular sieves causes a much broader pore size distribution than that seen in zeolites [47, 48].

The structure consists of microporous channels connected by ultramicroporous openings that have dimensions of the same order of magnitude as gas molecules [48, 49]. Figure 2.9 provides a schematic representation of this pore structure. The microporous channels provide the sorption capacity and means for rapid gas transport in the materials while the transport through ultramicroporous openings follows the expected activated transport mechanism of a molecular sieve.

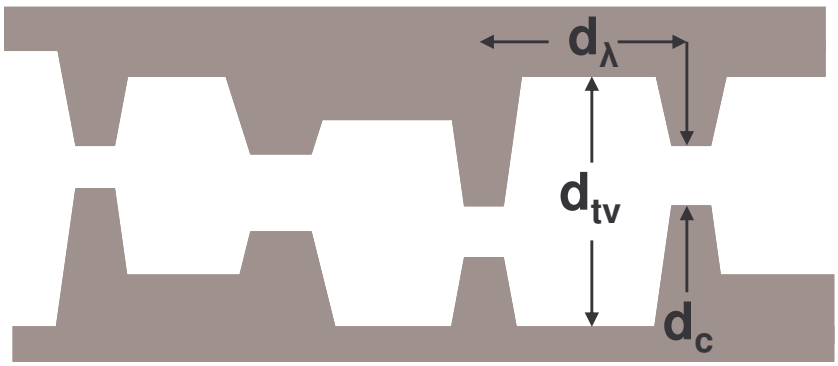

Figure 2.9 The pore structure of a carbon molecular sieve consists of microporous channels with ultramicroporous openings, adapted from Steel and Koros [48, 49]. Here $\mathbf{d_c}$ is the ultramicropore dimension, $\mathbf{d_{tv}}$ is the tranverse dimension (or the size of the adsorptive micropore), and $\mathbf{d_\lambda}$ is the jump length.

Despite the less regular structure of CMSs with respect to zeolites, there are some important advantages to their use. One of the most important advantages is the ability to regularly produce homogeneous, defect free CMS films that allow the material properties to be tested and used for gas separation applications. Another major advantage of the CMS materials is the ability to "tune" their properties by the careful control of pyrolysis conditions. This ability provides much more flexibility in the application of CMSs than with zeolites. Alteration of the structure of a zeolite is limited by the templates that can be reliably produced as well as the physical characteristics of the zeolite components. Research into the control of the pyrolysis process in the formation of CMSs suggests that these materials can be engineered to possess a wide range of properties that are not restricted by obtainable crystalline conformations [2, 24, 48, 50, 51].

Carbon molecular sieves are generally produced from the high temperature pyrolysis (thermal decomposition) of polymers or other precursor materials. This process can be further activated by chemical means, but the production of carbon materials for gas separation membranes is typically performed using a thermal process in an inert atmosphere. The hybrid materials studied in this work were formed using CMSs as the dispersed phase. Because of the importance of these materials to this work, their development will be discussed in further detail.

2.2.2.3. *Formation of Carbon Membranes*

Because carbon membranes may be formed by the controlled heating of a polymeric membrane, the available forms of carbon membranes are quite numerous [51]. Two broad categories that encompass most of these membranes are supported and unsupported. Supported membranes are formed by casting a thin layer of precursor

material on a surface and then pyrolyzing. The support surface is typically a porous inorganic flat sheet or tubular structure. Unsupported membranes are formed in similar fashion to polymer membranes with the additional step of pyrolysis after the membrane has been formed. These membranes are most commonly found in one of three primary configurations: dense flat films, asymmetric hollow fibers, and asymmetric flat films.

As previously discussed, the pore structure of a carbon molecular sieve is the determining factor in the separation performance achieved. Several factors have been determined to have a significant impact on the pore size distribution of the CMS produced during pyrolysis [51].

- Precursor composition
- Maximum pyrolysis temperature and ramp rate
- Thermal soak time at maximum pyrolysis temperature
- Pyrolysis atmosphere
- Post treatment conditions

While other factors have shown some influence, these variables have been established as the most important engineering parameters for the formation of carbon membranes. These factors are discussed in some detail in the following sections, but a more thorough treatment of the effects and possible underlying causes can be found in the work recently presented by Williams.

2.2.2.3.1. Precursor Composition

Carbon membranes have been produced from a number of different precursors including several different classes of polymers. The first hollow fiber carbon membrane was produced by Koresh and Soffer through the pyrolysis of cellulose hollow fibers [52]. Many other classes of materials have been tested as precursors for carbon membranes

including polyacrylonitrile, phenolic resin, polyfurfuryl alcohol, poly(vinylidene) based polymers, cellulose derivatives, and polyimides [48, 49, 52-61]. Of these materials, polyimides are often preferred because of their excellent physical properties and separation performance as a class of polymers. Another important characteristic for the precursor recommended by Koresh and Soffer is that the material used will not flow during pyrolysis [52]. More detailed reviews of results obtained from different precursors pyrolyzed under similar conditions can be found elsewhere, the important point is that the precursor plays a major role in the transport properties of the resulting polymer. Recent work by Williams has further shown some of the more specific relationships present between the precursor and the carbon membrane produced [51]. One important factor is the amount and type of byproducts evolved during the decomposition process. Larger molecules and larger amounts of byproducts both increase the permeability of the resulting CMS material. Another strong correlation was seen between the free volume of the precursor and the permeability of the CMS. Higher free volume in the precursor material generated higher permeabilities in the carbon membranes, even when amounts and types of byproducts were the same. This work is the first known study to deconvolute the source of dependence between the properties of the carbon and the precursors.

2.2.2.3.2. Maximum Pyrolysis Temperature

The highest temperature used in the pyrolysis process is commonly referred to as the pyrolysis temperature. This temperature should not be confused with the decomposition temperature where the precursor begins to break down and evolve byproducts. Several studies have been conducted to show the relationship between pyrolysis temperature and carbon properties [2, 48, 62, 63]. Generally, increasing the pyrolysis temperature causes the selectivity to increase and the permeability to decrease. There are some

cases where specific characteristics of the precursor and the pyrolysis protocol cause local changes contrary to these trends, but overall these trends apply. One good example was presented in the work reported by Shoa et al. dealing with the pyrolysis of the polyimide 6FDA-durene [62, 63]. They used pyrolysis temperatures ranging from 250 ^{o}C (near the glass transition temperature) to 800 ^{o}C (well above the decomposition temperature).

2.2.2.3.3. Ramp Rate and Thermal Soak Time

Carbon membranes formed from thermal decomposition are seldom if ever produced in actual equilibrium processes due to the kinetics associated with their formation. The rates associated with decomposition and evolution of byproducts as well as pore sintering, realignment of the carbon structure, that occurs after decomposition cause time dependent changes [48]. As a result of the kinetics of the process, both the ramp rate used during pyrolysis and the thermal soak time can impact the resulting properties of the carbon [4]. The ramp rate is the speed at which the temperature is increased during the pyrolysis, and the thermal soak time is the amount of time that the carbon is held at the pyrolysis temperature.

Higher ramp rates tend to cause lower selectivities and higher permeabilities. There are two primary reasons proposed for the relationship between ramp rate and carbon properties. First, the increasing the ramp rate is believed to increase the rate at which byproducts are evolved during decomposition. When the residence time of the byproducts in the pyrolyzing material is higher, they have potential to react further before being fully removed from the precursor [64]. Second, reducing the ramp rate increases the amount of “pyrolysis time” that the material is exposed to by increasing the time

between the decomposition temperature and the pyrolysis temperature. Most recent studies employ lower ramp rates (<5 ^{o}C) in order to obtain increased selectivities.

In a manner similar to the ramp rate, the thermal soak time is important to the final structure of the carbon membrane. Increasing the thermal soak time can have two major impacts on the carbon produced: further decomposition and pore sintering [48]. In most cases, increasing this time leads to increased selectivity with a reduction in permeability. The extent of these changes and their relationship to the thermal soak time has a strong relationship to the pyrolysis temperature. Increasing thermal soak in pyrolysis at higher temperatures tends to see only small changes in selectivity with greater changes in permeability while pyrolysis at lower temperatures can see significant changes in both selectivity and permeability [48].

2.2.2.3.4. Pyrolysis Atmosphere

The atmosphere in which pyrolysis is performed is a controlled inert environment to prevent the complete decomposition of the precursor. This atmosphere most commonly takes the form of either vacuum or an inert purge gas such as helium or argon. Studies have shown that the use of a purge gas can result in properties that differ substantially from those obtained in vacuum [24, 50, 65]. Geiszler and Koros proposed that these differences are likely the result of enhanced heat and mass transfer facilitated by the purge gas [50]. These conclusions were further supported by the changes seen in carbons produced under different purge gas flow rates. Additional work by Williams has shown the importance of trace amounts of oxygen in the system during pyrolysis [51]. Comparison of the results based upon a calculated oxygen exposure coefficient proved capable of explaining much of the variability seen in pyrolysis performed in different atmospheres. Williams proposes that the defect sites that form the ultramicropores in

the carbon membrane are also the most reactive towards oxidation. As a result, increasing the amount of oxygen present during pyrolysis increases the amount of oxidation that occurs in the ultramicropores near the surface of the carbon. Up to a point, the result of this oxidation is a reduction in permeability with an associated increase in selectivity; however, continued oxidation beyond this point leads to higher permeability and reduced permselectivity. Clearly, the atmosphere present during pyrolysis plays a major role in the microstructure of the CMS material formed during pyrolysis; therefore, it must be carefully controlled to provide reproducible and desirable results.

2.2.2.3.5. Post Treatment Conditions

After the thermal pyrolysis is completed, there is still significant potential to influence the pore structure of the carbon membrane through the use of post treatment processes. The most common post treatment used to alter the pore structure of the CMS material is "low" temperature oxidation [51]. Temperatures ranging from 100-400 ^{o}C have been used with carbon membranes in an oxidative atmosphere such as pure oxygen, carbon monoxide, or a mixture of oxygen and nitrogen. Adjusting the post treatment temperature and the time allowed for oxidation can be used to control the impact of post treatment on the pore size distribution. Extensive oxidation from long post treatment has even shown the ability to enlarge pores enough to change the transport mechanism [66]. This is one of the pathways used in the development of selective surface flow membranes that have potential to show selectivities for highly condensable penetrants over smaller permanent gas molecules [66, 67].

2.2.2.3.6. Conclusions

The previous sections demonstrate the large number of engineering parameters that provide the means for adjusting the pore structure of the CMS produced from thermal pyrolysis. These tools can be used to provide a well tuned CMS designed to provide the ideal separation performance based on the target system. While these parameters allow the carbon to be engineered to possess the desired properties, it is also important that all of these factors be carefully controlled to provide consistency.

2.3. Modeling Transport in Hybrid Systems

Rational design of hybrid membrane systems requires some method for prediction of membrane properties from the intrinsic properties of the components included in the membrane [68]. The use of an appropriate model will provide a method to evaluate the effectiveness of a hybrid system in performing gas separations. In addition, model predictions can be used to direct the matching of the polymer and inserts needed to provide the best performance enhancements. Several reviews have been performed on the ability of different models to predict the transport properties of hybrid gas separation membranes [23, 24, 68, 69], and the model generally accepted as one of the best tools for these systems is an adaptation of the Maxwell equation developed in the late 1800s for the description of dielectric properties in composite materials [70]. The following sections discuss the adaptation of this model to hybrid gas separation membranes and its use in material selection.

2.3.1. *Hybrid Membrane Modeling with Maxwell's Equation*

Several approaches have been considered for analysis of hybrid gas transport membranes [71], and one of the most useful models was adapted from work developed by Maxwell in 1873 to predict permittivity in composite dielectrics [70]. The governing

equations for electrical permittivity and mass flux through a membrane are mathematic analogs allowing the Maxwell model to be adapted for membrane analysis [72]. The resulting equation is the solution for effective permeability of a hybrid membrane of dilute ellipsoids,

$$P_{eff} = P_c\left[\frac{nP_d + (1-n)P_c - (1-n)\phi_d(P_c - P_d)}{nP_d + (1-n)P_c + n\phi_d(P_c - P_d)}\right] \tag{2.18}$$

where P_{eff} is the effective permeability, P_c is the permeability of the continuous phase, P_d is the permeability of the dispersed phase, ϕ_d is the volume fraction of the dispersed phase, and n is a shape factor of the inserts. When n = 0, the result is parallel transport through two different phases and permeability is given by the arithmetic average of the two phases:

$$P_{eff} = P_c(1-\phi_d) + P_d\phi_d \tag{2.19}$$

If n = 1, the model simplifies to represent transport in series through two phases:

$$P_{eff} = \frac{P_cP_d}{P_d(1-\phi_d) + \phi_dP_c} \tag{2.20}$$

However, for analysis in this project, a spherical particle is assumed which relates to a shape factor of n = 1/3, and the result is known as the Maxwell equation [73]:

$$P_{eff} = P_c\left[\frac{P_d + 2P_c - 2\phi_d\left(P_c - P_d\right)}{P_d + P_c + \phi_d\left(P_c - P_d\right)}\right] \tag{2.21}$$

One shortcoming of this model is that it does not account for interactions between the particles, and as a result, the model is not originally intended for use at higher concentrations, although there is some debate on this issue [71-73]. Petropoulos has even shown that if the system under analysis remains well dispersed, the Maxwell equation can be expected to perform adequately over the whole range of composition [71]. This analysis, combined with previous success using this model to analyze hybrid membrane performance, makes it an appropriate guide for use in this study.

2.3.2. *Material Selection with the Maxwell Equation*

Using the Maxwell equation to predict the hybrid membrane properties exposes a maximum improvement in the performance of the membrane when the polymer and the sieve are properly paired. Figure 2.10 shows the predicted results of forming hybrid films from polymers located on the upper bound curve with a selected sieve. As the sieve loading is increased, the presence of a “maximum” becomes more apparent. Using the location in the curve that provides the maximum displacement from the upper bound as the point of “maximum improvement” allows these curves to be compared to find the best match. This analysis has been performed for several sieves, and as a rule of thumb, the best match between polymer and sieve is obtained when the sieve permeability for the fast gas is equivalent to three times that of the polymer. The physical explanation for this maximum can be understood by briefly considering the limiting cases. In a situation where the polymer permeability is much higher than that of the sieve, both of the gases will simply bypass the sieve resulting in a decrease in the permeability of the system with little or no change in selectivity. In a system where the

polymer permeability is much lower than the sieve permeability, both gases may have enhanced permeability to the point that the system sees little selectivity enhancement from the sieve. As a result, the best match occurs somewhere in between these extremes, and due to the much better separation performance of the sieves, the best match occurs when the polymer permeability for the fast gas is slightly lower than that for the sieve.

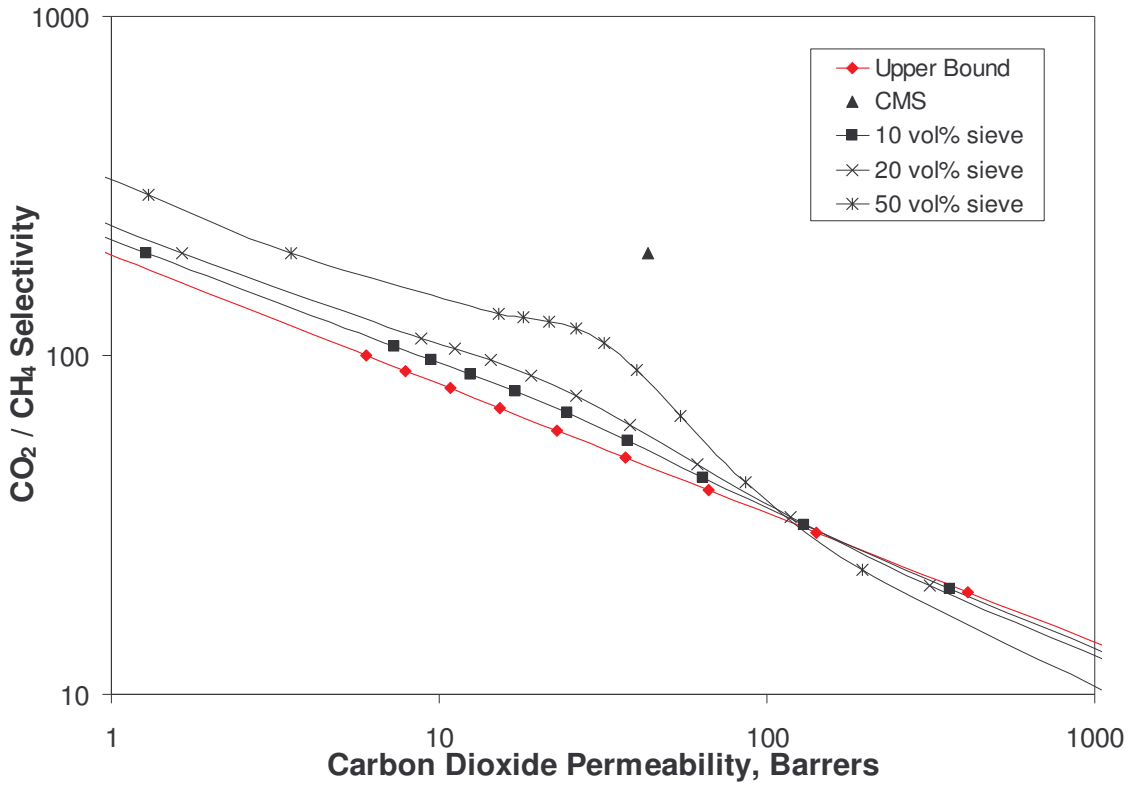

Figure 2.10 Maximum enhancement is obtained for a mixed matrix system when the permeability of the fast gas in the dispersed phase is nearly three times that of the continuous phase.

2.4. Previous Work with Hybrid Gas Separation Membranes

The combination of inorganic components in an organic matrix is not a new concept. Composite materials have been developed for some time in order to enhance the

mechanical properties of the polymer matrix [74-76]. However, the majority of work in the application of these materials to advanced gas separations has taken place in the past 10 to 15 years. Barrer and James were the first to report the use of inorganic fillers as a pathway to enhance transport properties in hybrid films [77, 78]. They used zeolite powder dispersed in a polymeric filler to provide ion exchange membranes with properties controlled by the zeolite. The work showed that the primary defect encountered in the hybrid membranes was the formation of a gap between the polymer matrix and the zeolite particles. In this application, the gap would fill with electrolyte solution causing reduced performance of the membrane. While filling the voids with an inert liquid or synthesizing the polymer in situ would enhance performance, the membranes still suffered over time, and this change in performance was attributed to degradation of the interface. Control of the interfacial region is still the limiting factor in hybrid membrane performance [23].

An important development in hybrid membrane research was achieved by Paul and Kemp when they observed an increase in the permeation time lag for silicone rubber (PDMS) with the incorporation of zeolite 5A [79]. They recognized an immobilizing sorption of CO_2 and CH_4 when the zeolite was incorporated in the membranes, but the steady state permeation properties showed little effect. This lack of significant change is most likely a result of the large pore size of zeolite 5A which has pores too large to discriminate between the gases used by Paul and Kemp to study the membrane properties. However, this study was instrumental in showing the important role that inorganic particles can play in the sorption properties of a hybrid system.

Much of the initial work in the area of hybrid gas separation membranes focused on the use of rubbery polymers for pervaporation applications. The higher chain flexibility of the

rubbery polymers reduces the presence of gaps between the polymer and inserts. As early as 1987, te Hennepe et al. were able to show enhanced performance of silicone rubber, poly(dimethyl siloxane) (PDMS), membranes through the incorporation of hydrophobic silica-based molecular sieves as an alcohol selective adsorbent [80]. Further work by this group was performed to analyze other alcohols, and they were able to describe much of the enhancement obtained using a resistance model [81, 82]. Other work focused on improving ethanol/water pervaporation has been done using zeolites Y and ZSM-5 in PDMS, zeolites 4A and 13X in cellulose acetate, and zeolite ZSM-5 in poly(vinyl alcohol) [83-86]. The silicalite-filled PDMS membranes have also been tested for other pervaporation appliications including the removal of halogenated hydrocarbons and aroma compounds from water [87-89]. Vankelecom et al. also tested carbon fillers for pervaporation applications [90]. Unlike the zeolite filled membranes, the carbon based membranes did not show enhanced properties, but rather they showed a decrease in permeability that was attributed to dead end pores in the carbon molecular sieves. Improvements in selectivity were observed only when the conditions were adjusted to greatly reduce membrane swelling. These results contrast those shown for zeolites where the zeolites are believed to provide a source of crosslinking (both physical and chemical) for the polymer chains [86].

There have been fewer reports of gas separation properties of hybrid films formed using rubbery polymers. One of the primary reasons for this shortage is likely the poor initial properties of rubbery polymers for forming gas separation membranes. Still, there have been some reports of this work, and the results provide useful analysis of the hybrid membrane systems. Silicalite filled PDMS membranes produced by Jin et al. for the pervaporation of ethanol and water have also shown enhancement of the O_2/N_2 separation performance compared to neat PDMS [91, 92]. At the high loading of 70 wt%

silicalite in PDMS, they report selectivity enhancements of O_2/N_2 from 2.14 to 2.92 and CO_2/CH_4 from 3.42 to 8.86. Other work in this area was reported by Duval et al. using both zeolites and carbon molecular sieves in various rubbery polymers [93]. Some of the best results were shown for the incorporation of zeolite KY at 46 vol% in nitrile butadiene rubber which had a CO_2/CH_4 selectivity improvement from 13.5 to 35. Hybrid membranes formed using the commercial CMSs, in contrast, showed no performance enhancement. Again, this failure was attributed to the presence of dead end pores in the carbon material [93].

While some of the hybrid membranes previously described showed significant enhancement over the neat rubbery polymer membranes, most of the results still fall below the upper bound for solution processable polymers. Only in a few of the cases with the highest loadings did the performance exceed what is attainable with neat glassy polymer membranes. Another advantage of glassy polymers is that they may be spun as asymmetric hollow fibers with a very thin selective layer that improves the economics of membrane application, but this process is very difficult with rubbery polymers [23]. With this motivation, continued work has been reported with the intention of using glassy polymers as the matrix for hybrid membrane systems.

While the nature of glassy polymers provides greatly enhanced transport properties, successful formation of hybrid membranes using a glassy matrix has proven to be more challenging than with rubbery polymers. The earliest known report of successful formation of a hybrid membrane using a glassy polymer is shown in the patent literature of Kulprathipanja et al. where silicalite was successfully used to enhance the performance of cellulose acetate membranes [94]. Unfortunately, Duval et al. were unsuccessful at producing similar performance when incorporating silicalite into cellulose

acetate membranes [95]. Voids between the polymer and sieve were blamed for the poor performance of the hybrid membranes. Several processing improvements were attempted to improve the interface including modification of the external zeolite surface, membrane formation above the polymer Tg, and heat treatment after membrane formation [95]. While the membrane structure showed improvements as observed by scanning electron microscopy, the gas permeation properties did not show concomitant improvement. Work by Gür showed good morphology in membranes prepared using polysulfone and zeolite 13X [96]; however, the large 10 Å pores of the zeolite were too large to provide any size discrimination for the gases tested. Other work using polyethersulfone and zeolites 4A and 13X was reported by Süer et al. [97]. These membranes showed some enhancement over the neat polymer properties, but the resulting performance was still well below the polymer upper bound. Vankelecom showed that polyimide-based hybrid films using various fillers (borosilicate, silicalite, or zeolite Y) resulted in interfacial voids [98, 99]. While no gas permeation results were reported, no selectivity enhancement would be expected for gas separations. Even so, the membranes did show some improvement in the xylene isomer selectivity, but xylene may condense in the void space limiting the effect of sieve bypassing.

A major step in improving the research of hybrid membranes was taken in 1997 when an effective model was introduced by Zimmerman et al. for the estimation of properties in these systems [68]. By applying the Maxwell equation to hybrid membrane systems, researchers now have a tool that allows results to be further analyzed to determine if non-ideal properties result from poor interfacial characteristics or poor pairing between the polymer and the sieve. Further work by Zimmerman et al. showed how the model could be used to better design the hybrid systems for a specific separation to obtain the maximum performance [100].

When Mahajan and Koros reported successful hybrid membrane performance in 2000 [69, 101], analysis of the results with the model led to the identification of a new phenomenon labeled “matrix rigidification” in which the polymer matrix mobility in the region surrounding the sieve is restricted sufficiently to cause a reduction in permeability with an associated increase in selectivity [102]. By adapting the Maxwell equation to account for this effect, they were able to show significant agreement between the model and the hybrid films produced. Further work by Mahajan and Koros highlighted important issues that should be controlled in the production of mixed matrix membranes using glassy polymers [42, 101, 102]. They emphasized the need for matching between the polymer and the sieve, selecting a sieve with molecular dimensions capable of enhancing the desired separation, and good interactions between the polymer and the sieve. Hybrid film formation using silane coupling agents was attempted to improve the interfacial interactions; however, gas permeation results were not ideal. Another technique used to improve the hybrid membrane properties increasing the polymer flexibility during film formation through the use of plasticizers or elevated temperatures. While some success was seen with these methods, they may not be ideal for industrial membrane development [24].

Vu et al. produced hybrid films using CMSs as the disperse phase [73, 103]. After increasing the viscosity of the casting dope to prevent agglomeration of the CMS particles, they were able to produce hybrid films with enhanced performance using both Ultem® and Matrimid® as the matrix polymers. By using material synthesized under conditions known to produce effective CMS membranes, Vu et al. were able to avoid the limiting “dead end” pores that other researchers have encountered. They also showed that under “mild” contaminant conditions, the membranes were able to maintain most of the enhanced performance seen in the pure gas tests [104].

While recent work has produced some of the best hybrid film performance to date, there are still very few examples of systems where the performance has exceeded the polymer upper bound. In order for this objective to be achieved, there is a desire to continue working with even higher performance matrix polymers. Some of the polymers with the best membrane performance are fluorinated polyimides and polypyrrolones [105]. It is desirable to use these materials as a matrix for hybrid film formation so that property enhancements will carry the films beyond the polymer upper bound. Attempts to use 6FDA-6FpDA (an upper bound polymer) as the continuous phase were reported by Vu [24], but the membranes only showed increased permeability with no selectivity enhancement, which is a characteristic response of voids at the interface. Other groups have attempted similar work using 6FDA-6FpDA and 6FDA-6FpDA:DABA with zeolite inserts [106-111]. Membranes formed using 6FDA-6FpDA failed to show any selectivity enhancements with the zeolite fillers used; however some slight enhancements have been seen with the 6FDA-6FpDA:DABA based membranes. The DABA group increases the flexibility of the polymer backbone as well as providing hydroxide groups that may hydrogen bond or react with the surface of the zeolite particles. Jeong et al. [112] had some success with the incorporation of aluminophosphate “flakes” in a 6FDA-6FpDA:DABA matrix providing significant enhancement of the O_2/N_2 separation leading to performance above the polymer upper bound. Still, the development of a hybrid membrane with enhanced properties exceeding the polymer upper bound for CO_2/CH_4 has not, to the author’s knowledge, been published in the literature. It is the primary goal of this work to use CMS particles to enhance the properties of an upper bound polymer pushing the performance above the polymer upper bound for CO_2/CH_4.

Because of the challenges associated with the formation of hybrid materials with glassy polymers, Moore recently completed a detailed analysis of several of the factors that

have a strong influence on the success and reproducibility of hybrid membrane formation [23]. He showed the strong influence of polymer flexibility, polymer/sieve affinity, and membrane preparation conditions. This included a detailed look at the stress generated during membrane formation and the impact of this stress on performance. Further work looked at the impact of various changes in material selection, dope preparation, and membrane formation. The findings of this work were compiled to provide a better framework for the future development of hybrid membranes with properties that approach theoretical predictions.

2.5. References

1. Hines, A.L. and Maddox, R.N. (1985). Mass Transfer. Upper Saddle River, Prentice Hall PTR.
2. Singh, A. (1997). Membrane Materials with Enhanced Selectivity: An Entropic Interpretation. Chemical Engineering. Austin, The University of Texas at Austin. Doctor of Philosophy: 263.
3. Singh, A. and Koros, W.J. (1996). "Significance Of Entropic Selectivity For Advanced Gas Separation Membranes." Industrial & Engineering Chemistry Research 35(4): 1231-1234.
4. Suda, H. and Haraya, K. (1997). "Gas Permeation Through Micropores Of Carbon Molecular Sieve Membranes Derived From Kapton Polyimide." Journal of Physical Chemistry B 101(20): 3988-3994.
5. Wijmans, J.G. and Baker, R.W. (1995). "The Solution-Diffusion Model - A Review." Journal of Membrane Science 107(1-2): 1-21.
6. Rautenbach, R. and Albrecht, R. (1989). Membrane Processes. Chichester, John Wiley & Sons.
7. Perry, J.D., Nagai, K., et al. (2006). "Polymer Membranes For Hydrogen Separations." Mrs Bulletin 31(10): 745-749.
8. Paul, D.R. and Koros, W.J. (1976). "Effect of Partially Immobilizing Sorption on Permeability and Diffusion Time Lag." Journal of Polymer Science Part B-Polymer Physics 14(4): 675-685.
9. Koros, W.J. and Hellums, M.W. (1989). Transport Properties. Encyclopedia of Polymer Science and Engineering, John Wiley & Sons, Inc. Supplement Volume: 724-802.
10. Chern, R.T., Koros, W.J., et al. (1983). "Implications of the Dual-Mode Sorption and Transport Models for Mixed Gas Permeation." Acs Symposium Series 223: 47-73.
11. Ganesh, K., Nagarajan, R., et al. (1992). "Rate of Gas-Transport in Glassy-Polymers - a Free-Volume Based Predictive Model." Industrial & Engineering Chemistry Research 31(3): 746-755.
12. Jordan, S.S. and Koros, W.J. (1995). "A Free-Volume Distribution Model Of Gas Sorption And Dilation In Glassy-Polymers." Macromolecules 28(7): 2228-2235.

13. Koros, W.J., Chan, A.H., et al. (1977). "Sorption and Transport of Various Gases in Polycarbonate." Journal of Membrane Science 2(2): 165-190.
14. Koros, W.J., Paul, D.R., et al. (1976). "Carbon-Dioxide Sorption and Transport in Polycarbonate." Journal of Polymer Science Part B-Polymer Physics 14(4): 687-702.
15. Vieth, W. R. and Amini, M. A. (1974). "Generalized Dual Sorption Theory." Abstracts of Papers of the American Chemical Society: 49-49.
16. Vieth, W. R., Howell, J. M., et al. (1976). "Dual Sorption Theory." Journal of Membrane Science 1(2): 177-220.
17. Ismail, A.F. and Lorna, W. (2002). "Penetrant-Induced Plasticization Phenomenon In Glassy Polymers For Gas Separation Membrane." Separation and Purification Technology 27(3): 173-194.
18. Madden, W.C. (2005). The Performance Of Hollow Fiber Gas Separation Membranes In The Presence Of An Aggressive Feed Stream. Chemical and Biomolecular Engineering. Atlanta, Georgia Institute of Technology. Doctor of Philosophy: 240.
19. Jackson, W.J. and Caldwell, J.R. (1965). "Antiplasticizers For Bisphenol Polycarbonates." Advances in Chemistry Series 48: 185.
20. Maeda, Y. and Paul, D.R. (1987). "Effect of Antiplasticization on Gas Sorption and Transport.1. Polysulfone." Journal of Polymer Science Part B-Polymer Physics 25(5): 957-980.
21. Maeda, Y. and Paul, D.R. (1987). "Effect of Antiplasticization on Gas Sorption and Transport.2. Poly(Phenylene Oxide)." Journal of Polymer Science Part B-Polymer Physics 25(5): 981-1003.
22. Dubinin, M.M. (1989). "Fundamentals of the Theory of Adsorption in Micropores of Carbon Adsorbents - Characteristics of Their Adsorption Properties and Microporous Structures." Pure and Applied Chemistry 61(11): 1841-1843.
23. Moore, T.T. (2004). Effects of Materials, Processing, and Operating Conditions on the Morphology and Gas Transport Properties of Mixed Matrix Membranes. Chemical Engineering. Austin, TX, The University of Texas at Austin. Doctor of Philosophy: 312.
24. Vu, D.Q. (2001). Formation and Characterization of Asymmetric Carbon Molecular Sieve and Mixed Matrix Membranes for Natural Gas Purification. Chemical Engineering. Austin, TX, The University of Texas at Austin. Doctor of Philosophy.
25. Knudsen, M. (1952). The Kinetic Theory of Gases; Some Modern Aspects. London, Methuen.
26. Hwang, S.T. and Kammerme, K. (1966). "Surface Diffusion in Microporous Media." Canadian Journal of Chemical Engineering 44(2): 82.
27. Lee, K.H. and Hwang, S.T. (1986). "The Transport of Condensable Vapors through a Microporous Vycor Glass Membrane." Journal of Colloid and Interface Science 110(2): 544-555.
28. Masaryk, J.S. and Fulrath, R.M. (1973). "Diffusivity of Helium in Fused Silica." Journal of Chemical Physics 59(3): 1198-1202.
29. Breck, D.W. (1974). Zeolite Molecular Sieves. New York, John Wiley & Sons.
30. Koros, W.J. and Fleming, G.K. (1993). "Membrane-Based Gas Separation." Journal of Membrane Science 83(1): 1-80.
31. Crank, J. and Park, G.S. (1968). Diffusion in Polymers. New York, Academic Press.
32. Koros, W.J. and Mahajan, R. (2000). "Pushing The Limits On Possibilities For Large Scale Gas Separation: Which Strategies?" Journal of Membrane Science 175(2): 181-196.

33. Zolandz, R.R. and Fleming, G.K. (1992). Gas Permeation Applications. Membrane Handbook. W. S. W. Ho and K. K. Sirkar. New York, Chapman and Hall: 78-94.
34. Anand, M., Langsam, M., et al. (1997). "Multicomponent gas separation by selective surface flow (SSF) and poly-trimethylsilylpropyne (PTMSP) membranes." Journal of Membrane Science 123(1): 17-25.
35. Bondar, V.I., Freeman, B.D., et al. (2000). "Gas Transport Properties Of Poly(Ether-B-Amide) Segmented Block Copolymers." Journal of Polymer Science Part B-Polymer Physics 38(15): 2051-2062.
36. Merkel, T.C., Gupta, R.P., et al. (2001). "Mixed-Gas Permeation Of Syngas Components In Poly(Dimethylsiloxane) And Poly(1-Trimethylsilyl-1-Propyne) At Elevated Temperatures." Journal of Membrane Science 191(1-2): 85-94.
37. Pinnau, I., Casillas, C.G., et al. (1996). "Hydrocarbon/Hydrogen Mixed Gas Permeation In Poly(1-Trimethylsilyl-1-Propyne) (PTMSP), Poly(1-phenyl-1-propyne) (PPP), and PTMSP/PPP Blends." Journal of Polymer Science Part B-Polymer Physics 34(15): 2613-2621.
38. Pinnau, I. and He, Z.J. (2004). "Pure- And Mixed-Gas Permeation Properties Of Polydimethylsiloxane For Hydrocarbon/Methane And Hydrocarbon/Hydrogen Separation." Journal of Membrane Science 244(1-2): 227-233.
39. Raharjo, R.D., Lee, H.J., et al. (2005). "Pure Gas And Vapor Permeation Properties Of Poly[1-Phenyl-2-[P-(Trimethylsilyl)Phenyl]Acetylene] (PTMSDPA) And Its Desilylated Analog, Poly[Diphenylacetylene] (PDPA)." Polymer 46(17): 6316-6324.
40. Robeson, L.M., Burgoyne, W.F., et al. (1994). "High-Performance Polymers for Membrane Separation." Polymer 35(23): 4970-4978.
41. Ferry, J.D. (1936). "Statistical Evaluation Of Sieve Constants In Ultrafiltration." Journal of General Physiology 20(1): 95-104.
42. Mahajan, R. and Koros, W.J. (2002). "Mixed Matrix Membrane Materials With Glassy Polymers. Part 1." Polymer Engineering and Science 42(7): 1420-1431.
43. Caro, J., Noack, M., et al. (2000). "Zeolite Membranes - State Of Their Development And Perspective." Microporous and Mesoporous Materials 38(1): 3-24.
44. Husain, S. (2006). Mixed Matrix Dual Layer Hollow Fiber Membranes for Natural Gas Separation. School of Chemical and Biomolecular Engineering. Atlanta, Georgia Institute of Technology. Doctor of Philosophy: 235.
45. Wallace, D.W. (2004). Crosslinked Hollow Fiber Membranes for Natural Gas Purification and Their Manufacture from Novel Polymers. Chemical Engineering. Austin, The University of Texas at Austin. Doctor of Philosophy: 221.
46. Pierson, H.O. (1990). Handbook of Carbon, Graphite, Diamond, and Fullerenes. Park Ridge, NJ, Noyes Publication.
47. Jenkins, G.M. and Kawamura, K. (1976). Polymeric Carbons - Carbon Fiber, Glass and Char. London, Cambridge University Press.
48. Steel, K.M. (2000). Carbon Membranes For Challenging Gas Separations. Chemical Engineering. Austin, TX, The University of Texas at Austin. Doctor of Philosophy.
49. Steel, K.M. and Koros, W.J. (2003). "Investigation Of Porosity Of Carbon Materials And Related Effects On Gas Separation Properties." Carbon 41: 253-266.
50. Geiszler, V.C. (1997). Polyimide Precursors For Carbon Molecular Sieve Membranes. Chemical Engineering. Austin, TX, The University of Texas at Austin. Doctor of Philosophy.

51. Williams, P.J. (2006). Analysis of Factors Influencing the Performance of CMS membranes for Gas Separation. School of Chemical and Biomolecular Engineering. Atlanta, Georgia Institute of Technology. Doctor of Philosophy: 238.
52. Koresh, J.E., Soffer, A. (1983). "Molecular Sieve Carbon Permselective Membrane. Part 1. Presentation Of A New Device For Gas Mixture Separation." Separation Science and Technology 18: 723-734.
53. Acharya, M. and Foley, H. C. (1999). "Spray-coating of Nanoporous Carbon Membranes for Air Separation." Journal of Membrane Science 16(1-2): 1-5.
54. Acharya, M., Raich, B. A., et al. (1997). "Metal-supported Carbogenic Molecular Sieve Membranes: Synthesis and Applications." Industrial & Engineering Chemistry Research 36(8): 2924-2930.
55. Centeno, T.A. and Fuertes, A.B. (2000). "Carbon Molecular Sieve Gas Separation Membranes Based On Poly(Vinylidene Chloride-Co-Vinyl Chloride)." Carbon 38(7): 1067-1073.
56. David, L.I.B. and Ismail, A.F. (2003). "Influence Of The Thermastabilization Process And Soak Time During Pyrolysis Process On The Polyacrylonitrile Carbon Membranes For O2/N2 Separation." Journal of Membrane Science 213(1-2): 285-291.
57. Fuertes, A.B. and Menendez, I. (2002). "Separation Of Hydrocarbon Gas Mixtures Using Phenolic Resin-Based Carbon Membranes." Separation and Purification Technology 28(1): 29-41.
58. Shiflett, M.B. and Foley, H.C. (1999). "Ultrasonic Deposition Of High-Selectivity Nanoporous Carbon Membranes." Science 285(5435): 1902-1905.
59. Shiflett, M.B. and Foley, H.C. (2000). "On The Preparation Of Supported Nanoporous Carbon Membranes." Journal of Membrane Science 179(1-2): 275-282.
60. Shiflett, M.B. and Foley, H.C. (2001). "Reproducible Production Of Nanoporous Carbon Membranes." Carbon 39(9): 1421-1425.
61. Wang, S.S., Zeng, M.Y., et al. (1996). "Asymmetric Molecular Sieve Carbon Membranes." Journal of Membrane Science 109(2): 267-270.
62. Shao, L., Chung, T.S., et al. (2005). "The Evolution Of Physicochemical And Transport Properties Of 6fda-Durene Toward Carbon Membranes; From Polymer, Intermediate To Carbon." Microporous and Mesoporous Materials 84(1-3): 59-68.
63. Shao, L., Chung, T.S., et al. (2004). "Casting Solvent Effects On Morphologies, Gas Transport Properties Of A Novel 6FDA/PMDA-TMMDA Copolyimide Membrane And Its Derived Carbon Membranes." Journal of Membrane Science 244(1-2): 77-87.
64. Hatori, H., Yamada, Y., et al. (1996). "The Mechanism Of Polyimide Pyrolysis In The Early Stage." Carbon 34(2): 201-208.
65. Geiszler, V.C. and Koros, W.J. (1996). "Effects Of Polyimide Pyrolysis Conditions On Carbon Molecular Sieve Membrane Properties." Industrial & Engineering Chemistry Research 35(9): 2999-3003.
66. Fuertes, A.B. (2001). "Effect Of Air Oxidation On Gas Separation Properties Of Adsorption-Selective Carbon Membranes." Carbon 39(5): 697-706.
67. Fuertes, A.B. (2000). "Adsorption-Selective Carbon Membrane For Gas Separation." Journal of Membrane Science 177(1-2): 9-16.
68. Zimmerman, C.M., Singh, A., et al. (1997). "Tailoring Mixed Matrix Composite Membranes For Gas Separations." Journal of Membrane Science 137(1-2): 145-154.

69. Mahajan, R. (2000). Formation, Characterization and Modeling of Mixed Matrix Membrane Materials. Chemical Engineering. Austin, The University of Texas at Austin. Doctor of Philosophy: 259.
70. Maxwell, J.C. (1873). A Treatise on Electricity and Magnetism, Vol. 1. London, Oxford University Press.
71. Petropoulos, J.H. (1985). "A Comparative Study Of Approaches Applied To The Permeability Of Binary Composite Polymeric Materials." Journal of Polymer Science, Polymer Physics 23: 1309-1324.
72. Bouma, R.H.B., Checchetti, A., et al. (1997). "Permeation Through A Heterogeneous Membrane: The Effect Of The Dispersed Phase." Journal of Membrane Science 128(2): 141-149.
73. Vu, D.Q., Koros, W.J., et al. (2003). "Mixed Matrix Membranes Using Carbon Molecular Sieves - II. Modeling Permeation Behavior." Journal of Membrane Science 211(2): 335-348.
74. Bosnyak, C.P., Burba, J.L., III, et al. (1997). Polymeric Composites With Crystalline Mixed Metal Hydroxide Particles Dispersed Therein. U. S. P. Office. United States, Dow Chemical Company. 5,658,653.
75. Nunes, S.P., Schultz, J., et al. (1996). "Silicone Membranes With Silica Nanoparticles." Journal of Materials Science Letters 15(13): 1139-1141.
76. Rong, M. Z., Zhang, M. Q., et al. (2001). "Structure-Property Relationships Of Irradiation Grafted Nano-Inorganic Particle Filled Polypropylene Composites." Polymer 42(1): 167-183.
77. Barrer, R. M. and James, S. D. (1960). "Electrochemistry of Crystal-Polymer Membranes.1. Resistance Measurements." Journal of Physical Chemistry 64(4): 417-421.
78. Barrer, R. M. and James, S. D. (1960). "Electrochemistry of Crystal-Polymer Membranes.2. Membrane Potentials." Journal of Physical Chemistry 64(4): 421-427.
79. Paul, D.R. and Kemp, D.R. (1973). "Diffusion Time Lag in Polymer Membranes Containing Adsorptive Fillers." Journal of Polymer Science Part C-Polymer Symposium(41): 79-93.
80. te Hennepe, H.J.C., Bargeman, D., et al. (1987). "Zeolite-Filled Silicone-Rubber Membranes.1. Membrane Preparation and Pervaporation Results." Journal of Membrane Science 35(1): 39-55.
81. te Hennepe, H.J.C., Boswerger, W.B.F., et al. (1994). "Zeolite-Filled Silicone-Rubber Membranes Experimental-Determination of Concentration Profiles." Journal of Membrane Science 89(1-2): 185-196.
82. te Hennepe, H.J.C., Smolders, C.A., et al. (1991). "Exclusion and Tortuosity Effects for Alcohol Water Separation by Zeolite-Filled PDMS Membranes." Separation Science and Technology 26(4): 585-596.
83. Bartels-Caspers, C., Tusellanger, E., et al. (1992). "Sorption Isotherms of Alcohols in Zeolite-Filled Silicone-Rubber and in Pva-Composite Membranes." Journal of Membrane Science 70(1): 75-83.
84. Okumus, E., Gurkan, T., et al. (1994). "Development of a Mixed-Matrix Membrane for Pervaporation." Separation Science and Technology 29(18): 2451-2473.
85. Vankelecom, I.F.J., Depre, D., et al. (1995). "Influence of Zeolites in PDMS Membranes - Pervaporation of Water/Alcohol Mixtures." Journal of Physical Chemistry 99(35): 13193-13197.
86. Vankelecom, I.F.J., Scheppers, E., et al. (1994). "Parameters Influencing Zeolite Incorporation in PDMS Membranes." Journal of Physical Chemistry 98(47): 12390-12396.

87. Dotremont, C., Vankelecom, I.F.J., et al. (1997). "Zeolite-filled PDMS Membranes.2. Pervaporation of Halogenated Hydrocarbons." Journal of Physical Chemistry B 101(12): 2160-2163.
88. Vankelecom, I.F.J., DeBeukelaer, S., et al. (1997). "Sorption And Pervaporation Of Aroma Compounds Using Zeolite-Filled PDMS Membranes." Journal of Physical Chemistry B 101(26): 5186-5190.
89. Vankelecom, I.F.J., Dotremont, C., et al. (1997). "Zeolite-Filled PDMS Membranes.1. Sorption Of Halogenated Hydrocarbons." Journal of Physical Chemistry B 101(12): 2154-2159.
90. Vankelecom, I.F.J., DeKinderen, J., et al. (1997). "Incorporation Of Hydrophobic Porous Fillers In PDMS Membranes For Use In Pervaporation." Journal of Physical Chemistry B 101(26): 5182-5185.
91. Jia, M.D., Peinemann, K.V., et al. (1991). "Molecular-Sieving Effect of the Zeolite-Filled Silicone-Rubber Membranes in Gas Permeation." Journal of Membrane Science 57(2-3): 289-296.
92. Jia, M.D., Peinemann, K.V., et al. (1992). "Preparation and Characterization of Thin-Film Zeolite PDMS Composite Membranes." Journal of Membrane Science 73(2-3): 119-128.
93. Duval, J.M., Folkers, B., et al. (1993). "Adsorbent Filled Membranes for Gas Separation.1. Improvement of the Gas Separation Properties of Polymeric Membranes by Incorporation of Microporous Adsorbents." Journal of Membrane Science 80(1-3): 189-198.
94. Kulprathipanja, S., Funk, E.W., et al. (1988). Separation of a Monosaccharide with Mixed Matrix membranes. U. S. P. Office. United States, UOP Inc. 4,735,193.
95. Duval, J.M., Kemperman, A.J.B., et al. (1994). "Preparation of Zeolite Filled Glassy Polymer Membranes." Journal of Applied Polymer Science 54(4): 409-418.
96. Gur, T.M. (1994). "Permselectivity of Zeolite Filled Polysulfone Gas Separation Membranes." Journal of Membrane Science 93(3): 283-289.
97. Suer, M.G., Bac, N., et al. (1994). "Gas Permeation Characteristics of Polymer-Zeolite Mixed Matrix Membranes." Journal of Membrane Science 91(1-2): 77-86.
98. Vankelecom, I.F.J., Merckx, E., et al. (1995). "Incorporation of Zeolites in Polyimide Membranes." Journal of Physical Chemistry 99(35): 13187-13192.
99. Vankelecom, I.F.J., VandenBroeck, S., et al. (1996). "Silylation To Improve Incorporation Of Zeolites In Polyimide Films." Journal of Physical Chemistry 100(9): 3753-3758.
100. Zimmerman, C.M., Mahajan, R., et al. (1997). "Fundamental And Practical Aspects Of Mixed Matrix Gas Separation Membranes." Polym. Mater. Sci. Eng 77: 328-329.
101. Mahajan, R. and Koros, W.J. (2000). "Factors Controlling Successful Formation Of Mixed-Matrix Gas Separation Materials." Industrial & Engineering Chemistry Research 39(8): 2692-2696.
102. Mahajan, R. and Koros, W.J. 2002). "Mixed Matrix Membrane Materials With Glassy Polymers. Part 2." Polymer Engineering and Science 42(7): 1432-1441.
103. Vu, D.Q., Koros, W.J., et al. (2003). "Mixed Matrix Membranes Using Carbon Molecular Sieves - I. Preparation And Experimental Results." Journal of Membrane Science 211(2): 311-334.
104. Vu, D.Q., Koros, W.J., et al. (2003). "Effect Of Condensable Impurity In CO2/CH4 Gas Feeds On Performance Of Mixed Matrix Membranes Using Carbon Molecular Sieves." Journal of Membrane Science 221(1-2): 233-239.

105. Walker, D.R.B. (1993). Synthesis and Characterization of Polypyrrolones for Gas Separation Membranes. Chemical Engineering. Austin, TX, The University of Texas at Austin. Doctor of Philosophy: 168.
106. Cornelius, C.J., Hibshman, C., et al. (2001). "Hybrid Organic-Inorganic Membranes." Separation and Purification Technology 25(1-3): 181-193.
107. Cornelius, C.J. and Marand, E. (2002). "Hybrid Silica-Polyimide Composite Membranes: Gas Transport Properties." Journal of Membrane Science 202(1-2): 97-118.
108. Cornelius, C.J. and Marand, E. (2002). "Hybrid Inorganic-Organic Materials Based On A 6fda-6fpda-Daba Polyimide And Silica: Physical Characterization Studies." Polymer 43(8): 2385-2400.
109. Hibshman, C., Cornelius, C.J., et al. (2003). "The Gas Separation Effects Of Annealing Polyimide-Organosilicate Hybrid Membranes." Journal of Membrane Science 211(1): 25-40.
110. Hibshman, C., Mager, M., et al. (2004). "Effects Of Feed Pressure On Fluorinated Polyimide-Organosilicate Hybrid Membranes." Journal of Membrane Science 229(1-2): 73-80.
111. Pechar, T.W., Kim, S., et al. (2006). "Preparation And Characterization Of A Poly(Imide Siloxane) And Zeolite L Mixed Matrix Membrane." Journal of Membrane Science 277(1-2): 210-218.
112. Jeong, H.K., Krych, W., et al. (2004). "Fabrication Of Polymer/Selective-Flake Nanocomposite Membranes And Their Use In Gas Separation." Chemistry of Materials 16(20): 3838-3845.

CHAPTER 3

MATERIALS AND EXPERIMENTAL PROCEDURES

This chapter details the materials used to produce carbon molecular sieves and gas separation membranes. The procedures used to process carbon molecular sieves and to form gas separation membranes are also described. Furthermore, the analytical methods used to study these materials are explained.

3.1. Materials

This section discusses the materials used in this work and the properties and criteria that led to their selection.

3.1.1. Polymers

The polymers used in this study are all polyimides. As a class, polyimides are rigid, high T_g, thermally stable polymers. Most commonly, these polymers are formed from the condensation reaction of diamines and dianhydrides [1]. The polymers used in this study will be discussed in two groups: polymers used for membrane formation and polymers used for pyrolysis.

The polymers used in membrane formation were selected based on their desirable performance. Four different polymers were used as the matrix for hybrid membranes: Ultem® 1000, Matrimid® 5218, 6FDA-6FmDA, and 6FDA-6FpDA. The structures of these polymers can bee seen in Figure 3.1. Ultem® 1000 is a polyetherimide commercially available from GE Plastics, Mount Vernon, IN. It is synthesized from 2,2'-bis[4-(3,4-dicarboxyphenoxy)phenyl] propane dianhydride (BPADA) and 1,3-

phenylenediamine (mPDA). Matrimid® 5218 is formed from the condensation reaction of 3,3',4,4',-benzophenone tetracarboxylic dianhydride (BTDA) and 5(6)-amino-1-(4'-aminophenyl)-1,3-trimethylindane (DAPI). Matrimid® is available commercially from Vantico, Inc., Brewster, NY. The two polymers 6FDA-6FmDA and 6FDA-6FpDA are not available for purchase and must be synthesized. 6FDA-6FmDA is synthesized from 4,4'-(hexafluoroisopropylidene) diphthalic anhydride (6FDA) and 3,3'-(hexaflurorisopropylidene) dianiline (6FmDA). The 6FDA-6FmDA used in this work was provided through a joint venture with Hoescht Celanese. Similarly, 6FDA-6FpDA is synthesized from the 6FDA monomer and 4,4'-(hexaflurorisopropylidene) dianiline (6FpDA). This polymer was synthesized as part of this work, and the details of the synthesis are presented in Appendix A.

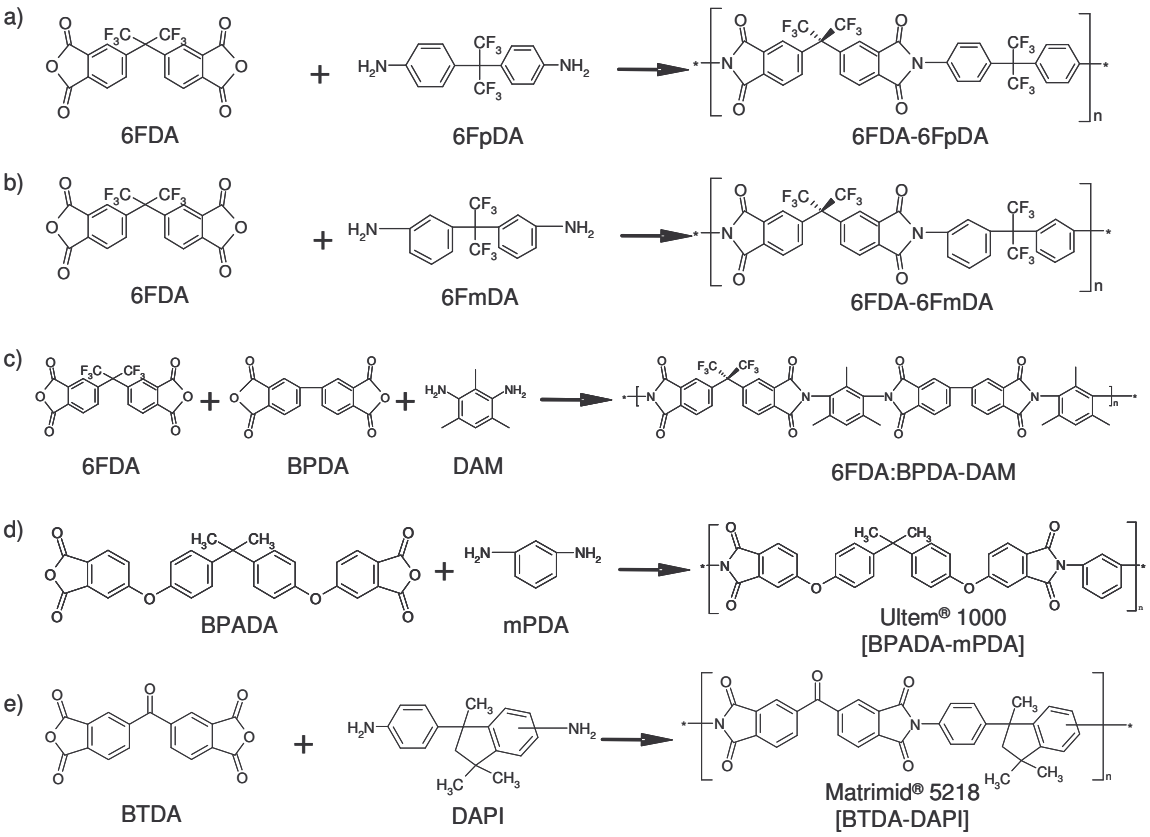

Figure 3.1 The polyimides used in this research are formed from the condensation polymerization of a dianhydride and a diamine:

a) 6FDA-6FpDA is from 4,4'-(hexafluoroisopropylidene) diphthalic anhydride (6FDA) and 4,4'-(hexafluoroisopropylidene) dianiline (6FpDA).
b) 6FDA-6FmDA is from 4,4'-(hexafluoroisopropylidene) diphthalic anhydride (6FDA) and 3,3'-(hexafluoroisopropylidene) dianiline (6FmDA).
c) 6FDA:BPDA-DAM is from 4,4'-(hexafluoroisopropylidene) diphthalic anhydride (6FDA), 3,3'-4,4'-biphenyl tetracarboxylic acid dianhydride (BPDA), and 2,4,6-trimethyl-1,3-phenylene diamine (DAM)
d) Ultem® 1000 is from 2,2'-bis[4-(3,4-dicarboxyphenoxy)phenyl] propane dianhydride (BPADA) and 1,3-phenylenediamine (mPDA)
e) Matrimid® 5218 is from 3,3',4,4'-benzophenone tetracarboxylic dianhydride (BTDA) and 5(6)-amino-1-(4'-aminophenyl)-1,3,3-trimethyldane (DAPI),

The ether linkage in the backbone of Ultem® adds to the polymer flexibility, as demonstrated by its lower glass transition temperature. Table 3.1 shows physical properties of the polymers used in this work. All of the polymers used as the continuous phase in the formation of hybrid membranes are soluble in several common solvents such as dichloromethane (CH_2Cl_2) and 1-methyl-2-pyrrolidone (NMP). These polymers

can be easily cast from solution, and the solubility is also an important characteristic in further development of membranes as asymmetric hollow fibers.

Table 3.1 Selected properties of polymers used in this work.

Polymer	***Density (g/cm^3)***	***T_g (^{o}C)***	***Source***
6FDA-6FpDA	1.466	320	[1, 2]
6FDA-6FmDA	1.439	254	[2]
Ultem®	1.27	209	[1]
Matrimid®	1.24	302	[1]
6FDA:BPDA-DAM	1.33	255	[1]

The selection criteria for polymers used in pyrolysis were described earlier in section 2.2.2.3.1. For this work, two different polymers were considered as precursor materials: Matrimid® 5218 and 6FDA:BPDA-DAM (1:1). These materials were selected based on previous knowledge of the properties achieved through established pyrolysis protocols for these materials [1, 4, 5]. The synthesis of Matrimid® was described above, but the synthesis of 6FDA:BPDA-DAM (1:1) follows a slightly different pathway. As with the synthesis of all of the polyimides used in this work, this polymer is formed form the combination of a one to one ratio of diamine to dianhydride. The primary difference in the case of 6FDA:BPDA-DAM (1:1) is the use of two dianhydrides. This polymer is formed from the reaction of equal amounts of 6FDA and 3,3'-4,4'-biphenyl tetracarboxylic acid dianhydride (BPDA) with 2,4,6-trimethyl-1,3-phenylene diamine (DAM) in an amount equivalent to the entire dianhydride concentration. The 6FDA:BPDA-DAM used in this work was synthesized by P. Jason Williams using a protocol very similar to that described for 6FDA-6FpDA in Appendix A.

3.1.2. *Molecular Sieves*

The molecular sieves used in this study are carbon molecular sieves created from the high temperature pyrolysis of a synthetic polymer precursor. The two precursor polymers, Matrimid and 6FDA:BPDA-DAM, were described in the previous section. Both polymers can be solution cast to form dense film membranes prior to pyrolysis, and this will be described in section 3.2.2.

The formation of carbon molecular sieve membranes begins with the formation of a dense, flat film. The films used for pyrolysis are typically cast to about 2 mils thick (1 mil = 0.001 inch). The films are then removed from the casting surface and dried in a vacuum oven to remove all of the residual solvent. Individual samples are then cut from the film as one inch diameter circles. These samples are weighed individually and placed on a ribbed quartz sample plate that is used in the pyrolysis process as shown in Figure 3.2. The ribbed plate allows air flow below the samples so that byproducts evolved during pyrolysis can leave from both sides of the film.

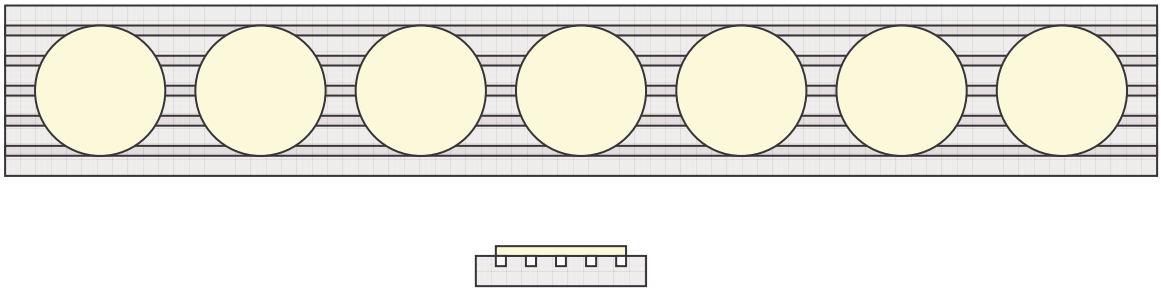

Figure 3.2 Films are pyrolyzed on a grooved quartz plate to allow byproducts to be removed from both sides of the film during decomposition.

The quartz sample holder is then placed inside the quartz tube of the Thermacraft Model 23-24-1ZH three zone tubular furnace used for pyrolysis. Quartz is used for the

components of the furnace because of its ability to withstand the high temperatures experienced during the pyrolysis while glass will deform at these temperatures. Figure 3.3 shows the arrangement of the pyrolysis system. One end of the quartz tube is closed with only a small opening sealed with an o-ring valve. The other end of the tube is open to allow the samples to be put into the system. Once the samples are in place, the end is sealed with a Pyrex® glass cap that seals against a large o-ring. The glass cap has a small opening sealed with an o-ring valve. The small openings in the two ends of the closed furnace tube allow the atmosphere to be controlled during pyrolysis either by inert gas purge or by continuous active vacuum.

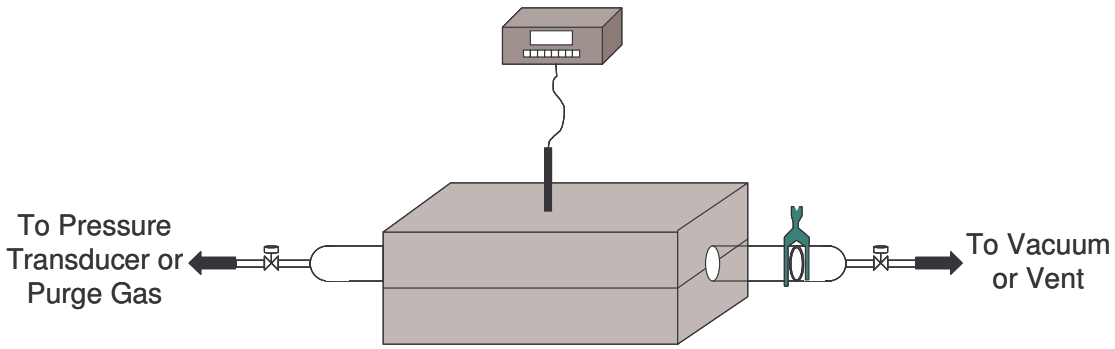

Figure 3.3 Pyrolysis is performed in a quartz tube that is heated by a split tube furnace.

Once the samples are sealed in the pyrolysis tube, the system is evacuated (vacuum pyrolysis) or purged (inert purge pyrolysis) for several hours to remove as much of the oxygen from the system as possible, since even very small quantities of oxygen have been shown to have a dramatic effect on the performance of the resulting carbon. Once the system has been fully evacuated, the pyrolysis may be started. The pyrolysis is performed using a well-controlled temperature profile selected as previously described to provide the desired impact on the carbon produced. Two sample temperature profiles can be seen in Figure 3.4. These profiles are similar to those used by several

researchers to study CMS formation [1, 4-10]. Once the temperature profile is completed and the system has cooled to near room temperature (<50 °C), the samples are removed and either tested as dense film membranes or further processed for use as CMS particles.

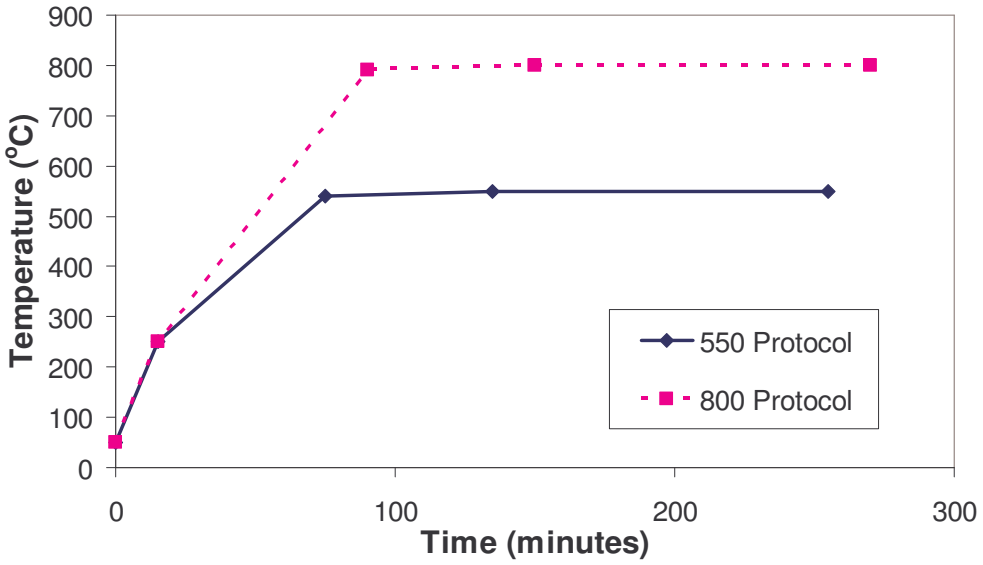

Figure 3.4 Consistent temperature profiles were used to form carbon molecular sieves.

Carbon molecular sieves used to form hybrid membranes must be further processed after pyrolysis. Because the final application of hybrid membranes is likely to take the form of asymmetric hollow fibers, it is necessary to use very small molecular sieve particles. The selective skin of a hollow fiber may be as thin as 100 nm [11], so it is ideal to use particles with sub-micron dimensions to reduce the chance of forming defects that persist through the entire selective layer of the hollow fiber. In order to produce sub-micron sized CMS particles, the pyrolyzed carbon was powdered in a SPEX CertiPrep 8000M Mixer/Mill. First the carbon was placed in the 2 ¼ inch diameter by 3 inch high hardened steel vial along with six stainless steel ball bearings (2 – ½ inch, 4 – ¼ inch). The vial, top, carbon, and ball bearings were then dried in a vacuum oven at 200 °C overnight prior to milling to degas the sieves and remove any moisture that might be

present. After drying, an o-ring was placed between the top and the vial and the cap was used to tighten the top securely. The vial was then clamped in the ball mill/mixer and agitated for 90 minutes. The vigorous shaking of the ball mill/mixer causes the ball bearings to crush the brittle molecular sieves into a very fine powder. After the milling was completed, the vial was allowed to rest for at least 2 hours to cool down and allow the particles to settle before the powder was recovered from the vial.

In order to remove any large particles that remain in the powder after the milling, the carbon was decanted prior to film formation or modification. To decant the carbon, a small amount of carbon (< 100 mg) was placed in a 40 ml ICHEM vial and dispersed in 35 ml of dichloromethane by sonicating in an ultrasonic bath for 30 minutes. The dispersion was then allowed to settle for 6 hours before decanting the solution to remove the larger particles that settled out. The decanted solution was then distilled to recover the CMS particles. Typically, several batches would be decanted and distilled together to provide a larger amount of small particles. These particles were then used for film formation or modification.

3.1.3. Coupling Agents

One of the important advancements of this work was the use of a coupling agent to form a covalent link between the polymer and the CMS insert. The selection process for this agent will be discussed later in Chapter 4, but the final result was the use of an agent with two primary aromatic diamine groups available for reaction. One amine group is used to bond to the CMS [12] while the other is left available to bond with the polyimide [13, 14]. Further analysis of the impact of the coupling agent on the membrane system was also performed using some agents containing only one amine group. Table 3.2 shows the different agents used in the modification and analysis of the hybrid membrane

systems. All modification agents were obtained from Aldrich Chemicals in the highest available purity. The primary molecule used in the modification of the CMSs for incorporation in the hybrid membranes was 1,4-phenylenediamine which proved successful in enhancing the performance of the hybrid membranes.

Table 3.2 Chemical agents used in the modification and analysis of the hybrid membrane systems.

Name	*Chemical Structure*
(6FpDA)	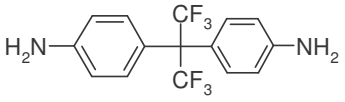
(p-phenylenediamine)	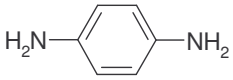
(ethylenediamine)	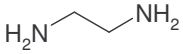
(aniline)	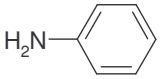
(tert-butylamine)	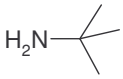
(propylamine)	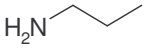

3.1.4. Gases

All of the gases used in this study were obtained from either Air Products or Airgas with purities at or above 99.999%.

3.2. Procedures

This section describes the experimental procedures and processes used to perform the tests in this work. This discussion is intended to provide sufficient information for these experiments to be repeated.

3.2.1. Modification of Carbon Molecular Sieves

The process used to modify the surface of the carbon molecular sieves used in this research was based on methods developed for modification of carbon nanotubes by Bahr and Tour [12]. The work that led to this procedure will be discussed in detail in Chapter 4, but the basic modification procedure is given here.

The decanted and dried CMSs were used in the modification procedure. The modification was performed under positive pressure nitrogen in very dry conditions. Figure 3.5 shows the primary reaction setup used for the modification. The glassware and stir bar are heated in a vacuum oven at 200 ^{o}C overnight to remove adsorbed moisture, and then they were set up in the hood prior to reaction and flame dried three times. Flame drying is accomplished using a propane torch to heat the glassware under alternating nitrogen and vacuum atmospheres. This is a commonly established laboratory procedure used to prepare glassware for use in moisture sensitive experiments. Once the glassware and the stir-bar were dried, the carbon was measured and added to the 3-neck flask. In a typical modification reaction, 100mg of decanted carbon was added to a 250ml 3-neck flask. The 175ml of 1,2-dichlorobenzene (ODCB) was added from a sure seal container using a double ended needle. A pressure drop was created between the two vessels by controlling the nitrogen purge lines, and pressure and gravity were used to transfer the solvent into the reaction vessel. Once the solvent was added, the reaction vessel was sonicated for 30 minutes in an ultrasonic bath (Branson 1510, ½ gallon, 40kHz) to disperse the carbon. The mixture was then placed in an oil bath and stirred under nitrogen purge. The diamine was added next. The amount of diamine used was limited to reduce the impact of the modifier on the polymer matrix. This issue is further discussed in Chapter 5. Once the diamine was measured, it was dissolved in 5ml of anhydrous ODCB. The fully dissolved diamine was

then added to the reaction vessel using a syringe. The solution was allowed to stir for five minutes before adding 1.5ml of the catalyst, isoamyl nitrite. Isoamyl nitrite caused the primary amine groups to form highly reactive diazonium groups in solution which then react with the surface giving off molecular nitrogen as a byproduct [12, 15]. The reaction solution was then heated to 60 ^{o}C using an oil bath with a hot plate/magnetic stirrer combo. When the temperature reached 60 ^{o}C, the nitrogen purge was adjusted to a very slow rate, and the solution was allowed to react for 24hrs.

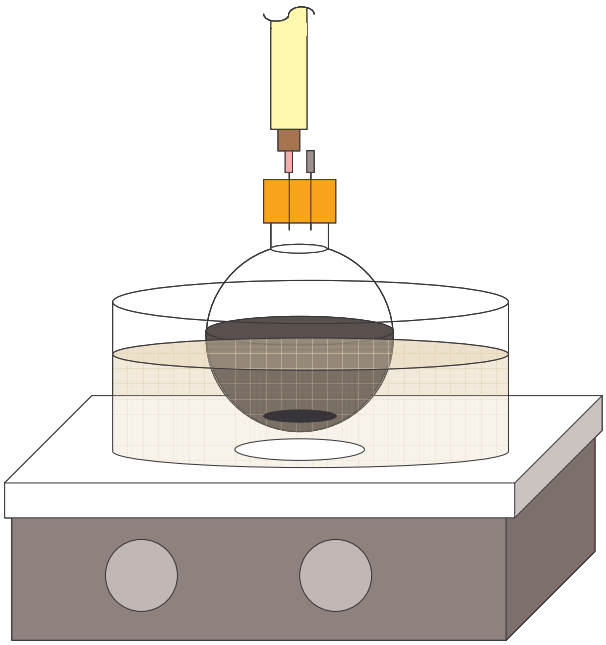

Figure 3.5 The modification reaction was carried out in dried glassware held at a constant temperature by a heating plate and oil bath.

When the reaction completed, the solution was removed from the heating oil and allowed to cool to room temperature. After cooling, 75ml of N,N-dimethylformamide (DMF) was added to dilute the solution. This solution was then filtered over a 0.2µ Whatman 47mm nylon membrane filter using up to 100 psig of nitrogen in a Pall Corporation 4280 high pressure filter as shown in Figure 3.6. After fitering the initial reaction product, 150ml of DMF was added to the filter and sonicated for two minutes using a VibraCell^{TM} 50 watt high-intensity ultrasonic processor equipped with a ¼ inch

titanium probe. The DMF is then filtered and this process is repeated at least three times. The filtrate is usually dark brown in color after the first filtration, light yellow after the second filtration, and clear for each subsequent filtration. After repeating the DMF filtration three times, one more filtration is performed using dichloromethane. This step removes much of the residual solvent from the reaction and washing of the carbon. When the final filtration has been completed, the carbon is immediately placed in a vacuum oven and heated to 200 ^{o}C for one hour to remove residual solvents and dry the CMSs. As soon as the drying is completed, the carbon is removed from the oven and either used to start mixed matrix solutions or stored under a nitrogen blanket. Because of the sensitivity of primary amines to oxidation it is important that the modified carbons not be left exposed to the atmosphere for extended periods of time.

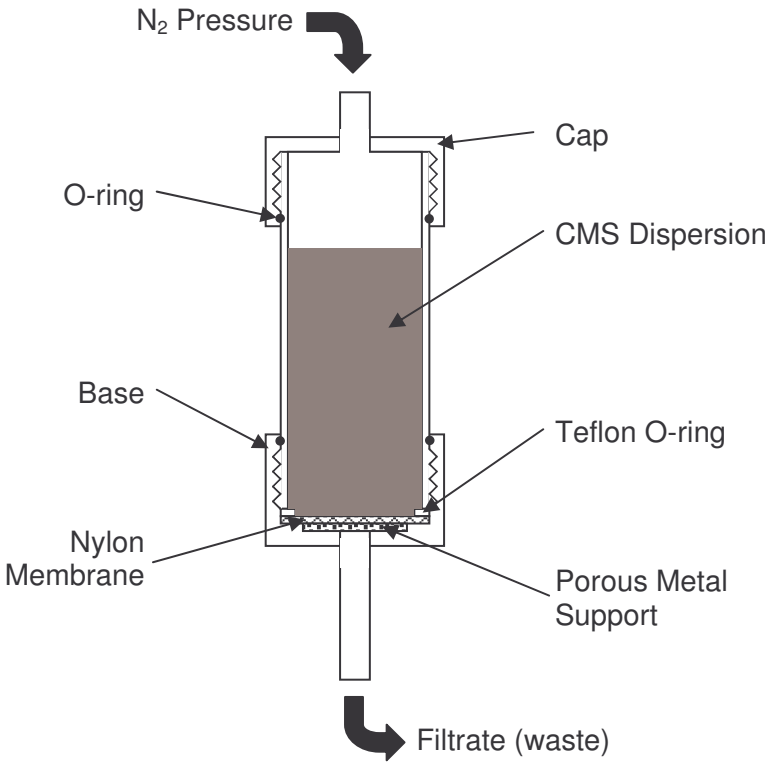

Figure 3.6 The modified carbon particles were washed and recovered using a high pressure filtration system.

3.2.2. Membrane Preparation

The membranes used in this study were all tested as dense flat films. The formation processes used were selected with the intention of producing homogeneous membranes with no asymmetry. Two primary methods were used to cast dense film membranes: solution casting and draw casting.

3.2.2.1. Solution Casting

In solution casting, a dilute solution, 2-5 wt%, was prepared and then poured into a casting ring. The first step in solution preparation was to dry the polymer, typically in a vacuum oven at 110 ^{o}C for 12 hours, to remove any moisture absorbed during storage. An appropriate amount of polymer was measured to provide the desired film thickness, typically 0.002 inches (2 mils), based on the density of the polymer and the diameter of the casting ring. Two different casting rings were used based on the desired membrane size: 7cm or 10cm. The rings are constructed from stainless steel, and the dimensions given are the inside diameters. These rings were placed on a mirror backed glass plate that is set on a leveling base that allows the plate to be leveled to promote even film formation. Figure 3.7 shows the setup used to form solution cast membranes. Once the polymer was weighed, approximately 10ml of dichloromethane was added to the polymer in a 20ml ICHEM vial. The vial was then agitated either by rolling or shaking for at least one hour to allow sufficient time for the polymer to dissolve.

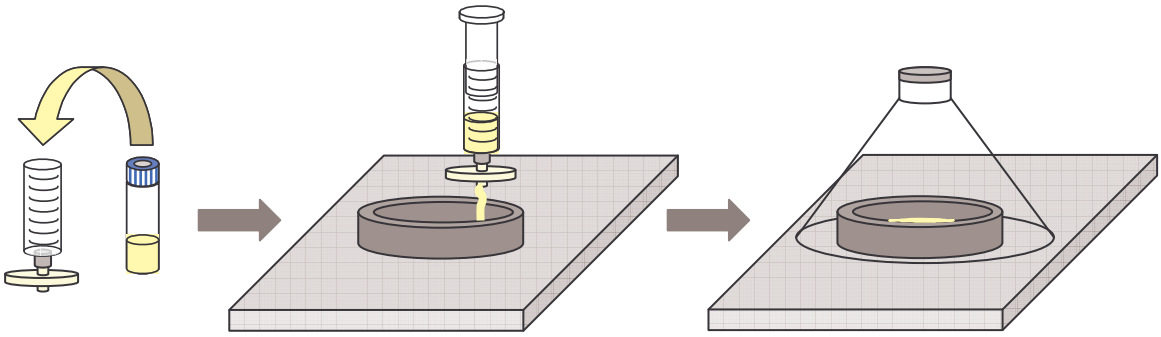

Figure 3.7 Pure polymer membranes were solution cast by syringe on a glass surface inside a metal ring. An inverted funnel was then used to slow the solvent evaporation and prevent contamination of the membrane during drying.

Solution casting is most often used for homogeneous polymer membranes, and the solution is cast using a syringe equipped with a 0.02μ filter to remove any contaminant particles that may be present in the solution. Once the solution was syringed into the casting ring, the ring was covered with a funnel to reduce the time of solvent evaporation to the range of 6 to 12 hours. Rapid solvent evaporation can cause temperature fluctuations leading to convective motion in the solution (ie. Marangoni/Benard flows). This motion can result in uneven evaporation and thickness variations in the membrane. The funnel used to cover the solution while the solvent is evaporating also prevented dust and other contaminants from being trapped in the membrane. The solvent was allowed to evaporate until the membrane is fully vitrified, which is determined by a change in the appearance of the membrane. Often, the membrane would partially or fully delaminate from the casting surface after the solvent evaporated, but even if this did not occur, there was usually a noticeable change in the appearance of the membrane when the solvent fully evaporated.

Once the membrane vitrified, it was removed from the glass and the casting ring. If the membrane was not fully delaminated when vitrified, the film was removed either by

gently pulling on an available portion of the membrane, by carefully lifting the edge with a razor blade, or by floating the membrane off of the surface with water. Water was used in most cases that have more than a very small portion of the membrane still attached to the glass since floating membranes on water causes the least amount of stress to the film and is effective even if there is not enough delaminated membrane area to allow direct removal. Once the membrane was removed from the glass and the casting ring, it was dried in a vacuum oven at 110 ^{o}C for at least 12 hours to remove any residual solvent and water that may remain in the film.

3.2.2.2. Draw Casting

Draw casting is the preferred method of film formation for hybrid systems. Much higher polymer concentrations are used in draw casting than in solution casting. Typical dopes (casting solutions) used for draw casting have a solids (polymer and sieve) content of 15-25 wt%. These solutions are much more viscous and will not spread evenly if "solution cast", therefore they are drawn onto the casting plate. Similar to solution casting, the first step of the process is to prepare the dope used to cast the membrane. Since hybrid systems contain both polymer and CMS particles, it is necessary to dry both prior to the dope formation. The polymer was dried as previously mentioned, and the CMSs were dried in a vacuum oven at 200 ^{o}C to remove sorbed water. The dry CMSs, typically 0.050-0.100g, were placed in a 20ml ICHEM vial and ~10ml of dry dichloromethane was added to the sieves. The solution was then sonicated in an ultrasonic bath (Branson 1510, ½ gallon, 40kHz) for 30 minutes to provide a well dispersed sieve solution. Once the sieves were well dispersed, they were primed with polymer. The priming process was developed to improve the interaction of the polymer and the sieve by allowing the sieves to be coated with a small amount of polymer while the solution is still very dilute [1, 3, 16]. The amount of polymer added was typically

close to 1/10 of the total polymer used in the final dope. Once the priming polymer was added to the solution, the dope was then sonicated again for 30 minutes. This solution was then placed on a roller or shaker to be agitated overnight and allow the priming polymer to react with the modified sieves and form a bond with the particles. After agitating overnight, the dope was sonicated again for 30 minutes to break up any agglomerates that may have formed during the priming process and to redistribute any of the CMS particles that settled. The remainder of the polymer needed for the dope was then added to the solution and the resulting solution was agitated by hand for about 30 seconds to dissolve most of the polymer added. The dope was then sonicated for 30 minutes to provide a well dispersed polymer/sieve solution.

Once the well dispersed solution was formed, the dope must be prepared for casting. In order to obtain an appropriately viscous casting dope, some of the solvent must be evaporated. The amount of solvent remaining in the solution before draw casting was selected qualitatively in order to produce the desired viscosity as observed by the motion of the solution in the vial, but generally the casting dope would contain 75-85% solvent by weight with the balance consisting of polymer and sieves. In order to remove the excess solvent from the dope, the vial was purged with nitrogen while being held in the ultrasonic bath. Initial trials simply used a nitrogen purge to remove the solvent, however agglomerates were still persistent in the membranes, and the use of the ultrasonic bath was established as a means to reduce the formation of agglomerates during the solvent evaporation. The effects of these changes will be further discussed in chapter 6. The setup used in the solvent evaporation can be seen in Figure 3.8. The solution was simultaneously purged with nitrogen and sonciated for 15 minutes, and then the nitrogen purge would be stopped and the solution sonicated with some mild agitation by hand to remove the polymer and sieve that dried on the sides of the vial.

Repeating this process three times for a sample initially created using 10 ml of solvent was typically sufficient to remove the desired amount of solvent. After the solvent had been removed, the viscous dope was then rolled on a very slow roller (1-5 rpm) for 20-30 minutes to promote a homogeneous solution.

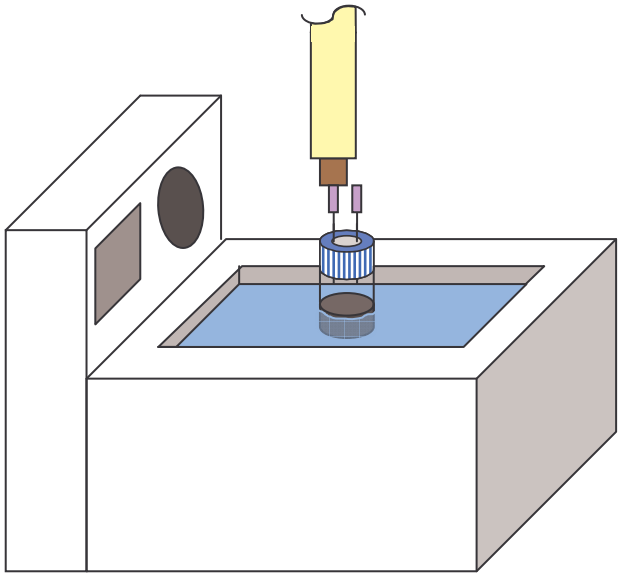

Figure 3.8 Solvent was evaporated from the solutions using a nitrogen purge while the solution was immersed in an ultrasonic bath.

The casting dope was then ready to be cast, and the draw casting process was carried out in a glove bag (Two-hand AtmosBag, Aldrich). Because the primary solvent, dichloromethane, has such a high vapor pressure, it was necessary to cast the films in a saturated atmosphere to reduce the evaporation rate of the solvent. The same casting plate was used in draw casting as in solution casting, only the plate was set up inside a glovebag for draw casting. With the level casting surface set up in the glovebag, the sample was placed in the bag, and four Petri dishes were filled with ~50 ml dichloromethane to provide a source of vapor saturation for the bag. The bag was then sealed and allowed to equilibrate for approximately two hours. After the solvent in the glovebag had time to reach equilibrium, the film was cast by pouring the dope in a short

line on the casting plate. A variable height drawing knife set to 12-16 mil was then slowly drawn across the dope to spread the film on the casting plate. This process is illustrated by Figure 3.9. The film was then left in the glovebag until all of the solvent in the film and in the Petri dishes had evaporated (usually 6-12 hrs). Most of the films cast using the draw knife were removed using water, and then dried with the same protocol as described for solution cast films.

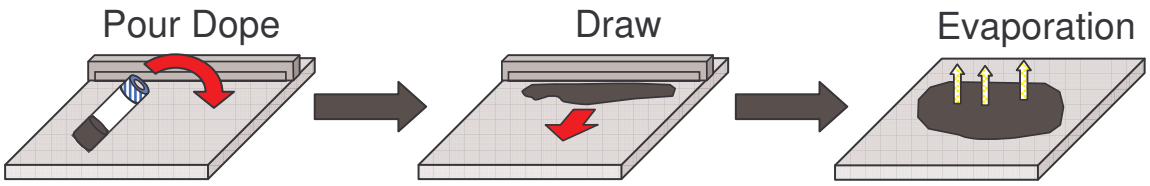

Figure 3.9 Hybrid membranes were draw cast in a glovebag saturated with solvent vapor to reduce the rate of evaporation while the film vitrifies.

3.2.3. Gas Permeation Measurements

All of the membranes prepared in this work were analyzed for their pure gas permeation properties. These tests are performed using a standard constant volume, variable pressure permeation system [17-19] shown in Figure 3.10.

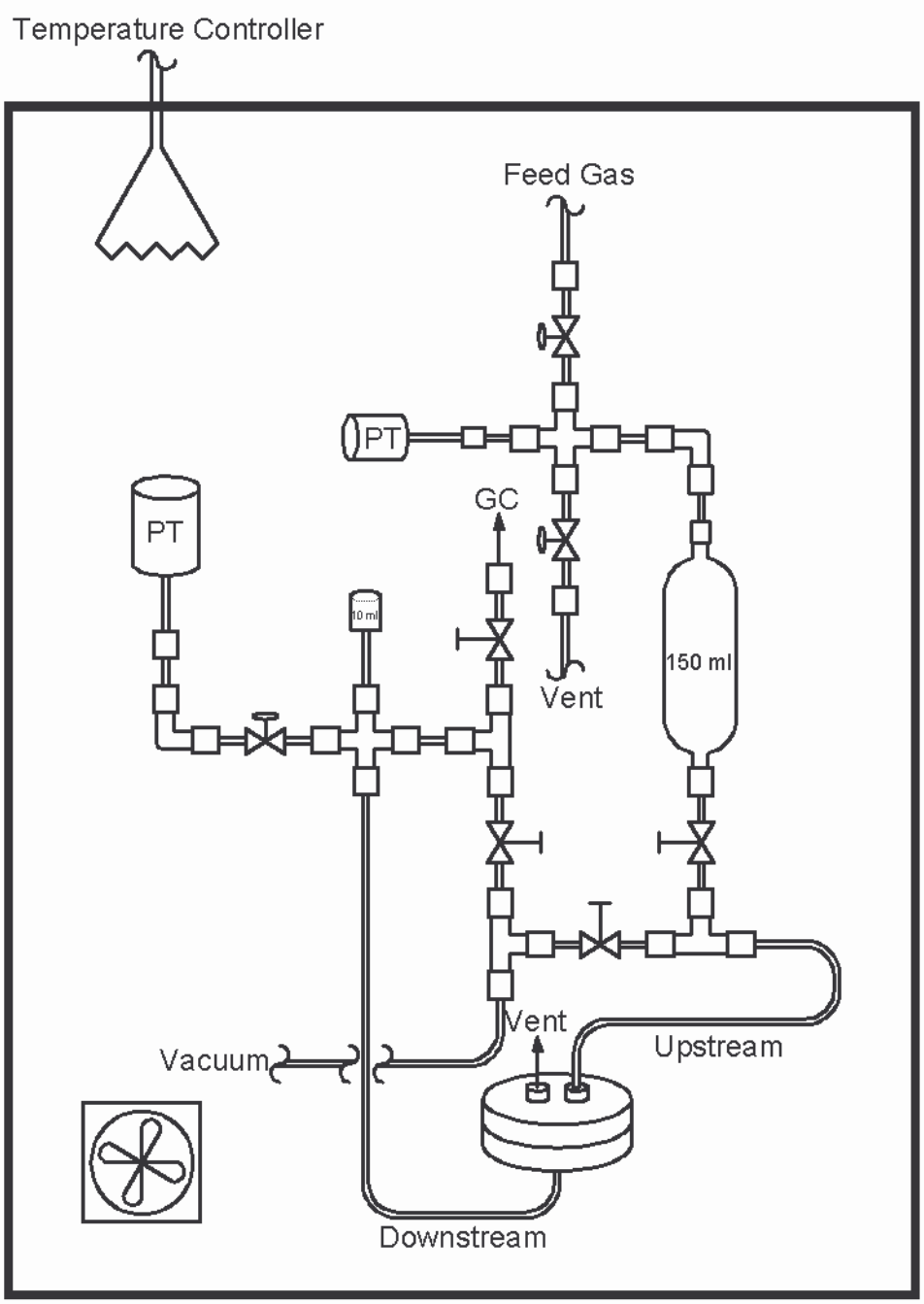

Figure 3.10 Permeation testing was performed using a constant volume, variable pressure permeation system.

By maintaining a low downstream pressure throughout the test (<10 torr), the

permeability of the membrane is directly proportional to the steady state pressure

change (dp/dt) in the downstream through the use of the ideal gas law. Equation 3.1 shows this relationship,

$$P = \left(\frac{dp}{dt}\right)\left(\frac{1day}{86400s}\right)\left(\frac{101325Pa}{760torr}\right)V\left(\frac{m^3}{10^6 ccm^3}\right)\left(\frac{mol \cdot K}{8.31451 m^3 \cdot Pa}\right)\left(\frac{1}{T}\right)X \qquad (3.1)$$

$$\left(82.056\frac{cm^3 \cdot atm}{mol \cdot K}\left(\frac{273.15K}{1atm}\right)\right)\ell\left(\frac{2.54cm}{1000mil}\right)\frac{1}{A}\frac{1}{p_f}\left(\frac{14.6959\,psi}{76cmHg}\right)\left(\frac{10^{10}\,Barrer}{\frac{cm^3(STP)\cdot cm}{s \cdot cm^2 \cdot cmHg}}\right)$$

where P = Permeability, Barrer

$\left(\frac{dp}{dt}\right)$ = Steady state pressure change, torr/day

V = Volume, cm^3

T = Temperature, Kelvin

ℓ = Thickness, mil

A = Area, cm^2

p_f = Feed pressure, psia.

Time lag, θ, is another important value obtained from the permeation experiment since the upstream and downstream sides of the membrane are initially under vacuum prior to the start of the test. The time lag, shown in Figure 3.11, is the location of the intersection of the x-axis with a line drawn through the steady state portion of the permeation data. The time lag can be used to determine the diffusivity of the material being tested by using Equation 3.2,

$$\theta = \frac{\ell^2}{6D} \qquad (3.2)$$

with ℓ = thickness (cm) and D = diffusivity (cm^2/s). Also, since the permeability is equal to the product of the diffusivity and the solubility, from Equation 2.8, the sorption coefficient may also be calculated. Another important use of the time lag is to help insure steady state has been obtained. After permeation has continued for four time lags, the dp/dt is at 99.9% of its steady state value. Using this relationship as a guide, data is typically taken for at least 10 time lags before calculating the permeability to assure that the true steady state permeation is measured. Another advantage of taking data for this length of time is that it also allows anomalies with slower kinetics to be identified, such as certain types of leaks or some polymer relaxation effects which may otherwise be unnoticed and unaccounted.

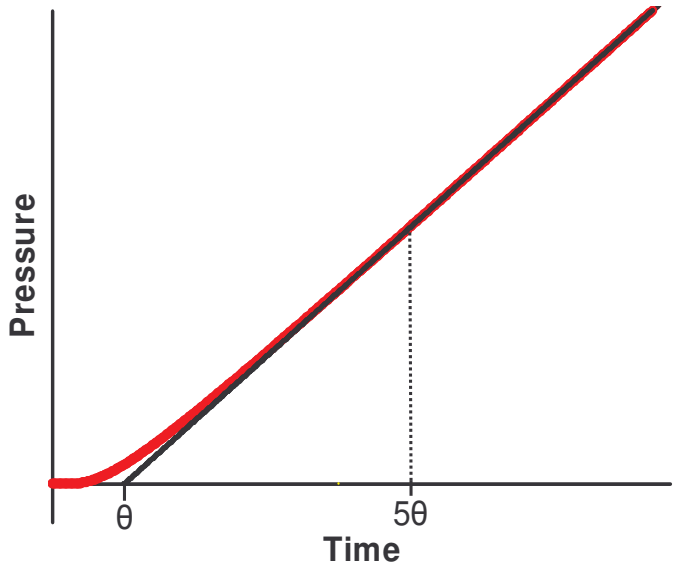

Figure 3.11 The intersection of the x-axis and a line drawn through the steady state portion of a permeation curve is known as the time lag, θ. The location of time 5θ is shown as a reference.

3.2.3.1. Preparation of Membranes for Permeation Measurements

Once a film is dried after casting, several sections were cut out for membrane testing. Typically 1 inch diameter circles were cut out with a metal die and a rubber mallet.

These membranes were then masked with adhesive backed aluminum tape to prepare them for testing. Figure 3.12 shows a cross section of a masked film in a permeation cell with a detailed view of the masked membrane. The membrane sample was "sandwiched" between two pieces of 1-5/8 inch diameter aluminum tape. The piece of tape used for the upstream side of the membrane had a ½ inch diameter hole cut out of the center while the piece used for the downstream side of the membrane had a 5/8 inch diameter hole in the center. The larger hole on the downstream side was used to provide a more accurate measurement of the area based on the smaller hole in the upstream side only. This precaution was particularly necessary with the hybrid membranes since the CMSs made them completely opaque, preventing the holes from the two sides of the mask from being aligned visually. Once the membrane was sandwiched in the aluminum tape, the sample was ready to be masked onto the permeation cell.

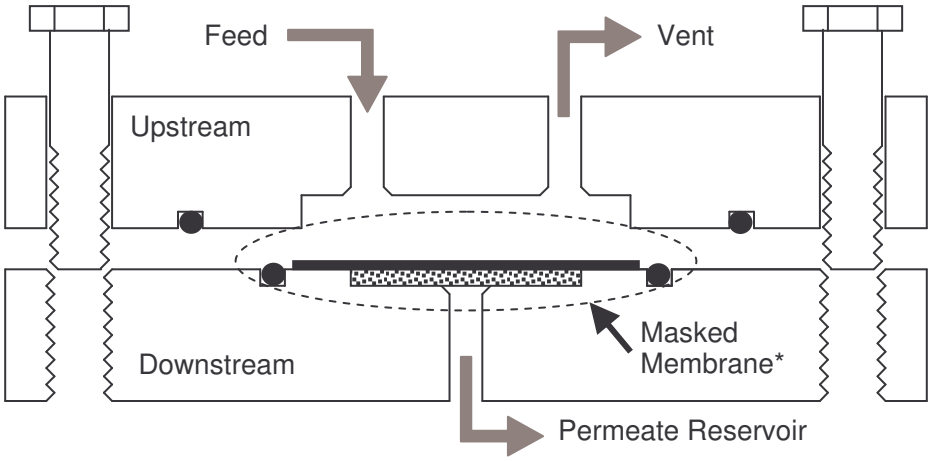

(A)

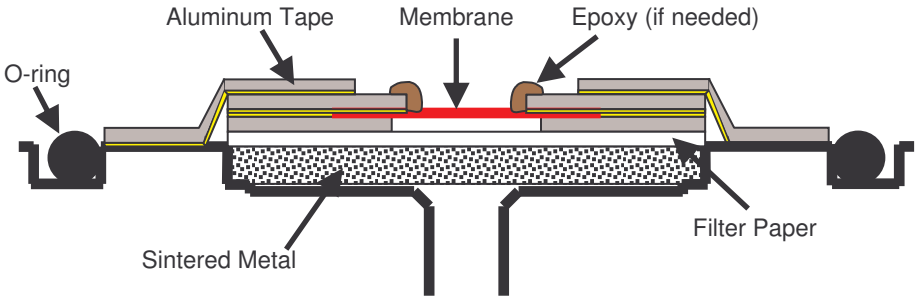

(B)

Figure 3.12 Membranes are masked into a permeation cell to allow permeability measurements. This figure shows the cell assembly (A) and a detailed cross-section of a masked film (B). Note: The figure is not drawn to scale.

With the smaller circle facing the upstream side of the permeation cell, the sandwiched membrane was placed on the permeation cell on top of two pieces of 1-5/8 inch diameter filter paper that sit directly over the sintered metal support disk in the permeation cell. These pieces were then masked onto the membrane using a 2 ¼ inch piece of aluminum tape with a ¾ inch diameter hole cut out of the center. All of the tape was then pressed into place as well as possible to reduce the potential for leaks. If visible defects or small sample sizes prevented a good seal from being formed in the masked membrane, Devcon 5 minute epoxy was used to cover the problem areas. Because the permeability of the epoxy is very slow, it is considered an impermeable

barrier compared to the membranes tested. With the epoxy cured and the membrane fully masked to the permeation cell, the upstream side of the cell was attached to the downstream side using six bolts. The cell was then connected to the permeation system using ¼ inch Swagelok® VCR connections.

3.2.3.2. Permeation Testing Procedure

The system used for permeation testing was shown previously in Figure 3.10. The permeation cell and gas reservoirs are fully contained in a temperature controlled box. The box was controlled by an RTD temperature controller connected to a small heating tape. A 5 inch axial fan was used to provide temperature uniformity within the box. The temperature controller can be used to regulate the system temperature between 25 and 75 ^{o}C; all of the permeation measurements in this work were performed at 35 ^{o}C. A two stage, mechanical vacuum pump (BOC Edwards, RV3 Rotary Vane Pump) was used to provide vacuum for the upstream and downstream of the system. The vacuum pump was equipped with a foreline trap containing replaceable aluminia to prevent vacuum pump oil from contaminating the vacuum lines. The system upstream pressure was measured using a 0-1000 psia pressure transducer from Honeywell Sensotec, Columbus, OH. The downstream pressure was measured with a 0-10 torr absolute pressure transducer from MKS Instruments, Inc., Wilmington, MA. The output from the downstream pressure transducer was sent to a five channel digital readout, which sends output to a Keithly KCPI-3107 data acquisition board that is connected to a desktop computer. Labview 6.0 data acquisition software was used to record the downstream pressure during the permeation experiment.

Once the membrane was masked and the permeation cell was connected to the permeation system, the downstream was evacuated for at least 15 minutes, and then

the upstream was also evacuated. Pulling vacuum on the downstream first served two purposes: 1) if the membrane has a major leak, the upstream pressure will decrease noticeably while only the downstream is being evacuated and 2) this procedure makes sure that the upstream pressure is never lower than the downstream pressure. Since the upstream side of the membrane is not supported, a lower upstream pressure can break a membrane or cause the mask to fail. The entire system was evacuated for a minimum of 12 hours prior to testing a membrane. This time under vacuum allowed the system to “degas” removing gases and vapors that may have sorbed in the system, the membrane, and the mask prior to testing.

After the system was degassed, a leak test was performed on the system. The leak rate was tested before any gases are run. This test was performed by closing the upstream and downstream vacuum valves and measuring the pressure rise in the downstream for several hours. This pressure rise was subtracted from the dp/dt measured for the pure gas permeations.

With the leak test completed, the entire system was evacuated again for at least 15 minutes. Next, the upstream reservoir was sealed off from the rest of the system and filled with the desired gas. Once the appropriate pressure was obtained, the system was closed and allowed to sit for ≥15 minutes to allow the gas and system temperature to equilibrate. Once the temperature had equalized, the gas was introduced to the upstream side of the membrane to begin the permeation test. Most of the permeation data in this work was collected with an upstream pressure of 50 psia, which is a common pressure used in membrane material research. If the pressure did not immediately spike, indicating a leak, the downstream valve was closed and the downstream pressure was recorded to provide the data for calculation of permeability. Upon completion of the

permeation test for a specific gas, the entire system was evacuated for an amount of time equal to at least three time lags before beginning the next gas to provide plenty of time for the membrane to fully degas.

After testing all of the gases for a sample, the membrane was removed from the permeation cell, and the sandwiched portion was cut out and retained. The membrane was then measured to allow permeability calculations. The thickness of the membrane was measured with a mechanical micrometer (B.C. Ames Co., Watham, MA, ±0.0001 inches) in several locations and the average value used. If epoxy was not used in a test, the diameter of the circle in the upstream side of the mask was used to calculate the area of the membrane, but if epoxy was used in the test, the membrane was scanned (Hewlett-Packard Scanjet 3970) and the area of the membrane was analyzed using Scion Image (Scion Corporation, Frederick, MD, version Beta 4.0.2) image processing software. Figure 3.13 shows a typical image used to analyze area. The thickness, area, and dp/dt are values needed for each individual membrane/gas combination to calculate the permeability using Equation 3.1.

Figure 3.13 Membrane images were scanned to allow area analysis when epoxy was used to seal the membrane mask.

3.2.4. Gas Sorption Measurements

Pressure decay sorption is a useful tool for evaluating the sorption of gases when pressures exceed 1 atm for various materials including polymers and molecular sieves [20, 21]. Figure 3.14 shows the apparatus used to perform pressure decay sorption. The sorption analysis of powders requires the use of a sample holder in the sorption system that is not required with larger samples. The sorption work presented here was performed on powder samples of carbon molecular sieves. Because this method of sorption analysis relies on the ability to perform a mole balance in the system, the volumes of the gas reservoir, sample chamber, sample holder, and sample (from density) must be known.

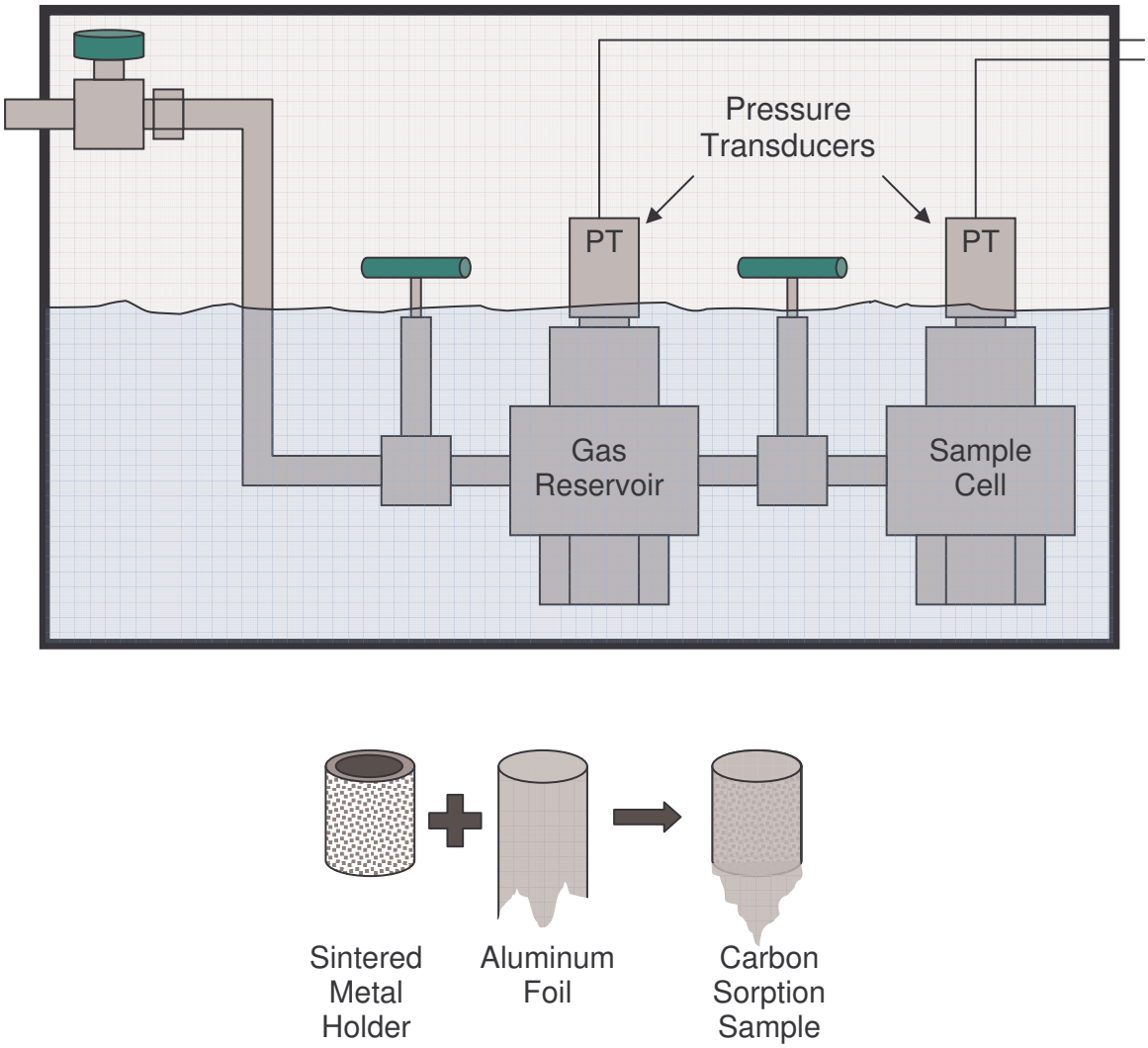

Figure 3.14 Pressure decay sorption was performed in this system. The detail of the sample holder is shown as well.

First, the samples must be dried prior to testing. The CMS powder was heated to 200 ^{o}C in a vacuum oven overnight prior to loading in the sorption system. The sample holder used for the powders was a 0.5 μ inline filter from Swagelok® (part # SS-8F-K4-05). The sample holder was then wrapped with aluminum foil to prevent the escape of the powder sample during testing. The sample holder is necessary to prevent powder from being pulled into parts of the sorption system other than the sample chamber during the analysis. The volume of the foil used is included in the sample holder volume because

the available volume in the sorption cell is critical to the mole balance used in sorption calculations. With the sample prepared, it is sealed in the sample chamber using a ¾ inch VCR gasket. The sorption cells are then reconnected with the rest of the sorption system.

Both the gas reservoir and the sample cell are fully immersed in a temperature controlled water bath to insure constant temperature during testing. The pressure transducers (0-1000 psia, Ametek Aerospace, Wilmington, MA) are not fully submerged in the water bath, but they are enclosed in an insulated chamber during the test to reduce fluctuations caused by ambient temperature changes during the experiment. Once the sample is loaded and the cells are reconnected, the entire sorption system is evacuated for at least 12 hours to remove gases and vapors that may have sorbed in the system or the sample prior to testing.

After the sample has degassed, the sorption test is started by introducing gas into the reservoir and recording the pressure. The valve separating the reservoir from the sample cell is then opened for just a few seconds and then closed again. When the valve is opened, some of the gas in the reservoir moves into the sample chamber. The pressure of both chambers is then carefully recorded as the gas in the sample chamber equilibrates with the sample. As the sample sorbs gas from the sample chamber, the pressure in the chamber falls until the system has reached equilibrium, and then the pressure in the sample chamber will become constant. The pressure of the reservoir and sample chamber at equilibrium can then be used in a simple mole balance before and after the pressure step to determine the amount of gas that has sorbed into the sample; however, it is important that compressibility factors for the gases be considered

due to the high pressures often used. The pressure in the reservoir is then changed and the cycle is repeated until the isotherm is completed.

In samples with regular geometries (uniform spheres, cylinders, flat sheets, etc.) the sorption kinetics can be used to determine the gas diffusivity [22]; however the size distribution of the molecular sieves used in this study is not known with enough certainty to allow this modeling. Even if the size distribution was very well known, the fact that the particle size is polydisperse rather than monodisperse would also make evaluation of diffusivities through kinetics extremely challenging [22]. Some qualitative comparisons are still possible between samples that have been processed in very similar ways, but quantitative measurements are not possible at this time.

3.2.5. Other Characterization Methods

Several other characterization techniques were used to varying degrees throughout this research. The general procedures for sample preparation and analysis will be given in this section.

3.2.5.1. TGA

Thermal gravimetric analysis (TGA) is a tool that allows the mass of a sample to be accurately measured during a well controlled temperature profile in a selected atmosphere. TGA experiments were performed on a Netzsch STA 409 PC Luxx TGA/DSC. The TGA may be operated under various purge gases or under vacuum conditions. Samples can be heated to temperatures in excess of 1500 ^{o}C at heating rates from about 1-20 ^{o}C/min. Sample sizes range from 10 mg up to about 10 g with the lower limit being set by the sensitivity of the balance and the upper limit by the size of the sample holder. When small weight changes are expected, larger samples were

used to provide greater resolution. The TGA is useful for studying a range of processes including drying effectiveness, weight loss during pyrolysis, or weight loss due to decomposition of modifiers. Because of the wide range of applications, no standard protocol exists for sample preparation across the entire spectrum, but samples were prepared in a fashion that very closely resembled the preparation they would undergo prior to the process being analyzed at the time.

3.2.5.2. FTIR

Fourier transform infrared spectroscopy provides information about the functional groups present in a sample. More specifically, bonds in a sample that can generate a dipole-dipole moment will be active to FTIR spectroscopy. The samples in this work were tested on a Bruker Tensor 27 FTIR with a Harrick MVP_2 micro ATR attachment. The ATR attachment allows samples to be tested when transmittance is not possible. The ATR attachment is well suited for testing film samples, and it is also equipped with a powder sample holder. The ATR has a slip wrench attachment that provides a consistent pressure to hold the samples against the SiO_2 crystal. Samples used for FTIR/ATR analysis were dried in a vacuum oven at 110 ^oC for at least 12 hours prior to testing to reduce the moisture content of the samples.

3.2.5.3. WAXD

Wide angle x-ray diffraction (WAXD) is useful in the analysis of angstrom scale crystalline structures. The WAXD results presented in this work were collected by P. Jason Williams using a Phillips Panalytical X-ray diffractometer with a Cu K_α source in the Nair research group at the Georgia Institute of Technology. All analyses were performed using either an X'pert Pro detector or a Miniprop detector with parallel plate collimator.

3.2.5.4. SEM

Scanning electron microscopy (SEM) can be used to directly observe some of the morphological characteristics of hybrid membranes including some information about the interface between the two phases and the distribution of sieves in the membrane. While the resolution is not small enough to clearly show the presence of angstrom scale defects believed to exist in some membranes, it can show larger voids that may occur in the film [3]. SEM samples are prepared by immersing a piece of a hybrid membrane in liquid nitrogen for at least 30 seconds and then breaking the piece to expose a cross section of the film. The samples are then mounted onto a metal sample holder using conductive carbon tape. The samples were tested using a Hitachi S-800 field emission scanning electron microscope (Hitachi High-Technologies Corporation, Tokyo, Japan). Because of the tendency of the polymer samples to charge during sampling, accelerating voltages of 10kV or less were used.

3.2.5.5. XPS

X-ray photoelectron spectroscopy (XPS), also known as electron spectroscopy for chemical analysis (ESCA), was used to analyze the atomic composition of the surface of CMS samples. XPS samples were prepared by drying at 200 ^{o}C overnight prior to loading in the analyzer. Samples would then be degassed in the XPS analyzer overnight prior to performing the analysis due to the need to maintain ultra high vacuum during the analysis. XPS analysis was performed with the assistance of Dr. Brent Carter of the School of Materials Science and Engineering at the Georgia Institute of Technology.

3.2.5.6. GPC

Gel permeation chromatography was used to analyze the molecular weight of various polymer samples generated during this work. The samples were prepared as 8 wt% polymer in THF. The analysis was performed by James Russum in the School of Chemical and Biomolecular Engineering at the Georgia Institute of Technology. The samples were analyzed based on a polystyrene standard, and while the numbers may not provide absolute quantitative results, they are accurate enough to provide estimates and applicable for qualitative comparison.

3.3. References

1. Vu, D.Q. (2001). Formation and Characterization of Asymmetric Carbon Molecular Sieve and Mixed Matrix Membranes for Natural Gas Purification. Chemical Engineering. Austin, TX, The University of Texas at Austin. Doctor of Philosophy.
2. Coleman, M.R. (1992). Isomers of Fluorine-Containing Polyimides for Gas Separation Membranes. Chemical Engineering. Austin, The University of Texas at Austin. Doctor of Philosophy: 262.
3. Moore, T.T. (2004). Effects of Materials, Processing, and Operating Conditions on the Morphology and Gas Transport Properties of Mixed Matrix Membranes. Chemical Engineering. Austin, TX, The University of Texas at Austin. Doctor of Philosophy: 312.
4. Steel, K.M. (2000). Carbon Membranes For Challenging Gas Separations. Chemical Engineering. Austin, TX, The University of Texas at Austin. Doctor of Philosophy.
5. Williams, P.J. (2006). Analysis of Factors Influencing the Performance of CMS membranes for Gas Separation. School of Chemical and Biomolecular Engineering. Atlanta, Georgia Institute of Technology. Doctor of Philosophy: 238.
6. Geiszler, V.C. (1997). Polyimide Precursors For Carbon Molecular Sieve Membranes. Chemical Engineering. Austin, TX, The University of Texas at Austin. Doctor of Philosophy.
7. Jones, C.W. and Koros, W.J. (1994). "Carbon Molecular-Sieve Gas Separation Membranes.I. Preparation and Characterization Based on Polyimide Precursors." Carbon 32(8): 1419-1425.
8. Jones, C.W. and Koros, W.J. (1995). "Characterization of Ultramicroporous Carbon Membranes with Humidified Feeds." Industrial & Engineering Chemistry Research 34(1): 158-163.
9. Jones, C.W. and Koros, W.J. (1994). "Carbon Molecular Sieve Gas Separation Membranes-II. Regeneration Following Organic Exposure." Carbon 32: 1427-1432.
10. Jones, C.W. and Koros, W.J. (1995). "Carbon Composite Membranes: A Solution To Adverse Humidity Effects." Industrial and Engineering Chemistry Research 34: 164.

11. Wallace, D.W. (2004). Crosslinked Hollow Fiber Membranes for Natural Gas Purification and Their Manufacture from Novel Polymers. Chemical Engineering. Austin, The University of Texas at Austin. Doctor of Philosophy: 221.
12. Bahr, J. L. and Tour, J.M. (2001). "Highly Functionalized Carbon Nanotubes Using in Situ Generated Diazonium Compounds." Chemistry of Materials 13: 3823-3824.
13. Liu, Y., Wang, R., et al. (2001). "Chemical Cross-Linking Modification Of Polyimide Membranes For Gas Separation." Journal of Membrane Science 189: 231-239.
14. Tin, P.S., Chung, T.S. (2003). "Effects Of Cross-Linking Modification On Gas Separation Performance Of Matrimid Membranes." Journal of Membrane Science 225: 77-90.
15. Carey, F.A. (1996). Organic Chemistry. New York, McGraw-Hill.
16. Mahajan, R. (2000). Formation, Characterization and Modeling of Mixed Matrix Membrane Materials. Chemical Engineering. Austin, The University of Texas at Austin. Doctor of Philosophy: 259.
17. Moore, T.T. (2004). Effects of Materials, Processing, and Operating Conditions on the Morphology and Gas Transport Properties of Mixed Matrix Membranes. Chemical Engineering. Austin, TX, The University of Texas at Austin. Doctor of Philosophy: 312.
18. Obrien, K.C., Koros, W.J., et al. (1986). "A New Technique for the Measurement of Multicomponent Gas-Transport through Polymeric Films." Journal of Membrane Science 29(3): 229-238.
19. Pye, D.G., Hoehn, H.H., et al. (1976). "Measurement of Gas Permeability of Polymers.1. Permeabilities in Constant Volume-Variable Pressure Apparatus." Journal of Applied Polymer Science 20(7): 1921-1931.
20. Costello, L.M. and Koros, W.J. (1992). "Temperature-Dependence of Gas Sorption and Transport-Properties in Polymers - Measurement and Applications." Industrial & Engineering Chemistry Research 31(12): 2708-2714.
21. Koros, W.J. and Paul, D.R. (1976). "Design Considerations for Measurement of Gas Sorption in Polymers by Pressure Decay." Journal of Polymer Science Part B-Polymer Physics 14(10): 1903-1907.
22. Zimmerman, C.M., Singh, A., et al. (1998). "Diffusion In Gas Separation Membrane Materials: A Comparison And Analysis Of Experimental Characterization Techniques." Journal of Polymer Science Part B-Polymer Physics 36(10): 1747-1755.

CHAPTER 4

IMPACT OF PROCESSING ON CARBON MOLECULAR SIEVE STRUCTURE AND PERFORMANCE

Chapters 1 and 2 emphasized the importance of carefully selecting the components in the development of a hybrid material system. In the formation of hybrid gas separation membranes, it is important to know the transport properties of the component materials that are used. It is of particular interest to know if the processing steps used in the formation of the hybrid material impact the properties of the components. If the properties change during the formation process, the changes must be considered in the engineering and analysis of these materials. This chapter discusses the changes that occur in the carbon molecular sieves when they are processed for hybrid membrane formation.

Previous researchers have performed substantial analysis to establish a base of knowledge about the CMS material used in this work. The carbon was produced from the pyrolysis of Matrimid® powder in an inert atmosphere at 800 ^{o}C for 2 hrs (CMS-800-2). The transport properties determined from analogous dense film characterization are given in Table 4.1. These values will serve as a basis of comparison for the analysis performed on the processed CMSs.

Table 4.1 Properties of Carbon Molecular Sieve CMS-800-2

Micropore Volume[1]	*Skeletal Density[1]*	*Bulk Density[1]*
0.186 cm^3/g	1.69 g/cm^3	1.29 g/cm^3

Permeability (Barrer)[2]		*Selectivity[2]*	
O_2	CO_2	O_2/N_2	CO_2/CH_4
24	43.5	13.3	200

4.1. Effects of Milling on Carbon Structure

It has been established that the pore size distribution of a CMS is the factor that most strongly influences the transport properties of the material [3, 4]. Chapter 2 discussed the importance of producing carbon with the appropriate pore size, and this carbon must maintain its transport properties during the formation of the hybrid membrane. One of the first steps in CMS preparation is to produce particles of appropriate size. As mentioned earlier, submicron particle sizes are desirable because of the very thin selective layer of asymmetric hollow fibers. Because the carbon used in this work was not produced in these sizes, it was necessary to ball mill the carbon into a powder with much smaller size particles. Initially, it was believed that the particles produced from this milling process would possess essentially the same physical properties as the bulk carbon starting material. However, the following discussion demonstrates how the milling process actually alters the properties of the material.

4.1.1. Particle Size

The primary motivation for the milling process was to provide carbon particles of submicron sizes. The process was successful in this regard. The carbon used in this work was produced from Matrimid® powder containing polymer particles with approximately 20-100 μ diameters. During the pyrolysis process, many of these polymer

particles clumped together, and the characteristic size of the newly formed CMS was predominantly ≥ 100 μ. After milling the carbon for 90 minutes in the ball mill, the majority of the carbon particles were reduced to submicron dimensions with a few remaining particles in the 1-10 μ range. Finally, the powder was suspended in solvent through the use of an ultrasonic bath, and the resulting suspension was then allowed to sit for at least 6 hours before decanting. This step removed many of the larger particles leaving primarily submicron CMS. Figure 4.1 shows scanning electron micrograph (SEM) images of the CMS particles produced from each stage of the process. The decanted carbons were recovered and analyzed with DLS to determine the average particle size. The average value returned from DLS for the particle suspensions tested was in the range of 150-250 nm for the particle diameters. These values agree fairly well with the image shown in Figure 4.1d showing the decanted carbon. This process has successfully allowed the CMS used in this work to be converted into submicron particles, but further analysis shows that this process has altered the structure and properties of the carbon material.

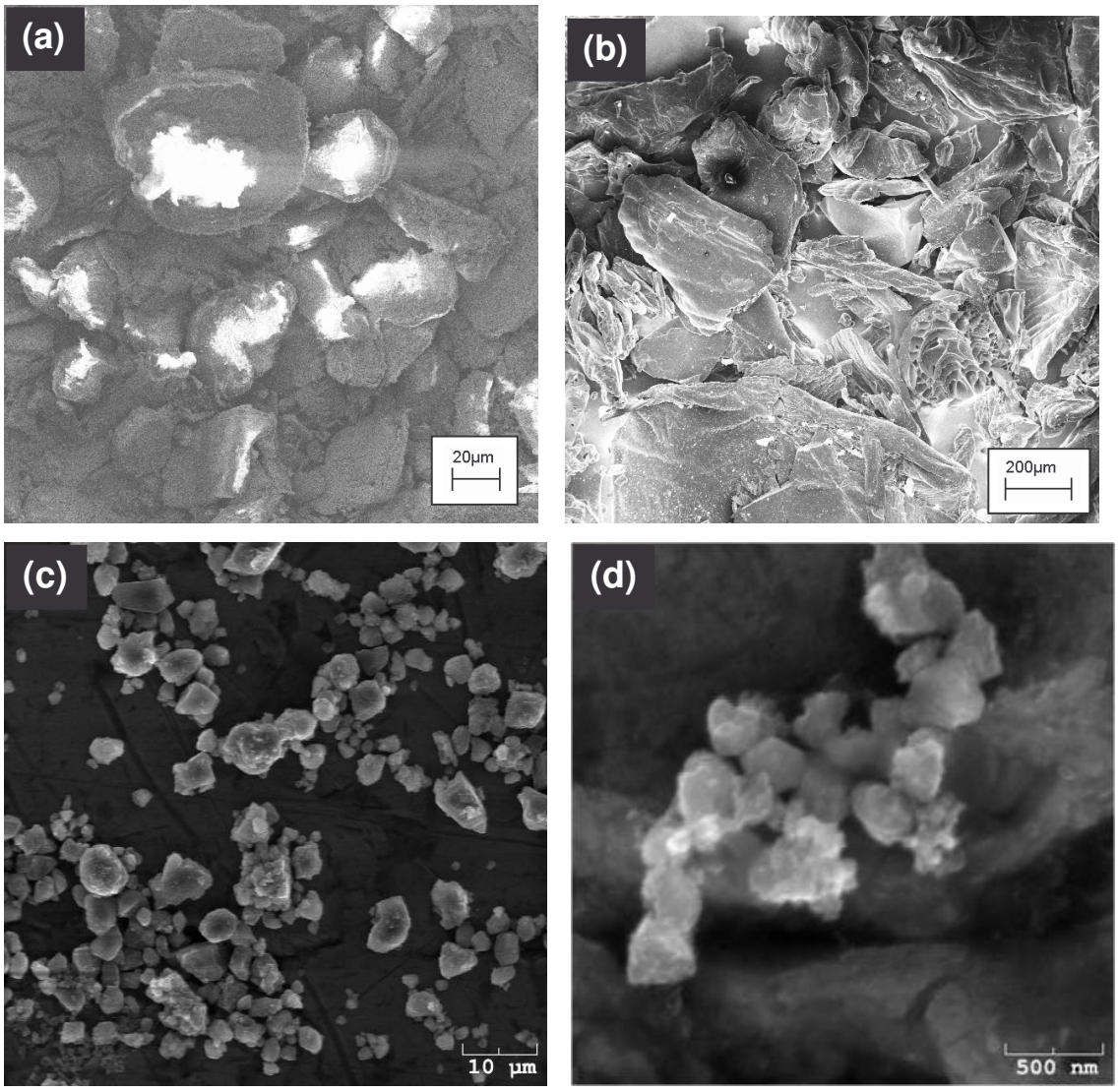

Figure 4.1 SEM images show the differences between the particle sizes of various samples of carbon molecular sieve particles and precursors: (a) Matrimid® powder, (b) CMS 800-2, (c) CMS 800-2 ball milled in air, and (d) CMS 800-2 ball milled in air and decanted after 6 hrs.

4.1.2. Equilibrium Sorption

The transport properties of the CMS are the most important characteristics for this work, and they must be monitored during the processing of the material. One of the best tools for analysis of transport properties in a powder is equilibrium sorption. Because the sorption capacity is a material property, it is not dependent on the geometry of the sample; therefore, size, amount, and shape of the material being tested do not affect the properties measured. As a result, the sorption in the carbon material would be

consistent for all of the samples, regardless of how they were milled, if the processing did not affect the sorption properties. Figure 4.2 shows the nitrogen and carbon dioxide sorption isotherms for CMS that has not been milled and for CMS that has been milled in air.

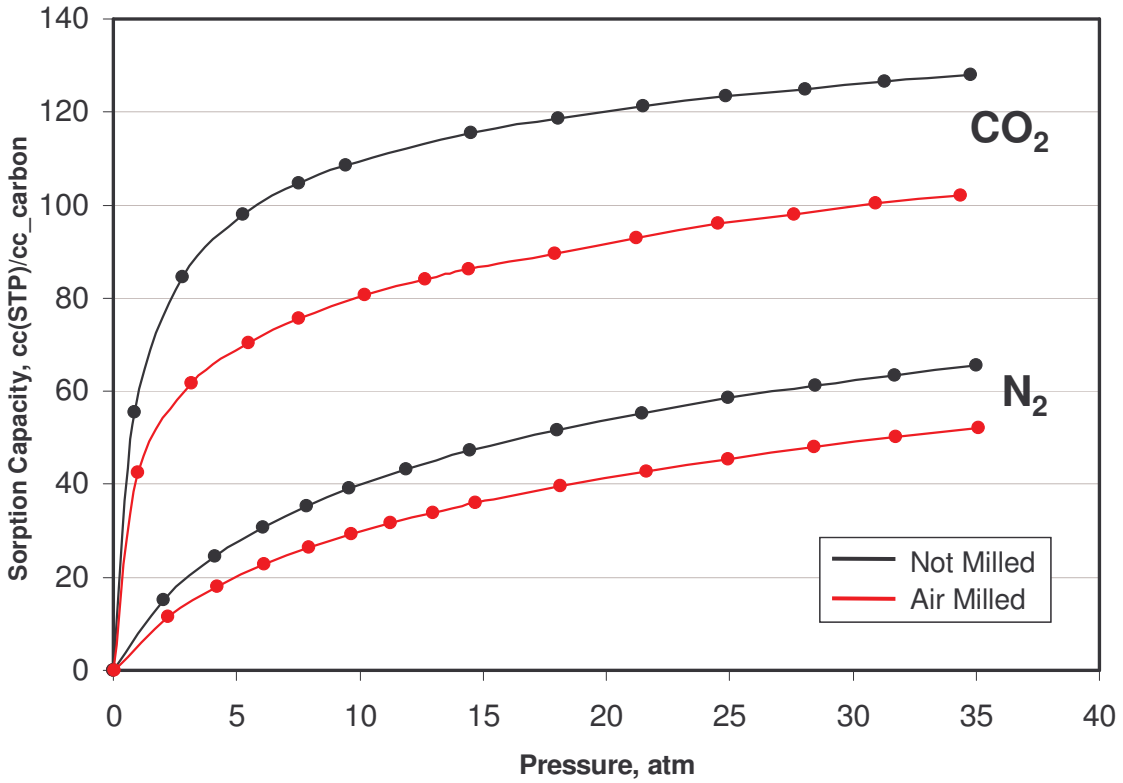

Figure 4.2 Equilibrium sorption changes significantly for carbon molecular sieves after ball milling. Sorption tested at 35 °C.

As this figure shows, the sorption capacity for the CMS was significantly reduced by ball milling. Because these sorption curves represent equilibrium sorption values, it is also clear that the change in sorption capacity is not just the result of a change in the surface characteristics of the carbon, but a change in the overall structure. One possible explanation for this change is the destruction of mesopores that exist in the particle clusters as they are broken apart during the ball milling procedure. If this is the primary cause of the changes, the atmosphere used during milling should not have a major

impact on the sorption properties of the resulting material. In order to test this relationship, some of the CMS was milled in an enriched nitrogen atmosphere. Rather than sealing the milling vial under ambient atmosphere, the vial was placed in a glove bag and purged with nitrogen several times before sealing in order to greatly reduce the oxygen content during the milling process. Figure 4.3 shows the carbon dioxide, methane, and nitrogen sorption isotherms for all three types of carbon.

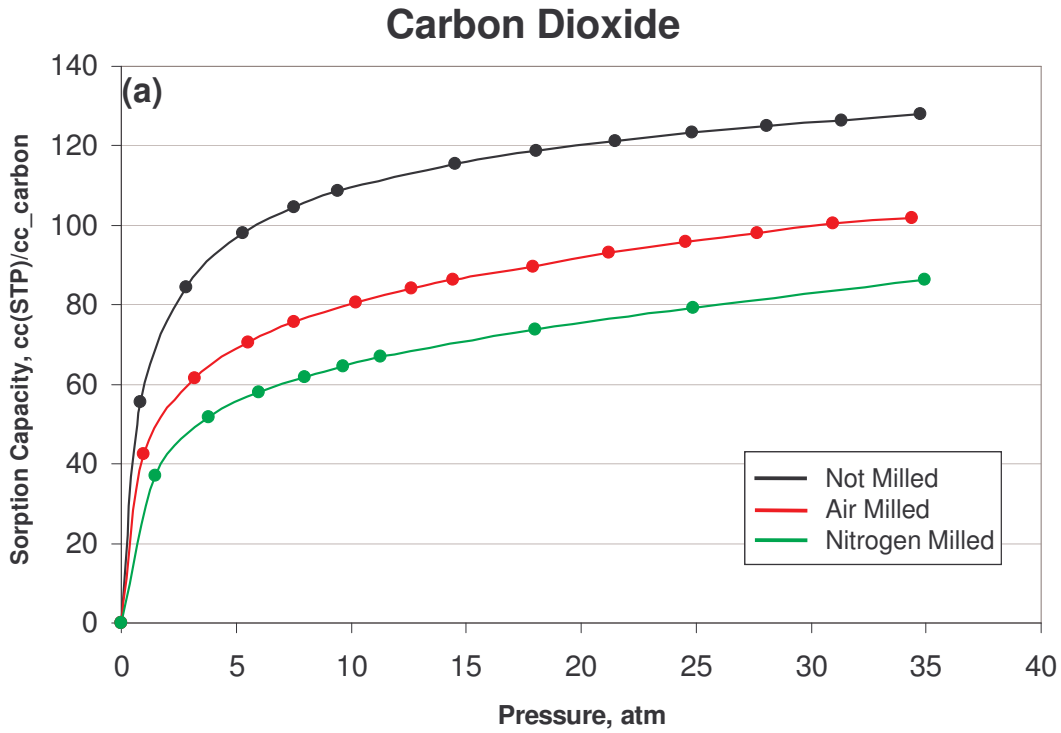

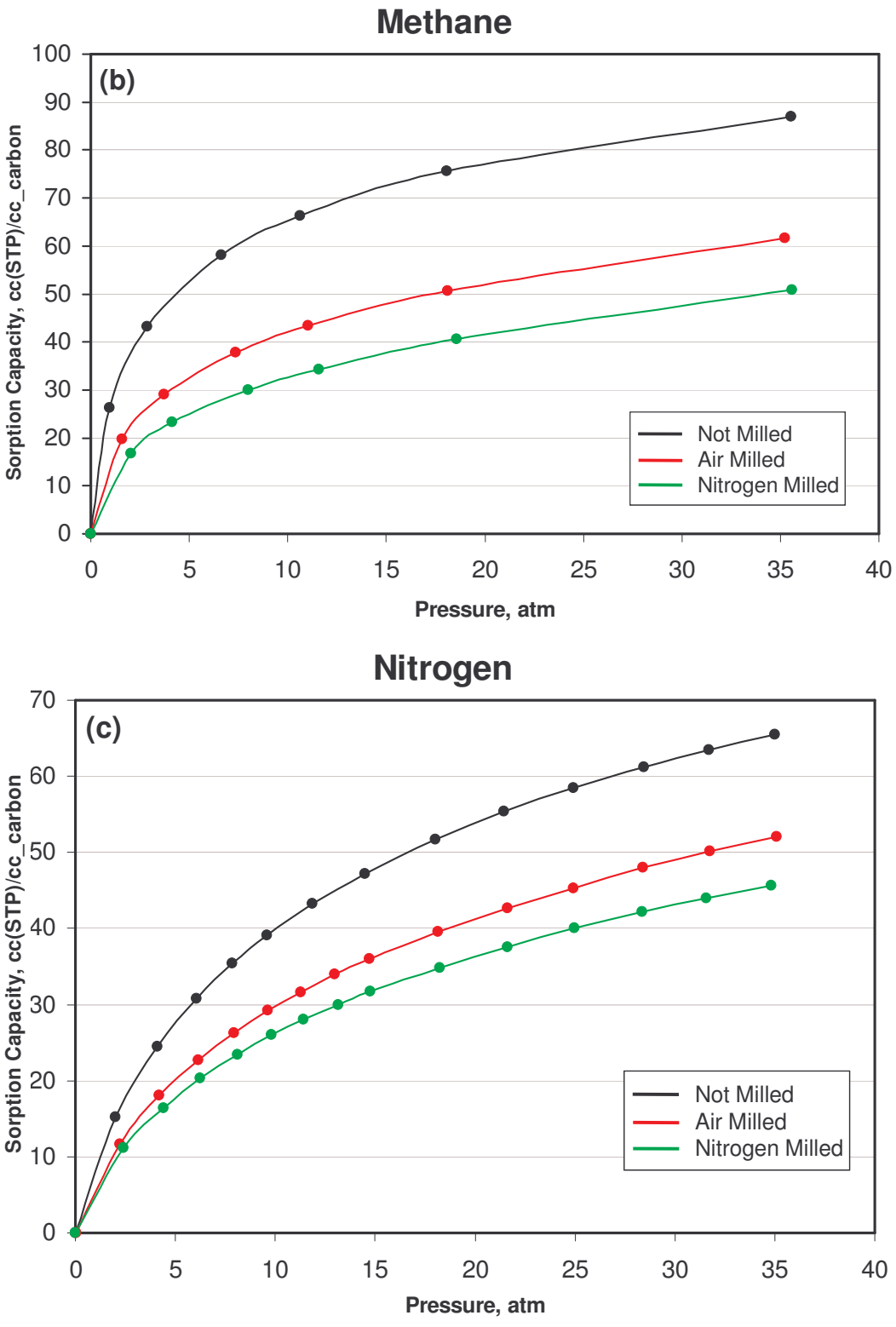

Figure 4.3 The ball milling atmosphere has a considerable impact on the equilibrium sorption capacity of the CMSs for various gases: (a) CO_2, (b) CH_4, and (c) N_2. Sorption tested at 35 °C.

Clearly, the sorption properties of the carbon are impacted not only by being milled into smaller particles, but also by the atmosphere present during the milling process. The changes in the CMS during milling were further studied by looking at the changes caused by two other milling conditions: 1) extensive milling by hand using a mortar and pestel and 2) milling in the ball mill for only 30 seconds. Figure 4.4 shows the carbon dioxide sorption isotherm for the five different milling states tested in this work.

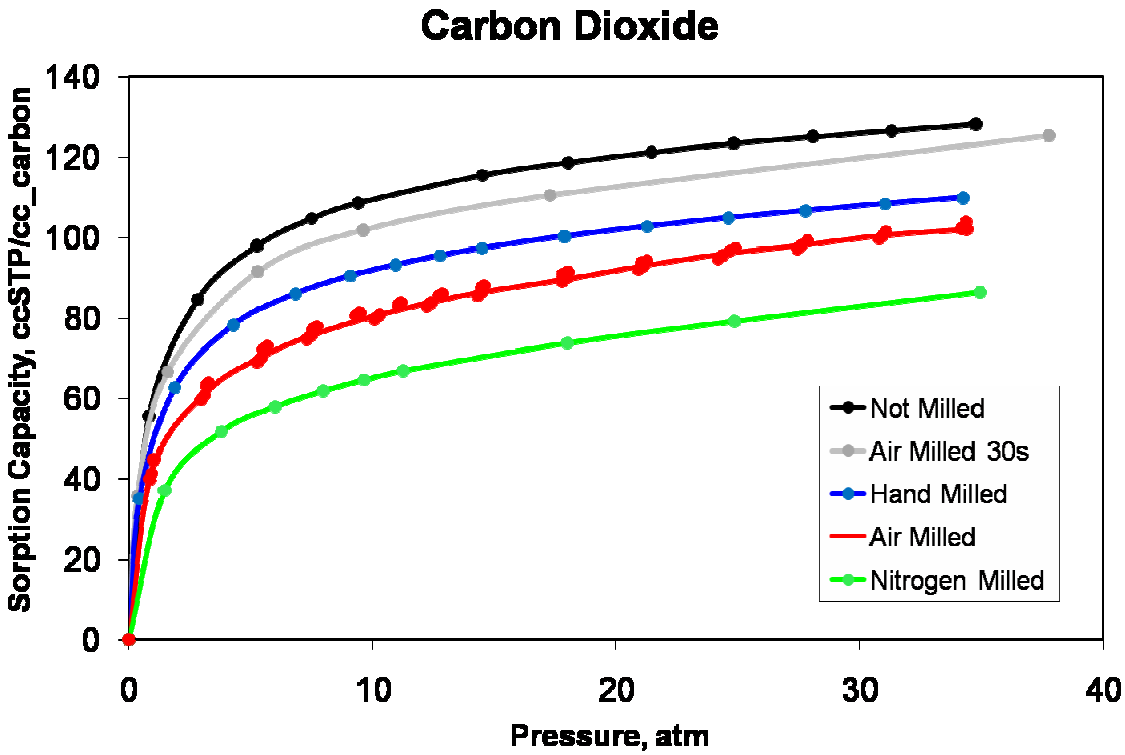

Figure 4.4 Carbon dioxide equilibrium sorption in CMS materials is very dependent on the milling process used to prepare the sample. Sorption tested at 35 °C.

It is evident from these tests that the sorption capacity of the milled CMS materials is very dependent upon the process used to mill the particles. Both the atmosphere and the milling type and duration impact the final properties of the material. As a result, the procedure used to produce the smaller particle sizes must remain consistent to eliminate additional variability from the products. Still, even though this work has shown considerable changes in the sorption properties of the CMS material, the previous work

by Vu et al. showed the ability of ball milled CMS to enhance the transport properties of hybrid membrane materials [2, 5, 6]. After considering these results, all of the carbon used for hybrid material formation in this work was produced by milling in air for 90 minutes and then decanting in dichloromethane for 6 hours. This process was selected for reproducibility and to provide better consistency between the remainder of this work, and previous work. To illustrate the reproducibility of the sorption measurements, the data from four separate sorption measurements are shown for the air milled sample in Figure 4.4. The four samples were from different batches of air milled carbon and tested using two different sorption systems.

4.1.3. Interplanar Spacing

An additional measure commonly used to analyze the structure of carbon molecular sieves is wide angle x-ray diffraction (WAXD). The average interplanar spacing between carbon planes in the CMS are given by the d-spacing of the WAXD measurements. Figure 4.5 shows the WAXD data for four of the milling conditions analyzed in this work. Chapter 2 discussed the amorphous nature of the CMS structure, and this characteristic is seen in the WAXD results presented in Figure 4.5. The presence of broad curves rather than sharp peaks is characteristic of amorphous materials; however, even without a sharp peak to provide a characteristic dimension, the location of the amorphous peak in the WAXD results can be used to provide important information about the relative structures of the different CMS materials [1].

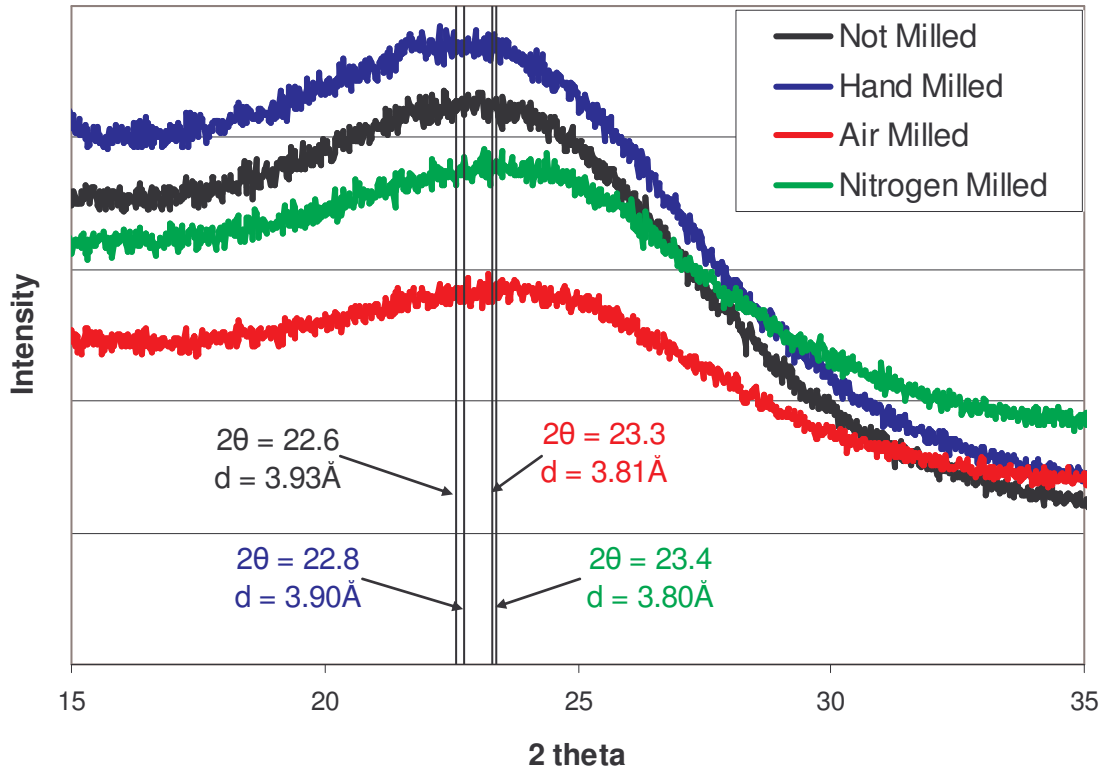

Figure 4.5 WAXD analysis of CMS samples shows changes in the average d-spacing when different milling processes are used.

It appears from the figure that there is a small shift in the average d-spacing of the carbon materials that have been milled under different conditions. In particular, the two samples prepared using the mechanical ball mill show reduced d-spacing in comparison to the sample milled by hand and the sample that was not milled. These data agree with the reduced sorption capacity for the ball milled samples as shown in Figures 4.2-4.4. Also, the shift in d-spacing seen in the WAXD results supports the hypothesis that the changes occurring in the carbon materials are not merely related to surface effects but to changes in the average structure of the material instead.

Another factor that appears in the WAXD analysis is the slight broadening of the amorphous peak in the ball milled samples. The broader peak indicates an increase in the disorder, or a further reduction in the regularity, of the d-spacing in the material. This

shift is in some ways similar to the destruction of crystallinity that was observed by Qiu et al. for the ball milling of cellulose acetate [7, 8]. The high energy of the ball mill was able to almost completely destroy the rugged crystalline structure of the cellulose acetate, and a similar increase in disorder was seen for this work. While the direct impact of these changes on the transport properties of the material are not fully understood, it is clear that the CMS structure was altered somewhat by the milling process. Further analysis with carbon dioxide adsorption was used to see how these changes relate to the pore size distribution in the CMSs as discussed in the next section.

4.1.4. Pore Size Distribution

Since the pore size distribution is such a major factor in the transport properties of the molecular sieves, carbon dioxide adsorption analysis was performed by Micromeretics Analytical Services for CMS that has not been milled and for CMS that has been milled in air. The primary goal was to determine if a clear shift in the pore size distribution could be seen in the samples after ball milling. Pore size analysis results are shown for the density functional theory model and the Dubinin-Astakhov model in Figures 4.6 and 4.7, respectively. Both differential and cumulative distributions are shown. The differential distributions show that the distribution of pore sizes was not greatly altered; however, the cumulative distributions agree with the results seen from the equilibrium sorption that the pore volume, which is related to sorption capacity, is reduced in the ball milled samples.

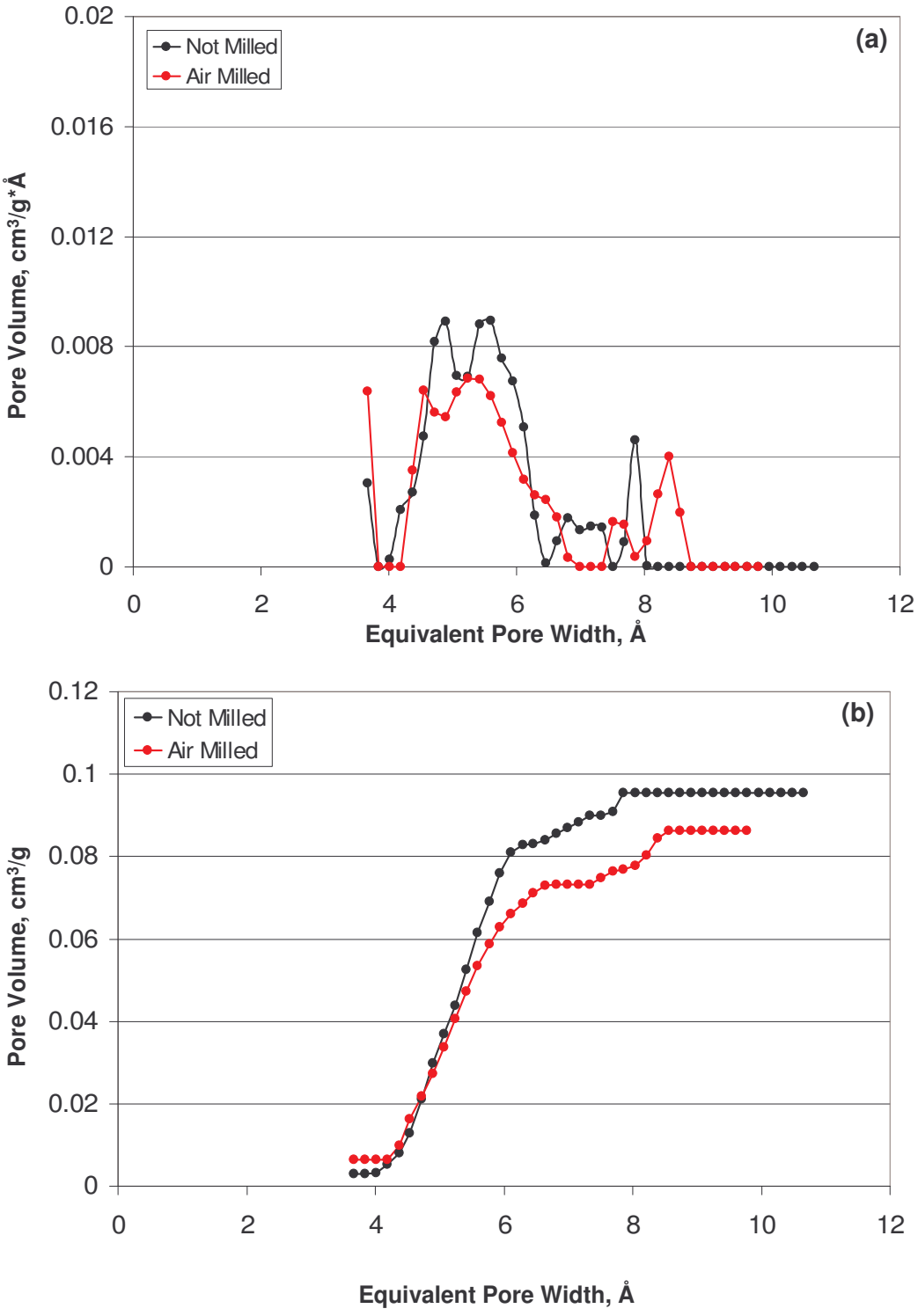

Figure 4.6 The density functional theory model was used with CO_2 adsorption analysis to provide data about the pore volume distribution of 4-10 Å pores in not milled and air milled CMS samples. Both differential (a) and cumulative (b) distributions are shown.

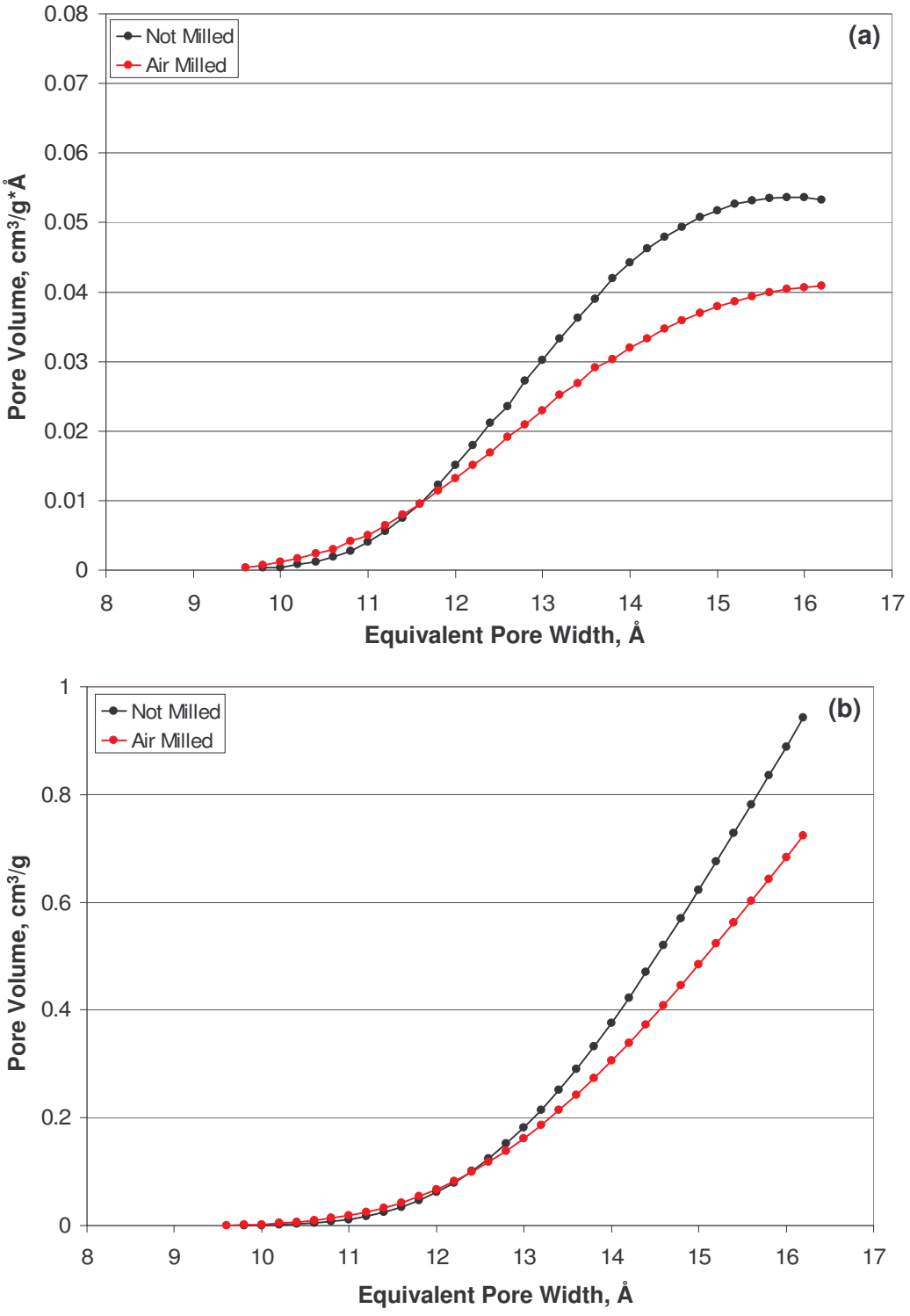

Figure 4.7 The Dubinin-Astakhov model was used with CO_2 adsorption analysis to provide data about the pore volume distribution of 10-16 Å in not milled and air milled CMS samples. Both differential (a) and cumulative (b) distributions are shown.

Since the sorption capacity for the carbon is reduced, it follows that the permeability would be similarly reduced. Unfortunately, current understanding does not allow direct prediction of the transport properties based only on sorption and porosity data, so the dense film data will still be used as the modeling basis for the analysis presented in this work. These data further support the need for consistency in the processing steps used to prepare the CMSs for incorporation in the hybrid matrix.

4.2. Surface Modification of Carbon Molecular Sieves

In order to improve the interfacial region of the hybrid membranes, the CMS surface was chemically modified with a linkage unit capable of covalently bonding the polymer to the sieve. The development of this modification process is discussed in this section.

4.2.1. Surface Chemistry

There are many types of preparation techniques available to engineer the CMS surfaces. One approach is to change the surface chemistry of the sieve itself. Chemical treatments can be used to strongly oxidize or reduce the surface in order to improve the "inherent" polymer-sieve interaction. One of the primary drawbacks of this technique is the likelihood of altering not only the external surface of the particle, but also altering the internal surface of the pore walls. Changes to the pore walls can lead to undesirable changes in the transport properties of the CMS. A more direct approach is to treat the surface of the sieve with a linkage group designed to directly bond the sieve to the polymer chain. This technique was selected for this work because it should result in a stronger, more resilient bond between the sieve and the polymer. Still, it introduces the need to carefully engineer the linkage unit to provide the desired interfacial properties.

Many of the interfacial issues faced by this project are very similar to complications present in the preparation of other composite materials such as those containing carbon fibers [9-22] and carbon nanotubes (CNTs) [23-35]. Even though the underlying motivations may be different, all of these materials benefit from good contact and strong adhesion between the inserts and the matrix. Another similarity is the difficulty often encountered in the chemical analysis of these high carbon content materials. Because of the extremely absorptive nature of the carbon structures, spectroscopic analytical techniques that are frequently used in the analysis of other materials such as polymers are commonly overwhelmed by these materials [10, 11, 22, 26, 27]. This problem limits the amount of specific information that is available about the surface chemistry and molecular composition of these compounds. However, atomic analytical techniques, such as XPS, are still able to provide important elemental analysis of the surfaces.

Because of the inherent difficulties in the detailed analysis of the molecular structure on the surface of these materials, the actual reactions resulting in modification of the surfaces and bonding agents to the surface are not precisely known. It *is* known that most CMS materials are in excess of 90% carbon, potentially leaving few reactive groups on the surface to aid the modification [1, 36]. However, techniques that have shown successful modification of CNTs, which have even higher carbon content and much more pristine surfaces, have potential to exploit the less “perfect” surface of the CMS particles sufficiently to provide a change in their effective surface chemistry.

Bahr and Tour demonstrated the ability to modify single-wall carbon nanotubes (SWNTs) by using diazonium chemistry to attach a primary aromatic amine to the surface as shown in Figure 4.8 [26]. Orthodichlorobenzene and tetrahydrofuran were used as solvents, and isoamyl nitrite was used as a catalyst to create the diazonium groups. The

reaction was conducted at 60 °C for 24 hours. After thorough washing, including repeated sonications, the modifying groups were still attached to the SWNTs as indicated by Raman spectroscopy.

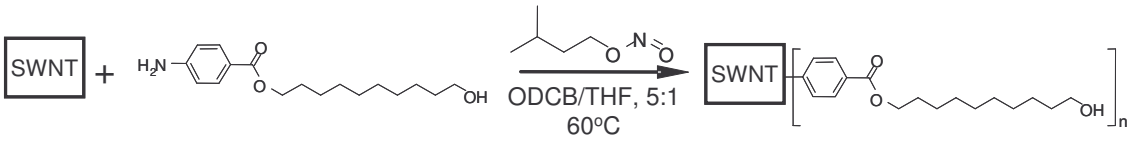

Figure 4.8 A primary aromatic amine was used to modify the SWNT surface [26].

This procedure was then adapted for use with the carbon molecular sieves produced for this work. The CMSs were substituted in the place of the SWNTs, and rather than using the primary aromatic amine described in the the work by Bahr and Tour, another primary aromatic amine was used. Apart from these two changes, the same procedure developed for the modification of SWNTs was followed for the modification of the CMS particles, and this basic reaction procedure was described in Chapter 3. Figure 4.9 shows the adapted reaction process used to modify the surface of the CMSs.

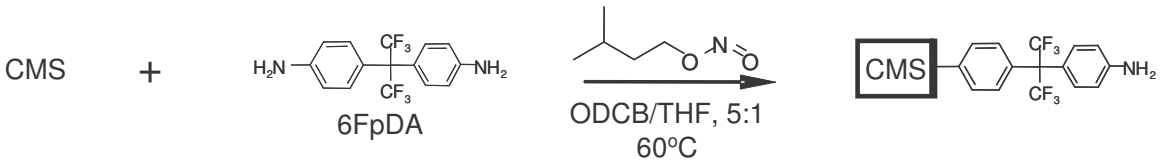

Figure 4.9 The SWNT modification shown in Figure 4.8 was adapted for use in the modification of CMS particles.

The attractions to this method of surface modification are two fold. 1) The modification reaction requires only one step for completion keeping the process simplified. 2) Primary amine groups have shown the ability to open the imide rings in the polymer backbone and form a covalent bond with the polymer (see Chapter 5) [37, 38]. As a result, the appropriate molecule containing terminal primary amine groups should have the ability to bond both to the surface of the sieve and to the polymer backbone.

4.2.2. Linkage Units

In addition to developing a chemical pathway to bond to the surface of the CMSs, it was necessary to determine the appropriate linkage agent to control the interface. Several aspects of this linkage unit influence the selection: rigidity, chemical composition, bulky groups, and length. Table 4.2 shows some potential linkage units along with some of their advantages and disadvantages. If the linkage agent is too flexible, then there is greater potential for both amine groups to bond to the surface of the sieve, preventing the desired covalent bond with the polymer. The chemical composition of the linkage unit is important because the linkage unit should improve the interaction between the sieve and the polymer. The presence of bulky groups in the linkage units may have a significant impact on the transport of gas molecules in the interfacial region. In contrast, a linkage molecule that is too small may have a greater tendency to plug the pores of the sieves. The overall length of the linkage unit must also be controlled. Potentially, a linkage that is too long may prevent the polymer from forming the necessary tight bond around the inserts, but if the linkage is too short, it may not possess the mobility needed to bond effectively with the polymer molecules. These characteristics must be considered, and the following candidate list illustrates some of the analysis considered during the selection process.

Table 4.2 Potential linkage units to improve the polymer-CMS interface.

Chemical Structure (name)	*Advantages*	*Disadvantages*
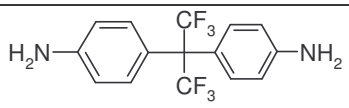 (6FpDA)	good polymer interaction rigid structure covalent linkage possible	bulky groups long molecule two bonds to surface?
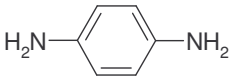 (1,4-phenylenediamine)	very rigid (linear) covalent linkage possible less likely to bond to surface twice	has bulky ring group little flexibility to bond with the polymer
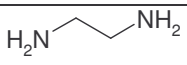 (ethylenediamine)	small molecule covalent linkage possible	may diffuse into pores two bonds to surface?
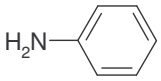 (aniline)	only one bond to surface modifies “surface” groups should not diffuse in pores	no covalent linkage has bulky ring group
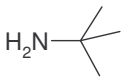 (tert-butylamine)	only one bond to surface modifies “surface” groups should not diffuse in pores	no covalent linkage
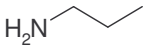 (propylamine)	only one bond to surface modifies “surface” groups	no covalent linkage may diffuse in pores

4.3. Impact of Modification on Sieve Properties

After considering these characteristics, 1,4-phenylenediamine was selected as the most desirable modifier based on the selection criteria listed above. It was used for the majority of the modification work presented here, but some initial modification trials were conducted using 6FpDA as the modifier. This compound was selected for initial testing for several reasons: 1) it contains fluorine which can be used with atomic analysis to verify the success of the modification, 2) it is one of the monomers for the polymer, which should lead to good interactions, 3) the bulky phenyl rings and fluorine groups

should prevent the molecule from diffusing into the pores of the sieve, and 4) the rigid structure and two amine groups should allow one end to bond to the carbon while the other remains available to bond with the polymer.

X-ray photoelectron spectroscopy (XPS) was used to analyze the atomic content of the surface of carbon particles before and after modification with 6FpDA. Figure 4.10 shows the results of this analysis, and Table 4.2 shows the atomic percentages for these samples. The most important characteristic is the presence of fluorine only after the modification. Since the XPS analysis of modified carbon was performed after vigorously washing four times with an ultrasonic horn, it is likely that the remaining fluorine persisted as a result of 6FpDA that was covalently bonded to the surface of the CMS particles [39].

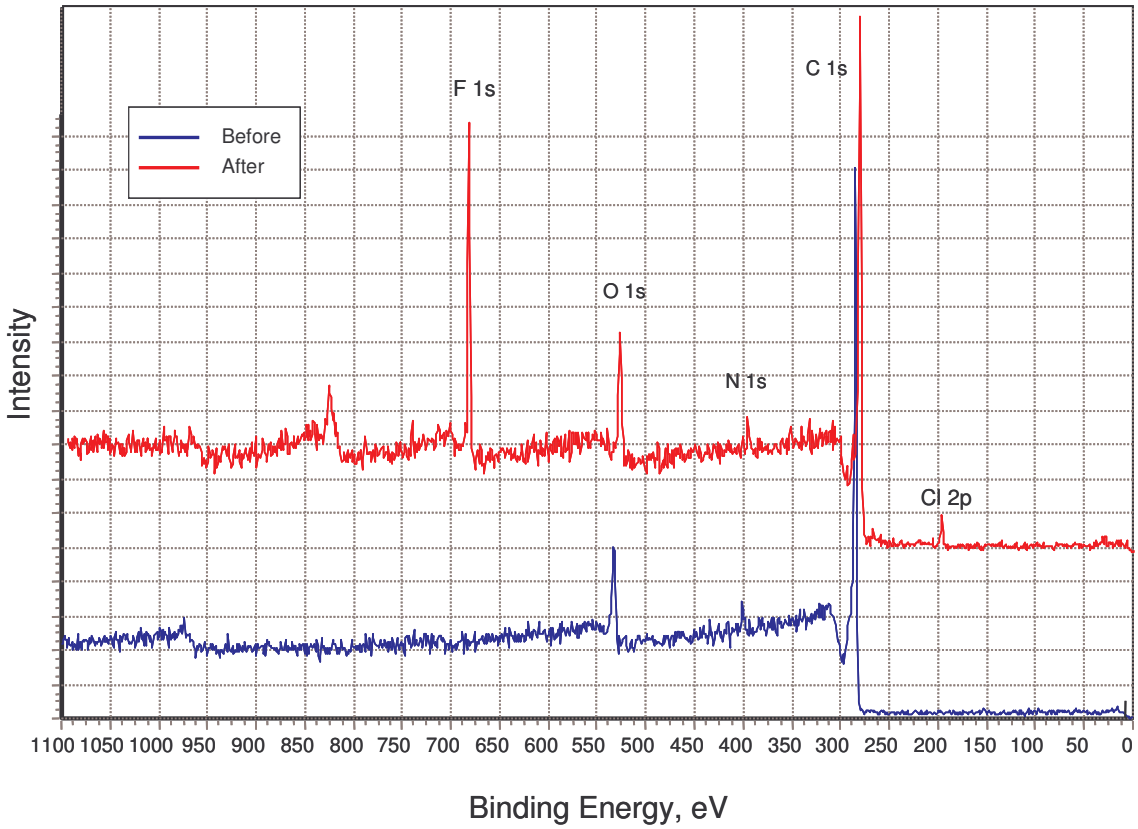

Figure 4.10 The presence of modifier on the surface of the CMSs after washing was verified by comparing XPS spectra of the sieves before and after modification.

Table 4.3 Atomic concentrations on the surface of CMSs before and after modification

Element	*Surface Atomic %*	
	Before Modification	After Modification
Carbon	89	78
Oxygen	8.8	7.9
Nitrogen	2.4	12
Fluorine	0.0	1.4
Chlorine	0.0	1.1

In addition to the issues related to *selecting* the appropriate linkage unit, there are also some important matters involving their *application* that must be considered. Previous uses of modifying agents on sieves and zeolites [40-42], have generally involved "full" coverage of the surface. While some coverage is necessary to promote adhesion, it is important to consider the effects of too much coverage: an effective barrier may be built

around the insert, plugging of the pores could increase, or multilayer formation may result. It is also important that the modifiers only bond to the sieve surface once. If the surface of the sieves is flat on the molecular level, the geometry of the molecules should be able to limit the ability of both ends to bond to the surface.

One very important test for the applicability of a modification technique is the analysis of the kinetic sorption data for the sample before and after modification. If the modifier is clogging the pores of the sieve, the kinetics of sorption should show a significant change as the gas molecules take more time to diffuse in the pores. Figure 4.11 shows the kinetic sorption data for carbon molecular sieves modified with 1,4-phenylenediamine compared to that for unmodified sieves. The modified and unmodified sieves were processed using the same procedures prior to sorption testing, so the particle size distributions should be very similar allowing qualitative comparison of the kinetic sorption data.

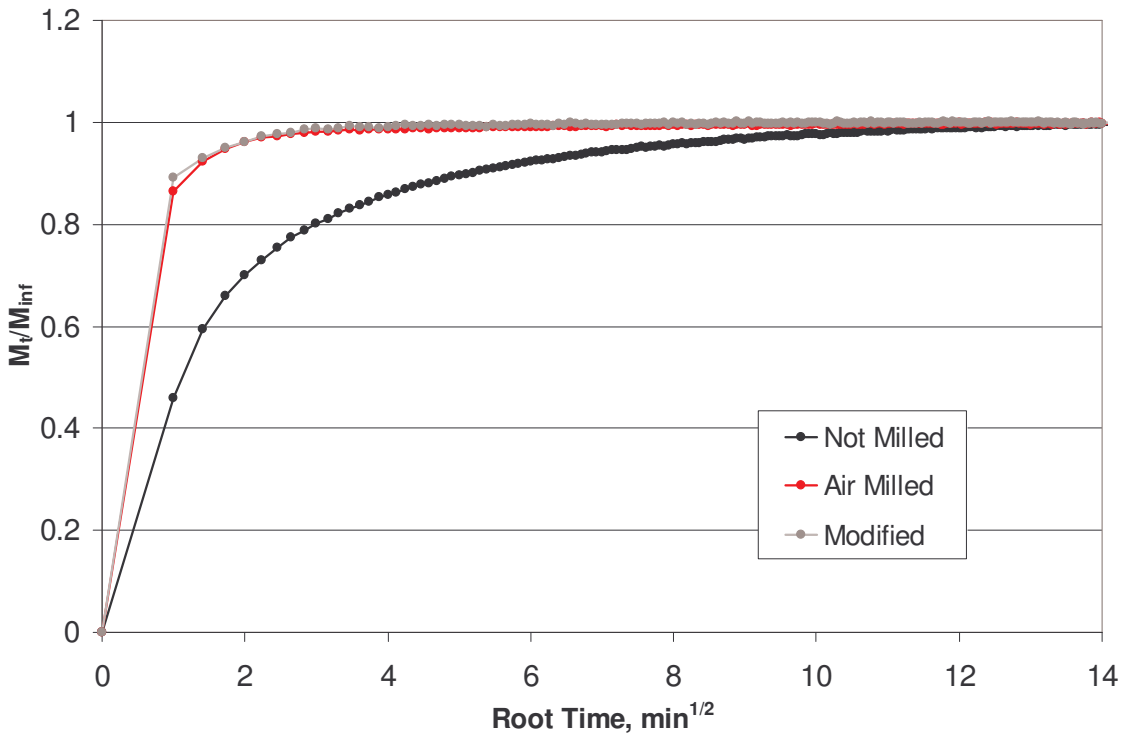

Figure 4.11 Comparison of the kinetic sorption data of CMS modified with 1,4-phenylenediamine and unmodified CMS samples milled under the same conditions showed little change. The response of the not milled sample is provided as a reference. Sorption tested at 35 °C.

The kinetic data are plotted as M_t/M_{inf} which is the ratio of the sorbed mass at time, t, to the amount sorbed at equilibrium. By plotting these values against the square root of time, if the diffusion is Fickian, as expected, the curves are dependent primarily on diffusion coefficient and size [43]. Since the modified and air milled samples possess very similar size distributions, changes in the kinetics would be primarily a result of changes in diffusion rates in the sample. The "not milled" sample, on the other hand, has a considerably larger average particle size that contributes to the slower sorption kinetics. These data provide a reference for the kinetic changes in the modified sieves. Within the error of the measurement, there was no difference in the kinetic sorption measured in the modified and unmodified samples. Unfortunately, the physical

limitations of the equipment used for these sorption measurements did not allow faster data collection times.

In addition to showing that the kinetics of sorption are not greatly affected by the modification, it is also important that the equilibrium sorption remain relatively unchanged. The isotherms shown in Figure 4.12 show little change in equilibrium sorption after CMS modification. The very small reduction in sorption capacity seen in the modified samples suggests that the linkage unit used was not excessively filling the pores of the CMSs during modification. These sorption data further support this modification as a viable processing step in the production of hybrid membrane materials.

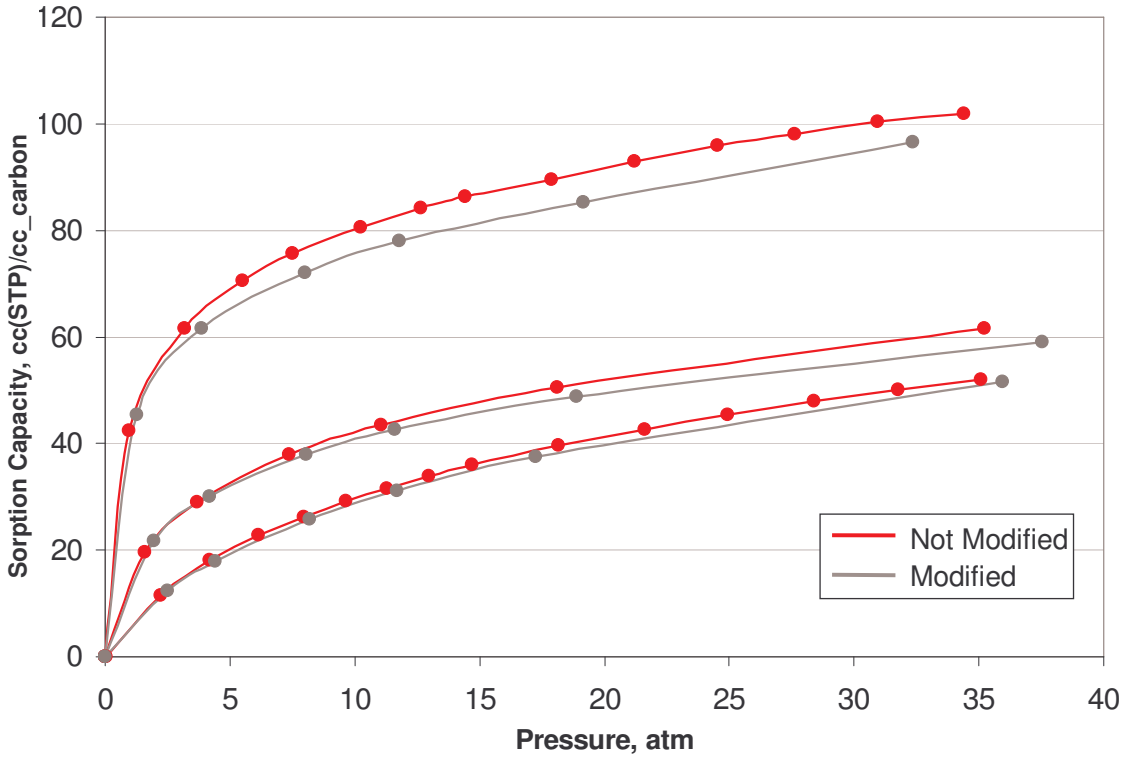

Figure 4.12 Equilibrium sorption in CMSs before and after modification with 1,4-phenylenediamine does not show large differences. Sorption tested at 35 °C.

4.4. Solution Stability

Another important factor in the successful formation of hybrid membrane systems is the ability to produce a stable membrane dope. A common technique used to produce stable suspensions of submicron particles is to use steric stabilization by attaching polymer molecules to the surface of the particles [44]. The polymer chains act as a buffer layer that prevents the small particles from agglomerating and becoming unstable. One major goal of the modification was to provide improved polymer-sieve interaction that would lead to higher stability in the membrane dopes. The stability of the suspensions was tested using modified and unmodified sieves in a very dilute polymer solution, since this "priming" phase is the most critical to the exclusion of agglomerates [44]. The stability was measured by simultaneously preparing solutions with three different sieve samples: 1) decanted, unmodified air milled particles, 2) modified carbons that have been exposed to the atmosphere for >24 hrs, and 3) modified carbon stored under nitrogen until the stability test.

The "exposed" sample was tested since primary amine groups are known to be relatively unstable when exposed to air. Particle stability was tested after atmospheric exposure to determine the impact of the chemical changes that occur on the suspension stability of the particles in a dilute polymer solution. Visual confirmation of the changes in the amine was seen with the 1,4-phenylenediamine as the crystals that are initially pure white will become fully brown if left exposed to the atmosphere overnight

Because of the ability of the CMS particles to strongly absorb light, even very dilute solutions of the particles are completely opaque. To provide a rough idea of this property, several samples of concentrations of increasing orders of magnitude were prepared as a guide. Figure 4.13 shows a picture of these samples with a strong back

light, and as the image indicates, solutions with concentrations of carbon greater than 1 mg/ml are completely opaque. Since the suspensions used to prepare hybrid membranes generally contained 5-10 mg/ml of carbon, visual or optical measurements of stability could only be used to determine if less than 10% of the initial carbon remained in solution. Until this low limit, the solutions remained opaque.

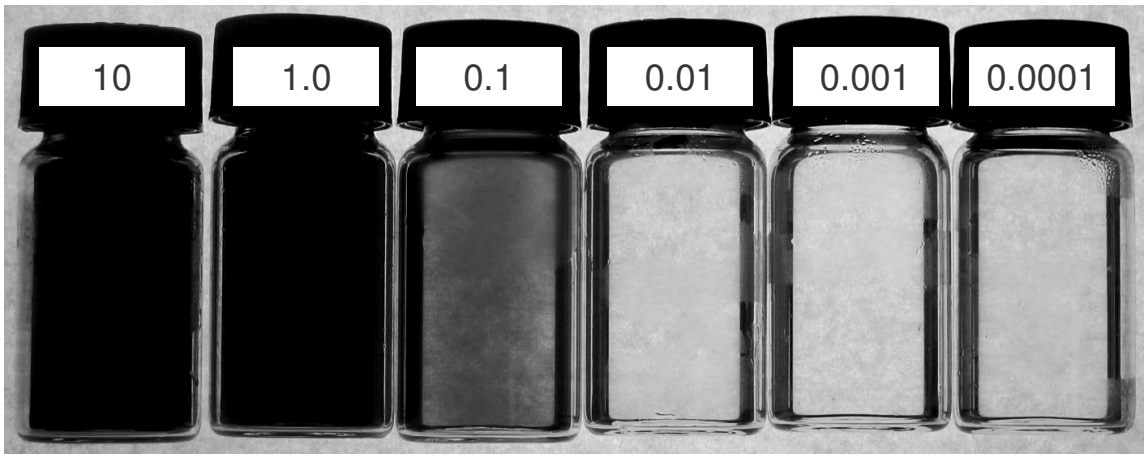

Figure 4.13 Even with very strong back lighting, the carbon molecular sieve suspensions must be very dilute before they become even partially transparent. Numbers indicate the mass concentration of carbon particles in dichloromethane solution with units of mg/ml.

Since an optical measure of the stability of sieves was impractical for characteristic concentrations, a mass based measure was performed to provide a quantitative means of comparison between the different carbon samples. The samples used to test the stability were prepared by adding 100 mg of carbon to 10 ml of a 2 wt% solution of 6FDA-6FpDA in dichloromethane to approximate the concentrations used in dope preparation. These mixtures were then sonicated for 1 hour to provide a well dispersed system for the stability test. Upon removal from the ultrasonic bath, 0.5 ml was removed from each sample and dried. A control sample was also prepared with no carbon to provide a measure of the amount of polymer contained in each sample as a baseline.

The baseline amount of polymer was subtracted from the mass of the dried polymer-carbon sample for each sample to provide the mass of carbon removed with each test. These values are shown in Figure 4.14 as the amount of carbon remaining suspended in the mixture after 6 hours, relative to the initial concentration. The test time of six hours was selected for the following reasons: 1) qualitative observation during experiments suggested that highly unstable suspensions would not remain suspended for that amount of time, 2) the sieves used in the modification were previously decanted after being suspended for 6 hours, so prior to modification they should be stable for this length of time in pure solvent, and 3) drying time of the hybrid films after casting should result in sufficient immobility after 6 hours to prevent any further settling or agglomeration.

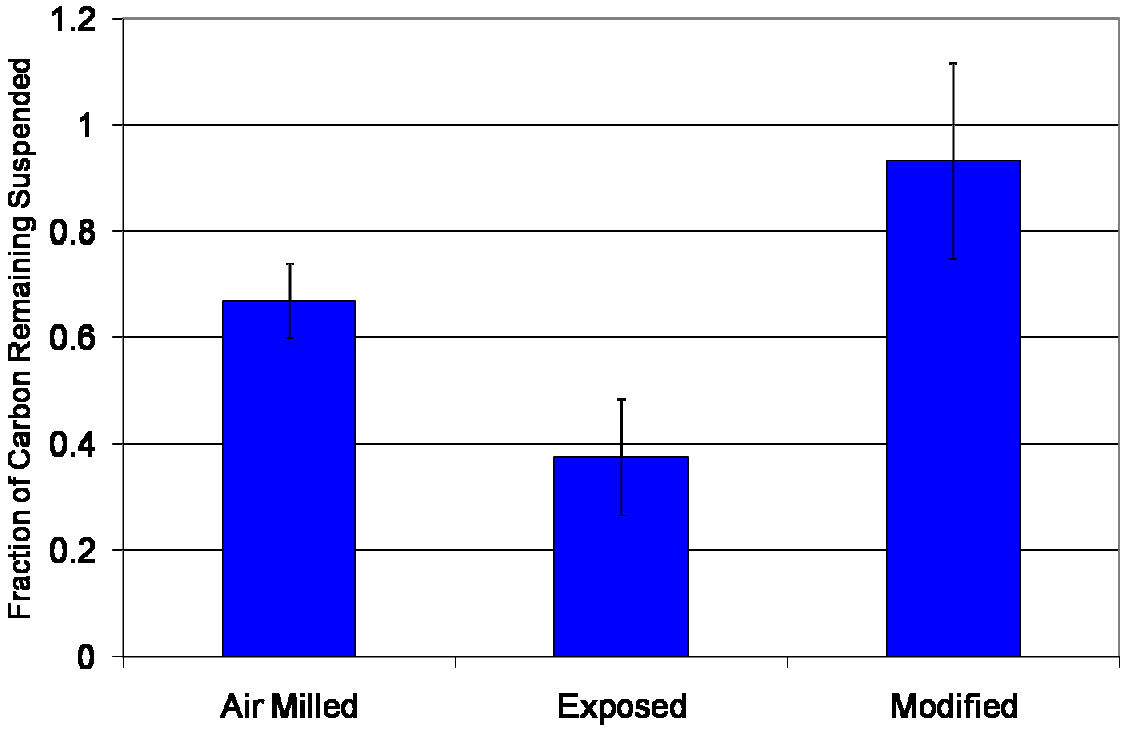

Figure 4.14 The stability of the carbon particles in a 2 wt% solution of 6FDA-6FpDA in dichloromethane is improved by the surface modification. All data shown are for carbon samples prepared after decanting to remove the larger particles. The air milled sample was tested without modification, the exposed sample was modified and exposed to the atmosphere for 24 hours before testing, and the modified sample was modified and stored under nitrogen until sample preparation.

As the figure shows, the stability of the carbon in the polymer solution was improved by the surface modification. As expected from previous observations, the exposed samples showed a significant decrease in stability, but the stability of the modified sieves was slightly improved over the unmodified samples. The need for enhanced stability of submicron particles used in hybrid film formation has been observed by other researchers [3,38,42]. This is one of the primary reasons for the development of the priming protocol used in dope preparation. Unfortunately, experimental results obtained with hybrid membranes revealed that the stability enhancement obtained from the surface modification was still not sufficient to prevent the formation of agglomerates in the hybrid membranes. This phenomenon will be further discussed in Chapter 6.

4.5. References

1. Steel, K.M. (2000). Carbon Membranes For Challenging Gas Separations. Chemical Engineering. Austin, TX, The University of Texas at Austin. Doctor of Philosophy.
2. Vu, D.Q. (2001). Formation and Characterization of Asymmetric Carbon Molecular Sieve and Mixed Matrix Membranes for Natural Gas Purification. Chemical Engineering. Austin, TX, The University of Texas at Austin. Doctor of Philosophy.
3. Rao, M.B. and Sircar, S. (1993). "Nanoporous Carbon Membranes for Separation of Gas Mixtures by Selective Surface Flow." Journal of Membrane Science 85(3): 253-264.
4. Williams, P.J. (2006). Analysis of Factors Influencing the Performance of CMS membranes for Gas Separation. School of Chemical and Biomolecular Engineering. Atlanta, Georgia Institute of Technology. Doctor of Philosophy: 238.
5. Vu, D.Q., Koros, W.J., et al. (2003). "Mixed Matrix Membranes Using Carbon Molecular Sieves - I. Preparation And Experimental Results." Journal of Membrane Science 211(2): 311-334.
6. Vu, D.Q., Koros, W.J., et al. (2003). "Mixed Matrix Membranes Using Carbon Molecular Sieves - II. Modeling Permeation Behavior." Journal of Membrane Science 211(2): 335-348.
7. Qiu, W.L., Endo, T., et al. (2004) “Interfacial Interactions Of A Novel Mechanochemical Composite Of Cellulose With Maleated Polypropylene.” Journal of Applied Polymer Science, 94(3) 1326-1335
8. Qiu, W.L., et al. (2004) “Milling-Induced Esterification Between Cellulose And Maleated Polypropylene.” Journal of Applied Polymer Science, 91(3) 1703-1709
9. Barbier, B., Pinson, J., et al. (1990). "Electrochemical Bonding of Amines to Carbon Fiber Surfaces Toward Improved Carbon-Epoxy Composites." Journal of the Electrochemical Society 137(6): 1757-1764.
10. Bascom, W.D. (1987). Interfacial Adhesion of Carbon Fibers. N. C. Report. 178306: 46.
11. Bascom, W.D., Drzal, L.T. (1987). The Surface Properties of Carbon Fibers and Their Adhesion to Organic Polymers. NASA Contractor Report. 4084: 94.
12. Broyles, N.S. Chan, R., et al. (1998). "Sizing Of Carbon Fibers With Aqueous Solutions Of Poly(Vinyl Pyrollidone)." Polymer 39(12): 2607-2613.
13. Broyles, N.S. Verghese, K.N.E., et al. (1998). "Fatigue Performance Of Carbon Fibre/Vinyl Ester Composites: The Effect Of Two Dissimilar Polymeric Sizing Agents." Polymer 39(15): 3417-3424.
14. Dilsiz, N., Wightman, J.P. (2000). "Effect Of Acid-Base Properties Of Unsized And Sized Carbon Fibers On Fiber/Epoxy Matrix Adhesion." Colloids and Surfaces A: Physicochemical and Engineering Aspects 164: 325-336.
15. Drzal, L.T., Rich, M.J., et al. (1983). "Adhesion of Graphite Fibers to Epoxy Matrices: I. The Role of Fiber Surface Treatment." Journal of Adhesion 16: 1-30.
16. Jenkins, S.D., Emmerson, G.T., et al. (1994). "Thermoplastic Sizing Of Carbon Fibres In High Temperature Polyimide Composites." Journal of Adhesion 45: 15-27.
17. Mader, E. (1997). "Study Of Fiber Surface Treatments For Control Of Interphase Properties In Composites." Composites Science and Technology 57: 1077-1088.
18. Panzer, U. (1991). "Characterization Of Solid Surfaces By Inverse Gas Chromatography." Colloids and Surfaces 57: 369-374.
19. Saito, M., Toki, H., et al. (1988). Sizing Agent for Carbon Fibers. U. S. Patent. United States, Tao Nenryo Kogyo Kabushiki Kiasha, Tokyo, Japan. 4,781,947.

20. Schultz, J., Lavielle, L. (1989). "Interfacial Properties of Carbon Fiber-Epoxy Matrix Composites." ACS Symposium Series 391: 185-202.
21. Thomas, Y., Parisi, J.P., et al. (1994). "Improvement Of Fiber/Matrix Bonding In Carbon-Fiber/Acrylic Composites By Electron-Irridation: Concept Of Difunctional Chemical Coupling Agent." Composites Science and Technology 52: 299-307.
22. Dilsiz, N., Wightman, J.P. (1999). "Surface Analysis Of Unsized And Sized Carbon Fibers." Carbon 37: 1105-1114.
23. Aizawa, M. S., Milo, S. P. (2003). "Silylation Of Multi-Walled Carbon Nanotubes." Chemical Physics Letters 368: 121-124.
24. Allongue, P. D., Delamar, M., et al. (1997). "Covalent Modification of Carbon Surfaces by Aryl Radicals Generated from the Electrochemical Reduction of Diazonium Salts." Journal of the American Chemical Society 119: 201-207.
25. Bahr, J. L., Mickelson, E.T., et al. (2001). "Dissolution Of Small Diameter Single-Wall Carbon Nanotubes In Organic Solvents?" Chemical Communications 2: 193-194.
26. Bahr, J. L. and Tour, J.M. (2001). "Highly Functionalized Carbon Nanotubes Using in Situ Generated Diazonium Compounds." Chemistry of Materials 13: 3823-3824.
27. Bahr, J. L. and Tour, J.M. (2002). "Covalent Chemistry Of Single-Wall Carbon Nanotubes." Journal of Materials Chemistry 12: 1952-1958.
28. Bahr, J.L., Yang, J.P. (2001). "Functionalization of Carbon Nanotubes by Electrochemical Reduction of Aryl Diazonium Salts: A Bucky Paper Electrode." Journal of the American Chemical Society 123: 6536-6542.
29. Canning, P.S.J. McCrudden, K., et al. (1999). "Rates And Mechanisms Of The Thermal Solvolytic Decomposition Of Arenediazonium Ions." Journal Of The Chemical Society-Perkin Transactions 2 12: 2735-2740.
30. Chen, J., Hamon, M.A., et al. (1998). "Solution Properties of Single-Walled Carbon Nanotubes." Science 282: 95-98.
31. Dyke, C.A. and Tour, J.M. (2003). "Solvent-Free Functionalization of Carbon Nanotubes." Journal of the American Chemical Society 125: 1156-1157.
32. Georgakilas, V., Tagmatarchis, N., et al. (2002). "Amino Acid Functionalisation Of Water Soluble Carbon Nanotubes." Chemical Communications 24: 3050-3051.
33. Liu, J., Rinzler, A.G., et al. (1998). "Fullerene Pipes." Science 280: 1253-1256.
34. Mitchell, C.A. Bahr, J.L., et al. (2002). "Dispersion of Functionalized Carbon Nanotubes in Polystyrene." Macromolecules 35: 8825-8830.
35. Peng, H., Reverdy, P., et al. (2003). "Sidewall Functionalization Of Single-Walled Carbon Nanotubes With Organic Peroxides." Chemical Communications 3: 362-363.
36. Geiszler, V.C. (1997). Polyimide Precursors For Carbon Molecular Sieve Membranes. Chemical Engineering. Austin, TX, The University of Texas at Austin. Doctor of Philosophy.
37. Liu, Y., Wang, R., et al. (2001). "Chemical Cross-Linking Modification Of Polyimide Membranes For Gas Separation." Journal of Membrane Science 189: 231-239.
38. Tin, P.S., Chung, T.S. (2003). "Effects Of Cross-Linking Modification On Gas Separation Performance Of Matrimid Membranes." Journal of Membrane Science 225: 77-90.
39. Kang, J.F., Perry, J.D., et al. (2002). "Growth and Morphology of Polythiophene on Thiophene-Capped Monolayers: 1. Single Component Monolayers." Langmuir 18: 10196-10201.

40. Mahajan, R. (2000). Formation, Characterization, and Modeling of Mixed Matrix Membrane Materials. Chemical Engienering. Austin, TX, The University of Texas at Austin. Doctor of Philosophy.
41. Mahajan, R. and Koros, W.J. (2002). "Mixed Matrix Membrane Materials With Glassy Polymers. Part 1." Polymer Engineering and Science 42(7): 1420-1431.
42. Mahajan, R. and Koros, W.J. 2002). "Mixed Matrix Membrane Materials With Glassy Polymers. Part 2." Polymer Engineering and Science 42(7): 1432-1441.
43. Crank, J. (1975). The Mathematics of Diffusion. New York, Oxford University Press.
44. Moore, T.T. (2004). Effects of Materials, Processing, and Operating Conditions on the Morphology and Gas Transport Properties of Mixed Matrix Membranes. Chemical Engineering. Austin, TX, The University of Texas at Austin. Doctor of Philosophy: 312.

CHAPTER 5

IMPACT OF MODIFICATION ON POLYMER STRUCTURE AND PERFORMANCE

The last chapter highlighted some of the changes that occur in the carbon molecular sieves during the processing steps needed to produce the hybrid membranes. As these membranes are constructed of both molecular sieve inserts and a matrix polymer, it is equally important to understand the impact of hybrid membrane formation on the polymer matrix. This chapter will deal with the changes that take place in the matrix polymer during the formation of the hybrid systems.

5.1. Initial Hybrid Membrane Results

The need to elucidate the source of membrane properties in a hybrid system is clearly illustrated by the initial membrane tests conducted with modified CMSs. Using the modification procedure described in Chapter 4, a batch of CMS particles were modified using an excess of modifier to provide the highest amount of surface coverage possible. These carbons were then used to form a hybrid membrane, and the resulting properties could not be described by simple interfacial phenomena commonly demonstrated by applications of the Maxwell equation. Figure 5.1 shows the results of this test along with some model predictions.

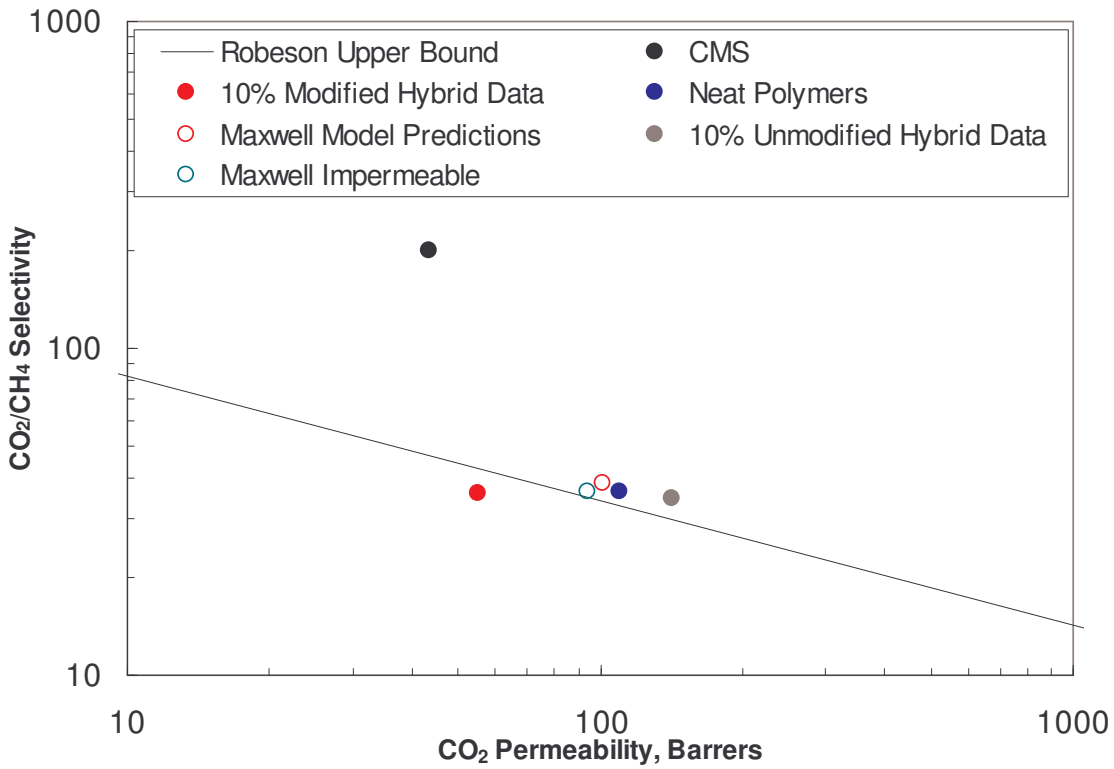

Figure 5.1 The properties obtained in the initial hybrid membranes formed with modified carbons could not be explained by model predictions. Permeabilities tested at 35 °C and 50 psia.

The membrane did not show the increase in selectivity expected for a hybrid membrane with an ideal interface. Instead, the selectivity remained nearly constant with a large decrease in permeability. This response is similar to that anticipated for a plugged sieve. Impermeable sieves with an ideal interface result in reduced permeability from the more tortuous path required for permeating molecules while the selectivity provided by the polymer remains unchanged. However, when the impact of a plugged sieve was compared to the hybrid membrane results, indicated in Figure 5.1 as an "impermeable sieve", the permeability change measured was much greater than that expected even for completely impermeable sieves. Since the properties obtained fall outside of those obtainable with inserts possessing physically realistic properties, the test suggested that the properties of the polymer have been changed significantly by the membrane

formation process. One of the most likely sources for this change was the linking agent added to the surface of the sieves. In order to further understand the nature of these changes, it is important to review the impact of polymer structure on the transport properties of the polymer.

5.2. Relationship of Polymer Structure and Transport Performance

Chapter 2 discussed some of the broad relationships observed between polymer structure and permeability and selectivity, but a more focused review of polyimides and some closely related polymers can provide some very useful insight for this work. Walker reported a study that helps to provide a good understanding of how important the structure of the polymer backbone is in determining the final transport properties of a polymer [1]. That work compared three related families of polymers: polyamides, polyimides, and polypyrrolones. The basic structures of the characteristic backbone unit in these polymers can be seen in Figure 5.2.

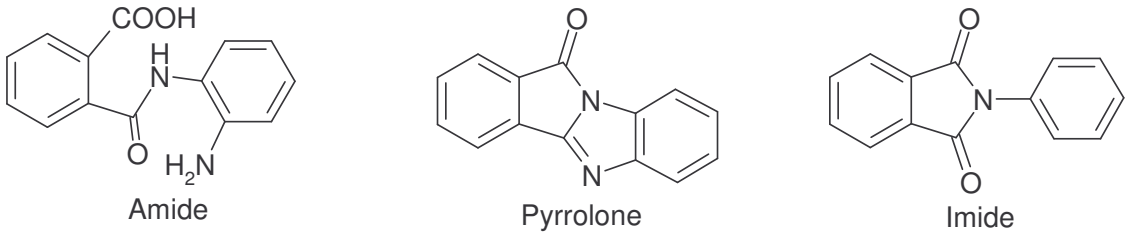

Figure 5.2 The structures of polyamides, polypyrrolones, and polyimides are differentiated by the structure of the nitrogen bonds in the backbone of the polymer chain.

These polymer classes are chemically similar with a slight change in the form of the nitrogen bond in the backbone. These changes affect the ability of the polymer to form hydrogen bonds, the rigidity of the polymer backbone, and the packing density of the polymer chains. However, even these fairly small changes in the structure of the

polymers cause significant differences in the transport properties obtained. Figure 5.3 shows the properties for a selection of polyamides, polyimides, and polypyrrolones, and the dotted lines connect polymers from each family that have identical structures differing only by the form of nitrogen bonds in the backbone.

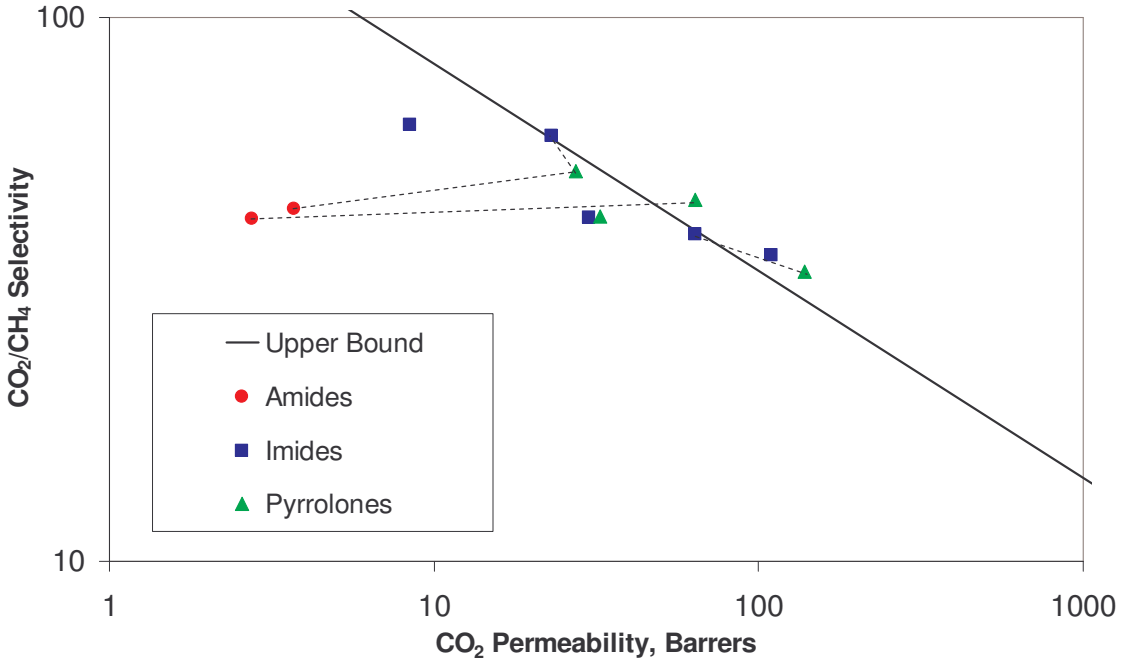

Figure 5.3 Properties of a selection of polyamides, polypyrrolones, and polyimides reveal the significant changes that a simple change in the polymer structure can cause in the transport properties of the polymer. The dotted lines connect polymers of similar structure differing only by the type of nitrogen bond in the backbone. Data from [1].

An interesting aspect of the data shown in Figure 5.3 is that the selectivities for the polymers shown vary by less than a factor of two while the permeabilities range well over an order of magnitude. This trend is very similar to the change seen in the hybrid membrane sample shown in Figure 5.1 where the permeability changed considerably with little change in selectivity.

Another illustration of the sensitivity of transport data to the backbone structure of the polymer chain is seen in the 6FDA-6FpDA and 6FDA-6FmDA polymer system. These two polymers are atomically identical with the only difference being in the location of the amine groups in the diamine used to synthesize the polymers. The transport properties for these polymers and blends of these polymers are shown in Figure 5.4.

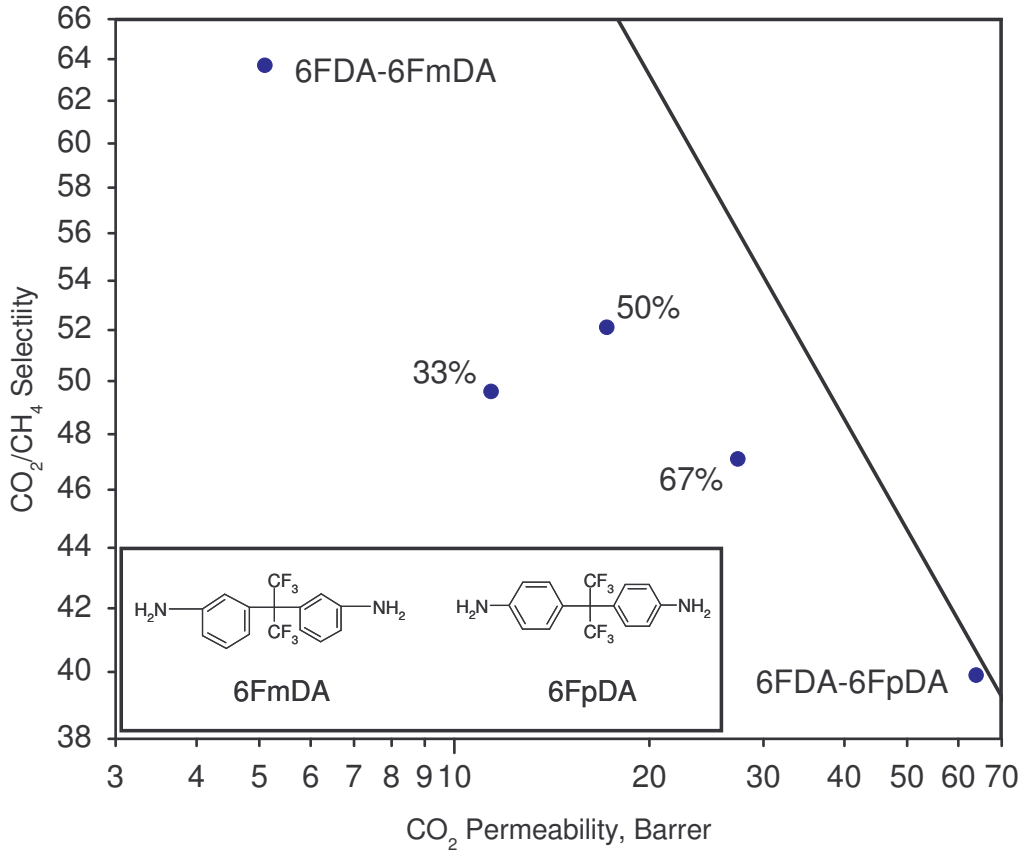

Figure 5.4 The transport properties of 6FDA-6FmDA and 6FDA-6FpDA and their blends show considerable differences despite their very similar structures [2]. Insert: Structures of the 6FmDA and 6FpDA monomers differ only by the location of the amine groups. Percentage of 6FDA-6FpDA labeled.

By changing the location of the amine groups from the para- position to the meta-position, the permeability drops by an order of magnitude while the selectivity nearly doubles. Since these two polymers are fully miscible with one another, Coleman was able to test a series of membranes formed from these polymers blended in different

ratios [2]. The transport properties resulting from that test are also shown in Figure 5.3. These examples illustrate the sensitivity of transport properties in a polymer to the nature of the backbone structure.

5.3. Modification of the Polymer

The mechanism by which the modifiers used in this work bond to the polymer involves the opening of the imide ring in the backbone to form two amide groups. One amide group remains in the backbone of the polymer chain, and the other group forms a covalent link to the modifier and, by extension, to the CMS. Primary amines have shown the ability to form covalent bonds in this manner through an S_N2, imide ring-opening reaction [3, 4] as shown in Figure 5.5.

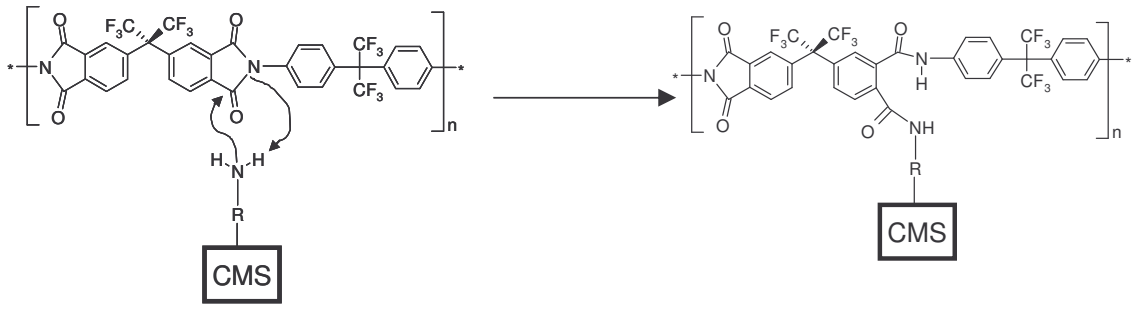

Figure 5.5 A primary amine has the ability to open the imide ring through an S_N2 reaction that forms two amide linkages creating a covalent bond between the polymer and the CMS.

Since the bond created between the polymer and the sieve effectively changes the backbone structure from an imide linkage to an amide linkage, it is conceivable that a major reason for the unexpected properties seen in the hybrid membrane is the result of a change in the transport properties of the matrix polymer. In order to show the extent of change that should be expected for the polymer bonded to the surface of the CMS

particles, a series of polymer membranes were formed using controlled amounts of modifier.

The initial step in these tests was to determine a realistic measure of the amount of amine groups that are present on the surface of the modified carbons. Full monolayer surface coverage and a footprint area for each linkage molecule equal to the area of a benzene ring parallel to the surface were assumed. The surface area per gram of carbon was estimated assuming spherical particles with a diameter of 200 nm and a bulk density of 1.29 g/cm^3 as previously discussed in Chapter 4. From these values a concentration of 0.769 mmoles per gram of carbon was calculated as a high end estimate of the amount of amines available for reaction with the polymer when forming a hybrid membrane using modified CMSs. In order to simulate this reactivity in polymer films without adding carbon, the modifiers were added directly to the polymer solution. The amount of modifier used was calculated to represent the number of active amine groups present in a hybrid membrane with 20 vol% carbon. As a result, the actual number of diamine molecules added to the solution was equal to half of the number of monoamine molecules added in order to maintain a consistent amine concentration. While these calculations are not expected to provide an exact measure, this process was selected as a best estimate with the expectation that most of the estimates used would cause the “actual” impact of the amines to be lower than that calculated by this method.

5.4. Properties of the Modified Polymer

Once the appropriate amount of modifier was calculated, a dilute polymer solution was formed (~2-5 wt%) and when the polymer was fully dissolved, the modifier was added to the solution and rolled for 12 hours to allow the solution to mix and react prior to casting

the membrane. The membranes were solution cast as described in Chapter 3, and the gas transport results for several "modified" polymer films can be seen in Figure 5.6.

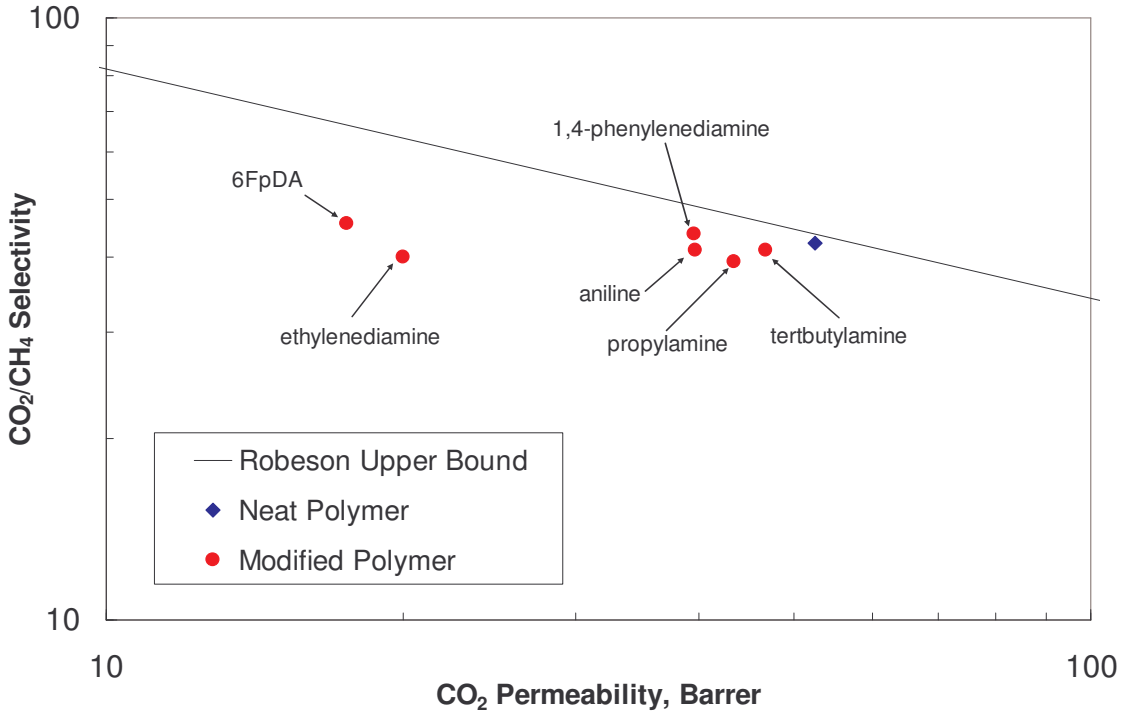

Figure 5.6 Polymer "modified" by amine groups shows significant reductions in permeability. Permeabilities tested at 35 °C and 50 psia.

Clearly the addition of the amines to the polymer solution had a substantial impact on the transport properties of the polymer. Most notably, the modifiers caused the permeability of the polymer to drop significantly, while the modification showed a relatively small influence on selectivity. Unfortunately, reductions of this magnitude in the permeability of the polymer matrix are not acceptable, and these changes must be circumvented for the successful application of this technology.

5.5. Reduced Modification of the Polymer

The next step in the analysis was to determine if the impact of the modifier on the polymer could be controlled by reducing the number of amine groups available for

reaction. Samples were prepared using 6FpDA, aniline, and 1,4-phenylenediamine as described above with the simple change that only one tenth of the modifier was added. This series was selected to represent the amount of amine groups available on molecular sieves modified under controlled conditions designed to prevent “full” surface coverage. Figure 5.7 shows the results of this test relative to the “full” coverage results.

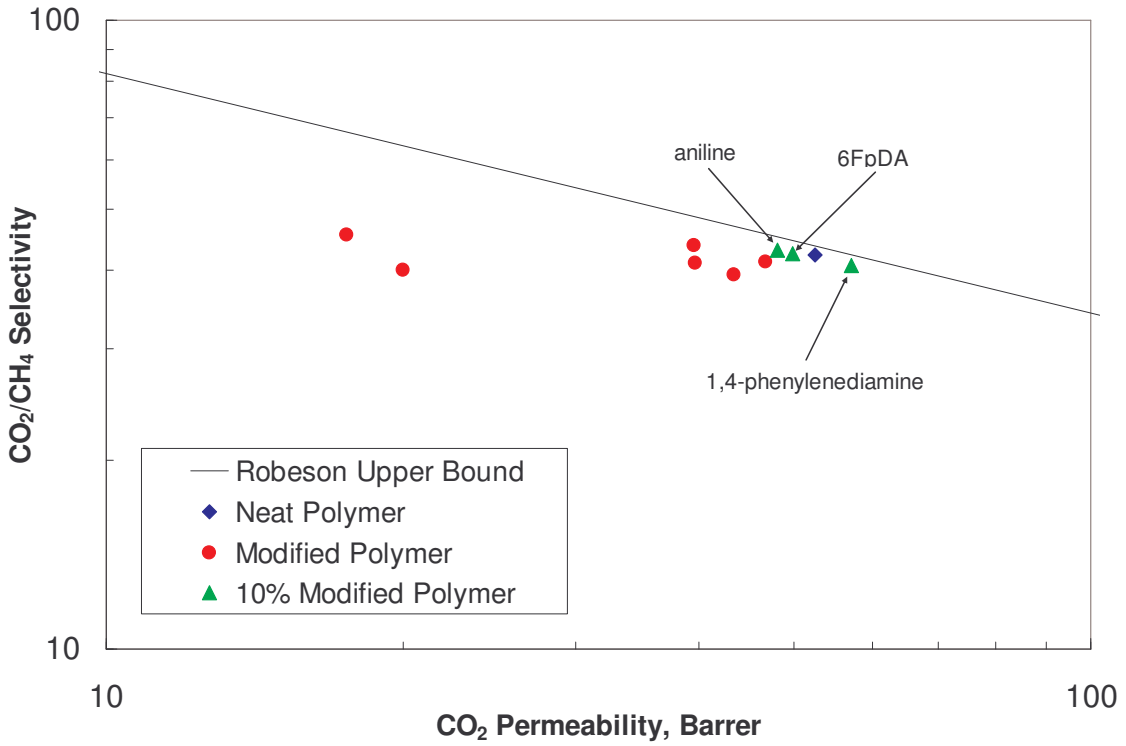

Figure 5.7 Controlled reduction of the modifier used on the polymer was able to limit the impact on transport properties. Permeabilities tested at 35 ^{o}C and 50 psia.

Clearly the reduction in amine groups has greatly reduced the impact of the modifier on the transport properties of the polymer. These results suggest that while the modifier has the potential to significantly change the performance of the polymer matrix, a controlled application may be used to promote adhesion without causing an unacceptable change in membrane performance.

Further evidence of the relationship between the amount of modifier and the performance of the membrane can be seen in Figure 5.8 which shows a series of "modified" membranes containing 6FpDA modifier. The neat polymer properties are plotted along with samples representing "full" coverage (from Figure 5.6), and coverage amounts equivalent to four times full coverage and one tenth of full coverage. In each case, the selectivity of the membrane is relatively constant while the permeability decreases monotonically with increasing amounts of modifier. These tests further support the hypothesis that careful control of the modifier used on the CMSs will allow hybrid membrane formation with enhanced transport properties.

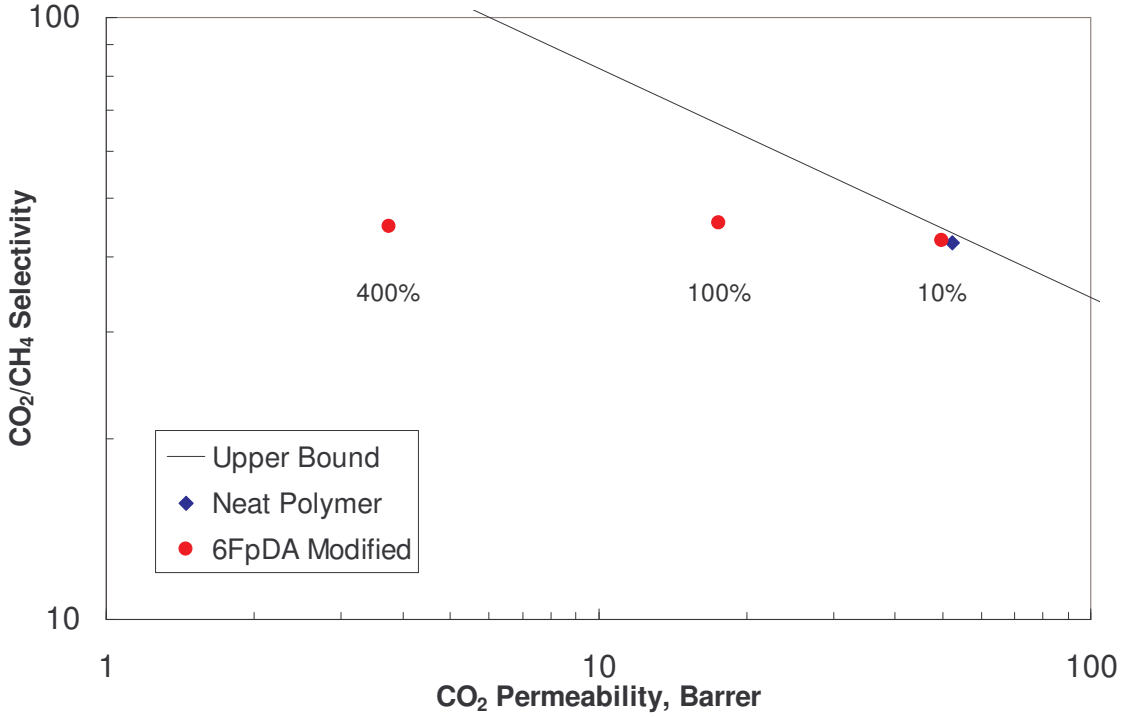

Figure 5.8 The decrease in permeability with increasing amounts of modifier illustrates the impact of the modification reaction on the transport properties of the polymer matrix. Permeabilities tested at 35 °C and 50 psia.

5.6. Molecular Weight of the Modified Polymer

Another aspect of the polymer system that must be investigated is the molecular weight of the polymer before and after modification. The molecular weight was tested using gel permeation chromatography with a polystyrene standard. As a result, the absolute values of the numbers may not be completely accurate, but the relative values are still viable for comparison. Figure 5.9 shows the CO_2 permeability and weight average molecular weight, Mw, together to show their relationship. The modification of the polymer lowered the molecular weight, demonstrating the presence of a reaction between the modifier and the polymer; however, the molecular weight change does not explain the measured changes in permeability.

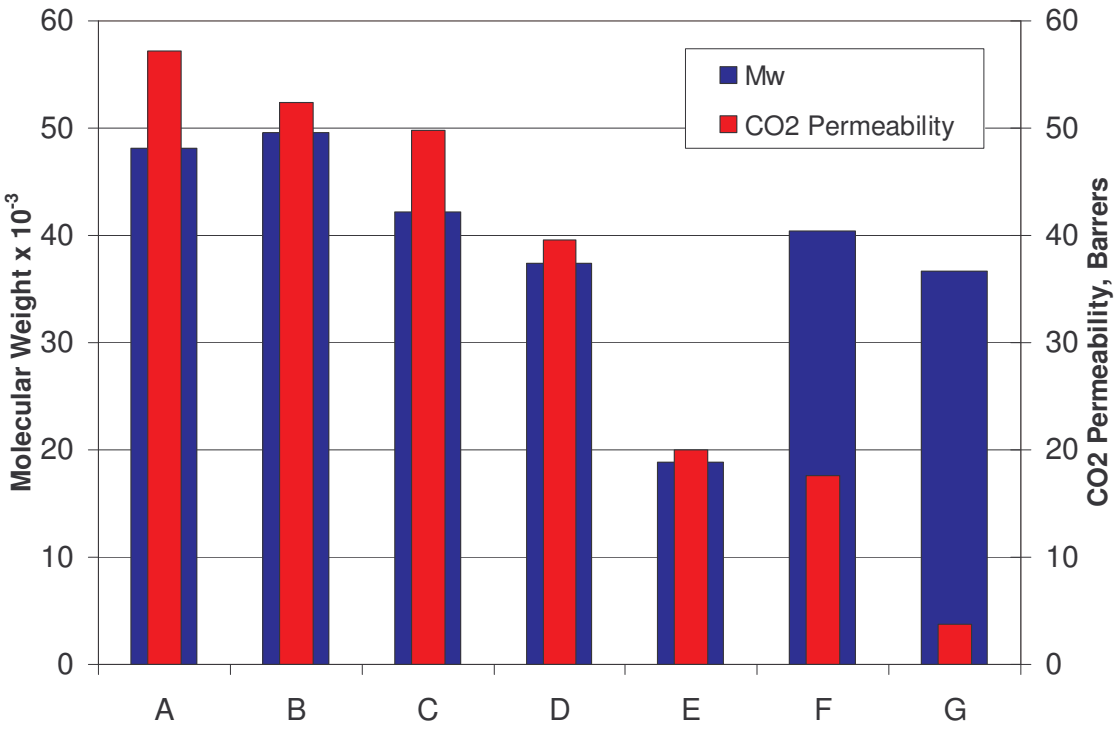

Figure 5.9 GPC results do not show a direct relationship between molecular weight and CO_2 permeability for the "modified" polymer samples A) 1,4-phenylenediamine (10%), B) neat 6FDA-6FpDA, C) 6FpDA (10%), D) 1,4-phenylenediamine, E) ethylenediamine , F) 6FpDA, and G) 6FpDA (4X).

While the molecular weight in these samples does not show a direct correlation to the permeability, it *is* important to the mechanical stability of the membrane. This dependence was clearly evident in the difficulty encountered in preparing a testable membrane modified with ethylenediamine. As the GPC results show, the ethylenediamine caused the most drastic reduction in molecular weight, and this was also evident in the membranes formed from this modified polymer. The films produced with ethylene diamine modifier were extremely brittle. In some cases, the adhesion of the polymer to the glass casting surface would cause the film to fracture into very small pieces during solvent evaporation. For this sample to be tested, a thicker film had to be prepared to keep the film from fracturing during solvent evaporation so that enough area was available to prepare samples of appropriate size for permeation measurement.

These results highlight another important characteristic of processing that must be monitored during the formation of hybrid membranes in order to insure the applicability of the resulting system. Fortunately, the systems prepared using reduced amounts of modifier showed relatively small reductions in molecular weight with no discernable changes in mechanical strength. By limiting the impact on molecular weight, the controlled modification provides a useful procedure for engineering the interface without degrading the transport or mechanical properties of the polymer matrix.

5.7. Annealing and Plasticization

Formation of successful hybrid membranes using 6FDA-6FpDA as the matrix polymer required above T_g annealing of the hybrid films after solvent evaporation. As with the other processing steps used in the formation of the hybrid membranes, it is important to study the impact of the annealing process on the transport properties of the polymer. Figure 5.10 shows the annealing temperature profile used for this work.

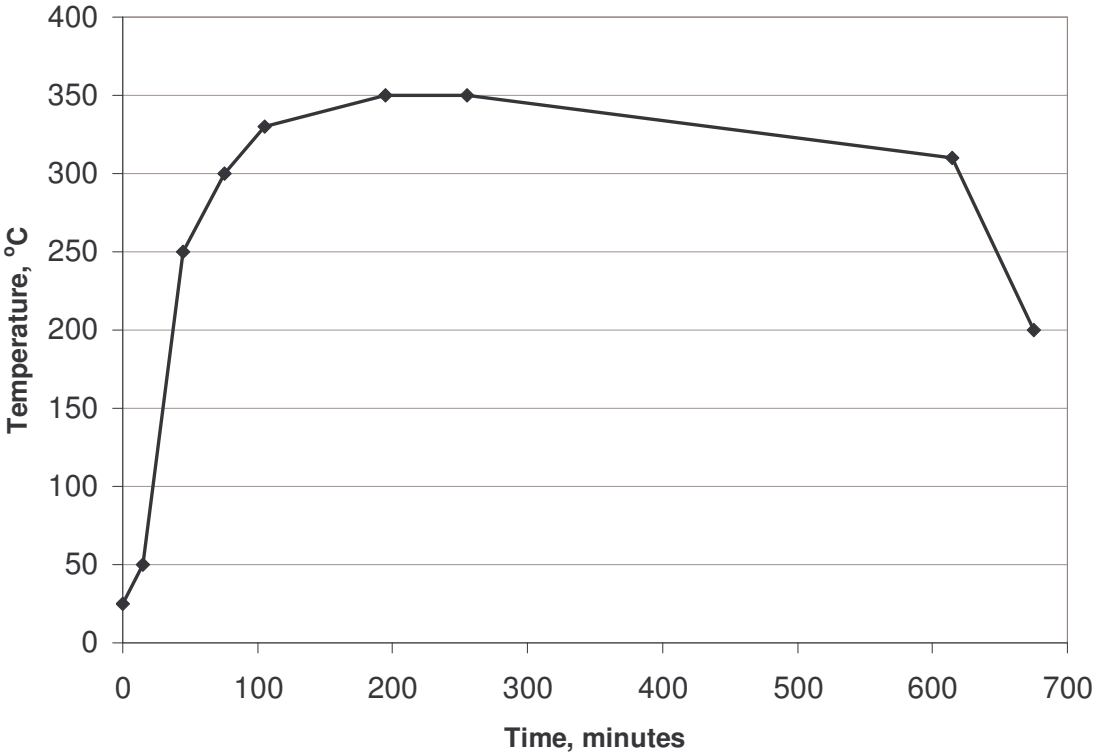

Figure 5.10 The temperature profile used to anneal the hybrid membranes used slow ramp rates to improve consistency in the transport properties.

Because the glass transition temperature of 6FDA-6FpDA is relatively high, 320 °C, the films could not be annealed in a regular vacuum oven, but the split tube furnace used for pyrolysis was used instead. The temperature profile was designed to provide one hour at the annealing temperature of 350 °C with a slow approach to avoid thermal overshoot from the oven. The cooling rate was also controlled to bring the polymer back below its T_g very slowly. If the polymer is rapidly cooled from above its glass transition temperature, the process can cause larger amounts of unrelaxed volume to become trapped in the polymer. The slower cooling rate induced by the temperature profile allows the polymer to relax closer to its equilibrium volume. This process also provides

more consistent results that are less sensitive to aging as compared to samples quenched rapidly from above T_g.

The annealing process causes some changes in the properties of the polymer. The most important property changes involve the transport performance before and after annealing. Figure 5.12 shows the permeability and selectivity of the 6FDA-6FpDA polymer before and after annealing for the two major gas separations tested: O_2/N_2 and CO_2/CH_4. In addition to pure gas analysis, the changes caused by annealing were analyzed using mixed gas for the CO_2/CH_4 separation to verify the trends seen with pure gas. The mixed gas analysis was performed with a CH_4:CO_2 ratio of 80:20 at a CO_2 partial pressure of 50 psia. The competition between the two gases from sorption and diffusion causes the permeability to be lower for the mixed gas test than for the pure gas test. At the same time, the higher condensability of CO_2 causes the sorption selectivity to increase over the pure gas increasing the selectivity measured in the mixed gas test over that measured in the pure gas test. Because of the additional analytical steps required for mixed gas testing, the error is somewhat larger than for pure gas testing; however, there was very good agreement between the mixed gas and pure gas properties measured for the polymer before and after annealing.

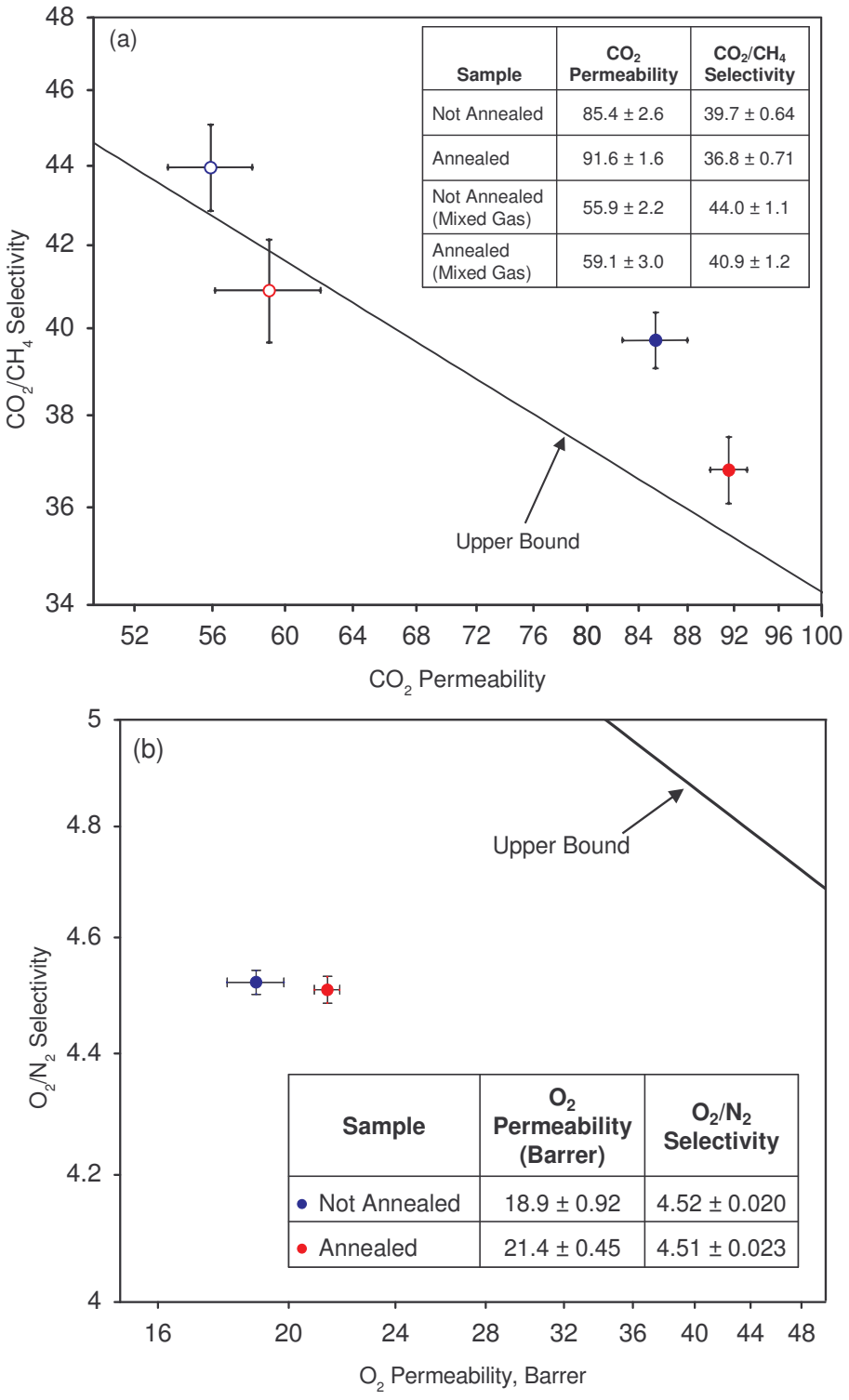

Figure 5.11 The transport properties of 6FDA-6FpDA change slightly after annealing above T_g. (a) CO_2 permeability increased with a small decrease in CO_2/CH_4 selectivity. Mixed gas was tested using an 80:20 ratio of CH_4 to CO_2. (b) O_2 permeability increased with no significant change in selectivity. Permeabilities tested at 35 ^oC and 50 psia.

Fortunately, using the controlled temperature profile shown in Figure 5.11 limits the extent of the change in transport properties that is caused by annealing. These changes are not extreme, and since they generally follow the upper bound, they do not render the polymer unable to perform well in gas separations. One important consideration at this point is that modeling used to predict the properties of hybrid materials must use the most appropriate properties available as input. Therefore, hybrid films that have been annealed will be modeled using the properties obtained for annealed polymer membranes whereas the hybrid films that have not been annealed will be modeled using the properties of the neat polymer.

While the annealing step causes an additional energy burden on the formation process, there are some advantages obtained from annealing above T_g, even for the neat polymer. Most importantly, the polymer shows a substantial increase in its resistance to plasticization. One of the major drawbacks in polymer based membrane applications is the ability of some aggressive feed streams to reduce the separation performance of a membrane [5]. As mentioned in Chapter 3, plasticization of the membrane can occur when sorption reaches a critical level. Unfortunately, the plasticization is almost always accompanied by a decrease in selectivity. The matrix polymer used in this study, 6FDA-6FpDA, has a plasticization pressure for carbon dioxide of approximately 100 psia. The membrane permeability decreases as the pressure is increased up to this pressure. The dual mode model of gas transport indicates this decrease is the result of filling of the Langmuir sorption sites. However, further increasing the pressure after this point leads to swelling of the polymer causing higher chain mobility and significant increases in permeability. Figure 5.12 shows the relationship of permeability to feed pressure for carbon dioxide in a 6FDA-6FpDA membrane before and after annealing.

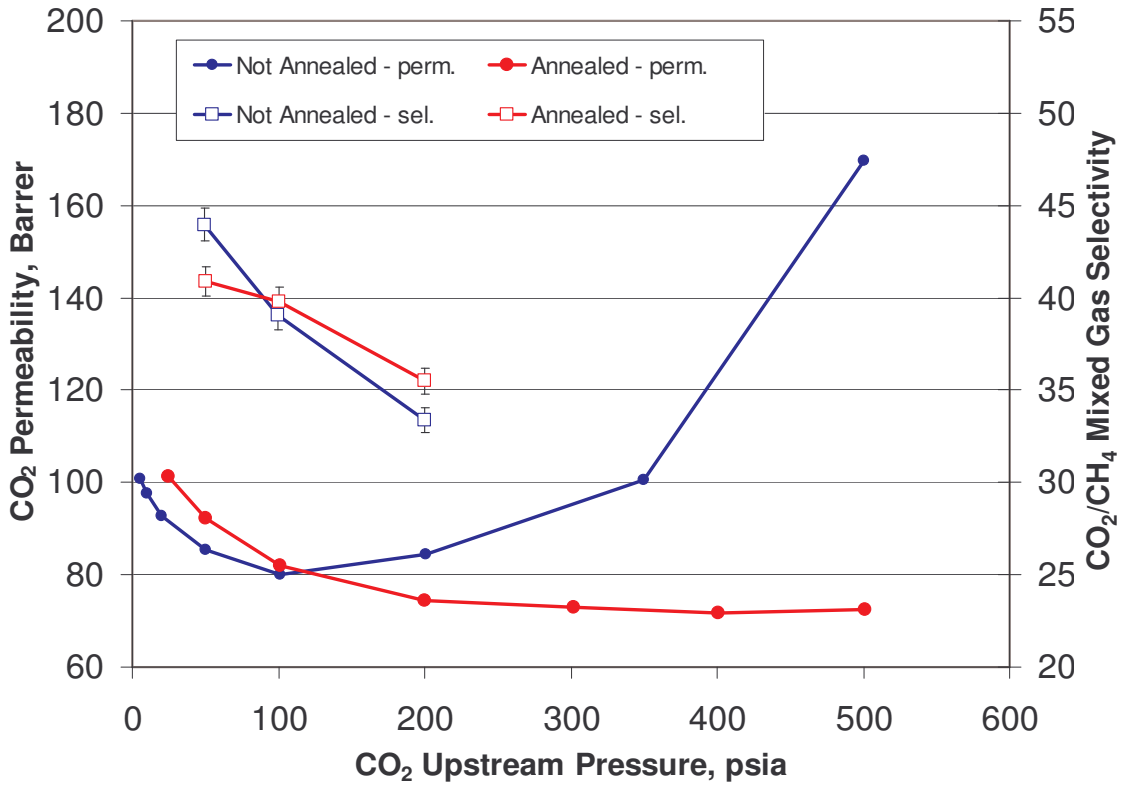

Figure 5.12 The pressure dependence of CO_2 permeability in 6FDA-6FpDA changes significantly after annealing above T_g. Selectivity decreases less in the annealed sample than in the sample that was not annealed. Permeability was measured at 35 °C, and selectivity was measured using an 80:20 CH_4:CO_2 mixed gas ratio.

The membrane that has not been annealed shows a very clear plasticization pressure with substantial increases in permeability as the upstream pressures exceed 100 psia. The annealed membrane, on the other hand, does not show a clear plasticization pressure in tests up to 500 psia. There is a slight rise in the permeability between 400 psia and 500 psia, but the change is within the error of the measurement and without testing at higher pressures, it is not certain if this is the onset of plasticization. Furthermore, the change in selectivity is significantly greater for the sample before annealing than for the sample after annealing. The exact cause of the increased resistance to plasticization is not completely known, but these properties could be attributed to the formation of charge transfer complexes [6-8].

Charge transfer complexes are known to form in polyimides from the interactions of regions of high and low electron density in the backbone of the polymer chain [9-13]. The six membered aromatic rings form areas of high electron density while the five membered rings possess lower electron density [14] (see Figure 3.1). It is believed that the increased mobility of the polymer chains at higher temperatures (even below T_g in some cases) is sufficient to allow the segments sufficient movement so that these areas of differing electron density can align [15]. When properly aligned, π-electron interactions occur that restrict the chain mobility. The Coulombic interactions that occur at these locations inhibit segmental motion of the polymer chains holding them together more tightly. As a result, it is more difficult for a penetrant to swell the material leading to a higher plasticization pressure. Recent work presented by Zhou was able to use fluorence spectroscopy to observe the formation of these complexes in Matrimid® that was annealed to 220°C [16]. Zhou showed that these complexes significantly reduced the plasticization effect of acetic acid and water on Matrimid® hollow fibers.

Another change caused by annealing is an increase in the carbon dioxide permeability prior to plasticization relative to the non-annealed polymer. Similar trends were seen by Madden for Matrimid® hollow fibers [15]. Figure 5.13 shows the response for Matrimid® hollow fibers annealed at 220 °C, and these results show very similar trends to the 6FDA-6FpDA polymer after annealing above T_g. These effects are not unlike the changes observed for some systems that can be crosslinked.

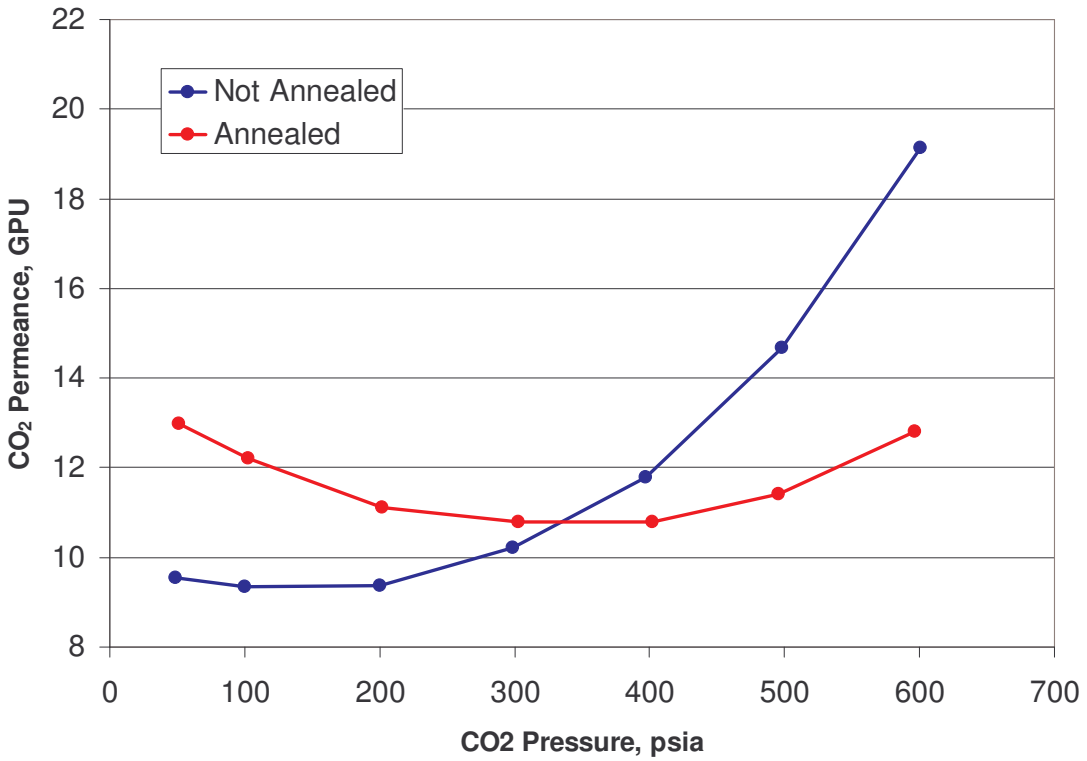

Figure 5.13 The pressure dependence of permeance in Matrimid® hollow fibers of similar age shows significant changes when the fibers are annealed at 220 °C [15].

Wind et al. showed that the use of small crosslinking agents in the 6FDA-6FpDA:DABA system caused the same effects seen in these annealed systems shown in Figures 5.12 and 5.13 [17-19]. The structure of 6FDA-6FpDA:DABA is shown in figure 5.14.

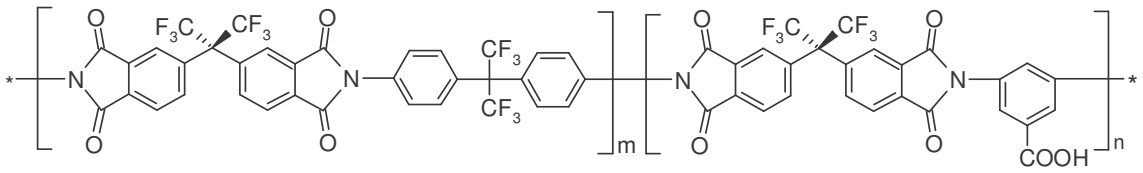

Figure 5.14 The carboxylic acid on the DABA group in the 6FDA-6FpDA:DABA (2:1) polymer provides a location for the formation of crosslinks between the polymer chains.

In this system, a diol may be used to crosslink the polymer by bridging two of the DABA groups. The use of the smaller crosslinking agent, ethylene glycol, led to a response in the 6FDA-6FpDA:DABA system that was very similar to that seen in the annealed 6FDA-

6FpDA and Matrimid® systems. The plasticization response of the 6FDA-6FpDA:DABA system crosslinked with ethylene glycol is shown in Figure 5.15. The increased permeability in the crosslinked sample was explained as a result of the inflexibility of the small crosslinking agent. The less flexible crosslink inhibited the packing structure of the polymer, essentially "propping" the chains apart causing higher carbon dioxide permeability. This effect was not seen for the larger crosslinking agents, presumably because their greater flexibility allowed better chain alignment.

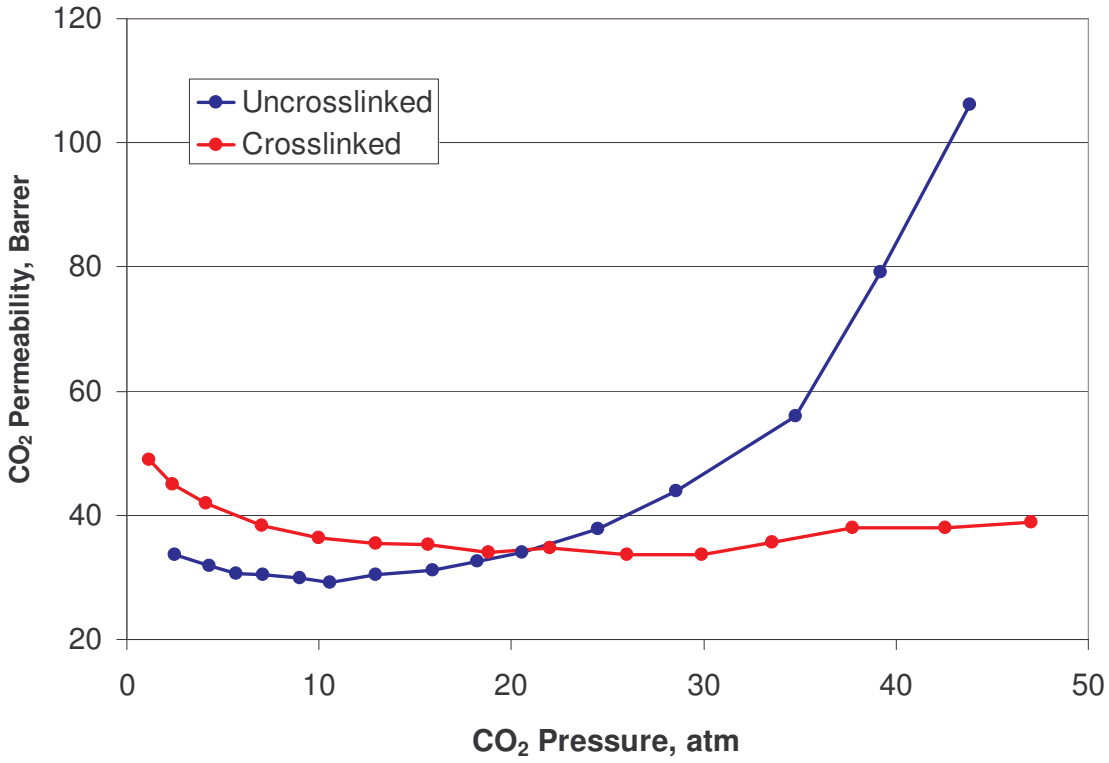

Figure 5.15 Crosslinking with ethylene glycol greatly suppresses plasticization in 6FDA-6FpDA:DABA (2:1) [17].

Due to the similar response shown by the annealed 6FDA-6FpDA and the crosslinked 6FDA-6FpDA:DABA systems, it is possible that the formation of charge transfer complexes in the annealed polymer act much like a short crosslinking agent in the network. The configuration imposed by the alignment of the regions of differing electron density may restrict the chain packing of the polymer enough to lead to the enhanced

permeability seen while at the same time increasing the segmental interactions sufficiently to inhibit the effects of plasticization. While the actual mechanism for these property changes is not known exactly, the ability of the polymer to withstand plasticization in the presence of higher feed pressures of CO_2 is a great benefit for applications in natural gas purification.

5.8. Summary

While the properties of the polymer phase are susceptible to changes during various processing steps, unlike the carbon molecular sieve powders, many of these changes can be monitored and measured directly through dense film characterization. This chapter has provided evidence to show how these changes may be prevented or controlled allowing a more complete understanding of the performance of the hybrid membranes to be obtained.

Chapters 4 and 5 have detailed many of the changes that occur in the two component phases of the hybrid membranes during the processing steps. These changes must be monitored and accounted for during the modeling and analysis of hybrid membrane systems. Chapter 6 will discuss the application of models to the hybrid membranes formed from these materials.

5.9. References

1. Walker, D.R.B. (1993). Synthesis and Characterization of Polypyrrolones for Gas Separation Membranes. Chemical Engineering. Austin, TX, The University of Texas at Austin. Doctor of Philosophy: 168.
2. Coleman, M.R. (1992). Isomers of Fluorine-Containing Polyimides for Gas Separation Membranes. Chemical Engineering. Austin, The University of Texas at Austin. Doctor of Philosophy: 262.
3. Liu, Y., Wang, R., et al. (2001). "Chemical Cross-Linking Modification Of Polyimide Membranes For Gas Separation." Journal of Membrane Science 189: 231-239.

4. Tin, P.S., Chung, T.S. (2003). "Effects Of Cross-Linking Modification On Gas Separation Performance Of Matrimid Membranes." Journal of Membrane Science 225: 77-90.
5. Ismail, A.F. and Lorna, W. (2002). "Penetrant-Induced Plasticization Phenomenon In Glassy Polymers For Gas Separation Membrane." Separation and Purification Technology 27(3): 173-194.
6. Bos, A., Punt, I.G.M., et al. (1998). "Plasticization-Resistant Glassy Polyimide Membranes For CO2/CO4 Separations." Separation and Purification Technology 14(1-3): 27-39.
7. Kawakami, H., Mikawa, M., et al. (1996). "Gas Transport Properties In Thermally Cured Aromatic Polyimide Membranes." Journal of Membrane Science 118(2): 223-230.
8. Mikawa, M., Nagaoka, S., et al. (1999). "Gas Transport Properties And Molecular Motions Of 6fda Copolyimides." Journal of Membrane Science 163(2): 167-176.
9. Dinan, F.J., Schwartz, W.T., et al. (1992). "Solid-State C-13-NMR Spectral Evidence For Charge-Transfer Complex-Formation In Aromatic Diimides And Dianhydrides." Journal of Polymer Science Part A-Polymer Chemistry 30(1): 111-118.
10. Dinehart, R.A. and Wright, W.W. (1971). "Study Of Some Properties Of Aromatic Imides." Makromolekulare Chemie 143(APR29): 189
11. Hasegawa, M., Kochi, M., et al. (1989). "Molecular Aggregation And Fluorescence-Spectra Of Aromatic Polyimides." European Polymer Journal 25(4): 349-354.
12. Huang, H.W., Horie, K., et al. (1999). "Differences In Thermo-Mechanical Properties And Intermolecular Charge-Transfer Characteristics Of The Aromatic Polyimide PI(BPDA/PDA) From Various Precursors." Macromolecular Chemistry and Physics 200(4): 791-798.
13. Ishida, H., Wellinghoff, S.T., et al. (1980). "Spectroscopic Studies Of Poly[N,N'-Bis(Phenoxyphenyl)Pyromellitimide].1. Structures Of The Polyimide And 3 Model Compounds." Macromolecules 13(4): 826-834.
14. Krol, J.J., Boerrigter, M., et al. (2001). "Polyimide Hollow Fiber Gas Separation Membranes: Preparation And The Suppression Of Plasticization In Propane/Propylene Environments." Journal of Membrane Science 184(2): 275-286.
15. Madden, W.C. (2005). The Performance Of Hollow Fiber Gas Separation Membranes In The Presence Of An Aggressive Feed Stream. Chemical and Biomolecular Engineering. Atlanta, Georgia Institute of Technology. Doctor of Philosophy: 240.
16. Zhou, F. (2005). Novel Pervaporation for Separating Acetic Acid and Water Mixtures Using Hollow Fiber Membranes. Chemical and Biomolecular Engineering. Atlanta, Ga, Georgia Institute of Technology. Doctor of Philosophy.
17. Wind, J.D. (2002). Improving Polyimide Membrane Resistance to Carbon Dioxide Plasticization in Natural Gas Separations. Chemical Engineering. Austin, TX, The University of Texas at Austin. Doctor of Philosophy: 232.
18. Wind, J.D., Staudt-Bickel, C., et al. (2002). "The Effects Of Crosslinking Chemistry On Co2 Plasticization Of Polyimide Gas Separation Membranes." Industrial & Engineering Chemistry Research 41(24): 6139-6148.
19. Wind, J.D., Staudt-Bickel, C., et al. (2003). "Solid-State Covalent Cross-Linking Of Polyimide Membranes For Carbon Dioxide Plasticization Reduction." Macromolecules 36(6): 1882-1888.

CHAPTER 6

PERFORMANCE OF HYBRID MEMBRANES WITH AN UPPER BOUND POLYMER MATRIX.

The previous chapters discussed the components of the hybrid matrix separately, and this chapter covers the application of these materials to the formation of hybrid membranes with enhanced separation performance. Modeling the transport in hybrid systems is paramount to a fully developed understanding of the experimental results. Models not only provide a means of predicting the properties for guidance in the design of a hybrid system, but they also provide a useful tool for determining the source of non-ideal properties that may be obtained in the formation of a hybrid gas separation membrane. This chapter begins with a detailed look at modeling that has been well established for application to hybrid membrane systems. With the model basis established, the remainder of the chapter will discuss the process developed for the enhancement of membrane performance in 6FDA-6FpDA, an upper bound polymer, through the use of carbon molecular sieves.

6.1. Model Predictions for Hybrid Gas Separation Membranes

The Maxwell equation was introduced in Chapter 2 as one of the most useful models in the prediction of transport properties in hybrid systems. While some more complex models are available the enhancement in model performance is marginal at best and unable to justify the added complexity, not only in calculations but also in evaluation of the model results [1, 2]. All of the model predictions shown in previous chapters describe systems with ideal, uniform properties. In practice, the interactions of the

polymer and the sieve often lead to regions of non-ideal properties near the interface. Of particular importance are materials in which voids are formed between the polymer and the sieve due to poor adhesion and materials in which the polymer properties are disrupted by the sieve particles. The following discussion shows how the Maxwell equation can be adapted to account for non-ideal regions that may form in the hybrid system. In particular, the model may be used to determine the effects of various interfacial phenomena that may occur where the polymer and sieve interact.

In order to account for these changes that occur near the interface of the hybrid system, Mahajan introduced the idea of modeling an interphase between the polymer and the sieve [3]. This interphase may be a void between the polymer and sieve, a region of polymer with properties altered by the presence of the sieve, or it may describe surface diffusion around the sieve. By applying the Maxwell equation two times, the three phase system may be modeled. Since the sieve is assumed to be fully enclosed by this interphase, the Maxwell equation may be applied to the interphase and sieve first to generate properties for a “pseudosieve” phase. The pseudosieve may then be modeled within the polymer matrix to describe the entire hybrid system. Figure 6.1 illustrates the pseudosieve concept.

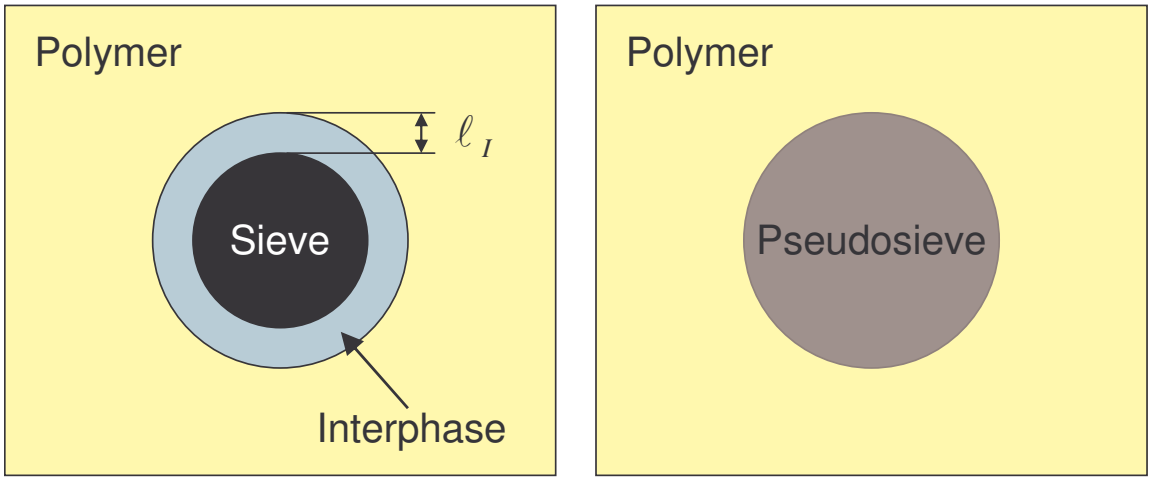

Figure 6.1 The sieve and the interphase are modeled together as a “pseudosieve” in the application of the three-phase Maxwell model.

By assuming that the interphase is continuous and fully surrounds the sieve, the Maxwell equation, shown previously (Equation 2.21), may be adapted to model the pseudosieve. In this application, the sieve is the dispersed phase and the interphase is the continuous phase:

$$P_{PS} = P_I\left[\frac{P_S + 2P_I - 2\phi_S\left(P_I - P_S\right)}{P_S + P_I + \phi_S\left(P_I - P_S\right)}\right] \tag{6.1}$$

where P_{PS} is the effective permeability of the pseudosieve phase, P_S is the permeability of the sieve, P_I is the permeability of the interphase, and ϕ_S is the volume fraction of the sieve in the pseudosieve. With a constant thickness of the interphase around the sieve, the volume fraction of the sieve in the pseudosieve follows the relationship shown in Equation 6.2

$$\phi_S = \frac{\phi_d}{\phi_d + \phi_I} = \frac{r_S^3}{\left(r_S + \ell_I\right)^3} \tag{6.2}$$

where ϕ_d and ϕ_I are the volume fractions of the sieve and the interphase in the overall membrane, respectively. The radius of the sieve is given by r_S, and ℓ_I is the thickness of the interphase around the sieve. This pseudosieve is then modeled as the dispersed phase in a second application of the Maxwell equation to the system with the permeability of the matrix polymer as the continuous phase, P_c, to provide the effective permeability of the three phase system, P_{3eff}.

$$P_{3eff} = P_c\left[\frac{P_{PS} + 2P_c - 2\left(\phi_d + \phi_I\right)\left(P_c - P_{PS}\right)}{P_{PS} + P_c + \left(\phi_d + \phi_I\right)\left(P_c - P_{PS}\right)}\right] \tag{6.3}$$

This expression will now allow the performance of a three phase membrane to be modeled if the permeability and thickness of the interphase can be estimated. In practice, one of these variables may be fit to data if the other can be reasonably

predicted. The following two subsections discuss methods of modeling the permeability in the interphase for two important morphologies: voids between the polymer and the sieve, and interactions that alter the performance of the polymer in the interphase when well bonded to the sieve surface.

6.1.1. Estimating Permeability in Molecular Scale Voids

One morphology commonly encountered in hybrid membrane systems is the presence of voids at the interface, also called “sieve-in-a-cage morphology”. This morphology can be seen in the SEM image of a hybrid membrane formed by Moore from the polysulfone Udel® and zeolite 4A shown in Figure 6.2 [4]. Although this morphology leads to increased permeability, there are several reasons that it should be avoided. First, the high permeability of the void compared to the sieve will cause most of the gas to bypass the sieve preventing selectivity enhancement in the membrane. If the size of the void is near the size of the penetrants or larger, the Knudsen selectivity will favor the lighter molecule resulting in selectivities below 1 in the void for the industrially important separations of O_2/N_2 and CO_2/CH_4. The presence of voids at the interface can also present significant problems when the hybrid membranes are formed as asymmetric hollow fibers. As the thickness of the selective layer of the fiber approaches the size of the sieve, voids at the interface can result in defects that essentially pass through the entire selective region of the membrane, greatly reducing the separation performance.

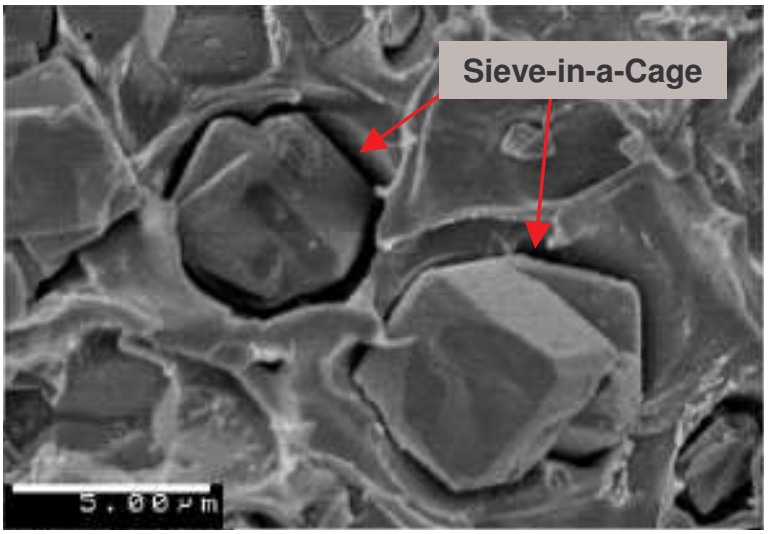

Figure 6.2 A hybrid membrane formed by Moore from the polysulfone Udel® and zeolite 4A demonstrates the sieve-in-a-cage morphology. Adapted from [4].

As discussed in Chapter 2, permeability is the product of the effective diffusion and sorption coefficients for a material. By assuming the penetrant in the void acts as an ideal gas, the sorption may be calculated by Equation 6.4.

$$S = \frac{C}{P} = \frac{n/V}{P} = \frac{1}{RT} = 0.012 \frac{cm^3(STP)}{cm^3 \cdot cmHg} \tag{6.4}$$

When the voids are very small, the sorption must be adjusted to account for the finite size of the penetrants. Ferry suggested the following correction for the Henry's law constant in a small pore for component A which may be adapted for the voids around the sieve [5]:

$$S_A = \frac{C_A}{P_A}\left(1 - \frac{\sigma_A}{2r_P}\right)^2 = \frac{1}{RT}\left(1 - \frac{\sigma_A}{2\ell_I}\right)^2 \tag{6.5}$$

where σ_A is the Lennard-Jones collision diameter of penetrant A, r_P is the radius of the pore, and ℓ_I is the thickness of the void at the interface. The pore radius and the void thickness in Equation 6.5 are related through the hydraulic diameter of the void based on the assumption that the width of the void is much greater than the thickness [4].

Because of the small size of the voids, the diffusion is assumed to fall in the in the Knudsen regime as discussed in Chapter 2. For this application, the diffusion is modeled by the empirical expression:

$$D = \frac{0.97x10^{-5}\,cm2\cdot(g/mol)^{1/2}}{s\overset{o}{\mathrm{A}}K^{1/2}}\sqrt{\frac{T}{M_P}}r_P = \frac{0.97x10^{-5}\,cm2\cdot(g/mol)^{1/2}}{s\overset{o}{\mathrm{A}}K^{1/2}}\sqrt{\frac{T}{M_P}}\ell_I \tag{6.6}$$

with the molecular weight of the penetrant, M_P, in g/mol, the absolute temperature, T, in Kelvin, and the pore radius, r_P, and interphase thickness, ℓ_I, both in angstroms. As with the sorption, this expression must be adapted to account for the finite size of the penetrant as shown [6]:

$$D = \frac{0.97x10^{-5}\,cm2\cdot(g/mol)^{1/2}}{s\overset{o}{\mathrm{A}}K^{1/2}}\sqrt{\frac{T}{M_P}}r_P\left(1-\frac{\sigma_A}{2r_P}\right) = \frac{0.97x10^{-5}\,cm2\cdot(g/mol)^{1/2}}{s\overset{o}{\mathrm{A}}K^{1/2}}\sqrt{\frac{T}{M_P}}\ell_I\left(1-\frac{\sigma_A}{2\ell_I}\right) \tag{6.7}$$

With these equations used to estimate the permeability of the void, the thickness of the void remains as a variable in the three phase model. Practical application of this modeling to permeation data often involves using the void thickness as an adjustable parameter. If the void size is as large as a few nanometers, SEM imaging may be able to provide some information. Unfortunately, angstrom sized voids are below the resolution of SEM analysis, and TEM must be used. Voids of this size can present a particularly important case in hybrid films as these defects can cause selectivities below that of the bulk polymer. Even with the application of high resolution imaging, it is difficult to obtain an accurate measure of the void dimensions due to inconsistencies in the void dimensions throughout the membrane as well as issues with sample preparation and problems associated with trying to average the properties from a small

sample. Therefore these tools are best used to support the modeling results rather than actually providing measurements of the average void size.

6.1.2. Estimating Permeability in Polymer with Altered Properties

In some situations, rather than forming voids, the polymer forms a good bond to the sieve, but interaction between the sieve and the polymer leads to changes in the transport properties in the polymer near the sieve. One form of this change is termed "matrix rigidification". Matrix rigidification occurs when the polymer chains experience reduced mobility in the region near the sieve leading to lower permeability. Rigidification has been observed near the interface for multiple composite materials causing deviations from model expectations such as decreased sorption [7], increased modulus [8-10], and even reduced permeability in semi-crystalline polymers [11]. Mahajan noticed that the effect of this reduction in permeability increased as the sieve loading increased [12], suggesting that the higher loading led to a greater fraction of affected polymer. In some cases, the affected region is believed to extend to as much as 1 μm [7, 13].

In order to account for the reduction in permeability experienced in the rigidified polymer, the permeability is assumed to decrease based on a chain immobilization factor, β, such that

$$P_I = \frac{P_c}{\beta}. \tag{6.8}$$

A similar approach has been used to model the permeability in the amorphous regions of semi-crystalline polymers [11, 14, 15]. Michaels et al. suggest that the value of β should depend on the penetrant [16]; however, for the similarly sized gases studied in this work, O_2, N_2, CO_2, and CH_4, the assumption of a constant value of β should introduce little

error [4]. As a reference, a value of β equal to 3 is commonly observed for oxygen and nitrogen in rigidified polymer [4]. For systems where the polymer is rigidified by the presence of the sieves, β has a value greater than one. It is suggested, however, that the interaction of the sieve and the polymer may result in permeability in the interphase that is higher than the bulk polymer [4].

This phenomenon causes a morphology known as a “stress dilated region”. The morphology of these regions is less well understood than the cases of matrix rigidification. There are multiple potential sources for this morphology: 1) addition of free volume to the polymer matrix near the interface by tensile stress insufficient to cause delamination of the polymer from the sieve, 2) disruption of the packing ability of the polymer chains (i.e. by nanoparticles), and 3) increased free volume near the interface due to poor interactions between the polymer and sieve [4]. Modeling of a stress dilated region involves the use of β values lower than 1.

The application of this model using the chain immobilization factor has one major limitation. The selectivity of the polymer is assumed to be constant even when the permeability changes from rigidification or stress dilation. These morphology changes are most likely the result of changes in the free volume of the polymer in this region. Since permeability and selectivity show dependence on free volume [4, 17], it is very likely that the selectivity does not remain constant; however, predicting the changes that would occur is speculative at best. While these estimates may not provide precisely accurate property estimates, they do provide insight about the morphology of the hybrid membranes based on the experimental results.

6.2. Applying Models to a Specific System

Moore developed a "map" of the properties predicted by these models for systems with Ultem and two different zeolites, 4A and HSSZ-13, as the insert phase [4]. By adapting these models to the system studied in this work, similar maps may be generated to provide insight to the sources of the properties obtained in the hybrid membranes. The "maps" for the hybrid system tested in this work can be seen in Figure 6.3 with some of the key results presented in Table 6.1. The predictions are shown for both the O_2/N_2 separation and the CO_2/CH_4 separation, with lines of constant β and ℓ_I / r_S included to show the effect of these parameters.

Table 6.1 Transport properties for important model predictions in hybrid membranes containing 10 vol% CMS in 6FDA-6FpDA. Predictions are for membranes operating at 35 °C and 50 psia.

Sample	Permeability (Barrer)		Selectivity	
	O_2	CO_2	O_2/N_2	CO_2/CH_4
Continuous Phase: 6FDA-6FpDA	18.9 ± 0.92	85.4 ± 2.6	4.52 ± 0.020	39.7 ± 0.64
Dispersed Phase: CMS-800-2 [18]	24	43.5	13.3	200
Maxwell Prediction 10 vol%	19.4	80.4	4.97	42.7
Impermeable Sieve 10 vol%	16.2	73.2	4.52	39.7
3 Å Sieve-in-a-Cage 10 vol%	22.0	82.8	4.20	29.3

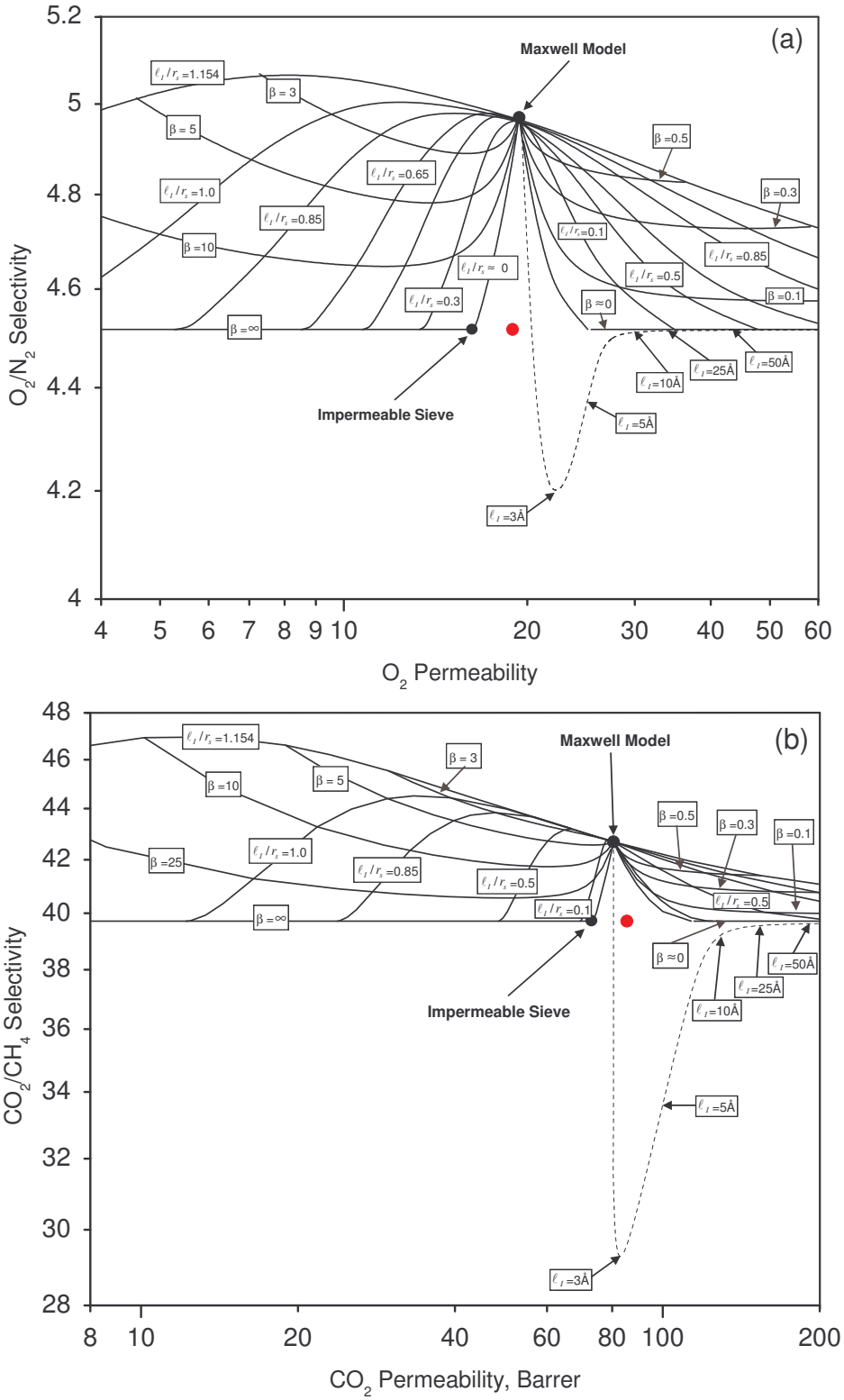

Figure 6.3 Transport properties are predicted for various hybrid membrane morphologies for a 10 vol% air milled carbon molecular sieves in 6FDA-6FpDA for (a) O_2/N_2 and (b) CO_2/CH_4. Predictions are for membranes operating at 35 °C and 50 psia. The red dot represents neat polymer.

The dashed lines in part a and b of Figure 6.3 represent the impact of voids between the polymer and the sieve. The occurrence of a minimum in these curves represents the effect of the reduced selectivity that can result from this type of defect. When the voids become large enough, the permeability for both gases increases to the point that the selectivity of the hybrid membrane is not changed. When the void size is smaller, the permeability in the void is still low enough that the selectivity of the hybrid membrane is reduced by the lower selectivity region of the void. The permeability in the voids is strongly dependent on the size of the void and the size of the penetrant. For both methane and nitrogen, the size of the molecules causes a sharp increase in permeability to be predicted in the region between 2.5 and 3.0 Å. Because of this permeability increase for the slow gases in this region, the maximum selectivity depression is predicted for a void size of 3 Å. At this point, the permeability of the gases becomes high enough to begin reducing the impact of the low selectivity in the void, and the selectivity of the hybrid membrane begins to approach that of the neat polymer while the overall permeability continues to increase.

When the hybrid system alters the properties of the polymer, the model predictions show deviations from the Maxwell equation. For the rigidified polymer, $\beta > 1$, the deviations fall to the left of the Maxwell prediction due to the lower permeability, and for the stress dilated polymer, $\beta < 1$, the deviations fall to the right of the Maxwell prediction. The upper boundary of the property map is formed when ℓ_I / r_S is equal to 1.154. This value corresponds to a system where the properties of the entire polymer matrix are impacted by the inserts. This value changes as the sieve loading changes. For a system containing 20 vol% inserts, this upper limit comes when ℓ_I / r_S is equal to 0.710.

Another interesting feature of these maps is the maximum selectivity predicted for systems with a high amount of rigidification. This increase in selectivity is caused by enhanced “matching” between the polymer and the sieve. In this case, the reduction in permeability predicted for the extensively rigidified polymer brings the fast gas permeability of the matrix closer to one third of that in the sieve. As discussed in Chapter 2, this relationship leads to the greatest predicted enhancement in hybrid membrane performance. If the fast gas permeabilities of the sieves used in this work were more than three times higher than that of the polymer, this maximum would occur in the stress dilated region of the map rather than the rigidified region.

When the rigidification of the polymer is modeled as infinite, the permeability in the interphase goes to zero, resulting in reduced permeability for the hybrid membrane with no change in selectivity, because the impermeable regions increase the tortuosity of the pathway for the penetrants while selectivity remains a material property. The limit of this effect as ℓ_I / r_S approaches zero models the response of an impermeable sieve insert as indicated in Figure 6.3.

Possibly the largest drawback to the use of these property maps is the assumption that the deviation from ideal transport properties in the hybrid membranes results from one dominant non-ideal morphology. Moore clearly showed the existence of multiple non-ideal morphologies within a single mixed matrix membrane [4], and this occurrence can easily be imagined in a membrane that possesses excellent polymer sieve adhesion while still having some amount of sieve agglomerates that exclude polymer-sieve contact. Such a system may easily experience matrix rigidification in regions where the sieves are well dispersed while the agglomerates impart properties similar to the sieve-

in-a-cage morphology. Further, more complicated combinations of non-ideal morphologies within a membrane can lead to nearly infinite combinations of voids and altered polymer properties with any number of β's and ℓ_I / r_S's. Accurate prediction and modeling of such systems is beyond any current capabilities; however, the use of the property maps based on one dominant morphology still provide a basis for the limits within which the properties of the hybrid material should fall. These figures provide a visual tool based on current knowledge of hybrid membrane morphologies and their impacts on transport properties that allows large amounts of data to be easily compared and analyzed. The remainder of this chapter will discuss the results of the hybrid membrane development carried out with the carbon molecular sieves and upper bound polymer studied in this work. Property maps similar to those shown in Figure 6.3 will be used as a basis for much of the analysis presented.

A comment about the data presented in the following sections is needed for clarification. All of the data plotted on the figures represent the properties measured for a specific *film* cast from one dope. The properties of a film were obtained by testing a minimum of three separate *membranes* from that film and averaging the results. The values given in the tables below indicate the average value for multiple *films* prepared under similar processing conditions.

6.3. Model Analysis of Initial Hybrid Membrane Results

The utility of these maps in the analysis of the hybrid membrane properties is illustrated by revisiting the initial tests performed with modified CMSs. Chapter 5 discussed, the properties leading to the conclusion that uncontrolled modification of the polymer backbone causes drastic changes in the properties of the polymer matrix. Table 6.2

gives the properties obtained, and Figure 6.4 shows those results (originally given in Figure 5.1) plotted on the morphology maps for both the O_2/N_2 and CO_2/CH_4 separations. In both cases, the permeability of the hybrid membrane is considerably lower than the bulk polymer while the selectivity showed only marginal changes.

Table 6.2 Transport properties for initial hybrid membranes formed with 10 vol% modified CMS in 6FDA-6FpDA. Permeabilities tested at 35 ^{o}C and 50 psia.

Sample	Permeability (Barrer)		Selectivity	
	O_2	CO_2	O_2/N_2	CO_2/CH_4
Continuous Phase: 6FDA-6FpDA	24.1 ± 1.6	110 ± 5.7	4.42 ± 0.22	36.5 ± 1.7
Dispersed Phase: CMS-800-2 [18]	24	43.5	13.3	200
Maxwell Prediction 10 vol%	24.1	102	4.82	38.8
Hybrid Membrane 10 vol%	12.3 ± 2.5	55.0 ± 8.5	4.49 ± 0.088	36.2 ± 0.37

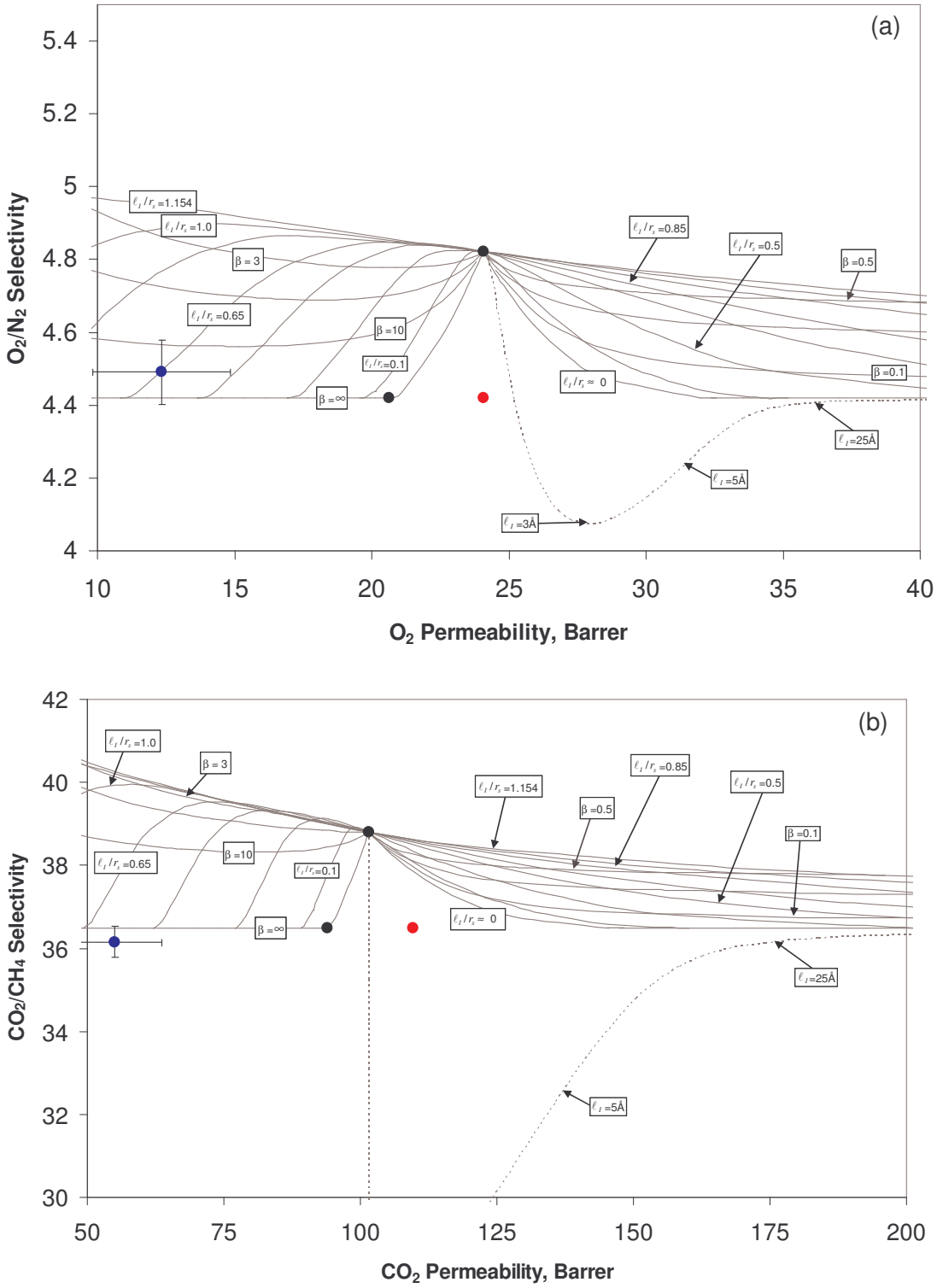

Figure 6.4 The initial hybrid materials created with 10 vol% modified CMS showed considerable impact on the transport properties of the bulk polymer for separation of (a) O_2/N_2 and (b) CO_2/CH_4. The red dot represents neat polymer. Permeabilities tested at 35 °C and 50 psia.

The location of these data on the maps falls in the range of very high β's (> 100) with ℓ_I / r_S in the range of 0.5 to 0.65. This explanation for the properties is most likely not physically realistic, but it does support the conclusion presented in Chapter 5 that the properties of the hybrid membrane did not result only from the properties of the neat component materials. As shown in the figure, the properties obtained could not be achieved with impermeable sieves alone. This example demonstrates the ability of these models to provide guidance in the analysis of hybrid systems even with the simplifying assumptions used in their development.

6.4. Hybrid Membranes Formed with "Controlled" Modification

The overwhelming impact of the modifier on the polymer matrix was controlled in subsequent applications by limiting the amount of linkage unit used in the modification of the sieves. The 1,4-phenylenediamine used to improve the interactions at the interface was limited in the solutions to between one and two times the amount needed to form a monolayer on the surface of the carbon molecular sieves following the calculations discussed in Chapter 5. This controlled modification was successful in limiting the impact of the diamine on the polymer transport properties; however, these membranes still did not possess the desired property enhancements from the incorporation of the molecular sieves. Figure 6.5 shows the O_2/N_2 and CO_2/CH_4 separation performance of several membranes formed from sieves modified with controlled amounts of diamine, and Table 6.3 gives the average values obtained.

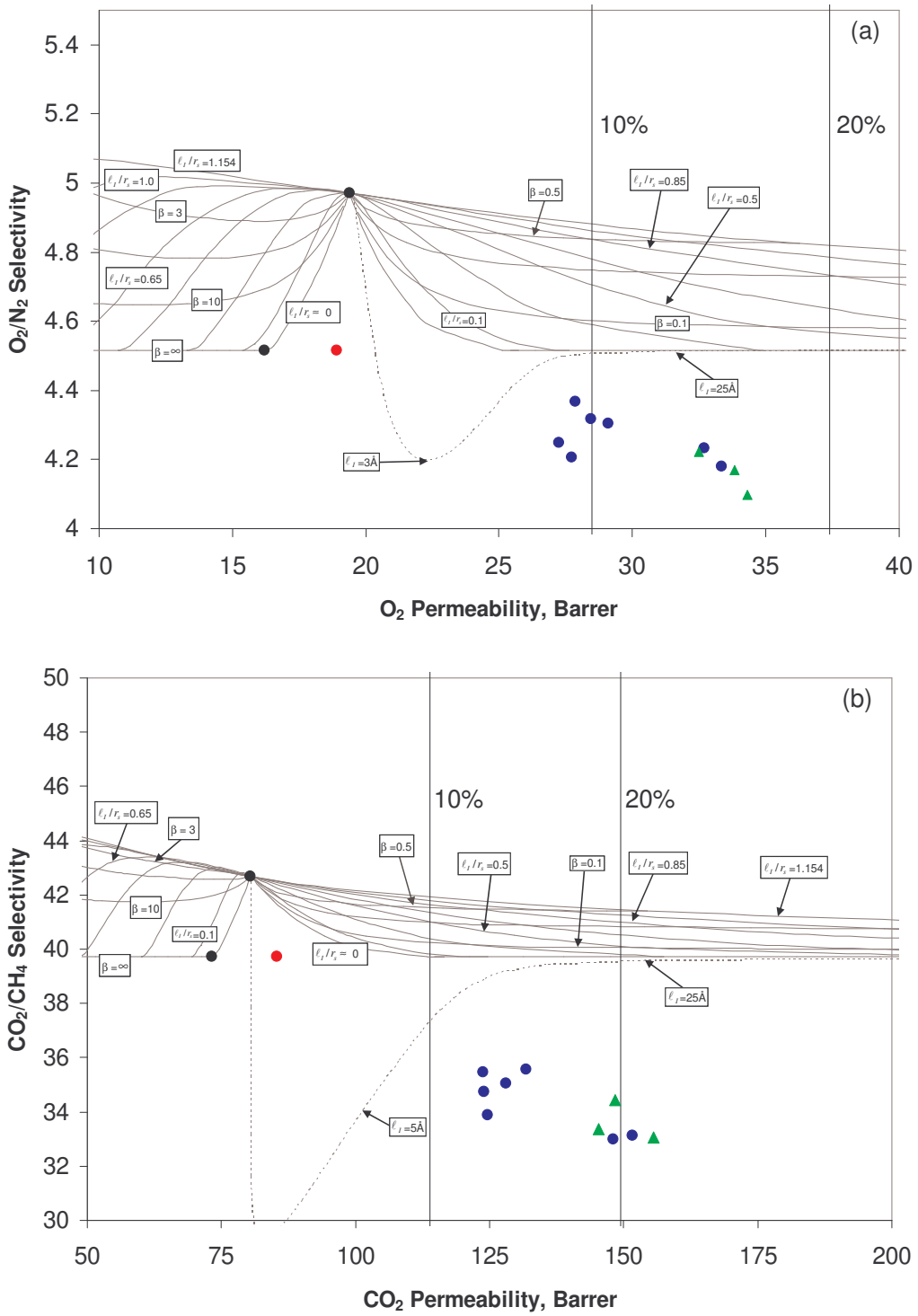

Figure 6.5 Hybrid membranes formed from 10 vol% CMS modified with controlled amounts of modifier (blue dots) showed very high permeabilities for the separation of (a) O_2/N_2 and (b) CO_2/CH_4. The red dot represents neat polymer. Green triangles represent hybrid membranes formed with unmodified CMS. Permeabilities tested at 35 °C and 50 psia.

Table 6.3 Transport properties for membranes formed from 10 vol% CMS modified with controlled amounts of modifier in 6FDA-6FpDA. Permeabilities tested at 35 °C and 50 psia.

Sample	Permeability (Barrer)		Selectivity	
	O_2	CO_2	O_2/N_2	CO_2/CH_4
Continuous Phase: 6FDA-6FpDA	18.9 ± 0.92	85.4 ± 2.6	4.52 ± 0.020	39.7 ± 0.64
Dispersed Phase: CMS-800-2 [18]	24	43.5	13.3	200
Maxwell Prediction 10 vol%	19.4	80.4	4.97	42.7
Modified Hybrid 10 vol%	29.5 ± 2.5	133 ± 12	4.27 ± 0.066	34.4 ± 1.1
Unmodified Hybrid 10 vol%	33.5 ± 0.93	150 ± 5.2	4.16 ± 0.062	33.6 ± 0.73

For both separations, the hybrid membranes showed significant increases in permeability with a slight depression in the selectivity. The green data points indicate the results of hybrid membranes formed using 10 vol% of unmodified sieves. Also included in Figure 6.5 are vertical reference lines that indicate the permeability expected for the incorporation of 10 and 20 vol% voids. All of the hybrid results shown in Figure 6.5 are for membranes produced from 10 vol% sieves, but almost all of the CO_2 permeabilities and several of the O_2 permeabilities were higher than they would be with the addition of 10 vol% voids rather than sieves. In order for the hybrid membranes to possess such high permeabilities, there must be significant voids throughout the membrane. As previously mentioned, the presence of substantial agglomeration in the membrane can lead to large voids that greatly increase the permeability of a hybrid membrane. These results make sense in light of the presence of visible agglomerates seen on the surface of the hybrid membranes cast under these conditions. To view the distribution of the CMS particles within the membrane, a sample of the membrane was etched in a 1N solution of potassium hydroxide for 30 minutes [19]. After etching in the stirred solution for 30 minutes, the sample was removed and dried. Measurement of a control sample showed a thickness reduction of between 5 and 10 microns, and the

slight graying of the solution indicated that enough of the polymer was etched to disperse some of the sieves into the solution. The dried sample was then viewed with a scanning electron microscope. Figure 6.6 shows the agglomerates that were clearly present in the hybrid membrane. At the same time, it is very likely that either very small defects that pass through the entire membrane, or a portion of sieves exhibiting sieve-in-a-cage morphology with voids in the range of 2-5 Å exist to cause the reduction in selectivity seen in the hybrid membranes.

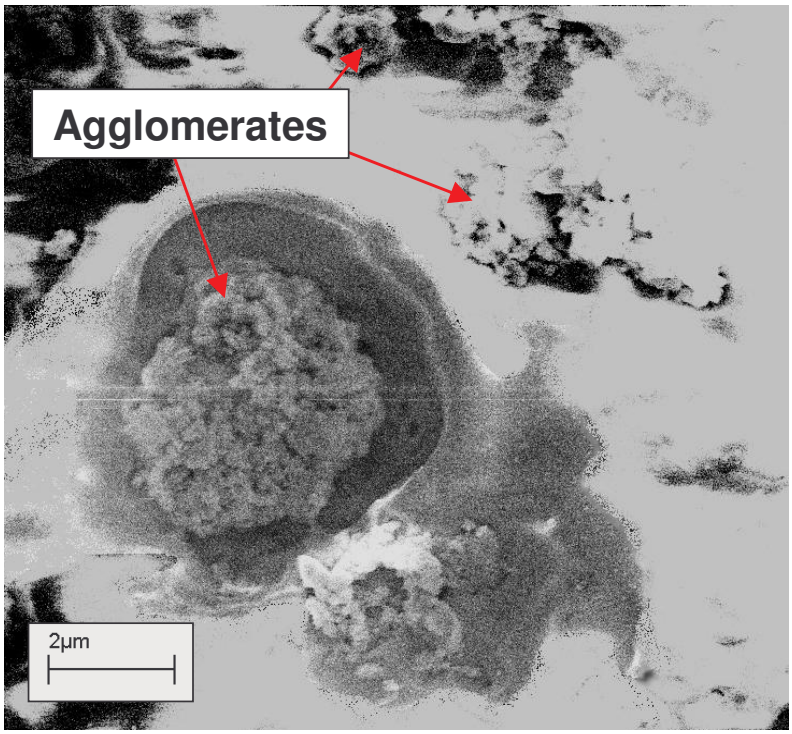

Figure 6.6 Large CMS agglomerates are visible in the SEM image of a hybrid membrane formed from 6FDA-6FpDA and modified CMSs. The film was etched in KOH solution to reveal the distribution of the sieves within the membrane.

These results include membranes cast from dopes of varying viscosities. Vu discovered that casting hybrid membranes using CMSs in Ultem® and Matrimid® required relatively high viscosities to eliminate the occurrence of the sieve-in-a-cage morphology [18]. Unfortunately, even using highly viscous dopes did not result in successful enhancement of the transport properties in this work.

6.5. Preventing Agglomerates in Hybrid Membranes with Sonication

The presence of the agglomerates in the membrane persisted in the hybrid membranes even with the high viscosity used to cast several of the films. Since the high viscosity should prevent the formation of agglomerates by limiting the mobility of the sieves in the dope, it is very likely that the agglomerates exist in the dope prior to casting the membrane. Further understanding of this hypothesis and the steps eventually developed to eliminate the agglomerates may be established by a more detailed description of the process used to form the high viscosity casting dopes used for these membranes.

Chapter 5 showed the impact of modification on the stability of the carbon molecular sieves in the priming polymer solutions. Unfortunately, these systems still did not possess full stability, and the results presented in Figures 6.5 and 6.6 above show the inability of the sieves to remain dispersed during film formation. In order to produce the high viscosity dopes used to form hybrid membranes, the final dope must possess a relatively low ratio of solvent to solids (sieves and polymer). In draw casting, the solvent content may be as low as 75 wt% (as opposed to 95-98 wt% for simple solution casting). The recovery process used after modification of the carbon molecular sieve particles cause the sieves to form a cake, and after drying, the particles must be separated prior to forming the hybrid membranes. Placing the particles in solution and agitating by hand or with stirring is insufficient to fully disperse the sieves; however, immersion of the solution in an ultrasonic bath is generally successful at producing a well dispersed suspension of modified CMS particles. Unfortunately, the dispersion of the modified CMS particles works best with sieve concentrations at or below 5 wt% in the solvent. Prolonged sonication at higher concentrations might be capable of providing the needed dispersion; however, the standard procedure of sonicating for 30 minutes used in this

work would not fully disperse highly concentrated solutions as evidenced by visible agglomerates that would almost immediately settle out of solution and remain on the wall of the glass vial used to form the casting dopes. As a result, the dopes were always started as dilute suspensions, and solvent was evaporated to provide the needed viscosity for casting the hybrid films.

In order to remove the excess solvent from the solutions, the vials were purged with N_2 while slowly rotated by hand to allow the solvent to evaporate without forming a vitrified film on the surface of the dope. The resulting dopes appeared viscous and free of agglomerates, but the high viscosity and complete opacity of the dope prevented visual characterization prior to casting. When the dope was cast, in the worst cases, visible agglomerates would appear on the surface immediately, but in most cases, the surface of the cured membrane would have the appearance of fine grit sand paper even if there were not large visible agglomerates, suggesting the presence of agglomerates as the sieves themselves should be too small to visually discern with the naked eye.

Since visual observation of the dope prior to evaporation of the solvent suggested the successful removal of agglomerates, it was apparent that the agglomerates were forming during the solvent evaporation given that the resulting membranes seemed to possess excessive agglomeration. In order to eliminate this unwanted effect of the solvent evaporation, sonication was added during the solvent removal to overcome the problem. Instead of rotating the vial by hand during solvent removal, the vial was immersed in the ultrasonic bath while being purged with N_2. The sonication provided sufficient agitation to prevent the formation of a vitrified film on the surface of the dope while at the same time acting to prevent the formation of sieve agglomerates while the solvent was evaporating. Because small amounts of the dope would dry on the sides of

the vial as the solvent level decreased, the solution was periodically rotated by hand while remaining in the ultrasonic bath to remove the dried dope from the walls of the vial. This process was continued until the desired viscosity was obtained for the solution, which usually consisted of three 15 minute intervals of purging with sonication each followed by several minutes of sonication without purging to remove the dried dope from the walls of the vial. This continued treatment with the ultrasonic bath during the solvent removal is believed to produce a dope that is free of excessive agglomeration and viscous enough to prevent agglomerate formation while the film dries, as discussed in the following section. This process is illustrated by the cartoon shown in Figure 6.7.

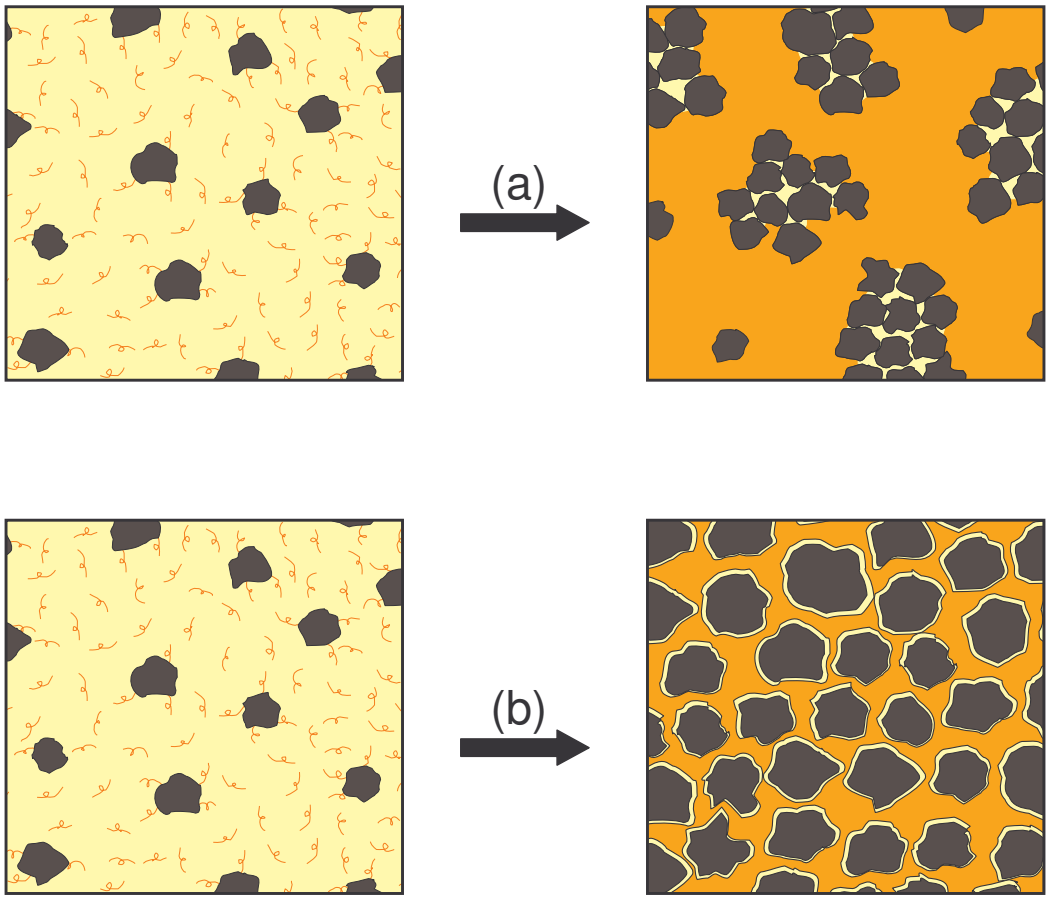

Figure 6.7 Solvent evaporation without continued sonication (a) lead to membranes with large sieve agglomerates, but modification of the solvent evaporation process to include continued sonication (b) eliminated most of the sieve agglomerates in the membranes.

6.6. Hybrid Films formed Without Agglomerates.

The films formed from dopes produced using the modified solvent evaporation procedure were visually improved over those formed using previous techniques. Not only were visible, large agglomerates no longer on the surface, but the films no longer had the appearance of sandpaper. Instead the films produced from these dopes appeared smooth and shiny on the surface. More importantly, the transport properties of these films were altered by the new formation process. Figure 6.8 shows the properties of the membranes produced using the new process, and Table 6.4 gives the average values obtained. The results for the films produced using the previous method are included as a reference.

Table 6.4 Transport properties for hybrid membranes formed from 10 vol% CMS prepared with the new solvent evaporation process in 6FDA-6FpDA. Permeabilities tested at 35 ^{o}C and 50 psia.

Sample	Permeability (Barrer)		Selectivity	
	O_2	CO_2	O_2/N_2	CO_2/CH_4
Continuous Phase: 6FDA-6FpDA	18.9 ± 0.92	85.4 ± 2.6	4.52 ± 0.020	39.7 ± 0.64
Dispersed Phase: CMS-800-2 [18]	24	43.5	13.3	200
Maxwell Prediction 10 vol%	19.4	80.4	4.97	42.7
New Modified Hybrid 10 vol%	24.5 ± 0.89	108 ± 3.7	4.27 ± 0.041	34.5 ± 0.62
New Unmodified Hybrid 10 vol%	28.4 ± 2.5	125 ± 11	4.96 ± 0.012	35.7 ± 0.30

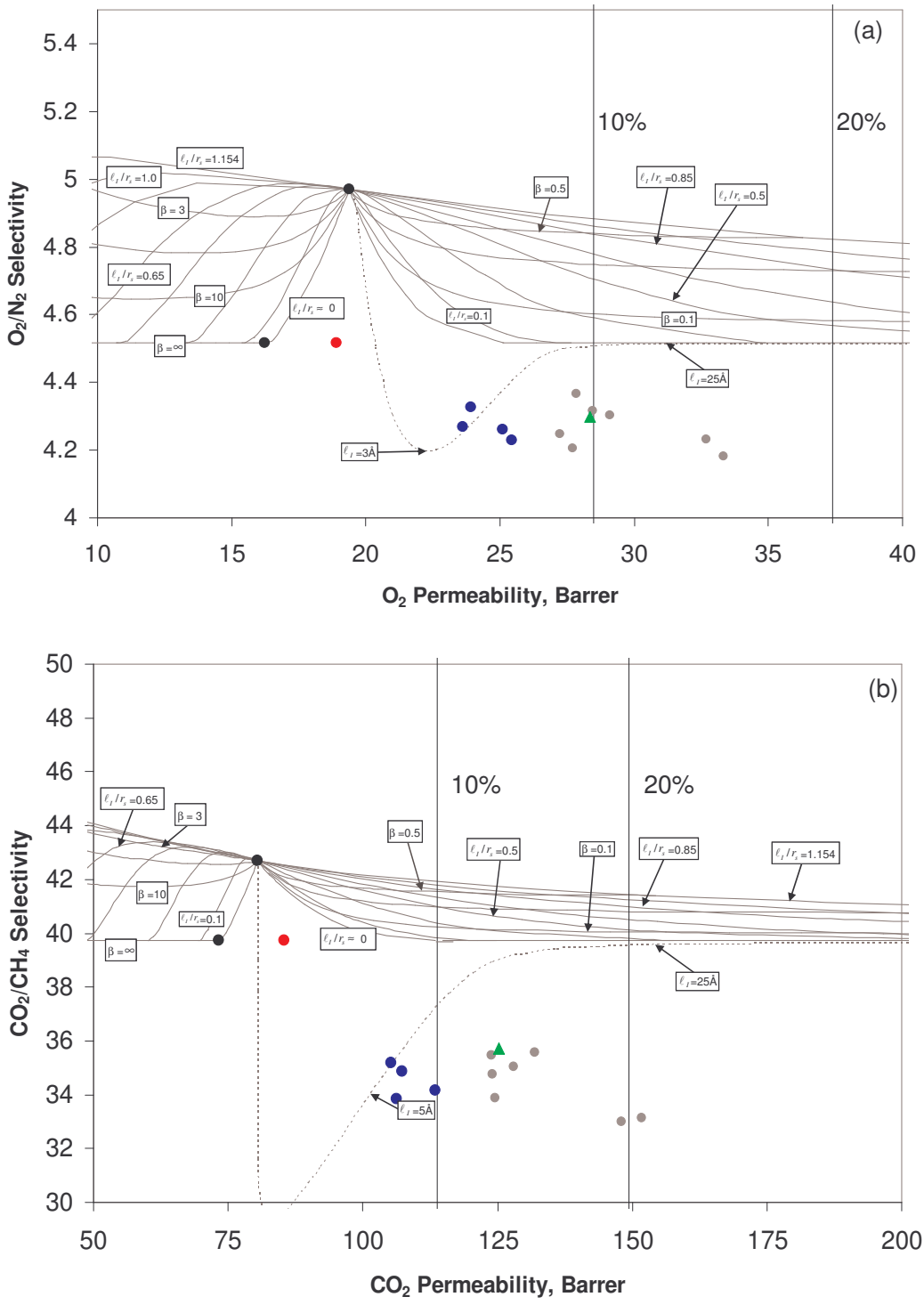

Figure 6.8 Hybrid membranes formed from 10 vol% CMS prepared with the new solvent evaporation process (blue dots) had properties very close to those predicted for systems with 4 to 6 angstrom voids for both (a) O_2/N_2 and (b) CO_2/CH_4. Also shown are neat polymer (red dot) and hybrid membranes formed with unmodified CMS (green triangle). Permeabilities tested at 35 °C and 50 psia.

The average properties of the films formed from the modified process have shown a decrease in permeability with little or no change in selectivity relative to the membranes formed from the earlier dopes. While these changes seem undesirable at first glance, further analysis shows that this trend is actually a move in the right direction. The results of the films from the modified process fall very near the model predictions for voids in the range of 4-6 Å for both the O_2/N_2 and CO_2/CH_4 separations. These sizes are on the order of magnitude of the gas molecules being separated in this work leading to the decreases in selectivity seen for these membranes. All of the samples prepared from the sonicated dopes also have permeabilities below those predicted for 10 vol% voids in the membrane. It appears that the new process greatly reduces the high permeability voids that were present in previous films. To view the distribution of the CMS particles within the membrane formed from the new dopes, a sample was etched and imaged with SEM as previously described. Figure 6.9 shows the well dispersed CMS particles within the sample prepared with the new solvent evaporation process. These results suggest some improvement in the membrane morphology, but the performance of the membranes still has not been enhanced as desired. Even when the new solvent evaporation process was used with unmodified CMSs, the hybrid membrane produced exhibited the response expected for large voids or excessive agglomeration.

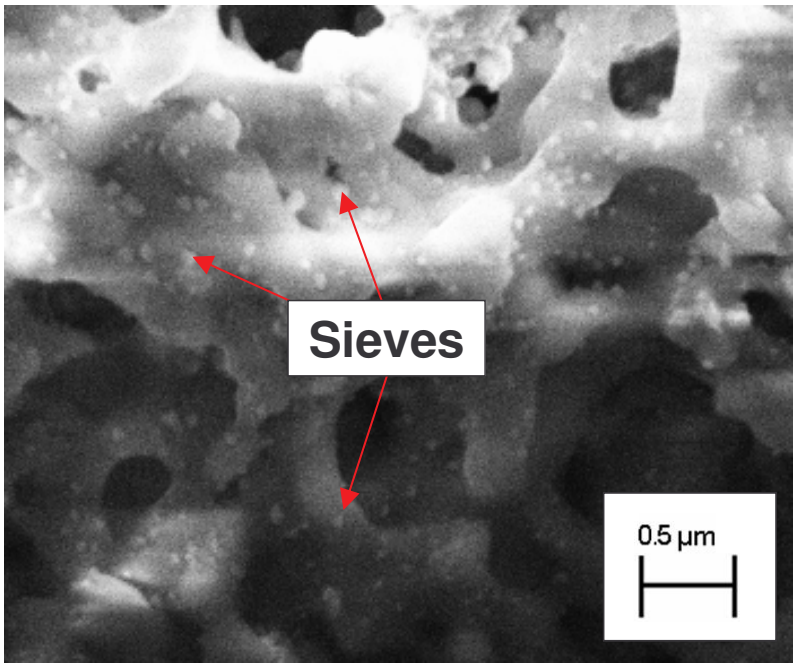

Figure 6.9 SEM revealed that the sieves in hybrid membranes formed from 6FDA-6FpDA and modified CMS using the new solvent evaporation protocol were well dispersed. The film was etched in KOH solution to reveal the distribution of the sieves within the membrane.

Small voids at the interface could lead to the properties seen in Figure 6.8. These voids may be the result of tensile stress generated during film vitrification. This stress could cause voids at the interface despite the presence of the modifier between the polymer and sieve. The significant reduction in permeability seen for these membranes formed using modified CMS with the enhanced process strongly suggests smaller voids than seen in previous membranes, but these voids must be further reduced before the performance of the membrane will be enhanced. Previous researchers have observed improvement in the performance of hybrid membranes that initially exhibit similar response by annealing near or above the T_g [4, 12], and this process was applied in this work as discussed in the following section..

6.7. Annealing Membranes to Improve Transport Performance

The proposed reason behind annealing the hybrid membranes is to relieve stress that accumulates during the curing process. Moore showed that the most successful techniques used to develop hybrid membranes involved reduction of tensile stress in the film as the solvent evaporates [4]. Since it is believed that the linkage units used in this work serve to form a covalent bond between the polymer and the sieve, it is possible that the evaporation of solvent from the membrane as it dries causes tensile stress between the polymer and the sieve where they are bound by the linkage unit. It is possible that annealing the polymer above its T_g would then allow the tensile stress to relax, hopefully reducing the size of the voids around the sieves sufficiently to allow enhanced separation performance from the molecular sieves. The average properties obtained can be seen in Table 6.5, and Figure 6.10 shows the transport properties of the annealed membranes for the separation of O_2/N_2 and CO_2/CH_4.

Table 6.5 Transport properties for hybrid membranes with 10 vol% CMS prepared from the new solvent evaporation process and above T_g annealing in 6FDA-6FpDA. Permeabilities tested at 35 °C and 50 psia.

Sample	Permeability (Barrer)		Selectivity	
	O_2	CO_2	O_2/N_2	CO_2/CH_4
Continuous Phase: Annealed 6FDA-6FpDA	21.4 ± 0.45	91.6 ± 1.6	4.51 ± 0.023	36.8 ± 0.71
Dispersed Phase: CMS-800-2 [18]	24	43.5	13.3	200
Maxwell Prediction 10 vol%	21.6	85.9	4.94	39.5
Annealed Modified Hybrid 10 vol%	19.9 ± 2.0	84.3 ± 9.1	4.6 ± 0.038	38.2 ± 0.22
Annealed Unmodified Hybrid 10 vol%	23.6 ± 1.2	99.6 ± 5.4	4.51 ± 0.056	36.7 ± 0.99

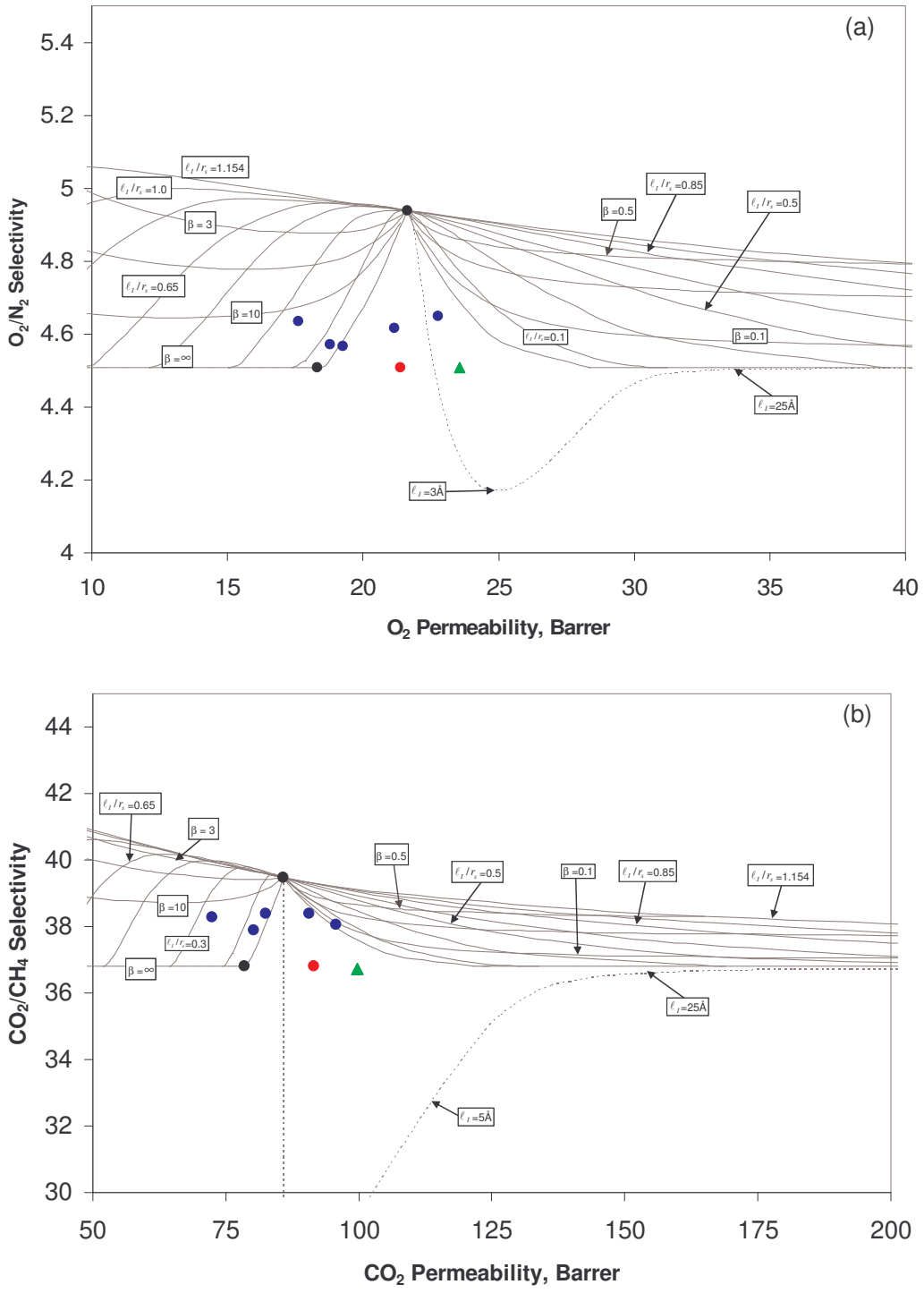

Figure 6.10 Hybrid membranes with 10 vol% CMS prepared from the new solvent evaporation process and above T_g annealing (blue dots) had enhanced transport properties in the direction predicted by the Maxwell equation for both (a) O_2/N_2 and (b) CO_2/CH_4. Also shown are neat polymer (red dot) and hybrid membranes with unmodified CMS (green triangle). Permeabilities tested at 35 °C and 50 psia.

The membranes that were annealed above T_g showed enhanced separation performance in the direction predicted by the Maxwell equation. Many of the data points for both separations fall in between the matrix rigidification and stress dilation regions of the maps shown, which may indicate the presence of multiple morphologies within the membranes. Again, these properties indicate that the majority of the large voids have been eliminated; however, it is not possible to completely rule out the ability of a complex morphology to possess some voids while at the same time providing the properties seen in the hybrid membranes.

6.8. Hybrid Membranes with Higher Sieve Loadings.

Membranes were prepared using a sieve loading of 20 vol% in order to further verify the conclusions drawn with lower sieve loadings and to show the ability of the process to further enhance membrane performance. The modified solvent removal process was used in the formation of the dopes for the 20 vol% hybrid membranes, and the resulting films were again free from visible defects. Figure 6.11 shows the transport properties for the O_2/N_2 and CO_2/CH_4 separations for hybrid films with 20 vol% CMS that were dried after casting but not annealed, and the average values obtained are shown in Table 6.6.

Table 6.6 Transport properties for hybrid membranes formed from 20 vol% CMS prepared with the new solvent evaporation process in 6FDA-6FpDA. Permeabilities tested at 35 °C and 50 psia.

Sample	Permeability (Barrer)		Selectivity	
	O_2	CO_2	O_2/N_2	CO_2/CH_4
Continuous Phase: 6FDA-6FpDA	18.9 ± 0.92	85.4 ± 2.6	4.52 ± 0.020	39.7 ± 0.64
Dispersed Phase: CMS-800-2 [18]	24	43.5	13.3	200
Maxwell Prediction 20 vol%	19.9	75.8	5.48	46.1
New Modified Hybrid 20 vol%	22.7 ± 2.6	102 ± 14	4.26 ± 0.19	33.0 ± 0.87
New Modified Hybrid 10 vol%	24.5 ± 0.89	108 ± 3.7	4.27 ± 0.041	34.5 ± 0.62

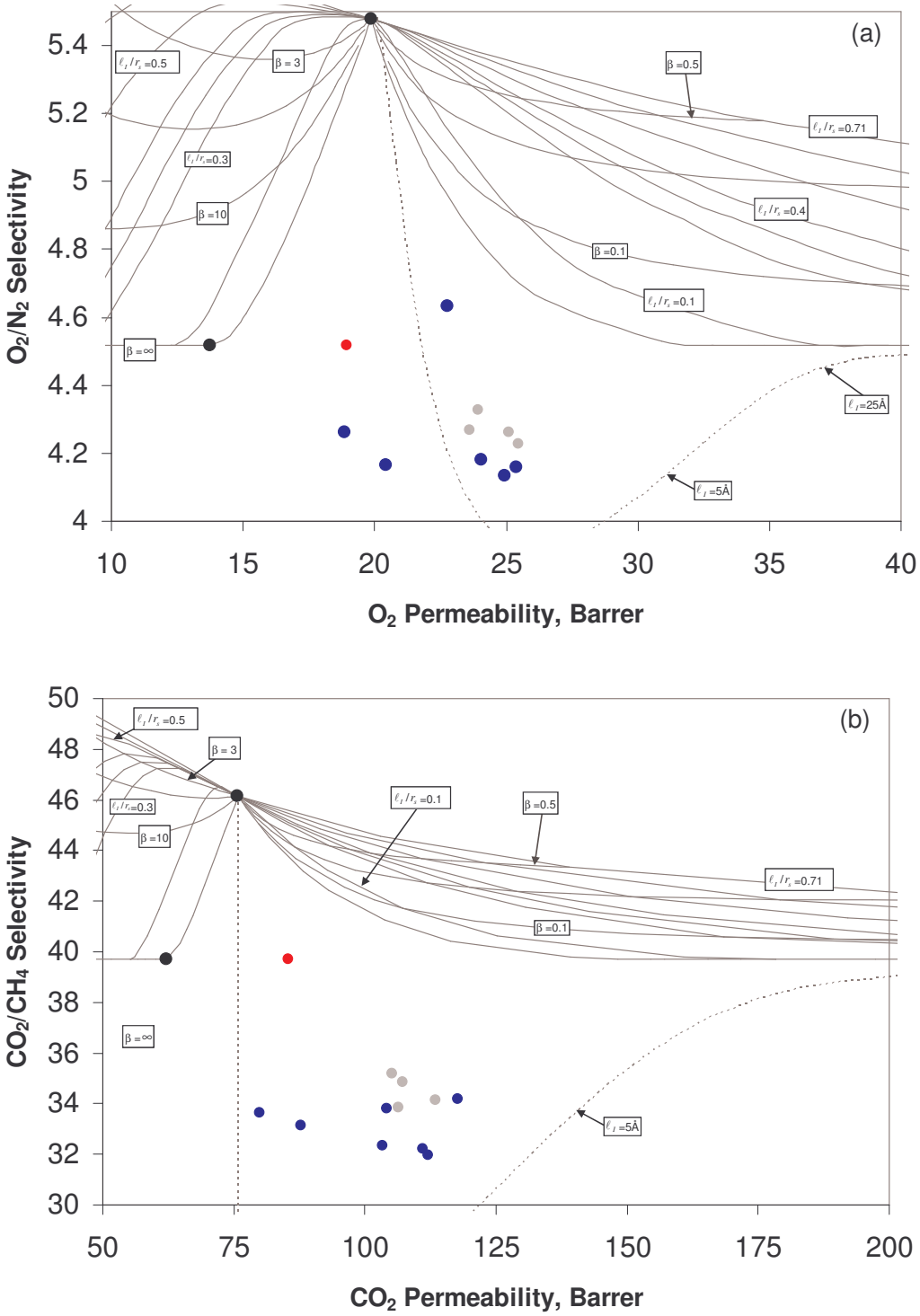

Figure 6.11 Hybrid membranes formed from 20 vol% CMS prepared with the modified solvent evaporation (blue dots) showed significantly decreased selectivity compared to the neat polymer (red dot) for both (a) O_2/N_2 and (b) CO_2/CH_4. Permeabilities tested at 35 °C and 50 psia. Results for 10 vol% also shown (gray dots).

The membranes prepared at higher loadings showed generally the same trend as the 10 vol% membranes; however, the selectivity of these hybrid membranes was slightly reduced over that for the films with lower loading. This further reduction in selectivity is consistent with the model predictions which show potential for considerably lower selectivities in these systems with higher loadings.

These films were then annealed following the same procedure used for the samples with 10 vol% loading, and the results of these trials can be seen in Figure 6.12. Table 6.7 shows the average properties obtained for these films. The transport properties for the O_2/N_2 and CO_2/CH_4 separations are shown, and the results from the samples with 10 vol% loading are included as a reference. Clearly, the increased CMS loading in these samples has further enhanced the separation performance of the membranes by providing additional enhancement of the selectivity in these films.

Table 6.7 Transport properties for hybrid membranes with 20 vol% CMS prepared from the new solvent evaporation process and above T_g annealing in 6FDA-6FpDA. Permeabilities tested at 35 °C and 50 psia.

Sample	Permeability (Barrer)		Selectivity	
	O_2	CO_2	O_2/N_2	CO_2/CH_4
Continuous Phase: Annealed 6FDA-6FpDA	21.4 ± 0.45	91.6 ± 1.6	4.51 ± 0.023	36.8 ± 0.71
Dispersed Phase: CMS-800-2 [18]	24	43.5	13.3	200
Maxwell Prediction 20 vol%	21.6	85.9	4.94	39.5
Annealed Modified Hybrid 20 vol%	23.2 ± 0.58	98.0 ± 2.8	4.68 ± 0.018	39.4 ± 0.56
Annealed Modified Hybrid 10 vol%	19.9 ± 2.0	84.3 ± 9.1	4.6 ± 0.038	38.2 ± 0.22

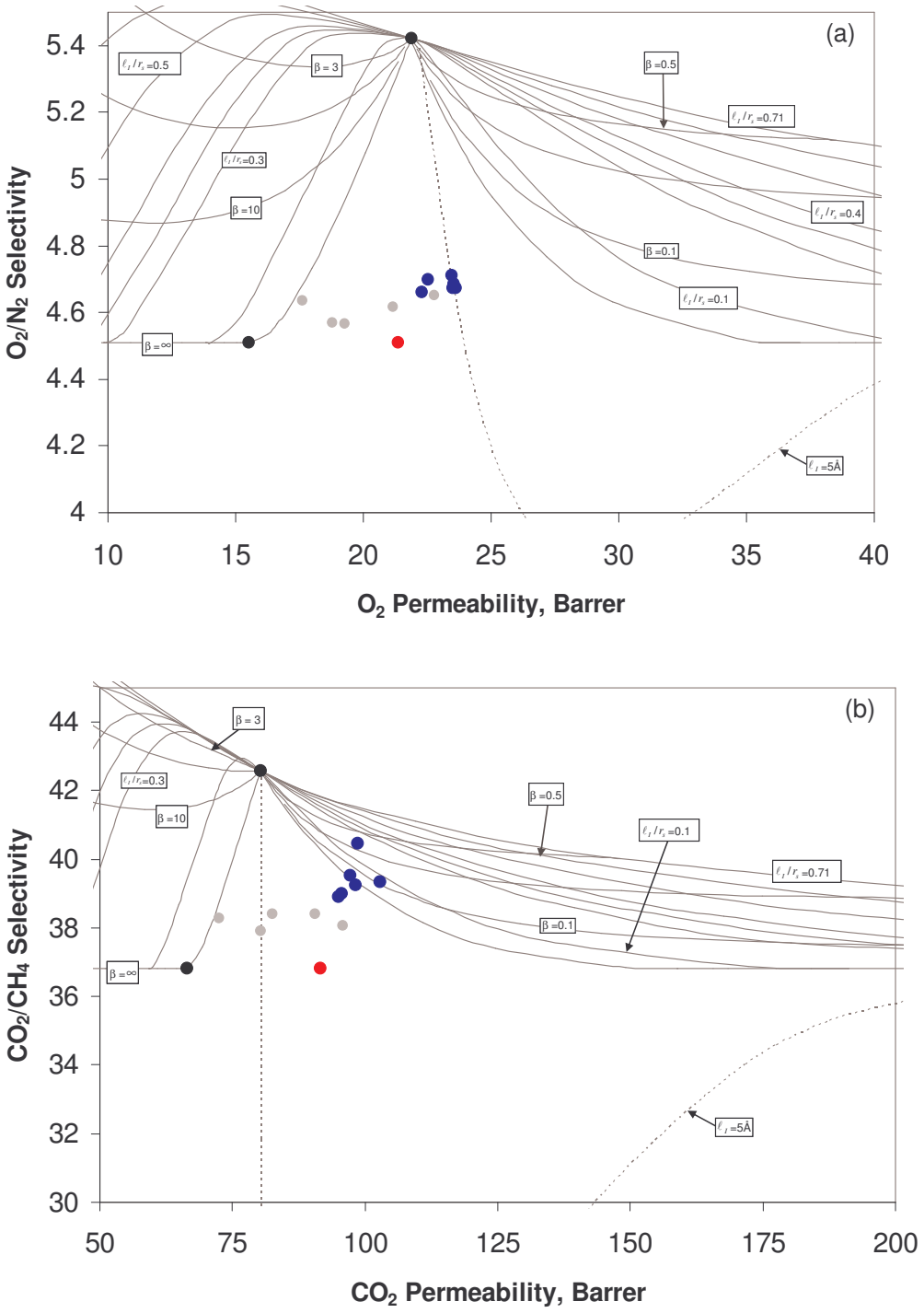

Figure 6.12 Hybrid membranes formed from 20 vol% CMS prepared with the modified solvent evaporation process and annealed above the T_g (blue dots) showed selectivity enhancements that exceeded those obtained for 10 vol% membranes (gray dots) for both (a) O_2/N_2 and (b) CO_2/CH_4. The red dot represents neat polymer. Permeabilities tested at 35 °C and 50 psia.

6.9. Summary

The work presented in this chapter has shown that carbon molecular sieve inserts may be used to enhance the separation performance of an upper bound polymer. To the author's knowledge, this is the first report of enhanced selectivity in a hybrid membrane prepared with an upper bound polymer matrix. The two major obstacles encountered in the formation of these hybrid membranes were excessive sieve agglomeration and residual stress in the vitrified membrane. Modification of the solvent evaporation process to include continual sonication was able to inhibit the formation of sieve agglomerates until the viscosity of the dope was high enough to sufficiently limit the particle mobility and prevent agglomeration. Analysis of the transport properties and SEM imaging of the membranes formed from the new process showed significant improvement over the previous methods. The resulting materials still did not possess the enhanced selectivity desired, most likely as a result of residual stress generated as the membrane vitrified after casting. In order to relieve the stress and improve the membrane performance, the hybrid films were annealed above the T_g of the material to allow the polymer to relax and repair the small voids caused by tensile stress at the interface. The annealing process successfully improved the interfacial region of the hybrid membranes to allow the sieves to increase the selectivity of the membranes above the neat polymer properties. Furthermore, the additional performance enhancement seen with increased sieve loading in the hybrid membranes, even though they may not equal the Maxwell prediction, shows the promise of this technology as a system to push the envelope of performance for polymer based gas separation membranes.

6.10. References

1. Bouma, R.H.B., Checchetti, A., et al. (1997). "Permeation Through A Heterogeneous Membrane: The Effect Of The Dispersed Phase." Journal of Membrane Science 128(2): 141-149.
2. Petropoulos, J.H. (1985). "A Comparative Study Of Approaches Applied To The Permeability Of Binary Composite Polymeric Materials." Journal of Polymer Science, Polymer Physics 23: 1309-1324.
3. Mahajan, R. and Koros, W.J. (2000). "Factors Controlling Successful Formation Of Mixed-Matrix Gas Separation Materials." Industrial & Engineering Chemistry Research 39(8): 2692-2696.
4. Moore, T.T. (2004). Effects of Materials, Processing, and Operating Conditions on the Morphology and Gas Transport Properties of Mixed Matrix Membranes. Chemical Engineering. Austin, TX, The University of Texas at Austin. Doctor of Philosophy: 312.
5. Ferry, J.D. (1936). "Statistical Evaluation Of Sieve Constants In Ultrafiltration." Journal of General Physiology 20(1): 95-104.
6. Suh, S.H. and Macelroy, J.M.D. (1986). "Molecular-Dynamics Simulation Of Hindered Diffusion In Microcapillaries." Molecular Physics 58(3): 445-473.
7. Manson, J.A. and Chiu, E.H. (1973). "Permeation Of Liquid Water In A Filled Epoxy Resin." Journal of Polymer Science Part C-Polymer Symposium(41): 95-108.
8. Galperin, I. and Kwei, T.K. (1966). "Dynamic Mechanical Properties Of Titanium Dioxide-Filled Poly(Vinyl Acetate) At 0-40 Degrees C." Journal of Applied Polymer Science 10(5): 673.
9. Kwei, T.K. and Kumins, C.A. (1964). "Polymer-Filler Interaction: Vapor Sorption Studies." Journal of Applied Polymer Science 8(3): 1483-1490.
10. Manson, J.A. and Sperling, L.H. (1976). Polymer Blends and Composites. New York, Plenum Press.
11. Michaels, A.S. and Parker, R.B. (1959). "Sorption And Flow Of Gases In Polyethylene." Journal of Polymer Science 41(138): 53-71.
12. Mahajan, R. (2000). Formation, Characterization and Modeling of Mixed Matrix Membrane Materials. Chemical Engineering. Austin, The University of Texas at Austin. Doctor of Philosophy: 259.
13. Moore, T.T. Mahajan, R., et al. (2004). "Hybrid Membrane Materials Comprising Organic Polymers with Rigid Dispersed Phases." AIChE Journal 50(2): 311-321.
14. Michaels, A.S., Barrie, J.A., et al. (1963). "Diffusion Of Gases In Polyethylene Terephthalate." Journal of Applied Physics 34(1): 13-20.
15. Michaels, A.S. and Bixler, H.J. (1961). "Solubility Of Gases In Polyethylene." Journal of Polymer Science 50(154): 393
16. Michaels, A.S. and Bixler, H.J. (1961). "Flow Of Gases Through Polyethylene." Journal of Polymer Science 50(154): 413
17. Park, J.Y. and Paul, D.R. (1997). "Correlation And Prediction Of Gas Permeability In Glassy Polymer Membrane Materials Via A Modified Free Volume Based Group Contribution Method." Journal of Membrane Science 125(1): 23-39.
18. Vu, D.Q. (2001). Formation and Characterization of Asymmetric Carbon Molecular Sieve and Mixed Matrix Membranes for Natural Gas Purification. Chemical Engineering. Austin, TX, The University of Texas at Austin. Doctor of Philosophy.
19. Moskowitz, P.A., Vigliotti, D.R., et al. (1984). Laser Micromachining of Polyimide Materials. Polyimides: Synthesis, Characterization, and Applications. K. L. Mittal. New York, Plenum Press. 1: 365-376.

CHAPTER 7

CONCLUSIONS AND RECOMMENDATIONS

7.1. Summary and Conclusions

As the first chapter indicated, the goal of this project was *to establish a framework for the development of gas separation membranes based on hybrid (polymer-carbon) materials that exceed the performance capabilities currently available with polymeric membrane systems*. In order to facilitate this goal, the hybrid membranes were formed with an upper bound polymer matrix. By using this matrix polymer, transport property enhancements over the neat polymer exceeded the properties obtainable by polymers alone. The development of this framework provided several important conclusions and highlighted the need for future research in some new areas. The primary conclusions drawn from the research objectives of this work are listed below and discussed in the subsequent paragraphs, and future work proposed for further development of this technology will be discussed in the following section.

1. Although the stability of submicron CMS suspensions was improved by surface modification and priming with polymer, a modified dope preparation technique was necessary to sufficiently suppress the formation of sieve agglomerates in the hybrid membranes.
2. A linkage unit capable of forming a covalent bond between the polymer and the sieve was successfully attached to the surface of the CMS particles without adversely affecting the transport properties of the sieve.
3. A modification technique was developed that prevents undesirable changes in the transport properties of the matrix polymer.

4. A formation protocol was developed that provides transport property enhancement in hybrid membranes formed with an upper bound matrix polymer. It appears that two of the primary steps necessary for property enhancement in hybrid systems are *prevention of agglomerates* and *reduction of stress* after film formation.

An important discovery relating to the processing of the sieves used in this work is the ability of milling the particles to not only reduce the size, but also to impact the bulk structure and transport properties of the sieves. The equilibrium sorption capacity of ball milled samples was significantly reduced, and WAXD showed changes in the average interplanar spacing. These changes were confirmed by CO_2 sorption measurements that indicated a shift in the pore size distribution within the carbon molecular sieves after ball milling.

Application of techniques developed for the modification of single-walled carbon nanotubes was successful at covalently attaching linkage units to the surface of the CMS particles without limiting the performance ability of the sieves in gas separation applications. The stability of the CMS particles suspended in a solution of priming polymer was slightly enhanced by the addition of the linkage unit; however, further process changes were required to fully prevent agglomeration in the dopes used to prepare hybrid membranes.

In a fashion similar to the sieves, an important discovery was made regarding the ability of linkage units to significantly alter the transport properties of the matrix polymer. Moderate to high amounts of modifier in the polymer matrix can significantly alter the transport properties of the material. For this system, the most common change was a

substantial drop in permeability with little or no change in the selectivity. Fortunately, this impact can be sufficiently reduced by limiting the amount of modifier used in the linkage.

Further work dealing with polymer annealed above the T_g showed slight changes in transport properties but more pronounced changes in the material response to plasticization in the presence of high CO_2 pressures. The onset of plasticization for the polymer was very near 100 psia of CO_2 at 35 ^oC before annealing, but after annealing, the plasticization pressure was near 400 psia under the same conditions.

The hybrid membrane work showed that previous methods used to stabilize particle suspensions (surface modification, priming with polymer, casting from viscous dopes) were unsuccessful at preventing the formation of agglomerates in the system studied in this work. Fortunately, modification of the dope formation process to include continual sonication was successful at preventing the excessive agglomeration that inhibited the previous trials.

Model analysis of the results indicated the presence of very small voids at the interface between the polymer and the sieve, and annealing of the hybrid membranes above the T_g was able to sufficiently “repair” the interfacial region so that the properties of the hybrid material were enhanced by the sieve inserts. Further work using higher loadings was also able to validate the applicability of this process to they polymer-sieve system studied in this work.

7.2. Recommendations for Future Work

While this work was successfully able to produce hybrid membranes with enhanced separation performance using an upper bound polymer matrix, the pathway towards this objective hilighted several important areas that could use further research and development work to advance hybrid membrane technology and improve its industrial viability. Several of these important research areas are discussed in the following subsections.

7.2.1. Determination of Transport Properties from Pore Size Distribution

Previous work has established the importance of pore size distribution in controlling the transport properties of molecular sieves [1]; however, accurate prediction of diffusivities and selectivities in carbon molecular sieves is not currently possible based on pore size distribution alone. Limitations in this area stem from difficulty in determining an "effective" pore size that describes the properties of the material [1]. The complexity of modeling the transport in these materials is further increased by the amorphous structure and irregular shapes of the pores.

Fortunately, research involved with carbon molecular sieve dense film membranes provides an excellent pathway towards the development of such predictive capabilities. Previous work has established the importance of several variables in determining the transport properties of CMS membranes [1-4], and the controlled variability of CMS membranes would allow a systematic study of the relationship between pore size distribution and gas transport properties. Preparation of CMS membranes with a wide range of transport properties would allow correlations between transport properties and pore size distributions to be developed using a large data set with considerable flexibility. It would also be of interest to analyze CMS materials prepared with different combinations of pyrolysis parameters that result in similar transport properties. For

example, it may be possible to prepare CMS membranes from precursors with considerably different free volumes under different temperature profiles such that the resulting CMS membranes possess nearly identical transport properties. Comparison of the pore size distributions of CMS materials prepared under such conditions could be very informative in building the knowledge base needed to develop predictive tools for the transport properties in these materials. One major advantage of such a predictive tool would be applicability to materials, such as CMS powders, that cannot be tested under traditional methods used for gas transport analysis.

7.2.2. Investigate Mechanism of Changes During Milling

This work showed the dramatic impact that ball milling can have on CMS physical properties. The milling process and atmosphere both showed significant effects on the final properties obtained in the CMSs. Further investigation should be performed to elucidate the mechanisms responsible for these property changes. One interesting series of tests to analyze these effects would be through the use of rigorously controlled atmospheres. Current results suggest that particles milled in air, oxygen enriched air, nitrogen, and helium could possess different properties. Williams has shown that CMS materials may be susceptible to oxidation that has the potential to dramatically impact gas transport in the sieves [1].

One tool that may be beneficial in studying the effects of oxidation on the CMS materials is high definition XPS analysis [5]. Several researchers have recently shown the ability to infer more detailed information about the oxidation state of carbon nanotubes by deconvoluting the C(1s) and O(1s) peaks obtained using high definition XPS [6-9]. Determining the chemical state of the oxygen on the surface of the CMS may help to resolve the mechanisms changing the CMS material during ball milling.

Extent of milling is another parameter that should be investigated. It is clear that increased milling initially changes the impact of processing on the CMS material; however, it is uncertain what limit these effects will approach under very extensive milling. It would be useful to determine if prolonged milling completely destroys the ability of CMS materials to perform gas separations, or if the changes in the material reach a limit while the material still maintains significant separation power. Understanding this relationship would be very beneficial in determining the optimal processing conditions for CMS particles.

Finally, it is important to establish the relationship between initial CMS properties and the impact that these processing parameters have on the physical properties. Consistency is very important in analyzing the impact of the various processing parameters on the CMS properties, but it is also important to determine if the trends established for one starting material are significantly altered when the initial properties of the CMS are changed.

7.2.3. Modified Casting Processes Without Annealing Above T_g

This work showed the need for stress relaxation in hybrid materials before the molecular sieve inserts were able to enhance the selectivity of the membranes. Moore also recognized the need for membrane preparation techniques that restrict the formation of stress in the polymer matrix during vitrification [10]. One approach that shows some promise in this area is the use of a dual solvent casting system to prepare the hybrid materials. In this type of process a high volatility solvent is used as the primary solvent to “freeze” the structure of the membrane while a second, low volatility solvent is used in small amounts to prevent vitrification. The low volatility solvent may then be removed under controlled conditions selected to vitrify the hybrid material very slowly. Initial trials

with this approach showed some selectivity improvement over other hybrid samples that were not annealed for the CO_2/CH_4 separation as shown in Figure 7.1.

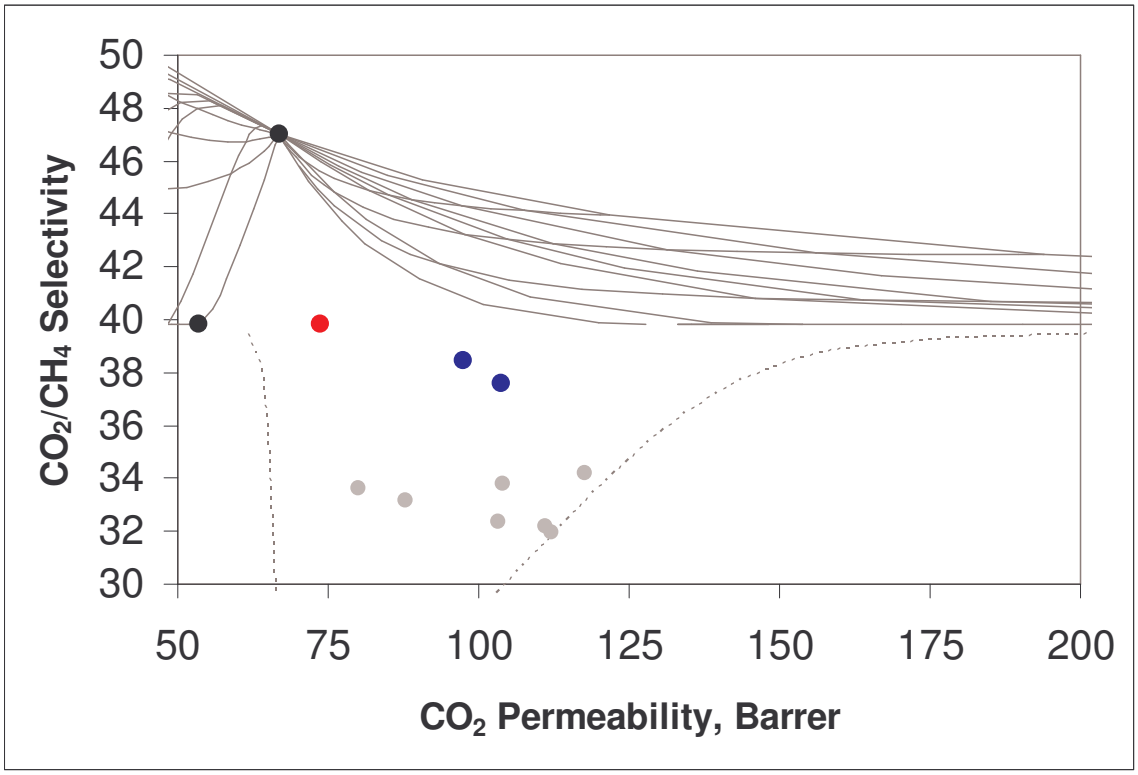

Figure 7.1 Hybrid membranes formed from 20 vol% CMS cast from a dual solvent system (blue dots) showed selectivity enhancements over membranes cast from CH_2Cl_2 alone (gray dots). The red dot represents neat polymer prepared from a dual solvent solution. Permeabilities tested at 35 °C and 50 psia. None of these samples were annealed above 200 °C.

The increased selectivity seen in the films prepared with the dual solvent dope suggests a smaller average void size at the interface. This relationship could result from a tighter bond between the polymer and the sieve, but it could also be the result of simply having a lower void fraction with similarly sized voids. Either situation represents an improvement over the previous casting technique, and it is possible that further optimization of this approach with an emphasis on the solvent ratio and drying procedure could result in the successful formation of hybrid membranes using the polymer-sieve combination studied in this work without the need for above T_g annealing.

7.2.4. Hybrid Membrane Performance in the Presence of Aggressive Feeds

One area of research involving hybrid membranes that still requires significant study is performance with aggressive feed streams. As a relatively new technology, much of the current work involving hybrid membrane development is involved in pushing the performance to higher levels through the use of higher performance polymers or higher sieve loadings, however industrial application of these membranes will require reliable performance in "real world" environments that often contain much more aggressive feeds than the pristine gas separations performed in the laboratory. In particular, high pressures of CO_2 or traces of highly condensable penetrants are possible in industrial applications [11]. Such feeds may be able to plasticize the polymer matrix [12, 13], and the impact of plasticization on hybrid membrane performance should be investigated. In some cases, particularly involving submicron inserts, hybrid membranes have shown plasticization resistance with the bonds between the polymer and the sieves acting as artificial cross links in the system [14-16] providing enhanced stability similar to that discussed in Chapter 5.

The impact of plasticization should be investigated using both high pressure CO_2 and highly condensable penetrants since the interactions at the interface of the polymer and sieve may change considerably for the different penetrants. Of particular importance is the ability of highly condensable penetrants to effectively fill voids at the interface allowing enhanced separation performance despite the presence of voids and the occurrence of plasticization in the polymer [17, 18]. It is possible for contaminants to sorb into the sieves sufficiently to alter the transport properties, and plasticization changes the polymer transport properties as well. While plasticization is generally expected to be accompanied by a loss in selectivity, there may be simultaneous

changes in the sieve properties or the effective matching between the polymer and the sieve that result in an overall increase in selectivity for the hybrid material.

Earlier work with aggressive feeds in polymeric membranes has shown the ability of certain feeds to effectively condition the membrane material resulting in a hysteresis when the transport properties do not return to those of the original polymer membrane after the aggressive feed stream is removed. In conjunction with studies of plasticization and contamination in hybrid membranes, it is important to determine the ability of these materials to maintain their performance capacity since membrane units are most often designed based on initial separation performance.

7.2.5. Hybrid Membranes as Asymmetric Hollow Fibers

One of the final stages of membrane development necessary to produce economically viable membrane separation systems is the formation of membranes as asymmetric hollow fibers. There are multiple new challenges faced in the formation of hollow fibers that are not present in the dense film trials or in the formation of polymeric hollow fibers. Recent work by Husain was able to identify several important parameters necessary for spinning hybrid asymmetric hollow fiber membranes [19], but there are still several areas in need of further development.

Issues associated with agglomeration are even more of a concern in the very thin selective layer of asymmetric hollow fibers. Even very small agglomerates may cause defects that pass through the entire skin effectively destroying the separation performance of the fibers. Other phenomena such as defect formation nucleated by the dispersed sieve particles must be further studied as well. The phase separation process that is used to form the asymmetric structure of the hollow fibers can be impacted by the

presence of the small sieve particles such that new defective morphologies, such as voids that pass through the entire selective skin layer of the membrane or nucleation of macrovoids in the fiber substructure, may form in the hollow fiber [19]. Further work is still needed to understand the fundamental causes for some of these phenomena as well as methods capable of controlling the formation process to provide defect free fibers.

7.3. References

1. Williams, P.J. (2006). Analysis of Factors Influencing the Performance of CMS membranes for Gas Separation. School of Chemical and Biomolecular Engineering. Atlanta, Georgia Institute of Technology. Doctor of Philosophy: 238.
2. Geiszler, V.C. (1997). Polyimide Precursors For Carbon Molecular Sieve Membranes. Chemical Engineering. Austin, TX, The University of Texas at Austin. Doctor of Philosophy.
3. Singh, A. (1997). Membrane Materials with Enhanced Selectivity: An Entropic Interpretation. Chemical Engineering. Austin, The University of Texas at Austin. Doctor of Philosophy: 263.
4. Steel, K.M. (2000). Carbon Membranes For Challenging Gas Separations. Chemical Engineering. Austin, TX, The University of Texas at Austin. Doctor of Philosophy.
5. Kelemen, S.R. and Freund, H. (1988). "XPS Characterization Of Glassy-Carbon Surfaces Oxidized By O2, CO2, And HNO3." Energy & Fuels 2(2): 111-118.
6. Fang, H.T., Liu, C.G., et al. (2004). "Purification Of Single-Wall Carbon Nanotubes By Electrochemical Oxidation." Chemistry of Materials 16(26): 5744-5750.
7. Liu, M. H., Y. L. Yang, et al. (2005). "Chemical Modification Of Single-Walled Carbon Nanotubes With Peroxytrifluoroacetic Acid." Carbon 43(7): 1470-1478.
8. Okpalugo, T.I.T., Papakonstantinou, P., et al. (2005). "Oxidative Functionalization Of Carbon Nanotubes In Atmospheric Pressure Filamentary Dielectric Barrier Discharge (APDBD)." Carbon 43(14): 2951-2959.
9. Xing, Y.C., Li, L., et al. (2005). "Sonochemical Oxidation Of Multiwalled Carbon Nanotubes." Langmuir 21(9): 4185-4190.
10. Moore, T.T. (2004). Effects of Materials, Processing, and Operating Conditions on the Morphology and Gas Transport Properties of Mixed Matrix Membranes. Chemical Engineering. Austin, TX, The University of Texas at Austin. Doctor of Philosophy: 312.
11. Baker, R. W. (2002). "Future Directions Of Membrane Gas Separation Technology." Industrial & Engineering Chemistry Research 41(6): 1393-1411.
12. Ismail, A.F. and Lorna, W. (2002). "Penetrant-Induced Plasticization Phenomenon In Glassy Polymers For Gas Separation Membrane." Separation and Purification Technology 27(3): 173-194.
13. Okamoto, K., Noborio, K., et al. (1997). "Permeation And Separation Properties Of Polyimide Membranes To 1,3-Butadiene And n-Butane." Journal of Membrane Science 134(2): 171-179.
14. Nunes, S.P., Schultz, J., et al. (1996). "Silicone Membranes With Silica Nanoparticles." Journal of Materials Science Letters 15(13): 1139-1141.

15. Sforca, M.L., Yoshida, I.V.P., et al. (2001). "Hybrid Membranes Based On SiO2/Polyether-B-Polyamide: Morphology And Applications." Journal of Applied Polymer Science 82(1): 178-185.
16. Vankelecom, I.F.J., Scheppers, E., et al. (1994). "Parameters Influencing Zeolite Incorporation in PDMS Membranes." Journal of Physical Chemistry 98(47): 12390-12396.
17. Vankelecom, I.F.J., Merckx, E., et al. (1995). "Incorporation of Zeolites in Polyimide Membranes." Journal of Physical Chemistry 99(35): 13187-13192.
18. Vankelecom, I.F.J., VandenBroeck, S., et al. (1996). "Silylation To Improve Incorporation Of Zeolites In Polyimide Films." Journal of Physical Chemistry 100(9): 3753-3758.
19. Husain, S. (2006). Mixed Matrix Dual Layer Hollow Fiber Membranes for Natural Gas Separation. School of Chemical and Biomolecular Engineering. Atlanta, Georgia Institute of Technology. Doctor of Philosophy: 235.

APPENDIX A

RESEARCH POLYMER 6FDA-6FPDA: SYNTHESIS AND PROCESSING EFFECTS

Consistency in membrane preparation is very important to successful studies involving research grade polymers. It has been shown in this work that the gas separation performance of a polymeric membrane can vary greatly as a result of changes that may initially seem fairly minor. Fortunately, consistent processing of the polymer membrane produces highly repeatable results. The first part of this appendix briefly discusses the process used to synthesize the polymer, and the subsequent sections discuss some observations regarding the impact of processing conditions on membrane transport properties.

A.1. Synthesis of 6FDA-6FpDA

As Chapter 3 discussed, the 6FDA-6FpDA used in this work was synthesized by the author using a procedure developed by previous members of the Koros Research Group. The overall synthesis occurs in two major parts: addition of equal molar amounts of a 4,4'-(hexafluoroisopropylidene) diphthalic anhydride (6FDA) and 4,4'-(hexafluoroisopropylidene) dianiline (6FpDA) to produce a polyamic acid, and conversion of the polyamic acid into a polyimide through a ring closing condensation reaction.

The first step in the synthesis was to obtain the two purified monomers. The 6FDA and 6FpDA used in this work are both obtained as white powders in >95% purity. Unfortunately, the high molecular weights needed for mechanical stability of the polymer

membranes can only be obtained with conversion factors in excess of 99% for the overall synthesis. Therefore, the monomers used must be further purified before synthesizing, and this purification is done by sublimation.

Figure A.1 shows the setup used to sublime the monomers. The system is held under vacuum at an absolute pressure of 0.001-0.005 torr. The monomer is then heated in an oil bath with a sublimation flask equipped with a cold finger located directly above the monomer powder. Under the pressures used in this lab (approximately 0.001-0.005 torr), 6FDA and 6FpDA sublime at around 220 ^{o}C and 180 ^{o}C, respectively. When the appropriate temperature is obtained, the monomer will sublime away from the bottom of the flask and condense on the cold finger that is maintained at a constant temperature by a continuous flow of water.

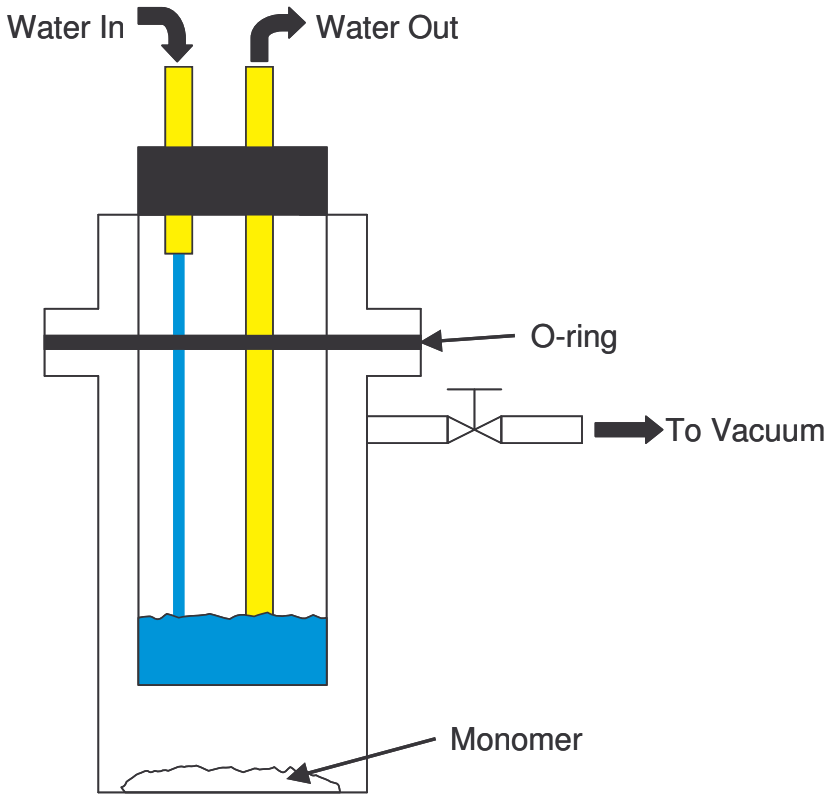

Figure A.1 The monomers were purified by sublimation in a glass sublimation flask as shown. The flask was submerged in a heating oil bath on a hotplate to provide the temperatures necessary for sublimation to occur.

Once the monomers have been purified, the synthesis can be performed. The polyamic acid synthesis was carried out in 1-methyl-2-pyrrolidone (NMP) at room temperature for a duration of 12 to 24 hrs. Because of the sensitivity of the reaction to precise stoichiometry, the reaction was performed in a rigorously dried environment. All glassware used was dried in a vacuum oven at 200 ^{o}C overnight and then flame dried three times in alternating nitrogen and vacuum atmospheres prior to the start of the reaction. All solvents used were obtained in anhydrous, sure seal containers, and further dried by storing over dried molecular sieves (Aldrich, Molecular Sieves, 4A, beads, 8-12 mesh). The reaction was performed under a positive pressure nitrogen blanket.

With all of the glassware and solvents dried, a precise amount of the diamine was added to the reaction flask. A small amount of NMP was then added to the flask to dissolve the diamine. When all of the diamine dissolved, the precise amount of dianhydride needed was added to the reaction flask, and the remainder of the NMP was added to provide a 20 wt% solution. The solution was then allowed to stir and react for 12 to 24 hrs. As the polyamic acid formed, the viscosity of the solution increased considerably.

After the polyamic acid formation was completed, the imidization was performed using one of two methods: chemical imidization or thermal imidization. For chemical imidization, a mixture of acetic anhydride and triethylamine was used to form the imide groups. The triethylamine acted as a catalyst for the ring closing reaction, and the acetic anhydride reacted with the water given off to form acetic acid. After the mixture was slowly added to the polyamic acid solution, the system was heated to 100 ^{o}C and allowed to react for at least one hour.

With thermal imidization, a mixture of ortho-dichlorobenzene (ODCB) and NMP was added. The NMP helped to dilute the viscous polymer solution, and the ODCB formed an azeotrope with the water that was released during the condensation reaction and removed it from the system by evaporation. The amount of ODCB added was calculated to provide an overall ODCB weight fraction of 0.15. With the ODCB/NMP mixture added, the solution was heated to 190 ^{o}C for at least 12 hrs to thermally imidize the polyamic acid. This temperature is high enough to promote the imidization reaction and to remove the water given off during the condensation reaction. Figure A.2 shows the major reaction steps.

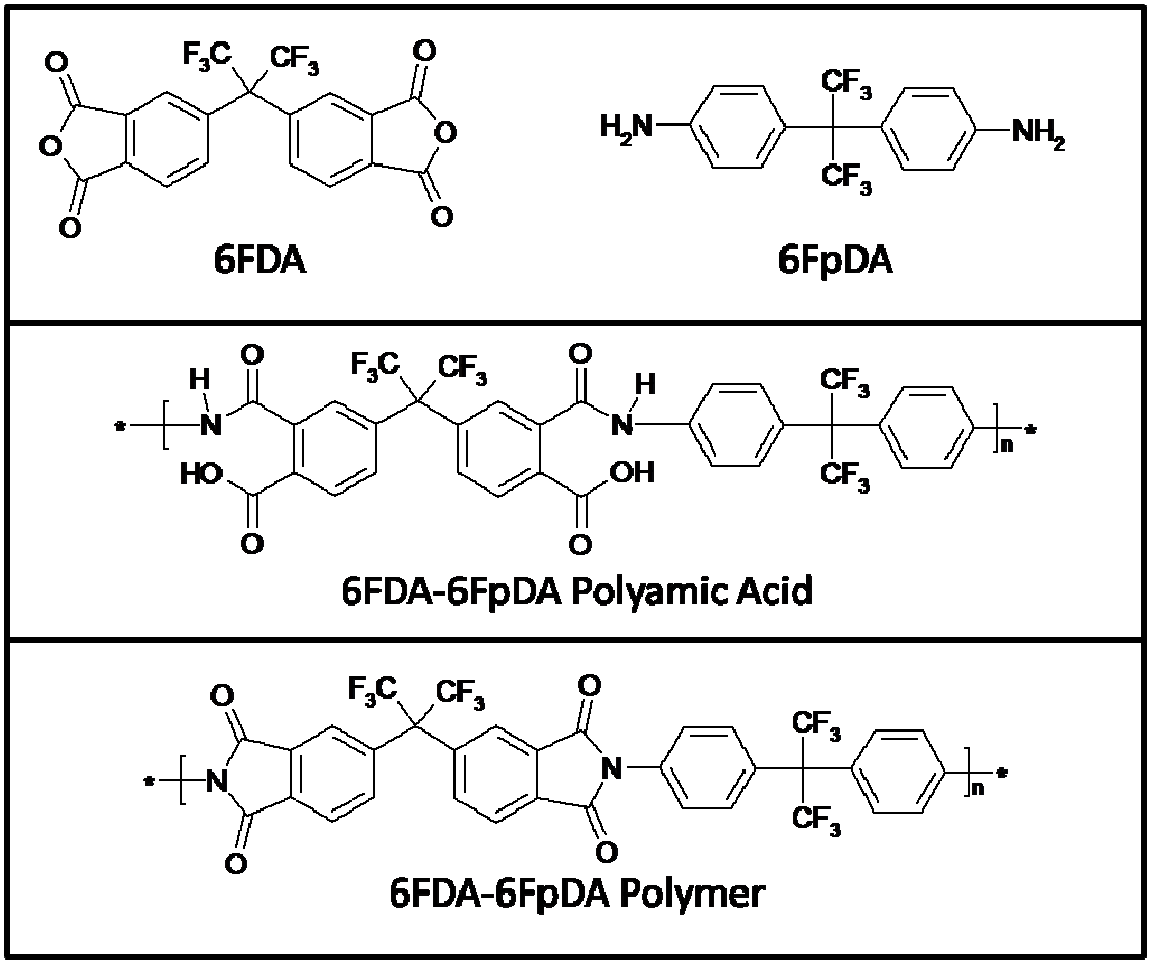

Figure A.2 Equal molar amounts of 4,4'-(hexafluoroisopropylidene) diphthalic anhydride (6FDA) and 4,4'-(hexafluoroisopropylidene) dianiline (6FpDA) were combined to form 6FDA-6FpDA polyamic acid which was then thermally imidized to form 6FDA-6FpDA polymer giving off water as a byproduct.

When the imidization is complete, the solution was allowed to return to room temperature and the polymer was recovered. The polymer was removed from solution by precipitating into a 50:50 mixutre of methanol and water. A large excess (generally ~10 times the reaction volume) of methanol/water solution was used for the precipitation. The solvent exchange caused a rapid phase change in the polymer system resulting in a continuous polymer fiber formed as the solution was slowly poured into the stirred methanol/water.

The resulting polymer fibers were then placed in a blender and just covered with fresh methanol/water solution. This solution was then blended thoroughly to produce a slurry of polymer pieces. The slurry was then filtered over a Buchner funnel, and the process was repeated once with a methanol/water solution and once with a pure methanol solution to remove residual solvents from the polymer. After the final filtration, the polymer was dried in a three step process: 1) dry overnight in a fume hood, 2) dry for ≥ 12 hrs at ambient pressure and 100 ^{o}C, and 3) dry for ≥ 12 hrs at full vacuum (<0.005 torr) and 200 ^{o}C. The polymer was then considered ready for use in experimental measurements, and the first test was always to characterize the gas transport properties of a pure polymer membrane formed form the synthesized polymer.

A.2. Effect of Polymer Synthesis and Drying Procedure

The process used to dry the polymer is important for several reasons. By slowly drying the polymer, the remaining solvents are not “flashed” which can cause practical problems with the equipment and the sample holders. Drying in vacuum at 200 ^{o}C insures full removal of the solvents used in the synthesis and recovery of the polymer. Heating the polymer samples to 200 ^{o}C also promotes full imidization of the polymer

backbone. The impact of this process on the performance of the polymer in gas separation can be seen in the two series presented in Figure A.3. The two series indicate the transport properties obtained for two batches of polymer: one synthesized using chemical imidization, and the other using thermal imidization.

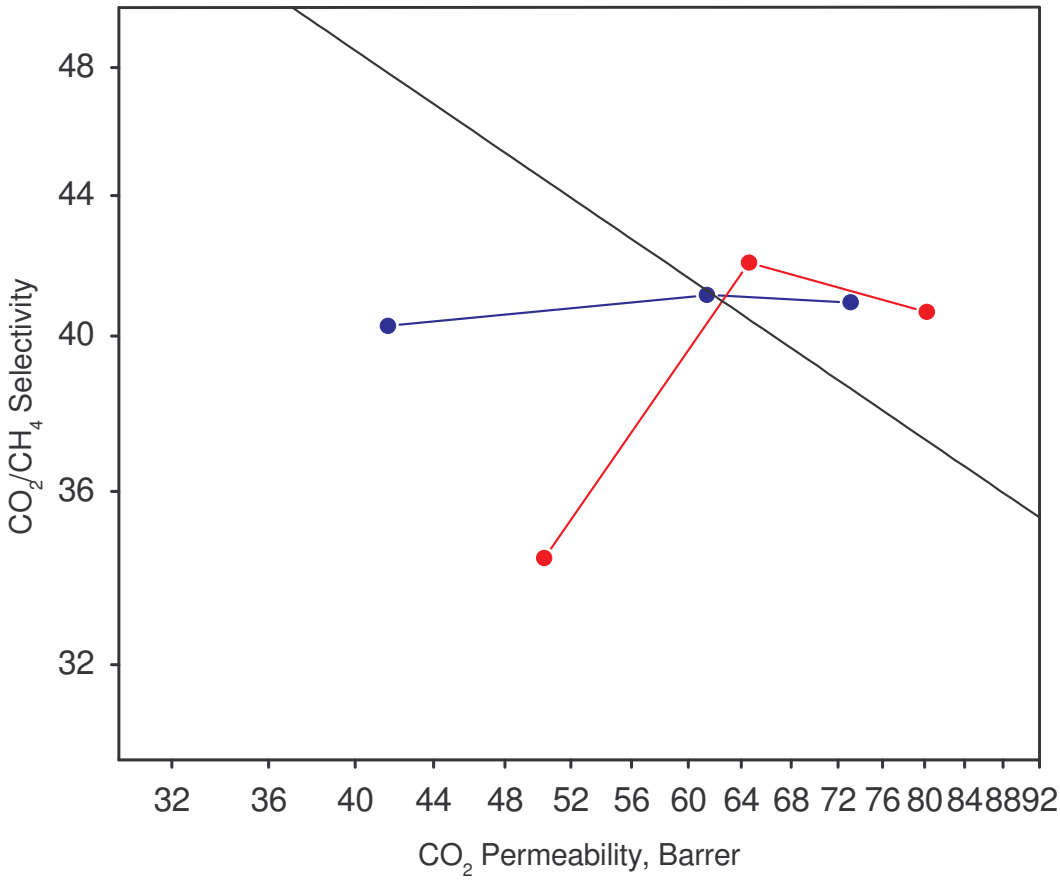

Figure A.3 The gas separation performance of the polymer is considerably altered by the drying conditions used after the synthesis. The temperatures shown indicate drying temperatures used prior to solution casting the membranes. All membranes were solution cast and then dried in vacuum at 110 °C. Permeabilities tested at 35 °C and 50 psia.

As the figure indicates, the gas separation properties of the polymers formed from the chemical and thermal imidization processes varied considerably prior to the final heat treatment and drying cycle at 200 ^{o}C. As the temperature approached the final drying temperature, the properties of the polymers tended to converge; however, the properties are still not quite equal. The gas transport properties obtained for several different batches of polymer are shown in Figure A.4. Several of the batches have properties near a CO_2 permeability of 75 Barrers with a CO_2/CH_4 selectivity of 41. The error bars in the figure show that while most of the differences in the transport properties are small, they are still significant because of the precision of the measurements. As a result of the small changes that can occur from one batch to another, the synthesis was scaled up to allow most of the work in this study to be performed with a consistent basis polymer, and the neat polymer references given throughout the dissertation were measured for the specific batch of polymer that was used in that part of the study.

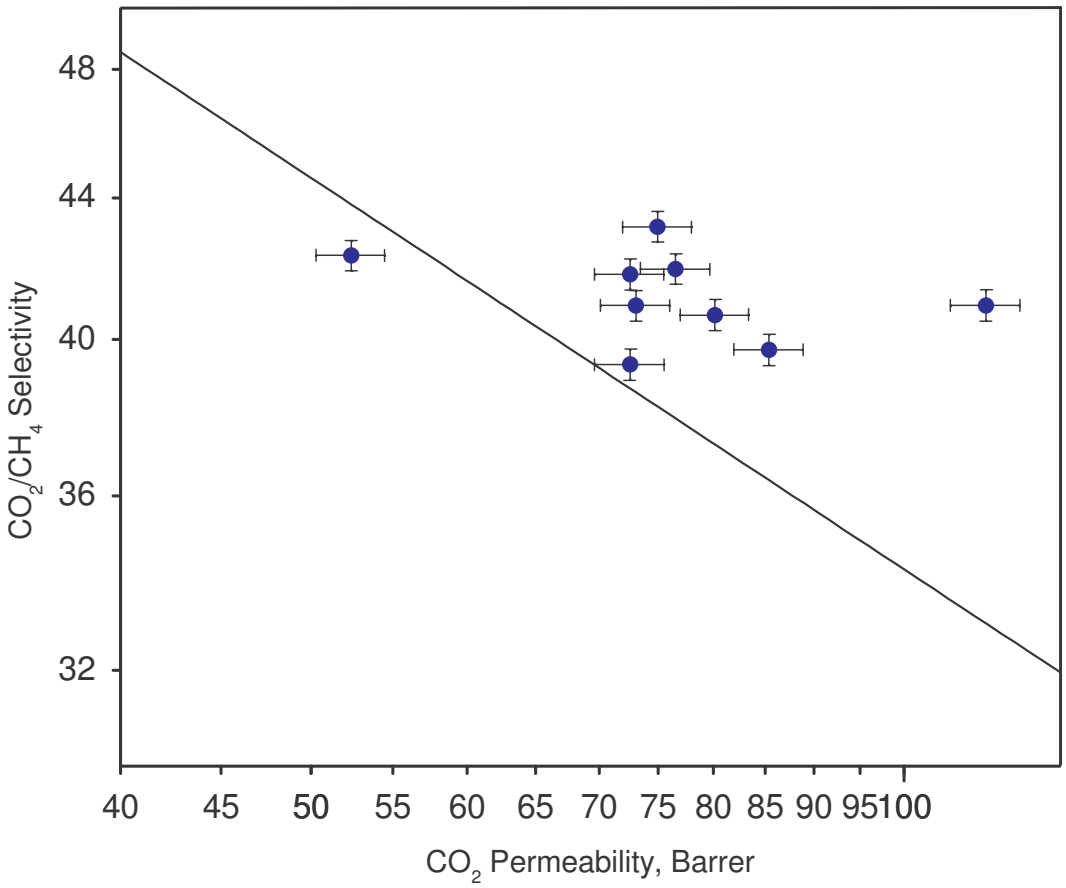

Figure A.4 Batches of 6FDA-6FpDA polymer synthesized separately may possess different gas separation properties. Permeabilities tested at 35 °C and 50 psia.

A.3. Effect of Film Drying Procedure

Another processing condition that must be controlled to reduce variability in the measurements is the film drying process. The solution casting procedure described in Chapter 3 with a drying temperature of 110 °C was used for each of the pure polymer films tested in this work with the exception of a few samples presented in this section. This process was adapted from the work reported by Vu [1]; however, other film drying procedures have been reported, such as extended drying at temperatures as high as 200 °C [2, 3]. In order to determine the impact of higher temperature drying on the transport properties of the membrane, a film cast from one of the polymer batches used in this work was dried at 200 °C for 20 hrs prior to testing. The gas separation properties

measured for the CO_2/CH_4 separation in this film and for a film dried at 110 °C are shown in Figure A.5. Also included in the figure are the properties measured for a films dried at 110 °C and 200 °C and then annealed above T_g using the process described in Chapter 5.

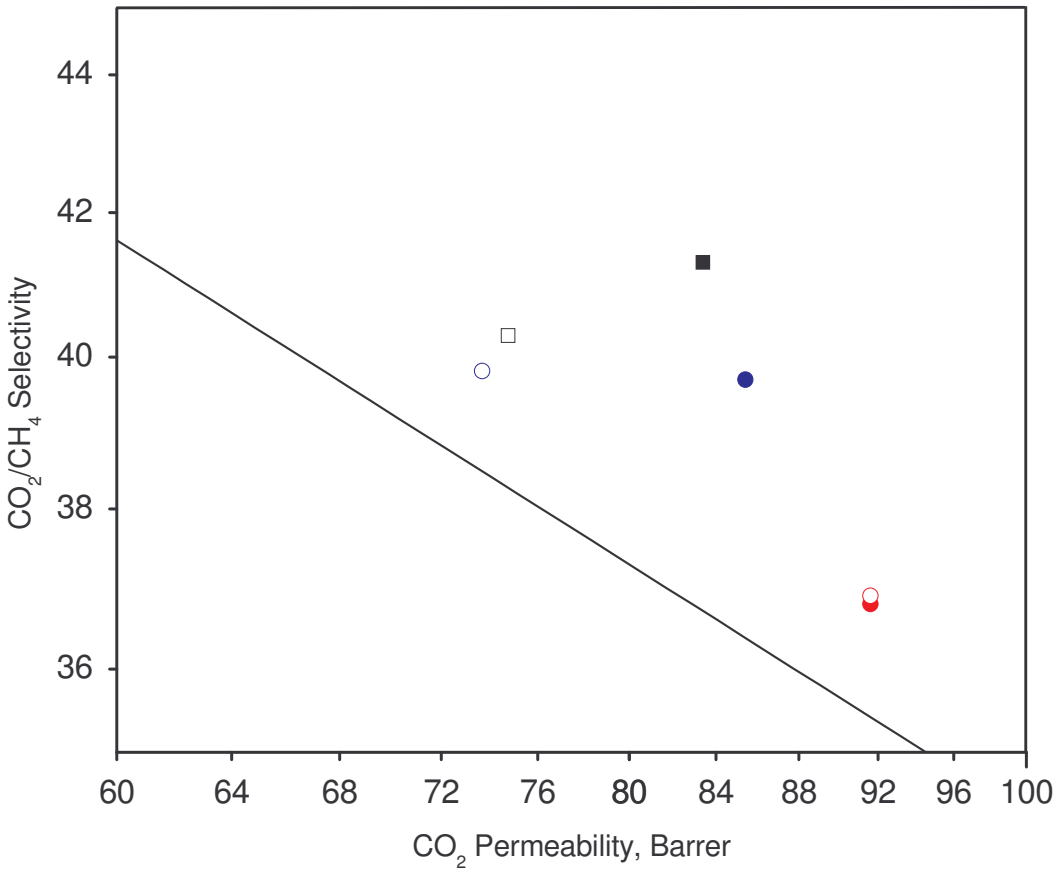

Figure A.5 The process used to dry the 6FDA-6FpDA films can impact the transport properties measured for the material. Filled data points are for films dried at 110 °C after casting, and opened data points are for films dried at 200 °C. Black squares are data from previous researchers [1, 2]. Blue circles are for films dried and directly tested. Red circles are for films dried and then annealed at 350 °C for 1hr. Permeabilities tested at 35 °C and 50 psia.

As the figure shows, the higher drying temperature caused a decrease in the permeability of the membrane with a very small increase in the selectivity. The permeabilities of the membranes prepared with the two drying temperatures agree with those reported by previous researchers that have used these drying protocols. It is also

clear that annealing the polymer sample above its Tg eliminates the effects of the thermal history of the film prior to annealing. These trends agree well with those reported previously for annealing and aging studies of the 6FDA-6FpDA and 6FDA-6FmDA polymer system [3, 4].

A.4. Consistency of Results

The previous discussion illustrates the importance of consistency in the preparation and measurement of polymeric gas separation membranes. Fortunately, carefully controlled processing used to prepare samples under the same conditions results in highly reproducible results. While changes in the processing conditions may change the permeabilities by as much as 20% or more, polymeric membranes prepared under consistent conditions generally have very low error with permeability variations in the range of 3-5% and typical selectivity variations of 1% or less. The reason for differences in variability between permeability and selectivity is that the largest errors introduced during the permeability measurement are associated with the measurement of the film thickness and area. Since these measurements have the same impact on all of the permeabilities calculated, the selectivity is unaffected by any errors in the dimensions.

It is also important to keep the changes discussed in this appendix in the proper perspective. For example, some of the polymers appear to possess properties a considerable distance above the upper bound [5]. However, when these properties are viewed relative to the data used to develop the upper bound [5], as shown in figure A.6, these differences appear less extreme, and the location relative to the upper bound appears more appropriate. Because of the precision possible with carefully controlled protocols, even small changes in the transport properties of the polymeric membranes may be studied and analyzed from a fundamental perspective.

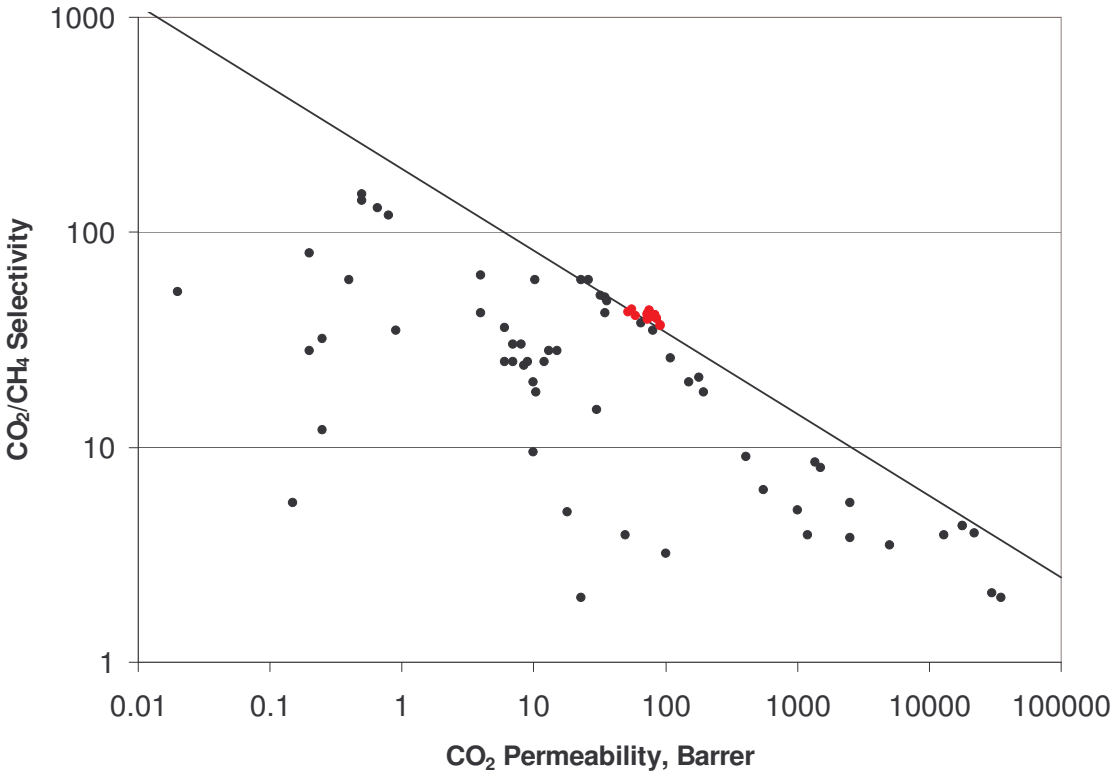

Figure A.6 Polymeric membranes may possess a very large range of gas separation properties. When viewed relative to properties of other polymer membranes, the property changes seen in 6FDA-6FpDA appear small. Red circles are data from figures A.3 and A.4.

A.5. References

1. Vu, D.Q. (2001). Formation and Characterization of Asymmetric Carbon Molecular Sieve and Mixed Matrix Membranes for Natural Gas Purification. Chemical Engineering. Austin, TX, The University of Texas at Austin. Doctor of Philosophy.
2. Coleman, M.R. (1992). Isomers of Fluorine-Containing Polyimides for Gas Separation Membranes. Chemical Engineering. Austin, The University of Texas at Austin. Doctor of Philosophy: 262.
3. Fuhrman, C., Nutt, M., et al. (2004). "Effect Of Thermal Hysteresis On The Gas Permeation Properties Of 6fda-Based Polyimides." Journal of Applied Polymer Science 91(2): 1174-1182.
4. Wind, J.D., Paul, D.R., et al. (2004). "Natural Gas Permeation In Polyimide Membranes." Journal of Membrane Science 228(2): 227-236.
5. Robeson, L.M. (1991). "Correlation of Separation Factor Versus Permeability for Polymeric Membranes." Journal of Membrane Science 62(2): 165-185.

VITA

JOHN DOUGLAS PERRY

John Douglas Perry was born on June 26, 1980, to Doug and Janice Perry in Easley, South Carolina. John graduated as valedictorian from Easley High School in May of 1998. He received his Bachelor of Science degree in Chemical Engineering with departmental honors from Clemson University in May of 2002, and began pursuing his Doctor of Philosophy in Chemical Engineering at the Georgia Institute of Technology in August of that year. In June 2004, John married Lindsay Michelle Martin of Anderson, South Carolina. They now live in Charleston, South Carolina, where John works in the Specialty Chemicals Division of MeadWestvaco Corporation.